University of Venda
Creating Future Leaders

UNIVERSITY OF VENDA

Adsorption of oxyanions of As, B, Cr, Mo and Se from coal fly ash leachates using Al^{3+}/Fe^{3+} modified bentonite clay

A Masters research submitted to the University of Venda, School of Environmental Sciences, Department of Ecology and Resource Management

By

Masindi Vhahangwele

Student No: 11572071

UNIVEN LIBRARY
Library Item : 20132631

Signature ..... Date 05/08/2013

Supervisor : Dr Wilson Mugera Gitari (University of Venda)

Signature ..... Date 05/08/2013

Co- supervisor : Dr Hlanganani Tutu (University of Witwatersrand)

Signature ..... Date 05/08/2013

© University of Venda

University of Venda
Creating Future Leaders

DEDICATION

This research is dedicated to my son (**Masindi Vhuthuhawe Jr**) for motivating and keeping me strong throughout this study.

UNIVERSITY OF VENDA
LIBRARY

© University of Venda

University of Venda
Creating Future Leaders

DECLARATION

I declare that "***Adsorption of oxyanions of As, B, Cr, Mo and Se from coal fly ash leachates using Al^{3+}/Fe^{3+} modified bentonite clay***" is my own work, that it has not been submitted for any degree or examination in any other university, and that all the sources I have used or quoted have been indicated and duly acknowledged by complete references.

Masindi Vhahangwele January 2013

Signature.....

© University of Venda

University of Venda
Creating Future Leaders

ABSTRACT

South African coal-fired power stations rely on the use of low grade bituminous coal for electricity generation. During coal combustion processes, this type of coal generates large volumes of waste materials which include Fly ash, bottom ash, boilers slag, flue gas desulphurization and un-captured particles. From the array of generated residues, coal fly ash constitute 90% and of this only 5% is beneficially used with the rest being disposed-off to land as ash dumps or slurried to ash retention ponds. On disposal, coal fly ash leaches out toxic chemical species on contact with the aqueous media hence posing hazardous effects to the aquatic and terrestrial environment. Of prime concern are Oxyanionic species such as As, B, Cr, Mo and Se. This study aims to investigate the adsorption of As, B, Cr, Mo and Se from coal fly ash leachates on Al^{3+}/Fe^{3+} modified bentonite clay.

Coal fly ash samples used in this study were collected from Tutuka, ESKOM power plant in Mpumalanga and Bentonite clay samples were collected from ECCA (pty) Ltd. pH, Electrical Conductivity (EC) and Total Dissolved Solids (TDS) of the samples were determined using a CRISON multimeter probe. Modifications of bentonite clay with Al^{3+} and Fe^{3+} cations were done in batch procedures and the parameters optimized included contact time, adsorbent dose and adsorbate concentration. Cation Exchange Capacity (CEC), Point of Zero Charge (pH_{pzc}) and Water Holding Capacity (WHC) of raw and modified bentonite clay were determined using standard methods. Surface areas of raw and modified bentonite clays were determined by BET. Elemental composition of raw and modified bentonite clay was determined by XRF and Mineralogical composition of raw and modified bentonite clay was determined by XRD. AAS and GFAAS were used to monitor Al^{3+} and Fe^{3+} concentration in the reaction mixture during and after modification while As, B, Cr, Mo, and Se were monitored using GFAAS, ICP- OES and ICP- MS. Adsorption of oxyanions of As, B, Cr, Mo and Se was carried out in batch experiments using synthetic solutions of the species. Effects of contact time, adsorbent dosage, adsorbate concentration and pH on the adsorption of As, B, Cr, Mo and Se were evaluated and optimized.

© University of Venda

The modification experiments revealed that loading of Al^{3+} onto bentonite clay interlayers is optimum at 60 minutes of contact time, 3 grams of adsorbent and 100 mg/L of adsorbate concentration and loading of Fe^{3+} onto bentonite clay matrices is optimum at 15 minutes of contact time, 2 grams of adsorbent and 100 mg/L of adsorbate. The CEC results showed that South African bentonite clay is characterized by high CEC of 262 meq/100g at pH 5.4 and 265.5 meq/100g at pH 7.4 which decreased to 186.9 meq/100g at pH 5.4 and 183.3 meq/100g at pH 7.4 on introducing Al^{3+} onto bentonite clay interlayers and 195.5 meq/100g at pH 5.4 and 188.9 meq/100g at pH 7.4 on introducing Fe^{3+} onto bentonite clay interlayers. The results show that CEC is independent of pH. BET results indicated that the loading of Al^{3+} onto bentonite clay interlayers increased the surface area from 16 m^2/g to 44.3 m^2/g and 50 m^2/g for Fe^{3+}, external surface area from 11.1 m^2/g to 33.1 m^2/g for Al^{3+} and 37.4 m^2/g for Fe^{3+}, micro-pore area from 4.9 m^2/g to 11.2 m^2/g for Al^{3+} and 12.5 m^2/g for Fe^{3+}. There was a slight difference in pH_{PZC} of Al^{3+} modified bentonite clay (8.2) as compared to raw bentonite (8.0). For Fe^{3+} modified bentonite clay, the pH_{PZC} was observed to increase from 8.0 for raw bentonite clay to 9.0. An increase in pH_{PZC} shows that modification will favour adsorption of anions from aqueous media. WHC of bentonite clay was determined to be 42.7%. Elemental composition by XRF showed SiO_2, Al_2O_3, Fe_2O_3, CaO, Na_2O, K_2O and MgO as the major chemical species. XRF results also confirmed that bentonite clay is an aluminosilicate material. XRD disclosed that bentonite clay is dominated by montmorillonite as the major mineral phase. Characterization of fly ash leachates revealed that coal fly ash leachates contains 53 µg/L of As, 1730 µg/L of B, 271 µg/L of Cr, 165 µg/L of Mo and 170 µg/L of Se. Adsorption of As, B, Cr, Mo and Se onto Al^{3+} modified bentonite clay revealed that 30 minutes of contact time, 4 grams of adsorbent dosage, 10 mg/L of adsorbate concentration and pH 10 are the optimum conditions for removing those species from aqueous media. The adsorption affinity of those species obeyed the following order: B = Se > Mo = Cr > As. Adsorption of As, B, Cr, Mo and Se onto Fe^{3+} modified bentonite clay revealed that 30 minutes of contact time, 4 grams of adsorbent dosage, 10 mg/L of adsorbate concentration and pH 10 are the optimum conditions for removing those species from aqueous media. The adsorption affinity of those species obeyed the following order: B = Se > Mo > Cr = As. The adsorption capacities of modified bentonite clays were greater than the adsorption capacities of raw bentonite clay. The data fitted well to both Langmuir and Freundlich adsorption isotherm hence showing that the adsorption is energetically favourable. The unmodified clay

© University of Venda

showed poor adsorption for these chemical species. Both Al^{3+} and Fe^{3+} modified bentonite clay successfully removed As, B, Cr, Mo and Se from generated coal fly ash leachates to below DWAF water quality guidelines at the optimized conditions. This shows that Al^{3+} or Fe^{3+} modified bentonite clay is an effective adsorbent for removal of oxyanionic species of As, B, Cr, Mo and Se from coal fly ash leachates and could be applied as a reactive barrier or liner in ash retention ponds.

Keywords: *Bentonite Clay, Coal Fly Ash Leachates, Batch Procedures, Adsorption, Oxyanions, Langmuir and Freundlich Isotherms*

© University of Venda

University of Venda
Creating Future Leaders

ACKNOWLEDGEMENTS

Firstly I would like to thank the Lord Almighty who is the reason why I am alive, thanking him for protecting me and everything he made possible for me.

I would like to express profound gratitude and sincere thanks to my supervisor **Dr Gitari.W.M**. A senior lecturer at the university of Venda, School of environmental sciences, Department of Ecology and resource management for his guidance, facilitation, supervision and concrete solid assistance throughout this project. Your contribution cannot be overstated because your advices made what looked almost impossible at the beginning very much possible at the end!

My sincere gratitude also goes to **Dr H Tutu** (Senior Lecturer University of Witwatersrand, School of Sciences, Department of chemistry), for his co-supervision, guidance and motivation.

I wish to thank all faculties and support staff of Department of ERM and Postgraduate students for their continuous support, constant help and extending the departmental facilities for my project work.

I would also like to thank the **University of Venda RPC, SKA grant and DST-NRF** Scholarship for financially supporting my study.

I would also like to thank my family for the roles they played in my life. For the special love and care they gave me. Your love is indispensable and immeasurable.

Lastly but not the least, I would like to extend my sincere thanks to my friend and fellow researcher **Mr Makoni Tonderai**, for his unconditional assistance and encouragement, for the stimulating discussions, for the sleepless nights we were working together before deadlines, and also to my friends **Mr P. C. Ngoetjane, Miss G Liabara, Miss F.P. Tshikovhi** and **Miss T Ngulube** for sincere help extended in completion of my project and for all the fun we have had in the last two years.

© University of Venda

University of Venda
Creating Future Leaders

ACADEMIC OUTPUTS

PRESENTATIONS AND CONFERENCES

Masindi V, Gitari, W.M; Tutu, H. Adsorption of oxyanions of As, B, Cr, Mo and Se from coal fly ash leachates using Al^{3+} modified bentonite clay. IGCP/SIDA Project number 606 Workshop on "**The quest for pragmatic solutions to complex health and environmental problems of small-scale mining**" International conference held in Kumasi, Ghana, NODA hotel from 27 – 30 June 2012.

Masindi V, Gitari, W.M; Tutu, H. Adsorption of oxyanions of As, B, Cr, Mo and Se from coal fly ash leachates using Fe^{3+}modified bentonite clay. ASSAf-DST-NRF Third Annual South African Young Scientists' Conference. Theme: "Our Energy Future" held in CSIR International Convention Centre, Brummeria, Pretoria. From 16-18 October 2012

Masindi V, Gitari, W.M; Tutu, H. Adsorption of oxyanions of As, B, Cr, Mo and Se from coal fly ash leachates using Fe^{3+}modified bentonite clay. Limpopo, University of Venda, School of Environmental Sciences Research day. 18 November 2012

MANUSCRIPTS BEING PREPARED FOR SUBMISSION TO INTERNATIONAL PEER REVIEWED JOURNAL

Masindi V, Gitari, W.M; Tutu, H. Adsorption of oxyanions of As, B, Cr, Mo and Se from coal fly ash leachates using Al^{3+} modified bentonite clay. To be submitted to an international peer reviewed journal in 2013

Masindi V, Gitari, W.M; Tutu, H. Adsorption of oxyanions of As, B, Cr, Mo and Se from coal fly ash leachates using Fe^{3+}modified bentonite clay. To be submitted to an international peer reviewed journal in 2013

© University of Venda

University of Venda
Creating Future Leaders

ACRONYMS AND ABBREVIATIONS

AAS	: Atomic adsorption Spectroscopy
BET	: Brunauer-Emmett-Teller method
CEC	: Cation Exchange Capacity
CFA	: Coal fly ash
DWAF	: Department of water affairs and forestry
EC	: Electrical conductivity
GFAAS	: Graphite Furnace Atomic Adsorption spectroscopy
ICP-OES	: Inductively Coupled Plasma- Optic Emission Spectrometer
pH	: Potential hydrogen
TDS	: Total dissolved solids
XRD	: X-ray diffraction
XRF	: X-ray fluorescence spectrometer
PZC	: Point of Zero Charge
WHC	: Water Holding Capacity

NOTE: Please refer to the periodic table for the elements

© University of Venda

University of Venda
Creating Future Leaders

TABLE OF CONTENTS

DEDICATION i
DECLARATION ii
ABSTRACT iii
ACKNOWLEDGEMENTS vi
ACADEMIC OUTPUTS vii
PRESENTATIONS AND CONFERENCES vii
MANUSCRIPTS BEING PREPARED FOR SUBMISSION TO INTERNATIONAL PEER REVIEWED JOURNAL vii
ACRONYMS AND ABBREVIATIONS viii
TABLE OF CONTENTS ix
LIST OF FIGURES xv
LIST OF TABLES xxvi
CHAPTER 2 xxvi
LIST OF APPENDICES xxviii

CHAPTER ONE 1

Introduction 1
1.1 Background Information 1
1.2 Problem Statement 3
1.3 Main Objective 3
1.4 Specific Objectives 3
1.5 Research Questions 4
1.6 Hypothesis 4
1.7 Research Rationale 4
1.8 Assumption 5
1.9 Structure of subsequent chapters 5

© University of Venda

University of Venda
Creating Future Leaders

CHAPTER TWO 6

Literature review 6

2.1 Introduction 6

2.2 Coal and Power Generation Worldwide and in South Africa 7

2.3 Coal Combustion Processes 7

2.4 By Products of Coal Combustion 8

2.5 Coal fly ash 9

2.5.1 Physical properties of fly ash 9

2.5.1.1 Particle size 9

2.5.1.2 Colour 10

2.5.1.3 Particle shape 10

2.5.1.4 Surface area 10

2.5.2 Chemical properties of fly ash 11

2.5.2.1 pH 13

2.6 Classification of fly ash 14

2.7 Beneficial applications of coal fly ash 15

2.7.1 CO_2 sequestration 16

2.7.2 Agriculture 16

2.7.3 Acid mine drainage treatment 17

2.7.4 Waste treatment and stabilization 17

2.7.5 Cement and concrete 17

2.7.6 Construction 18

2.8 Leaching properties of coal fly ash 18

2.8.1 Factors which dictate leaching of coal fly ash 20

2.8.1.1 Effects of pH on leaching of coal fly ash 20

2.8.1.2 Effects of particle size on leaching of coal fly ash 20

2.8.1.3 Effect of redox reaction on leaching of coal fly ash 21

2.9 Toxic species of concern to the environment 23

2.10 Potential Effects of oxyanions (As, B, Cr, Mo and Se) to living organisms 24

2.10.1 Arsenic 24

2.10.2 Boron 25

2.10.3 Chromium 25

2.10.4 Molybdenum 26

© University of Venda

University of Venda
Creating Future Leaders

2.10.5 Selenium 26
2.11 Clay materials and their applications in environmental remediation 26
2.12 Bentonite clay 27
2.13 Physicochemical properties of bentonite clay 28
2.13.1 Physical properties of bentonite clay 28
2.13.2 Chemical properties of bentonite clay 28
2.14 Applications of bentonite clay 31
2.16 DWAF water quality guidelines for oxyanions concentration in water bodies 33
2.17 Conclusion 34

CHAPTER THREE 35

Materials and methods 35
3.0 Introduction 35
3.1 Sampling 35
3.2 Determination of pH, Electrical conductivity (EC), temperature and total dissolved solids (TDS) 35
3.3 Preparations of Bentonite clay samples 35
3.4 Modification of bentonite clay with Al^{3+} and Fe^{3+} 36
3.4.1 Modification of raw bentonite clay with Al^{3+} species 36
3.4.1.1 Adsorption of Al^{3+} onto bentonite clay lattice as a function of contact time 36
3.4.1.2 Adsorption of Al^{3+} onto bentonite clay as a function of adsorbent dosage 36
3.4.1.3 Adsorption of Al^{3+} onto bentonite clay as a function of adsorbate concentration 37
3.4.1.4 Procedures for impregnating Al^{3+} onto bentonite clay crystal lattice 37
3.4.2 Modification of raw bentonite clay with Fe^{3+} cations 38
3.4.2.1 Adsorption of Fe^{3+} onto bentonite clay as a function of contact time 38
3.4.2.2 Adsorption of Fe^{3+} onto bentonite clay as a function of adsorbent dosage 38
3.4.2.3 Adsorption of Fe^{3+} onto bentonite clay as a function of adsorbate concentration 39
3.4.2.4 Procedures for impregnating Fe^{3+} onto bentonite clay crystal lattice 39
3.5 Physicochemical characterization of bentonite clay and coal fly ash leachates 39
3.5.1 Determination of Cation Exchange Capacity (CEC) 40
3.5.1.1 Preparation of ammonium acetate 40
3.5.1.2 CEC determination 40
3.5.2 Determination of elemental composition of modified and raw clays 40
3.5.3 Determination of surface area 41

© University of Venda

University of Venda
Creating Future Leaders

3.5.4 Determination of water holding capacity 41
3.5.5 Determination of point of zero charge (PZC) 41
3.5.6 Determination of the mineralogical composition of modified and raw bentonite clay 42
3.6 Generation of coal fly ash leachates 42
3.7 Removal of As, B, Cr, Mo and Se by raw and Al^{3+} Modified clay 43
3.7.1 Adsorption of As, B, Cr, Mo and Se onto bentonite clay as a function of contact time 43
3.7.2 Adsorption of As, B, Cr, Mo and Se onto bentonite clay as a function of dosage 43
3.7.3 Adsorption of As, B, Cr, Mo and Se onto bentonite clay as a function of concentration 44
3.7.4 Adsorption of As, B, Cr, Mo and Se onto bentonite clay as a function of pH 44
3.8 Interaction of coal fly ash leachates with raw and Al^{3+} modified bentonite clay under natural conditions 45
3.9 Interaction of coal fly ash leachates with raw and Al^{3+} modified bentonite clay under optimized conditions 45
3.10 Removal of As, B, Cr, Mo and Se onto raw and Fe^{3+} Modified clay 45
3.10.1 Adsorption of As, B, Cr, Mo and Se onto bentonite clay as a function of contact time 45
3.10.2 Adsorption of As, B, Cr, Mo and Se onto bentonite clay as a function of adsorbent dosage 46
3.10.3 Adsorption of As, B, Cr, Mo and Se onto bentonite clay as a function of adsorbate concentration 46
3.10.4 Adsorption of As, B, Cr, Mo and Se onto bentonite clay as a function of pH 47
3.11 Interaction of coal fly ash leachates with raw and Fe^{3+} modified bentonite clay under natural conditions 47
3.12 Interaction of coal fly ash leachates with raw and Fe^{3+} modified bentonite clay under optimized condition 48
3.13 Calculation of adsorption capacity of the synthesized adsorbent 48
3.14 Equilibrium adsorption models 48
3.14.1 The Langmuir Isotherm 49
3.14.2 The Freundlich Isotherm 49

CHAPTER FOUR 51

physicochemical characterization of raw and modified bentonite clay 51

4.0 Introduction 51

© University of Venda

University of Venda
Creating Future Leaders

4.1 Modification of raw bentonite clay with Al^{3+} polycations 51
4.1.1 Adsorption of Al^{3+} onto bentonite clay as a function of contact time 51
4.1.2 Adsorption of Al^{3+} onto bentonite clay as a function of adsorbent dose 54
4.1.3 Adsorption of Al^{3+} onto bentonite clay as a function of adsorbate concentration 57
4.2 Modification of bentonite clay with Fe^{3+} polycations 61
4.2.1 Adsorption of Fe^{3+} onto bentonite clay as a function of contact time 61
4.1.2.2 Adsorption of Fe^{3+} onto bentonite clay as a function of adsorbent dosage 64
4.1.2.3 Adsorption of Fe^{3+} onto bentonite clay as a function of adsorbate concentration .. 67
4.2 Physico-chemical characterization of raw and modified bentonite clay 70
4.2.1 Cation Exchange Capacity (CEC) 70
4.2.2 Elemental composition of raw and modified bentonite clays 72
4.2.3 Surface area of raw and modified bentonite clay 74
4.2.4 Water holding capacity 75
4.2.5 Point of zero charge (PZC) of raw and modified bentonite clay 76
4.2.6 Mineralogical composition of bentonite clay 78
4.3 Chemical composition of coal fly ash leachates 80

CHAPTER FIVE 82

Adsorption of As, B, Cr, Mo and Se onto Al^{3+} modified bentonite clay: optimization of adsorption conditions and application for coal fly ash leachates remediation 82
5.0 Introduction 82
5.1 Adsorption of oxyanions As, B, Cr, Mo and Se using Al^{3+} modified bentonite clay 82
5.1.1 Adsorption of As, B, Cr, Mo, Se as a function of contact time 82
5.1.2 Adsorption of As, B, Cr, Mo, Se as a function of adsorbent dosage 86
5.1.3 Adsorption of As, B, Cr, Mo, Se as a function of adsorbate concentration 89
5.1.4 Adsorption of As, B, Cr, Mo, Se as a function of pH 93
5.2 Adsorption capacity of raw and modified bentonite clay 98
5.3 Adsorption isotherms for As, B, Cr, Mo and Se onto Al^{3+} modified bentonite clay 98
5.4 Adsorption of As, B, Cr, Mo and Se from coal fly ash leachates using Al^{3+} modified bentonite clay under un-optimized and optimized conditions 106
Table 5.4: Adsorption of As, B, Cr, Mo and Se from coal fly ash leachates using Al^{3+} modified bentonite clay under un-optimized and optimized conditions and compare the product leachates with DWAF water quality guidelines (DWAF, 1996). 106

© University of Venda

University of Venda
Creating Future Leaders

CHAPTER SIX **108**

Adsorption of As, B, Cr, Mo and Se onto Fe^{3+} modified bentonite clay: Optimization of adsorption conditions and application for coal fly ash leachates remediation **108**

6.0 Introduction 108

6.1 Adsorption of oxyanions of As, B, Cr, Mo and Se using Fe^{3+} modified bentonite clay 108

6.1.1 Adsorption of As, B, Cr, Mo, Se as a function of contact time 108

6.1.2 Adsorption of As, B, Cr, Mo, Se as a function of adsorbent dosage 112

6.1.3 Adsorption of As, B, Cr, Mo, Se as a function of adsorbate concentration 115

6.1.4 Adsorption of As, B, Cr, Mo, Se as a function of pH 119

6.2 Adsorption capacities of raw and Fe^{3+} modified bentonite clay 123

6.3 Adsorption isotherms 124

CHAPTER SEVEN **133**

Conclusions and recommendations **133**

7.1 Conclusion 133

7.1.1 Modification of raw bentonite clay with Al^{3+}/Fe^{3+} polycations 134

7.1.2 Physicochemical characterization of raw and modified bentonite clay 134

7.1.3 Adsorption capacities and mechanisms of raw and Al^{3+}/Fe^{3+} modified bentonite clay for oxyanions of As, B, Cr, Mo and Se 135

7.2 Recommendations 136

REFERENCES **137**

APPENDICES **157**

© University of Venda

University of Venda
Creating Future Leaders

LIST OF FIGURES

CHAPTER 2

Figure 2.1: Schematic illustration of coal combustion process in coal fired power stations.

Figure 2.2: Structure of bentonite clay (Bradley and Weils, 2004)

CHAPTER 4

Figure 4.1: Variation of pH on adsorption of Al^{3+} onto bentonite clay as a function of contact time (1 gram of adsorbent dosage, 100 mg/L adsorbate concentration and 1/100 S/L ratios).

Figure 4.2: Variation of TDS and EC on adsorption of Al^{3+} onto bentonite clay lattices as a function of contact time (1 gram of adsorbent dosage, 100 mg/L adsorbate concentration and 1/100 S/L ratios).

Figure 4.3: Variation of Al^{3+} adsorbed onto bentonite clay with an increase in contact time (1 gram bentonite clay, 100 mg/L Al^{3+} and 1/100 S/L ratios).

Figure 4.4: Variation of pH profile on adsorption of Al^{3+} onto bentonite clay with an increase in adsorbent dosage (60 minutes of contact time, 100 mg/L adsorbate concentration and 1/100 S/L ratios).

Figure 4.5: Variation of TDS and EC on adsorption of Al^{3+} onto bentonite clay interlayers as a function of adsorbent dosage (60 minutes of contact time, 100 mg/L adsorbate concentration and 1/100 S/L ratios).

Figure 4.6: Variation of Al^{3+} concentration adsorbed onto bentonite clay lattice with an increase in adsorbent dosage (60 minutes of contact time, 100 mg/L of adsorbate concentration and 1/100 S/L ratios).

© University of Venda

Figure 4.7: Variation of initial and final pH during the adsorption of Al^{3+} onto bentonite clay matrices as a function of adsorbate concentration (60 minutes of contact time, 3 grams of adsorbent dosage, and 1/100 S/L ratios).

Figure 4.8: Variation of initial and final EC during the adsorption of Al^{3+} onto bentonite clay matrices as a function of adsorbate concentration (60 minutes of contact time, 3 grams of adsorbent dosage, and 1/100 S/L ratios).

Figure 4.9: Variation of initial and final TDS during the adsorption of Al^{3+} onto bentonite clay matrices as a function of adsorbate concentration (60 minutes of contact time, 3 grams of adsorbent dosage, and 1/100 S/L ratios).

Figure 4.10: Variation of initial and final pH during the adsorption of Al^{3+} onto bentonite clay matrices as a function of adsorbate concentration (60 minutes of contact time, 3 grams of adsorbent dosage, 100 mg/L of adsorbate concentration and 1/100 S/L ratios).

Figure 4.11: Variation of pH profile during the adsorption of Fe^{3+} cations onto bentonite clay matrices as a function of contact time (1 gram of adsorbent dosage, 100 mg/L of adsorbate concentration and 1/100 S/L ratios).

Figure 4.12: Variation of EC and TDS levels during the adsorption of Fe^{3+} onto bentonite clay as a function of contact time (1 gram of adsorbent dosage, 100 mg/L of adsorbate concentration and 1/100 S/L ratios).

Figure 4.13: Variation of Fe^{3+} adsorbed onto bentonite clay surfaces with an increase in contact time (1 gram of adsorbent dosage, 100 mg/L of adsorbate concentration and 1/100 S/L ratios)

Figure 4.14: Variation of pH profiles on loading of Fe^{3+} onto bentonite clay as a function of adsorbent dosage (15 minutes of contact time, 100 mg/L of adsorbate concentration and 1/100 S/L ratios).

Figure 4.15: Variation of EC and TDS levels on loading of Fe^{3+} onto bentonite clay as a function of adsorbent dosage(15 minutes of contact time, 100 mg/L of adsorbate concentration and 1/100 S/L ratios).

© University of Venda

Figure: 4.16: Variation of Fe^{3+} concentration adsorbed onto bentonite clay as a function of adsorbent dosage (15 minutes of contact time, 100 mg/L of adsorbate concentration and 1/100 S/L ratios).

Figure 4.17: Variation of initial and final pH of the solution with varying concentration ranges (15 minutes of contact time, 3 grams of adsorbent dosage and 1/100 S/L ratios).

Figure 4.18: Variation of initial and final EC of the mixture with varying concentration ranges (15 minutes of contact time, 3 grams of adsorbent dosage and 1/100 S/L ratios).

Figure 4.19: Variation of initial and final EC of the mixture with varying concentration ranges (15 minutes of contact time, 3 grams of adsorbent dosage and 1/100 S/L ratios).

Figure 4.20: Variation of % Fe^{3+} concentration adsorbed onto bentonite clay with increasing adsorbate concentration (15 minutes of contact time, 3 grams of adsorbent dosage and 1/100 S/L ratios).

Figure 4.21: PZC of Raw bentonite clay

Figure 4.22: PZC of Al^{3+} bentonite clay

Figure 4.23: PZC of Fe^{3+} bentonite clay

Figure 4.24: XRD diffractogram of bentonite clay.

© University of Venda

CHAPTER 5

Figure 5.1: Variation of pH, EC and TDS on adsorption of As, B, Cr, Mo and Se on Al^{3+} modified bentonite clay with contact time (1 gram of adsorbent dosage, 10 mg/L adsorbate concentrations, 26°C and 1g/100 mL S/L ratio).

Figure 5.2: Variation of pH, EC and TDS on adsorption of As, B, Cr, Mo and Se on raw bentonite clay with contact time (1 gram of adsorbent dosage, 10 mg/L adsorbate concentrations, 26°C and 1g/100 mL S/L ratio).

Figure 5.3: Variation of As, B, Cr, Mo and Se % removal for Al^{3+} modified bentonite clay with contact time (1 gram of adsorbent dosage, 10 mg/L adsorbate concentration, 250 rpm, 26°C and 1g/100 mL S/L ratio).

Figure 5.4: Variation of As, B, Cr, Mo and Se % removal for raw bentonite clay with contact time (1 gram of adsorbent dosage, 10 mg/L adsorbate concentration, 26°C and 1g/100 mL S/L ratio).

Figure 5.5: Variation of pH, EC and TDS with varying adsorbent dosage on adsorption of As, B, Cr, Mo and Se onto Al^{3+} modified bentonite clay (30 minutes of contact time, 10 mg/L adsorbate concentration, 250 rpm and 26°C).

Figure 5.6: Variation of pH, EC and TDS with varying adsorbent dosage on adsorption of As, B, Cr, Mo and Se onto raw bentonite clay (30 minutes of contact time, 10 mg/L adsorbate concentration, 250 rpm and 26°C).

Figure 5.7: Variation of As, B, Cr, Mo and Se % adsorption for Al^{3+} bentonite as a function of adsorbent dosage (30 minutes of contact time, 10 mg/L adsorbate concentration, 250 rpm and 26°C).

Figure 5.8: Variation of As, B, Cr, Mo and Se % adsorption for raw bentonite as a function of adsorbent dosage (30 minutes of contact time, 10 mg/L adsorbate concentration, 250 rpm and 26°C).

© University of Venda

Figure 5.9: Variation of initial and final pH profiles with an increase in adsorbate concentration for Al^{3+} modified bentonite clay (30 minutes of contact time, 4 grams of adsorbent dosage, 250 rpm, 26°C and 4g/100 mL S/L ratios).

Figure 5.10: Variation of initial and final pH profiles with an increase in adsorbate concentration for raw bentonite clay (30 minutes of contact time, 4 grams of adsorbent dosage, 250 rpm, 26°C and 4g/100 mL S/L ratios).

Figure 5.11: Variation of initial and final EC and TDS with an increase in adsorbate concentration for Al^{3+} modified bentonite clay (30 minutes of contact time, 4 grams of adsorbent dosage, 250 rpm, 26°C and 4g/100 mL S/L ratios).

Figure 5.12: Variation of initial and final EC and TDS with an increase in adsorbate concentration for raw bentonite clay (30 minutes of contact time, 4 grams of adsorbent dosage, 250 rpm, 26°C and 4g/100 mL S/L ratios).

Figure 5.13: Variation of As, B, Cr, Mo and Se % removal for Al^{3+} modified bentonite clay with an increase in adsorbate concentration clay (30 minutes of contact time, 4 grams of adsorbent dosage, 250 rpm, 26°C and 4g/100 mL S/L ratios).

Figure 5.14: Variation of As, B, Cr, Mo and Se % removal for raw bentonite clay with an increase in adsorbate concentration clay (30 minutes of contact time, 4 grams of adsorbent dosage, 250 rpm, 26°C and 4g/100 mL S/L ratios).

Figure 5.15: Variation of final pH at varying initial pH on adsorption of As, B, Cr, Mo and Se onto Al^{3+} modified bentonite clay (30 minutes of contact time, 4 grams of adsorbent dosage, 10 mg/L metals concentration, 250 rpm, 26°C and 4g/100 mL S/L ratios).

Figure 5.16: Variation of final pH at varying initial pH on adsorption of As, B, Cr, Mo and Se onto raw bentonite clay (30 minutes of contact time, 4 grams of adsorbent dosage, 10 mg/L metals concentration, 250 rpm, 26°C and 4g/100 mL S/L ratios).

Figure 5.17: Variation of EC and TDS with varying initial pH on adsorption of As, B, Cr, Mo and Se onto Al^{3+} modified bentonite clay (30 minutes of contact time, 4 grams of adsorbent dosage, 10 mg/L metals concentration, 250 rpm, 26°C and 4g/100 mL S/L ratios).

© University of Venda

Figure 5.18: Variation of EC and TDS with varying initial pH on adsorption of As, B, Cr, Mo and Se onto raw bentonite clay (30 minutes of contact time, 4 grams of adsorbent dosage, 10 mg/L metals concentration, 250 rpm, 26°C and 4g/100 mL S/L ratios).

Figure 5.19: Variation of As, B, Cr, Mo and Se % removal with varying pH on interaction with Al^{3+} modified bentonite clay (30 minutes of contact time, 4 grams of adsorbent dosage, 10 mg/L metals concentration, 250 rpm, 26°C and 4g/100 mL S/L ratios).

Figure 5.20: Variation of As, B, Cr, Mo and Se % removal with varying pH on interaction with raw bentonite clay (30 minutes of contact time, 4 grams of adsorbent dosage, 10 mg/L metals concentration, 250 rpm, 26°C and 4g/100 mL S/L ratios).

Figure 5.21: Langmuir adsorption isotherm for adsorption of As by Al^{3+} modified bentonite clay (30 minutes of contact time, 4 grams of adsorbent dosage, 250 rpm, 26°C and 4g/100 mL S/L ratios).

Figure 5.22: Langmuir adsorption isotherm for adsorption of B by Al^{3+} modified bentonite clay (30 minutes of contact time, 4 grams of adsorbent dosage, 250 rpm, 26°C and 4g/100 mL S/L ratios).

Figure 5.23: Langmuir adsorption isotherm for adsorption of Cr by Al^{3+} modified bentonite clay (30 minutes of contact time, 4 grams of adsorbent dosage, 250 rpm, 26°C and 4g/100 mL S/L ratios).

Figure 5.24: Langmuir adsorption isotherm for adsorption of Mo by Al^{3+} modified bentonite clay (30 minutes of contact time, 4 grams of adsorbent dosage, 250 rpm, 26°C and 4g/100 mL S/L ratios).

Figure 5.25: Langmuir adsorption isotherm for adsorption of Se by Al^{3+} modified bentonite clay (30 minutes of contact time, 4 grams of adsorbent dosage, 250 rpm, 26°C and 4g/100 mL S/L ratios).

Figure 5.26: Freundlich adsorption isotherm for adsorption of As by Al^{3+} modified bentonite clay (30 minutes of contact time, 4 grams of adsorbent dosage, 250 rpm, 26°C and 4g/100 mL S/L ratios).

Figure 5.27: Freundlich adsorption isotherm for adsorption of B by Al^{3+} modified bentonite clay (30 minutes of contact time, 4 grams of adsorbent dosage, 250 rpm, 26°C and 4g/100 mL S/L ratios).

© University of Venda

University of Venda
Creating Future Leaders

Figure 5.28: Freundlich adsorption isotherm for adsorption of Cr by Al^{3+} modified bentonite clay (30 minutes of contact time, 4 grams of adsorbent dosage, 250 rpm, 26°C and 4g/100 mL S/L ratios).

Figure 5.29: Freundlich adsorption isotherm for Freundlich adsorption isotherm for adsorption of Mo by Al^{3+} modified bentonite clay (30 minutes of contact time, 4 grams of adsorbent dosage, 250 rpm, 26°C and 4g/100 mL S/L ratios).

Figure 5.30: Freundlich adsorption isotherm for Freundlich adsorption isotherm for adsorption of Se by Al^{3+} modified bentonite clay (30 minutes of contact time, 4 grams of adsorbent dosage, 250 rpm, 26°C and 4g/100 mL S/L ratios).

© University of Venda

CHAPTER 6

Figure 6.1: Variation of pH, EC and TDS with adsorption of As, B, Cr, Mo and Se by Fe^{3+} bentonite clay as a function of contact time (1 gram of adsorbent dosage, 10 mg/L of adsorbate concentration, 250 rpm, 26°C and 1g/100 mL S/L ratios) the mixtures were shaked for 3 hours.

Figure 6.2: Variation of pH, EC and TDS on adsorption of As, B, Cr, Mo and Se on raw bentonite clay with contact time (1 gram of adsorbent dosage, 10 mg/L adsorbate concentrations, 26°C and 1g/100 mL S/L ratio).

Figure 6.3: Variation of As, B, Cr, Mo and Se % removal for Fe^{3+} modified bentonite clay as a function of contact time (1 gram of adsorbent dosage, 10 mg/L of adsorbate concentration, 250 rpm, 26°C and 1g/100 mL S/L ratios) the mixtures were shaked for 3 hours at the interval of 1, 5, 10, 15, 30, 60, and 180 minutes.

Figure 6.4: Variation of As, B, Cr, Mo and Se % removal for raw bentonite clay as a function of contact time (1 gram of adsorbent dosage, 10 mg/L of adsorbate concentration, 250 rpm, 26°C and 1g/100 mL S/L ratios) the mixtures were shaked for 3 hours.

Figure 6.5: Variation of pH, EC and TDS on adsorption of As, B, Cr, Mo and Se onto Fe^{3+} modified bentonite clay with varying adsorbent dosage (30 minutes of contact time, 10 mg/L of adsorbate concentration and 26°C). The dosages were varied from 0.5, 1, 2, 3, 4, and 5 grams.

Figure 6.6: Variation of pH, EC and TDS with varying adsorbent dosage on adsorption of As, B, Cr, Mo and Se onto raw bentonite clay (30 minutes of contact time, 10 mg/L adsorbate concentration, 250 rpm and 26°C).

Figure 6.7: Variation of As, B, Cr, Mo and Se % removal for Fe^{3+} modified bentonite clay as a function of adsorbent dosage (30 minutes of contact time, 10 mg/L of adsorbate concentration, 250 rpm and 26°C).

Figure 6.8: Variation of As, B, Cr, Mo and Se % removal for raw bentonite clay as a function of adsorbent dosage (30 minutes of contact time, 10 mg/L of adsorbate concentration, 250 rpm and 26°C).

© University of Venda

Figure 6.9: Variation of initial and final pH profiles for adsorption of As, B, Cr, Mo and Se by Fe^{3+} modified bentonite clay with an increase in adsorbate concentration (contact time of 30 minute, adsorbent dosage of 4 grams, 250 rpm, 26°C, and 4g/100 mL S/L ratios). The concentration was varied from 0.1, 0.5, 1, 3, 6, 10, and 15 mg/L.

Figure 6.10: Variation of initial and final pH profiles with an increase in adsorbate concentration for raw bentonite clay (30 minutes of contact time, 4 grams of adsorbent dosage, 250 rpm, 26°C and 4g/100 mL S/L ratios).

Figure 6.11: Variation of initial and final EC and TDS levels on adsorption of As, B, Cr, Mo and Se by Fe^{3+} modified bentonite clay with an increase in adsorbate concentration (contact time of 30 minute, adsorbent dosage of 4 grams, 26°C, 4g/100 mL S/L ratios, concentration varied 0.1, 0.5, 1, 3, 6, 10, and 15 mg/L).

Figure 6.12: Variation of initial and final EC and TDS with an increase in adsorbate concentration for raw bentonite clay (30 minutes of contact time, 4 grams of adsorbent dosage, 250 rpm, 26°C and 4g/100 mL S/L ratios).

Figure 6.13: Variation of As, B, Cr, Mo and Se % removal for Fe^{3+} modified bentonite clay with an increase in adsorbate concentration (contact time of 30 minute, adsorbent dosage of 4 grams, 250 rpm, 26°C, 4g/100 mL S/L ratios, concentration varied from 0.1, 0.5, 1, 3, 6, 10, and 15 mg/L).

Figure 6.14: Variation of As, B, Cr, Mo and Se adsorption for raw bentonite clay with an increase in adsorbate concentration (contact time of 30 minute, adsorbent dosage of 4 grams, 250 rpm, 26°C, 4g/100 mL S/L ratios, concentration varied from 0.1, 0.5, 1, 3, 6, 10, and 15 mg/L).

Figure 6.15: Variation of final pH on adsorption of As, B, Cr, Mo and Se by Fe^{3+} modified bentonite clay with varying initial pH (30 minutes of contact time, 4 grams of adsorbent dosage, 10 mg/L metals concentration, 26°C and 4g/100 mL S/L ratios).

Figure 6.16: Variation of final pH at varying initial pH on adsorption of As, B, Cr, Mo and Se onto raw bentonite clay (30 minutes of contact time, 4 grams of adsorbent dosage, 10 mg/L metals concentration, 250 rpm, 26°C and 4g/100 mL S/L ratios).

© University of Venda

Figure 6.17: Variation of EC and TDS levels on adsorption of As, B, Cr, Mo and Se by Fe^{3+} modified bentonite clay with varying initial pH (30 minutes of contact time, 4 grams of adsorbent dosage, 10 mg/L metal concentration, 250 rpm, 26°C and 4g/100 mL S/L ratios).

Figure 6.18: Variation of EC and TDS with varying initial pH on adsorption of As, B, Cr, Mo and Se onto raw bentonite clay (30 minutes of contact time, 4 grams of adsorbent dosage, 10 mg/L metals concentration, 250 rpm, 26°C and 4g/100 mL S/L ratios).

Figure 6.19: Variation of As, B, Cr, Mo and Se concentration on adsorption by Fe^{3+} modified bentonite clay with varying pH ranges (30 minutes of contact time, 4 grams of adsorbent dosage, 10 mg/L metals concentration, 250 rpm, 26°C and 4g/100 mL S/L ratios).

Figure 6.20: Variation of As, B, Cr, Mo and Se concentration on adsorption by raw bentonite clay with varying pH ranges (30 minutes of contact time, 4 grams of adsorbent dosage, 10 mg/L metals concentration, 250 rpm, 26°C and 4g/100 mL S/L ratios).

Figure 6.21: Langmuir adsorption isotherm for adsorption of As by Fe^{3+} modified bentonite clay (30 minutes of contact time, 4 grams of adsorbent dosage, 250 rpm, 26°C and 4g/100 mL S/L ratios).

Figure 6.22: Langmuir adsorption isotherm for adsorption of B by Fe^{3+} modified bentonite clay (30 minutes of contact time, 4 grams of adsorbent dosage, 250 rpm, 26°C and 4g/100 mL S/L ratios).

Figure 6.23: Langmuir adsorption isotherm for adsorption of Cr by Fe^{3+} modified bentonite clay (30 minutes of contact time, 4 grams of adsorbent dosage, 250 rpm, 26°C and 4g/100 mL S/L ratios).

Figure 6.24: Langmuir adsorption isotherm for adsorption of Mo by Fe^{3+} modified bentonite clay (30 minutes of contact time, 4 grams of adsorbent dosage, 250 rpm, 26°C and 4g/100 mL S/L ratios).

Figure 6.25: Langmuir adsorption isotherm for adsorption of Se by Fe^{3+} modified bentonite clay (30 minutes of contact time, 4 grams of adsorbent dosage, 250 rpm, 26°C and 4g/100 mL S/L ratios).

© University of Venda

Figure 6.26: Freundlich adsorption isotherm for adsorption of As by Fe^{3+} modified bentonite clay (30 minutes of contact time, 4 grams of adsorbent dosage, 250 rpm, 26°C and 4g/100 mL S/L ratios).

Figure 6.27: Freundlich adsorption isotherm for adsorption of B by Fe^{3+} modified bentonite clay (30 minutes of contact time, 4 grams of adsorbent dosage, 250 rpm, 26°C and 4g/100 mL S/L ratios).

Figure 6.28: Freundlich adsorption isotherm for adsorption of Cr by Fe^{3+} modified bentonite clay (30 minutes of contact time, 4 grams of adsorbent dosage, 250 rpm, 26°C and 4g/100 mL S/L ratios).

Figure 6.29: Freundlich adsorption isotherm for adsorption of Mo by Fe^{3+} modified bentonite clay (30 minutes of contact time, 4 grams of adsorbent dosage, 250 rpm, 26°C and 4g/100 mL S/L ratios).

Figure 6.10: Freundlich adsorption isotherm for adsorption of Se by Fe^{3+} modified bentonite clay (30 minutes of contact time, 4 grams of adsorbent dosage, 250 rpm, 26°C and 4g/100 mL S/L ratios).

© University of Venda

University of Venda
Creating Future Leaders

LIST OF TABLES

CHAPTER 2

Table 2.1: Average traces element composition in fly ash (EL-Mogazi et al., 1988; Young, 1993)

Table 2.2: Major chemical composition of selected South African fly ash (Gitari et al., 2008)

Table 2.3: ASTM standard classification of fly ash (ASTM C 618, 1993)

Table 2.4: New Canada specification of coal fly ash

Table 2.5: Oxides state of As, B, Cr, Mo and Se at varying pH conditions (Geert et al., 2008)

Table 2.6: Safe concentration of oxyanions as prescribed by DWAF (DWAF, 1996)

CHAPTER 4

Table 4.1: CEC of raw and modified bentonite clay in Milli-Equivalent (meq/100g)

Table 4.2: presents the results of XRF analysis of raw and modified bentonite clay

Table 4.3: Trace elements in raw and modified bentonite clay

Table 4.4: BET specific surface area and micro-pore area of raw and modified bentonite clay

Table 4.5: Minerals phases and their percentages (weight %) estimated using the Rietveld method (Autoquan Program).

Table 4.6: Major chemical composition of coal fly ash leachates

Table 4.7: Minor chemical composition of coal fly ash leachates

© University of Venda

CHAPTER 5

Table 5.1: Adsorption capacities of Al^{3+} modified and raw bentonite clay for As, B, Cr, Mo and Se

Table 5.2: Langmuir adsorption isotherm constant for adsorption of As, B, Cr, Mo and Se onto Al^{3+} modified bentonite clay

Table 5.3: Freundlich adsorption isotherm results on adsorption of As, B, Cr, Mo and Se onto Al^{3+} modified bentonite clay

Table 5.4: Adsorption of As, B, Cr, Mo and Se from coal fly ash leachates using Al^{3+} modified bentonite clay under un-optimized and optimized conditions and compare the product leachates with DWAF water quality guidelines (DWAF, 1996).

CHAPTER 6

Table 6.1: Adsorption capacities of raw and Fe^{3+} modified bentonite clay for oxyanions of As, B, Cr, Mo and Se

Table 6.2: Langmuir adsorption isotherms on adsorption of As, B, Cr, Mo and Se onto Fe^{3+} modified bentonite clay

Table 6.3: Freundlich adsorption isotherm of As, B, Cr, Mo and Se onto Fe^{3+} modified bentonite clay

Table 6.4: Adsorption of As, B, Cr, Mo and Se from coal fly ash leachates using Fe^{3+} modified bentonite clay under un-optimized and optimized conditions and compare the product leachates with DWAF water quality guidelines (DWAF, 1996).

© University of Venda

LIST OF APPENDICES

Table A1: pH_{Pzc} for raw bentonite clay at 0.1, 0.01, 0.001 KCl concentration

Table A2: pH_{Pzc} for Al^{3+} modified bentonite clay at 0.1, 0.01, 0.001 KCl concentration

Table A3: pH_{Pzc} for Fe^{3+} modified bentonite clay at 0.1, 0.01, 0.001 KCl concentration

Table A4: Variation of pH, TDS, EC, Temp and Al^{3+} with agitation time (1 gram of adsorbent dosage, 100 mg/L of adsorbate concentration and 26°C).

Table A5: Variation of pH, EC, TDS, Temp and Al^{3+} with adsorbent dosage (60 minutes contact time, 100 mg/L adsorbate and 26°C).

Table A6: initial pH, TDS (mg/L), EC (µS/cm), Temp (°C) before agitation with Al^{3+} adsorbate concentration (60 minutes of contact time, 3 grams of adsorbate concentration, 26°C and 3g/100 mL S/L ratios).

Table A7: Final pH, TDS, EC, Temp and Al^{3+} concentration with varying concentration ranges (60 minutes contact time, 3 grams ,26°C and 3g/100 mL).

Table A8: Variation of pH, TDS (mg/L), EC (µS/cm), Temp (°C) and Fe^{3+} with agitation time (3 gram adsorbent dosage, 100 mg/L adsorbate concentration, 26°C and 1g/100 mL S/L ratios).

Table A9: Variation of pH, TDS(mg/L), EC(µS/cm), Temp(°C) and Fe^{3+} ions with adsorbent dosage (15 minutes of contact time, and 100 mg/L adsorbate concentration, and 26°C).

Table A10: Variation of pH, TDS, EC, Temp and Fe^{3+} with initial adsorbate concentration before agitation (15 minutes contact time, 2 grams adsorbent dosage, 26°C and 2g/100 mL S/L ratios).

Table A11: Final pH, TDS(mg/L), EC(µS/cm), Temp(°C) and Fe^{3+} ions with adsorbate concentration (15 minutes of agitation, 2 grams of adsorbent dosage, 26°C and 2g/100 mL S/L ratios).

© University of Venda

Table A12: % removal of As, B, Cr, Mo and Se, pH, EC and TDS as a function of contact time onto raw bentonite clay (1 gram of adsorbent dosage, 10 mg/L of Adsorbate concentration, 26°C and 1g/100 mL S/L ratios).

Table A13: % removal of As, B, Cr, Mo and Se, pH, EC and TDS as a function of adsorbent dosage onto raw bentonite clay (30 minutes of contact time, 10 mg/L adsorbate concentration and 26°C).

Table A14: Initial pH, EC and TDS on adsorption of As, B, Cr, Mo and Se onto raw bentonite clay as a function of adsorbate concentration (30 minutes contact time, 4 grams adsorbate dosage, 26°C and 4g/100 mL S/L ratios).

Table A15: % removal of As, B, Cr, Mo and Se, pH, EC and TDS as a function of adsorbate concentration onto raw bentonite clay (30 minutes contact time, 4 grams adsorbate dosage, 26°C and 4g/100 mL S/L ratios).

Table A16: % removal of As, B, Cr, Mo and Se, pH, EC and TDS as a function of pH onto raw bentonite clay (30 minutes of contact time, 4 grams of adsorbent dosage, 10 mg/L of adsorbate concentration, 26°C and 4g/100 mL S/L ratios).

Table A17: % removal of As, B, Cr, Mo and Se, pH, EC and TDS as a function of contact time onto Al^{3+} modified bentonite clay (1 gram of adsorbent dosage, 10 mg/L of Adsorbate concentration, 26°C and 1/100 S/L ratios).

Table A18: % removal of As, B, Cr, Mo and Se, pH, EC and TDS as a function of adsorbent dosage onto Al^{3+} modified bentonite clay (30 minutes of contact time, 10 mg/L adsorbate concentration and 26°C).

Table A19: Initial pH, EC and TDS on adsorption of As, B, Cr, Mo and onto Al^{3+} modified bentonite clay as a function of adsorbate concentration (30 minutes contact time, 4 grams adsorbate dosage, 26°C and 4g/100 mL S/L ratios).

© University of Venda

Table A20: % removal of As, B, Cr, Mo and Se, pH, EC and TDS as a function of adsorbate concentration onto Al^{3+} modified bentonite clay (30 minutes contact time, 4 grams adsorbate dosage, 26°C and 4g/100 mL S/L ratios).

Table A21: % removal of As, B, Cr, Mo and Se, pH, EC and TDS as a function of pH onto Al^{3+} modified bentonite clay (30 minutes of contact time, 4 grams of adsorbent dosage, 10 mg/L of adsorbate concentration, 26°C and 4g/100 mL S/L ratios).

Table A22: Langmuir and Freundlich adsorption isotherms for Al^{3+} modified bentonite clay (30 minutes contact time, 4 grams adsorbate dosage and 1/100 mL S/L ratios).

Table A23: Langmuir and Freundlich adsorption isotherms for Al^{3+} modified bentonite clay (30 minutes contact time, 4 grams adsorbate dosage and 1/100 mL S/L ratios).

Table A24: Langmuir and Freundlich adsorption isotherms for Al^{3+} modified bentonite clay (30 minutes contact time, 4 grams adsorbate dosage and 1/100 mL S/L ratios).

Table A25: Langmuir and Freundlich adsorption isotherms for Al^{3+} modified bentonite clay (30 minutes contact time, 4 grams adsorbate dosage and 1/100 mL S/L ratios).

Table A26: Langmuir and Freundlich adsorption isotherms for Al^{3+} modified bentonite clay (30 minutes contact time, 4 grams adsorbate dosage and 1/100 mL S/L ratios).

Table A27: % removal of As, B, Cr, Mo and Se, pH, EC and TDS as a function of contact time onto Fe^{3+} bentonite clay (1 gram of adsorbent dosage, 10 mg/L of Adsorbate concentration, 26°C and 1/100 S/L ratios).

Table A28: % removal of As, B, Cr, Mo and Se, pH, EC and TDS as a function of adsorbent dosage onto Fe^{3+} bentonite clay (30 minutes of contact time, 10 mg/L adsorbate concentration and 26°C).

Table A29: Initial pH, EC and TDS on adsorption of As, B, Cr, Mo and Se onto Fe^{3+} bentonite clay as a function of adsorbate concentration (30 minutes contact time, 4 grams adsorbate dosage, 26°C and 4g/100 mL S/L ratios).

© University of Venda

Table A30: % removal of As, B, Cr, Mo and Se, pH, EC and TDS as a function of adsorbate concentration onto Fe^{3+} bentonite clay (30 minutes contact time, 4 grams adsorbate dosage, 26°C and 4g/100 mL S/L ratios).

Table A31: % removal of As, B, Cr, Mo and Se, pH, EC and TDS as a function of pH onto Fe^{3+} bentonite clay (30 minutes of contact time, 4 grams of adsorbent dosage, 10 mg/L of adsorbate concentration, 26°C and 4g/100 mL S/L ratios).

Table A32: Langmuir and Freundlich adsorption isotherms for Fe^{3+} modified bentonite clay (30 minutes contact time, 4 grams adsorbate dosage and 1/100 mL S/L ratios).

Table A33: Langmuir and Freundlich adsorption isotherms for Fe^{3+} modified bentonite clay (30 minutes contact time, 4 grams adsorbate dosage and 1/100 mL S/L ratios).

Table A34: Langmuir and Freundlich adsorption isotherms for Fe^{3+} modified bentonite clay (30 minutes contact time, 4 grams adsorbate dosage and 1/100 mL S/L ratios).

Table A35: Langmuir and Freundlich adsorption isotherms for Fe^{3+} modified bentonite clay (30 minutes contact time, 4 grams adsorbate dosage and 1/100 mL S/L ratios).

Table A36: Langmuir and Freundlich adsorption isotherms for Fe^{3+} modified bentonite clay (30 minutes contact time, 4 grams adsorbate dosage and 1/100 mL S/L ratios).

© University of Venda

University of Venda
Creating Future Leaders

CHAPTER ONE

Introduction

1.1 Background Information

In South Africa, ESKOM, the main power generating company principally relies on coal combustion for power generation (Petrik et al., 2005). Most prevalently, low grade bituminous coal is combusted for power generation and this type of coal generates huge volumes of waste materials such as bottom ash, fly ash, boiler slag, flue gas desulfurization sludge and non-captured particles (Page et al., 1979; Fytianos and Tsaniklidi, 1998; Petrik et al., 2005; Fatoba, 2008; ESKOM, 2010).

From coal combustion waste, of more concern is fly ash which is mainly collected from coal combustion power plant by means of mechanical devices such as bag house, electrostatic precipitators and scrubbers (Tyler and Miller, 2007; ESKOM, 2001; Gitari et al., 2010). After collection, fly ash is hydraulically transported to holding ponds, lagoons, landfills and slag heaps where it can be reacquired for treatment purposes or discarded. The transportation water is recollected as penstock overflow and recirculated for more ash slurry (Petrik et al., 2005; Gitari et al, 2006; Ramasubramania, 2002).

Approximately thirty seven million tons of fly ash (FA) are produced annually in South African power utilities (Petrik et al., 2005). Of this, only 5% of annual production is utilized beneficially for construction and agricultural purposes, treatment of waste water and formation of synthetic adsorbent such as zeolite (Fatoba, 2008; Petrik et al., 2005; Gitari et al., 2006). The remainder is discarded to surface impoundments such as ash retention dams where it continues to evolve chemically with environmental problems (Gitari et al., 2009).

Coal fly ash is dominated by a heterogeneous mixture of inorganic elements which are incorporated in coal during the coalification stages since they were associated with organic matrix (Fatoba, 2008). On ash disposal, the inorganic toxic pollutants such as anions (Cl^-, SO_4^{2-}), oxyanions of As, B, Cr, Mo, and Se and cations (Al, Ba, Ca, Cd, Cu, Fe, K, Mg, Na, Sr and Zn)

© University of Venda

are dispersed into different environmental compartments through leaching from ash retention ponds by the waste water originating from the ash slurry or by subsequent infiltration by rain upon disposal (Adriano et al., 1980; Eary et al., 1990; Mattigod et al., 1990; Reardon et al., 1995; Ramasubramania, 2002; Nameni et al., 2008; Gitari et al., 2010). Several studies have shown the mechanisms which dictate migration of leachates from fly ash to surface and subsurface water bodies through leaching (Wasay, 1992; Querol et al., 2001; Nugteren et al., 2001; Binay et al., 2009). When coal fly ash species leach-out to the surface and underground water resources, they change the chemical profile of water bodies hence causing hazardous effects to organisms in those water ecosystems (Gitari et al., 2009; Iziquiezdo et al., 2011).

Elements such as Arsenic, Boron, Chromium, Molybdenum and Selenium are toxic species of prime environmental concern (Adriano et al., 1980; Carson and Adriano, 1993; Abbott et al., 2001; Spears and Lee, 2004; Jankowski et al., 2006; Gitari et al., 2009) which are more likely to persist in fresh water bodies for a longer period of time without being transformed into stable compounds because they are adsorbed to positively charged sediments (Langmuir, 1997). As a result, fly ash leachates end up deteriorating the water quality hence making it unsuitable for numerous defined uses (DWAF, 1996).

Numerous techniques have been developed to eradicate and manage the problem of coal fly ash leachates. These include using fly ash for other beneficial uses such as construction purposes (ESKOM, 2010), agricultural soil amendment (Fatoba, 2008), synthesis of adsorbent such as zeolite (Petrik et al., 2005), synthesis of cement, amelioration of acid mine drainage (Gitari et al., 2006), carbon sequestration (Muriithi et al., 2011), and making of bricks (Ahmaruzzaman, 2010).

Several membrane (filtration, Reverse Osmosis, etc.) and non-membrane (Precipitation, adsorption, etc.) methods for waste water treatment have been developed to treat contaminated water bodies but the cost factor limit their implementation (Jiuhui, 2008; Sanjay et al., 2009). As a result, there is a constant search for a low cost technology that can remove coal fly ash leachates prior to fresh water contamination (Baba et al., 2008; Jiuhui, 2008). This study, therefore, aims to develop a low cost technology that uses Al^{3+}/Fe^{3+} modified Bentonite clay for removing the oxyanions from coal fly ash leachates.

© University of Venda

1.2 Problem Statement

When coal fly ash gets into contact with aqueous media, it leaches out toxic chemical species such as anions (Cl^-, SO_4^{2-}), oxyanions of As, B, Cr, Mo, and Se and cations (Al, Ba, Ca, Cd, Cu, Fe, K, Mg, Na, Sr and Zn) into the water bodies (Adriano et al., 1980; Eary et al., 1990; Mattigod et al., 1990; Reardon et al., 1995; Ramasubramania, 2002; Nameni et al., 2008; Gitari et al., 2010). This alters the chemical profile of surface and underground water resources and its suitability for other defined uses (Petrik et al., 2005; DWAF, 1996; Gitari, 2006). Trace metals availability in the environment is problematic, though present as a relatively small fraction in fly ash, are of special interest, due to their cumulative build up, long life and high toxicity to man, plants, and animals through air, water and soil intake (Fytianos and Tsaniklidi, 1998). Of more concern are oxyanions As, B, Cr, Mo, and Se which persist in fresh water for a long period of time without being transformed to stable species but rather get adsorbed to sediments (DWAF, 1996). The presence of these metals in aquatic environments has been known to cause severe health problems to living organisms including humans (Wasay, 1992, Jankowski et al., 2006).

1.3 Main Objective

The main objective of this study is to evaluate the application of Al^{3+}/Fe^{3+} modified bentonite clay for adsorption of oxyanions of As, B, Cr, Mo and Se from coal fly ash leachates.

1.4 Specific Objectives

- To assess the feasibility of modifying South African bentonite clay by introducing Al^{3+}/Fe^{3+} into the lattice.
- To evaluate the physicochemical properties of raw and modified bentonite i.e. Cation Exchange Capacity (CEC), surface area, point of zero charge (PZC), water holding capacity, Elemental composition, and Mineralogical composition of bentonite clay.
- To evaluate the adsorption capacities of modified and unmodified bentonite clay for the oxyanions As, B, Cr, Mo and Se from fly ash leachates.

© University of Venda

- To determine the adsorption mechanism of modified bentonite clay for the oxyanions in fly ash (FA) leachates.
- To assess the efficiency of modified Bentonite clay for oxyanions adsorption by comparing the concentration of the oxyanions in the product leachates to DWAF water quality guidelines.

1.5 Research Questions

- What is the feasibility of modifying South African bentonite clay by introducing Al^{3+}/Fe^{3+} into the lattice?
- What are the physicochemical properties of raw and modified bentonite i.e. Cation Exchange Capacity (CEC), surface area, point of zero charge (PZC), water holding capacity, Elemental composition, and Mineralogical composition of bentonite clay?
- What are the adsorption capacities of modified bentonite clay for the oxyanions As, B, Cr, Mo and Se from fly ash leachates?
- What are the adsorption mechanisms of modified and unmodified bentonite clay for the oxyanions in fly ash (FA) leachates?
- What is the efficiency of modified Bentonite clay for oxyanions adsorption in coal fly ash leachates as compared to DWAF water quality guidelines?

1.6 Hypothesis

The Al^{3+}/Fe^{3+} modified Bentonite clay can remove oxyanions As, B, Cr, Mo and Se from coal fly ash leachates.

1.7 Research Rationale

Water contamination by coal fly ash leachates is an ever more pronounced issue and has raised public concern globally. As such, there is a constant search for a wastewater decontamination technology that is effective and affordable. This study aims to develop a clay based low cost

© University of Venda

adsorbent for removing oxyanions As, B, Cr, Mo and Se from coal fly ash leachates. Several studies revealed that oxyanions have a strong affinity for electro positive materials and they can be easily adsorbed to positively charged clay materials such as bentonite (DWAF, 1996; Besq et al., 2003; Sanjay et al., 2009; Joubert, 2003). Bentonite is an aluminium phyllosilicate smectite clay material with high adsorption capacity and high cation exchange capacity (George, 1998). To further enhance its adsorption capacity, Bentonite can be modified with electro positive ions such as Al^{3+} and Fe^{3+}. The main reason for modifying bentonite clay with Al^{3+}/Fe^{3+} is because these elements are stable in aqueous media and they have been shown to have a strong affinity for oxyanions (DWAF, 1996; Zhang et al., 2003).

1.8 Assumption

It is assumed that the samples of fly ash used in this study will be representative of coal fly ashes generated in South Africa coal fueled power stations.

1.9 Structure of subsequent chapters

This research work presented an introduction section in chapter 1 giving a brief discussion on background information, the problem statement, main objective, specific objectives, hypothesis, research rationale and the assumptions. The literature review is presented in chapter 2. The other chapters are presented as follows:

Chapter 3: Materials and methods used in this study

Chapter 4: Modification and physiochemical characterization of raw and modified bentonite clay

Chapter 5: Adsorption of oxyanions of As, B, Cr, Mo and Se on Al^{3+} modified bentonite clay

Chapter 6: Adsorption of oxyanions of As, B, Cr, Mo and Se on Fe^{3+} modified bentonite clay

Chapter 7: Conclusions and Recommendations

© University of Venda

CHAPTER TWO

Literature review

This chapter presents a concise review of the literature relating to the generation of coal fly ash, elemental composition of coal fly ash, beneficiation of coal fly ash and its environmental implications. It also reviews various literatures on the physiochemical properties of bentonite clay and its application in wastewater decontamination together with the adsorption mechanisms involved during water purification processes.

2.1 Introduction

Coal is a black hard sedimentary rock which is formed from the decomposition of dead organic matter such as terrestrial plants which were buried beneath soil over 300-400 million years ago, under anaerobic and waterlogged conditions (Tyler and Miller, 2007). Coal is by far the most abundant energy source that is mostly burnt to generate electricity in many parts of the world (IEA, 2010). Primarily, it is dominated by carbon as a major element but it also contains small fractions of sulfur, nitrogen and other minerals which were incorporated in coal during coalification or carbonification stages. Sulphur and nitrogen oxides are released into the atmosphere as sulfur dioxide and nitrogen oxides during coal combustion. The carbon content in coal determines the value and ranking of coal (Boggs, 1995; Prothero, 1996; Petrik et al., 2005; IEA, 2010).

Over 5990 million tons (Mt) of hard coal are currently produced worldwide and about 913 Mt is brown coal (lignite) (IEA, 2010). The largest coal producing countries are not confined to one region of the world even though coal is said to be the most abundant resource in numerous parts of the world. The top six hard coal producers are China, USA, India, Australia, Indonesia and South Africa. Nevertheless, much of the global coal produced is used in the respective countries for production of electricity and only about 16% of the hard coal produced is exported to other countries (IEA, 2010).

© University of Venda

2.2 Coal and Power Generation Worldwide and in South Africa

Modern life depends upon electricity to cater for a variety of human activities such as lighting the houses, buildings, streets, providing domestic and industrial heat, and powering most equipment used in homes, offices and machinery in factories. Improving access to electricity worldwide is crucial to the alleviation of poverty (IEA, 2010). Coal plays a pivotal role in electricity generation worldwide and is currently fueling approximately 41% of global electricity demand amongst other power sources such as solar, nuclear, wind, geothermal and biomass fuel (Manaham, 1984; IEA, 2010). In some countries, coal fuels a higher percentage of electricity and the trends of coal to power generation worldwide are set to continue, with coal estimated to fuel an average of 44% of global electricity demand in 2030 (Barker, 1999; IEA, 2010).

2.3 Coal Combustion Processes

In power stations, large volumes of powdered coal are burned at a very high temperature in the combustion chamber to produce steam that propels the turbines to generate electricity (Fig 2.1) (ESKOM, 2010, IEA, 2010). Nevertheless, In South Africa, ESKOM's coal-fired power stations were noted to consume approximately 109 million tonnes of coal per annum, producing 25 million tonnes of ash, to supply the bulk of South Africa's electricity (Petrik et al., 2005, Gitari, 2006; Fatoba, 2008, ESKOM, 2010). In addition, the modern South African coal fired power station with a total output of 3600 MW consumes close to 50 000 tonnes of coal and produces close to 17 000 tonnes of ash residues per day (ESKOM, 2010). The coal demand trend in South Africa is prospected to increase in the upcoming years due to the exploding population growth which is leading to an increased energy demand in order to suit people's needs. As such, it can be stated that plenty of combustion by-products are going to be produced in large quantities (Willis, 1999; Petrik et al., 2005).

© University of Venda

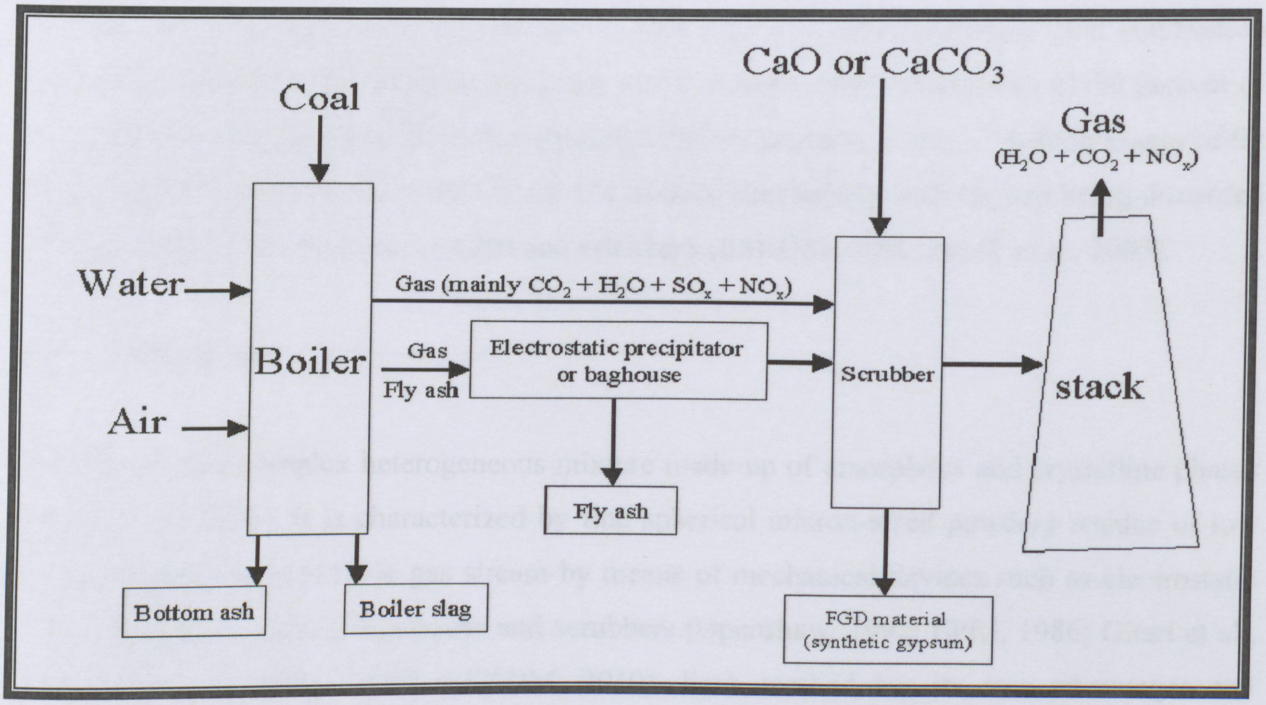


Figure 2.1: Schematic illustration of coal combustion process in coal fired power stations (Gitari et al., 2006).

2.4 By Products of Coal Combustion

The combustion of coal in power stations produces huge volumes of waste materials which include fly ash, bottom ash, flue gas desulfurization waste, fluidized bed combustion waste and un-captured particles (Adriano et al., 1980; Page et al., 1979; Petrik et al., 2005; Carlson and Adriano, 1993). Bottom ash and boiler slag settle to the bottom of the combustion chamber in the ash hopper and they consist of coarse particle sizes of approximately 19-75 mm in size. Low density particles called fly ash which are transported from the boilers by the flue gas streams and captured by means of electrostatic precipitators or scrubber and stored in the ash retention pond. Another by-product of coal combustion is the flue gas desulfurization (FGD) products which consists mainly of calcium sulfate ($CaSO_4$) or gypsum ($CaSO_4.2H_2O$). Flue Gas Desulphurization (FGD) products result from a chemical process which removal of gaseous sulfur dioxide from boiler exhausts gas. Primary types of FGD processes are wet scrubbers, dry scrubbers, and sorbent injection. Sorbents include lime, limestone, sodium based compounds,

© University of Venda

and high-calcium coal fly ash (Gitari et al., 2006; NRDC, 2007). Amongst coal combustion residues, fly ash is by far the most abundant waste material which constitutes 85-90 percent of coal combustion by products (Ramasubramania, 2002). Generally, about 37 million tonnes of fly ash is generated annually and only 5% of it is utilized beneficially with the rest being discarded off in holding ponds, lagoons, landfills and ash heaps (ESKOM, 2001; Petrik et al., 2005).

2.5 Coal fly ash

Coal fly ash is a complex heterogeneous mixture made-up of amorphous and crystalline phases (Petrik et al., 2005). It is characterized by fine spherical micron-sized powdery residue of low density trapped from the flue gas stream by means of mechanical devices such as electrostatic precipitator, fabric filters, bag house and scrubbers (Openshaw, 1992; EPRI, 1986; Gitari et al., 2006, Tyler and Miller, 2007, ESKOM, 2010). Each method has its own advantages and disadvantages, but aside from some gradation differences, the fly ash is not affected by the collection device (Openshaw, 1992). It is considered the most abundant, non-volatile, incombustible and thermally altered inorganic mineral matter derived from coal combustion (Scheetz and Earl, 1998). Its physicochemical properties depends on the chemical composition of parent coal materials, degree of coal preparation, cleaning and pulverization: design, type and operation of the power plant boiler unit; conditions during combustion; additives used to assist combustion; efficiency of the burner, efficiency of emission control devices; storage and handling of the by-products; and the prevailing climate (Adriano et al., 1980; EPRI, 1992; Openshaw, 1992; Fatoba, 2008; Petrik et al., 2005).

2.5.1 Physical properties of fly ash

2.5.1.1 Particle size

Fly ash is a light grey powder made-up of glass like spheres and very fine particles ranging from 0.01 to 100μm in diameter. It is spherically or irregularly shaped (Adriano et al., 1980). The glassy and transparency nature of the particles evolve from the melting of silica containing minerals and these play a significant role in determining the shape of fly ash (Petrik et al., 2005).

© University of Venda

2.5.1.2 Colour

The availability of iron rich materials determines the color of the fly ash. Mainly, it ranges from light red to dark red. The carbon contents also give fly ash the blackness or grayish colour. When the carbon is not completely combusted the fly ash will attain a darker colour but if it is combusted completely it will be lighter in colour (Openshaw, 1992; Young, 1993; Fatoba, 2008; Adriano et al., 1980, Gitari et al., 2006).

2.5.1.3 Particle shape

The fineness of the fly ash particles is determined by the pulverized coal size that is introduced into the burner and the combustion temperature whereas the regularity of particle size (spherical or irregular) is determined by the solidifying and rapidness of cooling of the molten materials. Fly ash also contains hallow spherical particles such as cenospheres and plerospheres particles which are filled with smaller amorphous particles and crystals (Mattigod et al., 1990; Openshaw, 1992; Campbell, 1999; Petrik et al., 2005). Moreover, particles morphology is significant because it reveals the physical properties and leaching behavior of the fly ash (Fisher et al., 1978)

2.5.1.4 Surface area

The smoothness and hydrophilicity of coal fly ash is determined by the presence of calcium oxide and surface area (Campbell, 1999; Iyer, 2002). As a result, coal fly ash dissolves faster in a solution leaving higher concentration of smooth glassy material in the residue (Gitari et al., 2009). Fly ash contains high specific surface area and varying ranges of particle size distribution and this dictates the reactivity of fly ash with the aqueous media (Mishra et al., 2010). The smaller particles of coal fly ash present high specific surface area and that enhances the probability of volatile matters to condense on the coal fly ash surface after combustion. The larger surface area is more susceptible to hydrolysis hence enhancing the leachability of coal fly ash leachates (Gitari et al., 2009).

© University of Venda

2.5.2 Chemical properties of fly ash

Depending on chemical composition of parent coal materials, degree of coal preparation, cleaning and pulverization: design, type and operation of the power plant boiler unit; conditions during combustion, additives used to assist combustion, efficiency of the burner, efficiency of emission control devices, storage and handling of the by-products, and the prevailing climate the composition of coal fly ash tends to vary widely (Adriano et al., 1980; EPRI, 1986; Openshaw, 1992; Zipper et al., 2002; Fatoba, 2008; Petrik et al., 2005). According to Gitari et al (2006), Coal fly ash is a ferro-alumino silicate material dominated by Al, Si, Fe, Ca, K, S, Mg and Na oxides in concentration higher than those found in the parent coal along with carbon, nitrogen and various trace elements which includes As, B, Be, Cd, Co, Cr, Cu, Ga, La, Mn, Hg, Ni, Pb, Sc, Ag, Tn, Sr, V, Y, Zn and Zr (Table 2.1) (Smith et al., 1980; Young, 1993; Ramasubramania, 2002; Zipper et al., 2002; Petrik et al., 2005; Gitari et al., 2006; Mahlaba et al., 2011; Kearsley et al., 2011; Koukouzas et al., 2011).

The aforementioned trace elements are partitioned on fly ash because they are more volatile and fly ash remains in the burner for a shorter period of time during combustion so they are released altogether with fly ash. On cooling those elements form spherical amorphous particles or coat the ash particles during condensation (Kutchko and Kim, 2006; Natush et al., 1975, Ramasubramania, 2002). Some elements occur in higher concentrations than the ones found in soil for example, Al, Ca and Fe occurs in concentrations which are similar to the ones that are found in soils. Na is available in concentrations generally exceeding the ones found in soils. The S content of fly ash is greater relative to soil and it plays a significant role in maintaining the pH of fly ash leachates which normally ranges from 4.5 to 12 (Mattigod et al., 1980; Murarka et al., 1991).

Trace elements (As, B, Pb, Ni, Se, Sr, V and Zn) occur in higher concentrations in fly ash relative to coal and soil (parent materials). The mineralogical composition of fly ash is determined by the parent coal material because each coal has varying mineralogical composition. The combustion temperature affects the degree of volatilization of some minerals (Gitari et al., 2006). Moreover, there is a relationship between particle size and element composition of coal

© University of Venda

fly ash (Ramasubramania, 2002). Petrik et al. (2005); Davidson et al. (1974) reported that there is an increase in elemental composition with a decrease in particle size for the following elements: As, Cd, Cu, Ga, Mo, Pb, S, Sb, Ti and Zn, these elements tend to be present as sulphide minerals or associated with organic fractions, and they are more volatile during combustion and tend to become enriched in particle size surfaces than silicate and oxides. But the non-volatile matter (Al, Fe, Si, Mn, Mg, Ba, Ca, Ti, Co, Ce, Eu, Hf, La, Rb, Sc, Sr, Ta, and Th) elements shows little partitioning by particle size. There are elements such as Na, K, Be, Cr, Ni, Sc, U, and V which show intermediate partition behavior (Adriano et al., 1980). Their concentration gradient is caused by the volatilization of element on combustion followed by their consecutive condensation on fly ash spherules. The most volatile element condenses the last on small particles. When elements are partitioned on small particles in higher concentration, the easier it takes to be leached when they are in contact with the aqueous media (Adriano et al., 1980; Eary et al., 1990; Petrik et al., 2005; Fatoba, 2008). EL-Mogazi et al. (1988) tabulated the average concentration of trace elements in fly ash (Table 2.1)

Table 2.1: Average traces element composition in fly ash (EL-Mogazi et al., 1988; Young, 1993)

Element	Concentrations (mg/g)	Element	Concentrations (mg/g)
As	2.3-312	Pb	31-241
B	10-600	Mo	6.6-41
Cd	0.2-3.9	Ni	1.8-15
Cu	45-259	Se	1.2-17
Cr	43-259	Zn	15-406

Gitari et al. (2006) showed the variation in the chemical composition of fly ash in South African power station (Table 2.2). The authors also observed that the variation in chemical composition of fly ash may be used to show the difference in the parent coal composition from which fly ash originated.

© University of Venda

Table 2.2: Major chemical composition of selected SA fly ash on %W/W (Gitari et al., 2008)

Element	Arnot	Matla	Secunda	Tutuka
SiO_2	534	538	500.6	561.3
TiO_2	13.4	14.4	16.3	16.1
AlO_3	234	262	257.1	243
FeO_3	47.2	34	27.3	47.2
MnO	0.6	0.5	0.5	0.4
MgO	26.7	24.8	24.6	19.3
CaO	84.3	85	86.7	64.4
Na_2O	3.5	4.9	2	-
K_2O	4.9	8.6	7.5	8.3
P_2O_3	3.4	6	6.2	3.1
Cr_2O_3	0.3	0.3	0.4	0.5

2.5.2.1 pH

Basically, pH refers to the measure of the acidity and alkalinity balance of water solution or soil (Mulder and Cresser, 1994; Alloways, 1995). It is dependent on the power of hydrogen or the measure of hydrogen ions (H^+) in solution or hydroxyl ions (OH^-) (Langmuir, 1997). According to Sparks (1997), pH is the principal variable which regulates ion exchange, dissolution/ precipitation, redox reactions, sorption and complexation reactions. Depending on the nature and type of coal being combusted, coal fly ash tends to vary in pH. However, coal fly ash can either be acidic or alkaline (Openshaw, 1992; Moitsheki et al., 2010). The pH of the solution also promotes the reusability of coal fly ash for other purposes (Fisher et al., 1978; Adriano et al., 1980; EL-Mogazi, 1988). Studies by Peffer (1982); Mattigod et al. (1990) and Manz (1999) reported that coal fly ashes from western regions are highly acidic due to the presence of S at high concentrations and CaO and MgO at low concentrations whereas Gitari et al. (2009) reported that South African coal fly ashes are highly alkaline due to the presence of CaO and MgO at very high concentrations. The mechanical collector also plays a crucial role in influencing the pH of the ash because they capture nitrogen and sulphur through a bag house, flue gas desulphurization and electrostatic precipitator (Carlson and Adriano, 1993). South

© University of Venda

African fly ashes are generally alkaline because they contain basic oxides such as CaO and MgO (Gitari et al., 2009).

2.6 Classification of fly ash

As aforementioned, the chemical properties of coal largely depend on the chemical content of the type of coal been burned (i.e. Peat, lignite, bituminous and anthracite) (Adriano et al., 1980). Based on chemical content, coal fly ash is classified into two classes by the American society for testing and material, namely class C and class F (ASTM, C618, 1993). They categorize them by checking the content of alumina, silica, and ferric oxides in fly ash (Table 2.4). If the sum of silica + aluminium + iron oxides is greater than 50% fly ash is classified as class C and when the sum of silica + aluminium + iron oxides is above 70% the fly ash is classified as class F. Class C fly ash is derived from the burning of young coals such as semi-bituminous and lignite coals and class F is derived from the burning of old coals such as bituminous and anthracites coals, in addition, both classes of coal fly ash have pozzolanic properties (ASTM, C618, 1993; Manz, 1999; ACCA, 2008). Class C fly ash contains self-cementing properties due to high content of calcium oxides whereas class F fly ash contains no cementing properties but can react with calcium hydroxide (CaOH), calcium sulphate ($CaSO_4$), and glass components in the presence of water to form cementing properties (Table 2.3) (Collins, 1988; Adriano et al., 1980; Openshaw, 1992; Petrik et al., 2005; Sheetz and Earl, 1998; NRDC, 2007). However, the specification was unable to categorize some types of coal fly ash since they have dualistic properties. In the light of the above, Canada attempted to simplify the classification process and develop Can A23.5-M86 (Table 2.4), which is very similar to C618, and though it classifies fly ash based on CaO content. If fly ash has < 8% of CaO content it is classified as class F and if fly ash has > 8% of CaO it is classified as class C (Manz, 1999). Based on literature, South African fly ash can be classified within class C coal fly ash (Willis, 1987; Gitari et al., 2006).

© University of Venda

Table 2.3: ASTM standard classification of fly ash (ASTM C 618, 1993)

Mineralogy	Class F	Class C
$SiO_2+Al_2O_3+Fe_2O_3$, min %	70	50
SO_3, max %	5	5
Moisture content, max %	3	3
LOI, max %	6	6
Available alkalis, max %	1.5	1.5

Table 2.4: New Canada specification of coal fly ash

Type	CaO
F	< 8
CI	8-20
CH	> 20

2.7 Beneficial applications of coal fly ash

Disposal problems associated with coal fly ash resulted in a lot of research studies which were attempting to establish possible ways in which coal fly ash can be beneficially utilized (Hodgson and Holiday, 1966; Zouboulis and Tszimou-Tsitouridou, 1990; Petrik et al., 2003; Gitari et al., 2009).Due to numerous concerns which have been raised to come up with alternatives to minimize environmental impacts associated with coal fly ash, to minimize the disposal costs of coal fly ash, to create less area which is reserved for disposal, thus, enabling others to sustainably use the virgin land and decrease disposal permits requirements, and to acquire some financial return from the sale of the waste product and replace the use of some scarce natural resources (Ahmaruzzaman, 2010). To date, Europe has been documented to be roughly reusing forty to fifty percent of their coal fly ash (Adriano et al., 1980), Japan has been reported to be reusing sixty percent (Wong and Wong, 1989), United States has been using approximately twenty to thirty percent (Chang et al., 1977; Theis and Gardner, 1990; Sandhu and Mills, 1991) and South Africa has been reported to be benefiting only five percent from their coal fly ash residues

(Petrik et al., 2005). Although many fly ash reutilization projects have been performed with positive results, most are still perceived as experimental primarily due to the environmental implications. A thorough knowledge of the physical characteristics, chemical composition, and properties is essential to understanding any possible environmental impacts (Jones, 1995). Variation in chemical and mineralogical compositions of fly ash altogether with particle size distribution and shape enhances the suitability of fly ash for a variety of uses (Fatoba, 2008; Hareeparsad et al., 2011).

2.7.1 CO_2 sequestration

CO_2 has been identified as one of the major greenhouse gas which enormously contributes to the process of global warming (Tyler and Miller, 2007). Muriithi et al. (2011) pointed out that the fly ash slurry has a strong affinity for atmospheric CO_2. In their study Muriithi et al. (2011) noted that CO_2 will react with CaO in fly ash/brine matrices hence leading to the formation of a mineral carbonate as illustrated in the equation below (eq 1) Since SA fly ash is enriched with high content of CaO. This will significantly minimize possible environmental impacts associated with CO_2 emission, brine and fly ash disposal since 1 ton of fly ash can store 799 kg of CO_2 and the formed carbonate can be used for mine backfilling and acidic water neutralization.

$$CO_{2(aq)} + CaO_{(S)} \rightarrow CaCO_{3(S)} \quad \text{(1)}$$

2.7.2 Agriculture

Coal fly ash is characterized by silt sized particles which are enriched by high concentration of major and trace elements which are crucial for plants to grow (Yanusa et al., 2006). Moreover, plants are also enriched with basic metals which are essential for neutralizing soil which is acidic (Martens et al., 1970; Taylor et al., 1988; Mittra et al., 2003; Thukre et al., 2010). Amelioration of agricultural soil by adding a certain ratio of coal fly ash to poor quality soils in agricultural fields will improve drainage and water-retention properties and the ability of the soil to sustain and maintain vegetative growth (Chang et al., 1977; Mittra et al., 2003). Fly ash also contains a wide range of essential trace elements such as iron, manganese, molybdenum, boron, copper and zinc that growing plants require the most in order to flourish. As such, mixing fly ash with poor

© University of Venda

quality soil enriches those nutrients to the soil hence making them available to be assimilated by plants (Adriano et al., 1980; Cheremisinoff, 1988).

2.7.3 Acid mine drainage treatment

South African coal fly ash is rich in CaO and MgO which are very crucial in neutralizing acidic water hence reclaiming it to a potable standard (Petrik et al., 2005). Gitari et al. (2006), reported that coal fly ash has the capacity to remove major inorganic contaminants from acid mine drainage to produce neutral and alkaline process waters. The efficiency of elements removal was directly linked to the amount of fly ash in the reaction mixture and to the final pH attained. Most elements were found to attain approximately 100 % removal only when the pH of minimum solubility of their hydroxides was achieved.

2.7.4 Waste treatment and stabilization

The Pozzolanic fly ashes with Portland cement and other cementation agents have been used successfully for stabilizing biological industrial sludge and liquid wastes from wastewater treatment. It can be mixed with solid sewage to synthesize fertilizers that can be used for soil supplement and replace the common fertilizers that are used to improve soil quality (NDEQ, 2004). The chemical stabilization provided by the cementing and pozzolanic reactions serves to reduce the leachability of the toxic substances within the waste, and results in the drying and thickening of the wastes to improve their handling and compaction characteristics. Metal-bearing wastes are particularly amenable to this type of stabilization and reduce the risk of surface and underground water contaminations (NDEQ, 2004; Kumpiene et al., 2006; ACAA, 2008).

2.7.5 Cement and concrete

The physicochemical properties of fly ash make it well-suited for use in cement and concrete productions. The variation in particle size distribution of fly ash is similar to that of Portland cement. When fly ash is used as a partial replacement for Portland cement in a concrete mixture, the fly ash spheres act as ball bearings within the concrete mix that can significantly lower the water requirements and improve the flow ability and workability of the concrete (Manz, 1999).

© University of Venda

South African low grade bituminous coals tend to have significantly higher amounts of Aluminium, Silicon, Iron and calcium oxides and it is categorized under class C (Gitari et al., 2006). Coal fly ash C contains self-cementing properties and they are pozzolanic due to higher concentrations of CaO (ASTM C618, 1993). South African coal Fly ash can be added to replace 50 % of Portland cement additives. The replacement of Portland cement additive by fly ash eliminates the potential environmental problems which are associated with fly ash disposal since the production of one ton of Portland cement produces close to one tone of CO_2 to the atmosphere as compared to CO_2 free fly ash (ASTM C618, 1993).

2.7.6 Construction

Outstanding physicochemical properties of coal fly ash have resulted in it being beneficially utilized in construction purposes. Addition of fly ash to soil can potentially improve the shear strength of soil and controls its swelling properties. The clay sized particles and pozzolan properties of fly ash also makes it best suitable for road embankment, brick making, mineral fillers, geo-polymers, roller compacted concrete, mine reclamation and flowable fill (Cheremisinoff, 1988; Collins, 1988; NDEQ, 2004; Fatoba, 2008).

2.8 Leaching properties of coal fly ash

Fly ash disposal on land creates potential problems of pollution to surface and underground water resources (Skodras et al., 2009; Jones, 1995; Dutta et al., 2009). During rainfalls water percolates through disposed coal fly ash hence leaching out wide range of toxic species to water bodies (Roy and Graffins, 1984; Cunningham, 1990; Wasay, 1992). This causes serious health problems to aqueous inhabitants and terrestrial organisms and ultimately disturbs the ecological and environmental balance (Wagner and Hlatshwayo, 2005).

Leaching kinetics and elemental speciation of coal fly ash leachates principally depend on several parameters such as mineralogical composition of coal fly ash, morphology of coal fly ash particles, contact time, redox reactions, temperature and the pH of leachant (Krebs et al., 1988; Ramasubramania, 2002; Pahara et al., 2002; Gitari et al, 2009). Recent research study by Gitari et al. (2009) indicated that major leaching processes entails neutralization and chemical

© University of Venda

weathering. However, a number of research investigations have been used to predict quantitative estimate on leaching and release of toxic elements from coal fly ash (Nugteren et al., 2001; Querol et al., 2001). The physicochemical characterization of coal fly ash leachates tend to vary significantly depending on the nature and characteristics of coal fly ash being leached (El-mogazi, 1988). Coal fly ash particles are essentially insoluble glasses (Openshaw, 1992). However, the enriched surface elements are soluble (Roy et al., 1981). The composition of any leachate depends on the solubility of trace metals and other components. As noted previously, sorption and solubility of most heavy metals (as cations) is low in basic environments (Spencer and Drake, 1987; Gitari et al., 2009). This can be attributed to metals precipitating or adsorbing onto hydrous iron, aluminum and manganese oxides (Golden, 1983; Openshaw, 1992). Theis and Gardner (1990) concluded that pH values below 7 favors the solubility of trace cations and pH values above 7 favored trace anions (As, B, Cr, Mo, Se).

Due to the presence of CaO and MgO in higher concentration in South African coal fly ash, it tends to release leachates which are alkaline in nature hence favoring mobility and speciation of oxyanions (Gitari et al., 2009; Iziquierol et al., 2011). In addition, the rate at which minor elements are leached from coal fly ash is also dictated by the abundance, surface morphology, accessibility and dissolution kinetics of the primary solids containing the trace elements (Eary et al., 1990). pH value, contact time and volume of leachant in contact with aqueous media plays a significant role in the leaching of coal fly ash as it accounts for the rate at which those species are released from coal fly ash (Steenari et al., 1999). To date, several leaching standard procedures have been developed to simulate factors which dictate mobility and speciation of trace species from coal fly ash in the ambient environment (Kim, 2002, Fatoba, 2008; Singh et al., 2007; Gitari et al., 2009; Hyks et al., 2009). The Toxicity Characteristic Leaching Procedure (TCLP), the Extraction Procedure Toxicity Test (EPTOX), the Synthetic Precipitation Leaching Procedure (SPLP), the Standard Test Method for Shake Extraction of Solid Waste with Water (ASTM-D3987), and the California Waste Extraction Test (WET) (Kim, 2002, Singh et al.,2007).

© University of Venda

University of Venda
Creating Future Leaders

2.8.1 Factors which dictate leaching of coal fly ash

2.8.1.1 Effects of pH on leaching of coal fly ash

pH plays a pivotal role in the leaching of trace elements from coal fly ash because it influences the rate of dissolution and leaching of species from coal fly ash (Gitari et al., 2009). Furr et al. (1978) reported that the pH of coal fly ash leachates is determined by the elemental composition of fly ash. Gitari et al., (2009) pointed out that South African coal fly ashes are highly alkaline due to the availability of basic oxides such as CaO and MgO hence favoring the mobility of oxyanions since they are more mobile at circumneutral to alkaline pH conditions. This has consistently collaborated results of the same rank obtained by Van der Hoek et al., 1994; Wagner and Hlatshwayo, 2005; and Iziquierol et al., 2011

The leaching of As and Se from a coal fly ash was studied by Van der Hoek et al. (1994). The authors showed that the leaching of those elements is more dependent on pH and their solubility is optimum at alkaline pH. Gitari et al. (2009) evaluated the effects of pH on the release of major and trace elements from coal fly ash and he demonstrated that many oxyanions such as Cr, Mo, As, and Se are highly soluble and mobile in alkaline conditions, except for B which is soluble in both acidic and alkaline conditions.

Ramasubramania, (2002) pointed out that the alkalinity and acidity controls the extractability of elements like As, B, Be, Cd, Cr, Cu, F, Mo, Se, V and Zn from coal fly ash. He also revealed that the aqueous extracts of an acidic fly ash contains high concentrations of Cd, Co, Cu, Mn, Ni, Zn, As, B, Be, Cd, F, Mo, Se and V. Nevertheless, some studies have reported that the extractability of trace elements increases with a decrease in pH and decrease with an increase in pH except for oxyanions (Wasay, 1992; Querol et al., 2001).

2.8.1.2 Effects of particle size on leaching of coal fly ash

Partitioning of trace elements within fly ash mainly depends on the combustion process because at high temperature, the inorganic minerals melt and becomes fluid or volatile or react with oxygen, and on cooling, they form crystalline solids, spherical amorphous particles or condenses

UNIVERSITY OF VENDA
LIBRARY

© University of Venda

as coating on the particles (Fatoba, 2008; Petrik et al., 2005; Adriano et al., 1980; Kutchko and Kim, 2006; Gitari et al., 2010). The fly ash particles contain a certain amount of leachable materials partitioned in varying proportion. The leachable elements are partitioned into two groups on the basis of their concentration depending upon particle size, (1) those with no enrichment in the smallest particle size and these include Mg, Na, K, Mo, Ce, Rb, Cs and Nb and they appear to have a smaller fraction volatilized during coal combustion or have significant variations in behavior between plants. Here the volatility is directly proportional to particle size (2) those which are enriched, they include elements such as Mn, Ba, V, Co, Cr, Ni, Ln, Ga, Nd, As, Sb, Sn, Br, Zn, Se, Pb, Hg and S which are usually volatile to a significant extent in the combustion process. The volatility for these elements is inversely proportional to the particle size. (Ahmaruzzaman, 2010; Gitari et al., 2009; Fatoba, 2008; Petrik et al., 2005; Ramasubramania, 2002; Adriano et al., 1980). Elements such as Si, As, Fe, Ca, Sr, La, Sm, Eu, Tb, Py, Yb, Y, Se, Zr, Ta, Na, Th, Ag and Zn show intermediate partition, they either are not volatilized or show minor trends which is related to the geochemistry of the mineral matter (Petrik et al, 2005; Fatoba et al., 2008; Gitari et al., 2009; Ramasubramania, 2002). Gitari et al (2009) noted that the smaller the particle size the larger the specific surface area, which is susceptible to hydrolysis.

Particles size plays an important role in the leaching of fly ash. It was shown that small particle sized flay ash is more susceptible to hydrolysis and is largely enriched with trace elements. This indicates that elements can be easily leached out of smaller particle size compared to a larger particle size. As such, it can be concluded that leaching of toxic metal species does not rely on pH only but it can also rely on fly ash particle size (Alloways, 1995).

2.8.1.3 Effect of redox reaction on leaching of coal fly ash

Redox reaction (reduction-oxidation reaction) is a chemical reaction in which both oxidation and reduction takes place. Oxidation is a process in which oxygen is gained, or hydrogen is lost; or, more generally, electrons are lost. Reduction is the opposite process, oxygen is lost, or hydrogen is gained; or, more generally, electrons are gained (Langmuir, 1997). Redox reactions are dependent on pH (Langmuir, 1997). Moreover, oxyanions are more sensitive to redox reactions

© University of Venda

and they tend to exist in numerous forms within an aqueous solution. As illustrated by the table below (Table 2.5) the most common forms of As are arsenate (pentavalent) which are present in coal fly ash leachates in the form of AsO_4^{3-}. B is prevalently present in coal fly ash in a trivalent form. Cr can exist as chromate (CrO_4^{2-}) or in a reduced form as $Cr(OH)_4^-$, which is usually considered more soluble, mobile, and bio-available than the sparingly soluble chromite (Cr(III)), which is normally present in soil as the precipitate $Cr(OH)_3$ (Langmuir, 1997). Mo exists in hexavalent form (MoO_4^{2-}). Similarly, Se can be present as selenates (SeO_4^{2-}) or in a reduced form recognized as selenites (SeO_3^{2-}). Just like As, the chemistry of Se is similar to Phosphate (Alloways, 1995).

When coal fly ash is exposed to aqueous media through rainfall, species enriched to coal fly ash particles tend to be transformed to a stable and non-toxic form whereas some are transformed to an unstable hazardous nature. In order to understand the most probable set of dissolution and redox reactions that can affect the concentrations of the trace elements in coal fly ash leachates, thermodynamic models and geochemical mechanisms can be applied to elucidate the relationship between solubility and elemental speciation (Eary et al., 1990). The redox reaction affects solubility hence controlling precipitates that can be formed and the sorption possibilities of the elements that can occur (Gitari et al., 2006). Oxyanions are highly soluble in alkaline aqueous media, therefore, it is of great interest to understand their geochemical mechanisms that dictates their leaching behavior, in particular, As, B, Cr, Mo and Se (Jones, 1995; Heebink and Hussett, 2001; Geert et al., 2008).

Table 2.5: Oxyanions of As, B, Cr, Mo and Se at varying pH conditions (Alloways, 1995; Gupta, 1997; Geert et al., 2008)

Element	Acidic condition < 3	Circum-neutral (5-8)	Alkaline > 9
As	$H_3AsO_3^-$	$H_2AsO_4^{2-}$	AsO_4^{2-}
B	$B(OH)^-_4$	$B(OH)_4^{2-}$	$B(OH)_4^{2-}$
Cr	$HCrO_2^{3+}$	CrO_4^{2-}	$Cr_2O_7^{2-}$
Mo	MoO^{2-}_4	MoO^{2-}_4	MoO^{2-}_4
Se	$HSeO_3$	$HSeO_3^-$	SeO_3^{2-}

© University of Venda

2.9 Toxic species of concern to the environment

Coal fly ash contains a total of 47 trace and rare elements (Alper et al., 2010). In their study, Alper et al. (2010), evaluated the availability of As, B, Ba, Be, Cd, Cu, Co, F, Hg, Mo, Ni, Pb, Sb, Se, Sn, Th, Tl, V, U and Zn in fly ash. Among these elements; As, Be, Cd, Cr, Co, Hg, Mn, Ni, Pb, Sb, Se, and radionuclide (e.g., Th and U) were also identified as being potentially hazardous air pollutants (HAPs) (U.S Environmental protection agency, 2007). In fly ash, of more concern are oxyanions As, Cr, B, Mo, and Se which are more toxic and they can persist in fresh water bodies for a prolonged period of time (DWAF, 1996; Gitari et al, 2006).

Different lists of potentially toxic elements have been compiled. Wagner and Hlatshwayo, (2005) listed As, B, Cd, Hg, Mo, Pb and Se, as elements of greatest environmental concern, Cr and Ni of moderate concern, and Li and Sb of minor environmental concern. The US national committee for geochemistry listed As, B, Cd, Hg, Pb, Mo, and Se as trace elements of major environmental concern, and Cr, Cu, F, Ni, V, and Zn of moderate concern (Nugteren et al., 2001). The Canadian Environmental Protection Agency listed As, Cd, Hg, Ni, and Pb as major toxic elements of environmental concern. Goodarzi et al. (2002), listed As, Cd, Cr, Cu, Hg, Mo, Pb, Se, V, and, Zn as elements of prime public and environmental concern. Based on the elements enumerated above, this study will particularly focus on oxyanions As, B, Cr, Mo, and Se which when leached from coal fly ash to leaching agent (water) poses hazardous effects to living organisms that consumes contaminated water. Manoharan et al. (2007) undertook a greenhouse study in an attempt to elucidate the elemental uptake by flora conola (*Brassica napus*) on acidic soil amended by unweathered fly ash. In their study, they found out that trace elements As, B, Cd, Cr, Mo, Ni and Se are required by plants in trace amounts but become toxic to the fauna and flora when they are available in excessive amounts. In pot experiments, Furr et al. (1978) observed elevated concentrations of B, Mo and Se in edible parts of beans, cabbage, millet and carrots and it has been revealed that oxyanions have the potential to bioaccumulate and biomagnify in living organisms. Though several technologies have been developed to minimize the environmental impacts of fly ash leachates, its impacts in the environment are proclaimed to be having detrimental impacts to living organisms (Vinso et al., 2011).

© University of Venda

Numerous studies have reported that coal fly ash leachates are characterized by varying ranges of oxyanions, In particular, Arsenic, Boron, Chromium, Molybdenum and Selenium (Gitari et al., 2009). Their average concentration in coal fly ash leachates are shown in Table 2.6.

Table 2.6: Concentration of As, B, Cr, Mo and Se in coal fly ash leachates (Booth et al., 2009; Huggins, 2002; Choi et al., 2002; Sear et al., 2003)

Element	Concentration (mg/L)
As	< 1
B	< 0.1 to 6
Cr	< 0.1
Mo	< 0.1 to 0.6
Se	< 0.01 to 0.15

2.10 Potential Effects of oxyanions (As, B, Cr, Mo and Se) to living organisms

In the past few decades, growing interest in the leaching behavior, speciation and environmental contamination by oxyanions As, B, Cr, Mo and Se have raised public concern globally (Singh et al., 2007; Geert et al., 2008). During rainfall, elements in coal fly ash particles are leached to surface and underground water ecosystems (Geert et al., 2008). When those elements are leached to the nearby water ecosystems they can pass through cell walls along differential permeable membranes and commonly interfere with the whole functioning of the body of the living organism hence affecting its health and wellbeing (Van den Berg et al., 2001; Gottlieb et al., 2010). Below is the possible impact that exposure to individual oxyanions cause.

2.10.1 Arsenic

In most coal seams, As is primarily associated with As-bearing pyrite rocks (Alloways, 1995). During the coal combustion process As is thermally decomposed and gives rise to a dominant surface association in the coal combustion residues (ashes). Arsenic condenses on the surface of coal fly ash particles as sparingly soluble arsenate species (Goodarzi et al., 2008). Leaching of

© University of Venda

As is highly dependent on pH of the solution (Iziquierol et al., 2011). When exposed to aqueous media it is more likely to be transformed to a variety of As species which can pose threats to human health and aquatic organisms. Human exposure to Arsenic through consumption of contaminated water can produce a variety of adverse health effects and ingesting a very high concentration can result in death. Chronic exposure to Arsenic through drinking Arsenic contaminated water can cause several cancers, such as skin cancer, bladder cancer, lung cancer, and kidney cancer. Recent studies have linked ingestion of high levels of As, primarily from drinking water to cardiovascular diseases, diabetes mellitus and neurological effects. Exposure to lower levels of As can cause nausea and vomiting, decreased production of red and white blood cells, and cardiovascular effects include abnormal heart beat rhythm, damage to blood vessels and damage to the peripheral nervous system (Wagner and Hlathwayo, 2005; NRDC, 2007; Gottlieb et al., 2010).

2.10.2 Boron

In coal fly ash B is organically associated with coal fractions during coalification stages (Reash et al., 2006). Such affinity enhances the volatility of B during coal combustion and the subsequent condensation of soluble admixed borate salts onto coal fly ash surfaces (Iziquierol et al., 2011). Reash et al. (2006) elucidated that the silicious materials lock B up during coal combustion. Exposure to B through drinking contaminated water can result in the damage of the testes, intestine, liver, kidney, and brain. Exposure to large volumes of B over a short period of time can eventually lead to death. When exposure to small amounts of B takes place irritation of nose, throats and eyes may occur (Reash et al., 2006; NRDC, 2007; Gottlieb et al., 2010).

2.10.3 Chromium

Chromium prevalently occurs in most bituminous coals as trichromate species in association with organic matrices during carbonation (Alloway, 1995; Goodarzi et al., 2008; Iziquierdo et al., 2011). In coal fly ash leachate chromium exists in different forms i.e. chromium (III) and Chromium (IV). Chromium (III) is an essential nutrient for plants and human. Chromium (IV) is highly toxic and if it happens that it is ingested through drinking contaminated water, it can

© University of Venda

cause stomach and small intestine ulcer. Frequent ingestion can cause anemia and stomach cancer (Reash et al., 2006; NRDC, 2007; Gottlieb et al., 2010).

2.10.4 Molybdenum

Mo is also linked with carboniferous material during the diagnosis of coal and is essentially concentrated on the surface of fly ash particles after coal combustion processes (Querol et al., 2001; Izquierdo et al., 2011). Spears and Martinez-Tarrazona (1996) estimated that the surface association can be close to 80% of Mo for UK coal fly ash. Mo in this mode of occurrence is three times more soluble than that associated with the magnetic fraction of fly ash (Iziquierol et al., 2011). Consumption of water rich in Mo can result in diarrhea, slowed growth, low birth weight and infertility, and can affect the lungs, liver and kidneys (Gupta, 1997).

2.10.5 Selenium

Occurrence of Se in coal fly ash leachates was due to the fact that it was affinitized with organic fraction during coal digenesis (Yudovich and Ketris, 2006; Izquierdo et al., 2011). Se can occur as sorbed selenate in oxidized coals (Yudovich and Ketris, 2006) and also be bonded to Fe oxides (Riley et al., 2007). Whether it occurs in pyrite or organically associated coal, such weak bonding allows Se to be easily released and almost completely volatilized during combustion. Irrespective of its mode of occurrence in the coal matrix, Se might react with Ca and form stable compounds such as $CaSeO_3$ condensing on the surface of ash particles (Querol et al., 2001). As by a number of laboratory studies, Se accumulation can cause developmental abnormalities in fish and amphibians and has led to the death of entire local fish population. Se is biomagnative, meaning that it passed up the food chain in increasing concentrations, and excessive amounts has been found in water snakes, small mammals, birds and humans (Alloways, 1995).

2.11 Clay materials and their applications in environmental remediation

Clays are fine grained and hydrous aluminosilicates materials which are mainly composed of colloid fractions of soils, sediments, rocks and water bodies (Hill and Paolo, 1997; Bhattacharyya and Gupta, 2008). They are the products of rock weathering and they play an

© University of Venda

exceptional role in determining the physical and chemical properties of soil (Alloways, 1995; Sparks, 1997). The clay fractions contain less than 2 μm diameter particle size (Bohn et al., 1979; Evangelou, 1998). They are also referred to as inorganic materials with sheet like structures of phylosilicates (Bradly and Weils, 2004; Sparks, 1997). The clay minerals are characterized by a two dimensional array of tetrahedral sheets of T_2O_5 composition, usually it is polycations of Al^{3+} or Si^{4+} sandwiched to pentagon oxygen, the octahedral sheet which is mainly characterized of Al^{3+}, Fe^{3+}, Fe^{2+}, or Mg^{2+} coordinated with oxygen or the hydroxyl anions (Bradly and Weils, 2004; Sparks, 1997; Langmuir, 1997). The tetrahedral and octahedral sheets are bonded together by oxygen (Alloways, 1995). Depending on charge valences, if trivalent species such as Al occupies the site arrangement it is called dioctahedral and if the octahedral sheet is dominated by divalent such as Mg, it is classified as trioctahedral (Bohn, 1979; Alloways, 1995). Depending on charge density and valency, species in octahedral sheet or tetrahedral sheet may replace each other through isomorphous substitution (Sparks, 1997). They are the most abundant and widely spread natural resources that are readily available on the earth surface. Depending on the nature and composition of clay materials, there are different types of clays and these include Smectite, Vermiculite, Kiolinite, Sepiolite, Chlorites, and Mica. Due to the negatively charged end of clay fraction, high surface area, and swelling properties clay minerals have the ability to scavenging positively charged species through adsorption and ion exchange (Katsumata et al., 2003; Bradly and weils, 2004). Subsequently, clays can adsorb anions to clay interlayers since they have high cation exchange capacity (Bradly and Weils, 2004). Clays containing Montmorillonite as the main mineral are referred to as bentonite clays and they are categorized within the Smectite family (Robertson, 1986; Christidis, 1998). A number of research studies have recommended bentonite clay as having good physico-chemical properties that result in it being an excellent adsorbent (Tahir and Naseem, 2007; Manohar et al, 2006; Ramesh et al., 2007; Grygar et al., 2007; Lian et al., 2009; Kamble et al., 2009; Sarkar et al., 2010; Su et al., 2011; Silva et al., 2011; Latif et al., 2012; Nassef and Eltaweel, 2012)

2.12 Bentonite clay

The term bentonite is ambiguous. As defined by geologists, it is referred to a crystalline silicate clay rock formed of highly colloidal and plastic clays largely dominated by Montmorillonite, a

© University of Venda

clay mineral of the smectite family (Alloways 1995; Langmuir, 1997; WHO, 2005).The formation of bentonite predominantly takes place in aqueous environmental conditions during or after deposition (Langmuir, 1997; WHO, 2005). In addition to Montmorillonite as the main mineral, bentonite may also contain feldspar, biotite, kaolinite, illite, cristobalite, pyroxene, zircon, and crystalline quartz moreover; this may also depend on the physiochemical properties of the parent weathered material being weathered (Sparks, 1997). Depending on the dominant element, bentonite clay can be classified into K, Na, Ca, Al and Fe bentonite (Lagaly, 1995, Spark, 1997). The chemical properties of bentonite can be modified by introducing a high ionic stable and higher density species to bentonite clay interlayer through a process known as ion exchange and sorption (Manohar et al., 2006; Ramesh et al., 2007; Grygar et al., 2007; Krishna et al., 2008).

2.13 Physicochemical properties of bentonite clay

2.13.1 Physical properties of bentonite clay

Bentonite is white to pale green or blue and, with exposure, darkens in time to yellow, red, or brown (Besq et al., 2003). It feels greasy and soap-like when touched (WHO, 2005). It contains flat and thin sheet crystal morphology which is irregularly shaped and can be up to 1,000μm in dimension. It has a large surface area of about 800m^2/gram and it significantly contributes to its high cation exchange capacity (Agnello, 2004). Nevertheless, bentonite has a high water holding capacity which enables it to swell 30 times its original size hence allowing it to retain water within its matrices for a long period of time thus promoting higher chemical reactivity between soil solution and bentonite clay (Bradly and Weil, 2004). This good physical property of clay enables it to scavenge polar pollutants and firmly hold them on clay fractions through weak Vander Waal forces or chemical bondings (Bohn et al., 1979; Bhattacharyya and Gupta, 2008).

2.13.2 Chemical properties of bentonite clay

Bentonite clay is mainly dominated by montmorillonite as the principal element. Montmorillonite is a very soft phyllosilicate group of minerals that typically forms in microscopic crystals. It is derived from volcanic glass, mica, feldspar, various FeMg silicates or

© University of Venda

precipitate directly from solution (Besq et al., 2003). Bentonite clay may also contain feldspar, biotite, kaolinite, illite, cristobalite, pyroxene, zircon, and crystalline quartz as impurities depending on the weathered parent materials (WHO, 2005). The basic crystal structure of smectite clay (bentonite) is an octahedral alumina sheet sandwiched to two tetrahedral silica sheets as shown (Figure 2.2), hence the name 2:1. As such, they are classified within the family of expansible 2:1 phyllosilicate clays having permanent charges that can undergo cation and anion exchange (Brady and Weil, 2004). Atoms in these sheets common to both layers are oxygen. These three-layer units are stacked one above another with oxygen in neighboring layers adjacent to each other (Alloways, 1995; Brady and Weil, 2004). This produces a weak bond, allowing water and other polar molecules to enter between layers and induce an expansion of the mineral structure (swelling). In the tetrahedral coordination, silicon may be substituted by aluminium or iron, in the octahedral coordination, aluminium may be substituted by magnesium, iron, lithium, chromium, zinc, or nickel by the process known as isomorphous substitution (Sparks, 1997; Langmuir, 1997; Brady and Weil, 2004). Differences in the substitutions within the lattice in terms of position and elemental composition give rise to the various montmorillonite clay minerals. The molecular formula for montmorillonite is usually expressed as:

$(M^{+}_{x} \cdot nH_2O)\ (Al_{2-y}Mg_x)Si_4O_{10}(OH)_2$, where $M^{+} = Na^{+}$, K^{+}, Mg^{2+}, or Ca^{2+} (exchangeable base cations) Ideally, x = 0.33 (Brindley and Brown, 1980; WHO, 2005).

© University of Venda

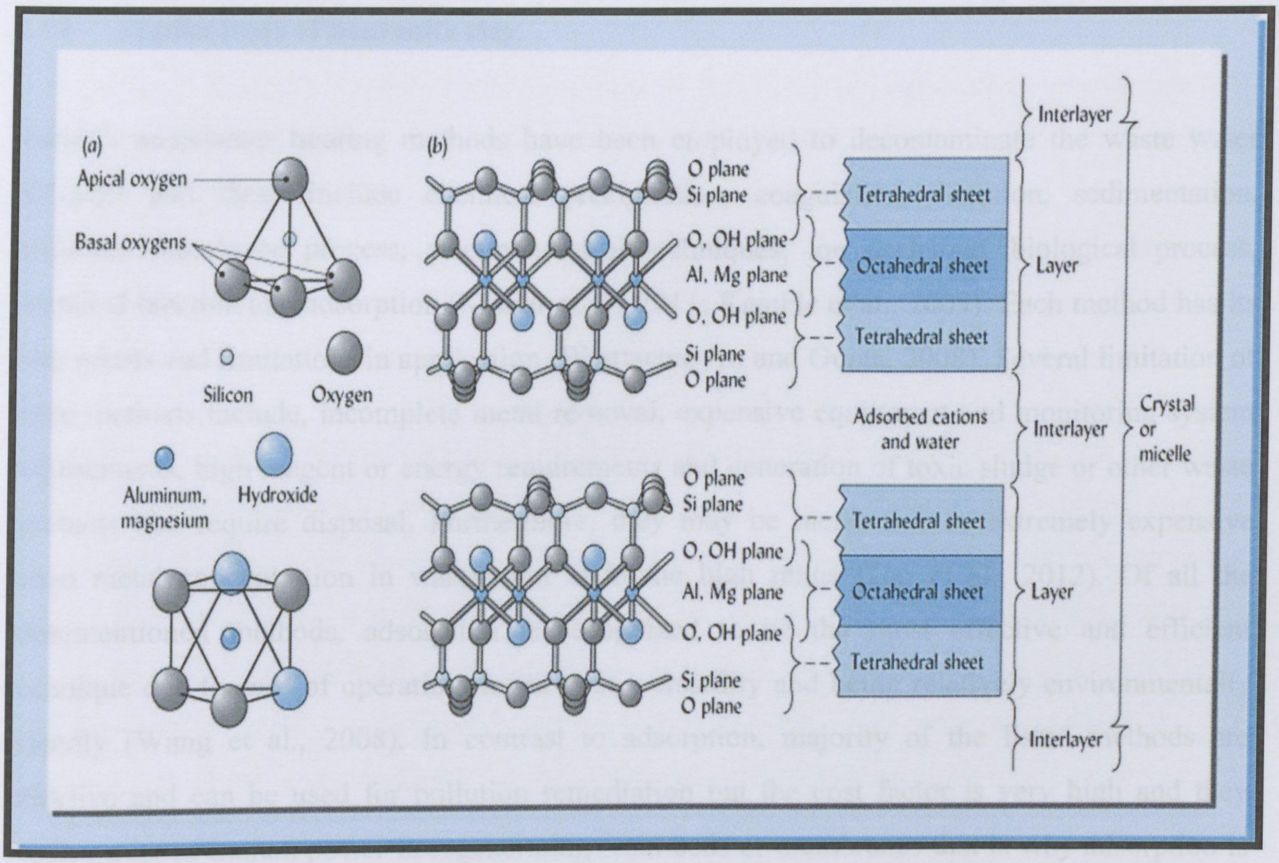


Figure 2.2: Structure of bentonite clay (Bradley and Weils, 2004)

Due to magnificent physicochemical properties bentonite clay is valued for versatile uses, sorption properties, catalytic action, bonding power, plasticity, high swelling and water holding capacity, high surface area and ion interchange capacity (CEC and AEC) (Kamble et al., 2009). The addition of water to the bentonite causes the platy particles of the clay to partly swell (Langmuir, 1997; Brady and Weil, 2004). The plates of this clay have negative charges on the edges which attract positively charged species on the surface using the electrostatic forces or weak Van der Waal forces. Bentonite clay can attract and hold a large number of water molecules, because the charges on the internal and external colloid surfaces attract the oppositely charged end of the polar water molecule (Bohn et al., 1979; Sparks, 1997). Water adsorbed between the crystal layers can cause the layer to move apart, making the clay more plastic and swell (Brady and Weil, 2004). The water in bentonite clay is driven off when clay is heated in air, and this then leads to the platy layers collapsing, hence causing the clay to have an undefined structure with an overall slightly negative charge (Brady and Weil, 2004).

© University of Venda

2.14 Applications of bentonite clay

Various wastewater treating methods have been employed to decontaminate the waste water effluents and these include chemical precipitation, coagulation, flotation, sedimentation, filtration, membrane process, electrochemical techniques, ion exchange, biological process, chemical reaction and adsorption (Kumar et al., 2011; Kamble et al., 2009). Each method has its own merits and limitations in application (Bhattacharyya and Gupta, 2008). Several limitation of these methods include, incomplete metal removal, expensive equipment and monitoring system requirements, high reagent or energy requirements and generation of toxic sludge or other waste products that require disposal. Furthermore, they may be ineffective or extremely expensive when metal concentration in wastewater is in the high range (Dar et al., 2012). Of all the aforementioned methods, adsorption is recognized to be the most effective and efficient technique due to ease of operation, lower cost, versatility and being relatively environmentally friendly (Wang et al., 2008). In contrast to adsorption, majority of the listed methods are effective and can be used for pollution remediation but the cost factor is very high and they require a lot of human power in regenerating resin beds or membranes that is why adsorption is the best (Petrik et al., 2005; Wang et al., 2008; Bhatnagar et al., 2011; Dilip et al., 2010). Also, the shortcomings of most of these methods including high operational and maintenance costs, secondary pollution (generation of toxic sludge, etc.) and complicated procedure involved in the treatment and adsorption (Petrik et al., 2005). Activated carbon, zeolite, saw dust, biomass and cellulose, peat, chitin, chitosan, orange waste, rice husk and wheat bran are some of the adsorbent with good adsorption characteristics (Petrik et al., 2005; Wang et al., 2008; Bhatnagar et al., 2011). Activated carbon is regarded the best adsorbent (Dilip et al., 2010; Silva et al., 2011). Due to the high cost, most of these substances have limited commercial applications (Rahardjo et al., 2011). In addition to cost, adsorptive properties and availability are other factors to look at for an adsorbent to be considered suitable for water decontamination (Dilip et al., 2010; Silva et al., 2011).

In the light of the above, the discovery of inexpensive, abundantly and readily available materials in nature as alternative adsorbents collectively offers the adsorption method a very attractive and excellent environmental remediation progress. In recent decades, different types of natural and

© University of Venda

readily available clay materials which can be used as low cost adsorbent for polluted water have been reported (Kim and Keane, 2002; Bhatnagar et al., 2011). To date, bentonite clay has been reported to be the only low cost material that is widely used in numerous fields of material science technology and the utilization of this clay material for treatment of wastewater containing hazardous substances has received great attention (Bhatnagar et al., 2011). Moreover, bentonite clay can also be modified by other exogenous species in an attempt to enhance its adsorption capacities (Ramesh et al., 2007; Grygar et al., 2007; Kamble et al., 2009)

Sepiolite and Al-pillared bentonite clay has been employed and examined for the removal of Co (II) from polluted water (Manohar et al., 2006; Kara et al., 2003). Natural and modified kaolinite and montmorillonite have also been noted as effective adsorbents for heavy metals such as As, Cd, Cr, Co, Cu, Fe, Pb, Mn, Ni, and Zn (Bhattacharyya and Gupta, 2008). Haghseresht et al (2009) examined the efficiency of lanthanum modified bentonite clay for the removal of phosphate from waste water through chemisorption process. The authors observed that the phosphate anion has a great affinity for the adsorbent surface and adsorption was more likely to be affected by high pH. (Guo et al., 2009) evaluated the efficiency of $CaCl_2$ modified bentonite clay for the removal of Congo red dye from aqueous solutions. Results of the study showed that 0.1 g of $CaCl_2$ modified bentonite clay (BCa^{2+}) could remove 95 % of the dye from 100 ml of 100 mg/l of Congo red solution.

Karthikeya et al. (2005) evaluated the removal of fluoride from aqueous media using montmorillonite clay. In that study, the uptake of fluoride from fluoride ladened water was highly dependent on pH and the obtained results revealed that the maximum uptake was at pH 2. This collaborates a study conducted by Kamble et al. (2009) which also evaluated the efficiency of bentonite clay modified with positively charged species such as Lanthanium, Magnesium and Manganese for the defluoridation of water. The authors observed that the uptake of fluoride from aqueous media was very high in acidic conditions as compared to alkaline conditions.

Dilip et al. (2010) undertook an intensive study which attempted to demonstrate the feasibility of modifying bentonite clay by incorporating magnesium into the bentonite clay lattice for deflouridation of drinking water. The authors observed that the magnesium modified bentonite clay had maximum fluoride adsorption capacity of 2.26 mg/g at an initial fluoride concentration

© University of Venda

of 5.52 mg/l. Dilip et al. (2010) observed that this pH was too low and less feasible to maintain during water defluoridation in the ideal environment and they aimed to maintain a pH 6-7 for their defluoridation work. Their study successfully achieved a low fluoride concentration of 1.5 mg/l as stipulated by WHO at neutral pH.

In Australia, Haghseresht et al. (2009) undertook an investigation to evaluate the ability of Lanthanum modified bentonite clay for the removal of phosphate from waste water. The study used the low cost and readily available clay material modified with Lanthanum. They observed that Lanthanum modified bentonite clay can remove close to 98 % of phosphate from waste water.

2.16 DWAF water quality guidelines for oxyanions concentration in water bodies

In South Africa, several regulations have been developed and implemented to assess, monitor and manage the suitability of water for different defined water uses. These regulations serve to ensure that water quality is within the prescribed range that is safe for drinking and other domestic uses. They also define the suitability of water resources for different water sectors. The department of water affairs and forestry (DWAF) is the main custodian which ensures that the water quality is within the required standards in South Africa. It is also stringent in assuring that prescribed water quality regulations are accordingly enforced and abided to. As such, DWAF has stipulated a certain range of chemical status for surface and underground water resources. Those ranges attempt to clarify whether water is fit for a recognized water use in various water user sectors i.e. domestic water use, recreational water use, industrial water use, and agricultural water use. This study will principally focus in the concentration of oxyanions As, B, Cr, Mo, and Se in water bodies for domestic use and agricultural irrigation (DWAF, 1996)

UNIVERSITY OF VENDA
LIBRARY

© University of Venda

Table 2.7: Guideline safe concentration of oxyanions as prescribed by DWAF (DWAF, 1996; DWAF, 2002)

Species	Domestic	Agricultural
As	0-0.01 mg/L	0-0.1 mg/L
B	Not specified	0-0.5 mg/L
Cr	0.05 mg/L	0-0.01 mg/L
Mo	Not specified	0-0.01 mg/L
Se	0-0.02 mg/L	0-0.02 mg/L

2.17 Conclusion

In this review, it was observed that environmental implications of coal fly ash due to improper and poor disposal practice have numerous environmental impacts that degrade the suitability of the environment to foster life. It was also noted that coal fly ash leaches toxic species to surface and underground water resources. Those species have been reported to potentially impair human health on exposure. As such, there is a need to come up with a low cost and effective decontamination technology which can be used as a permeable reactive barrier to capture pollutants prior to surface and underground water contamination. Clays has been documented to be low cost, effective, and readily available materials with good adsorption features. Due to its versatility, high surface area, Swelling capacities and high cation exchange capacity bentonite clay has received great attention in recent decades, particularly, in environmental remediation. This study will therefore, attempt to evaluate the adsorption efficiencies of modified bentonite clay for anionic species of As, B, Cr, Mo and Se generated in disposed coal fly ash leachates.

© University of Venda

CHAPTER THREE

Materials and methods

3.0 Introduction

This chapter seeks to present various methods and materials applied for data generation, analysis and interpretation.

3.1 Sampling

Bentonite clay was collected from ECCA pty (Ltd) in Cape Town, South Africa and coal fly ash was collected from Tutuka, ESKOM power plant in Mpumalanga, South Africa. All reagents used in this study were of analytical grade.

3.2 Determination of pH, Electrical conductivity (EC), temperature and total dissolved solids (TDS)

The pH, EC, TDS and Temperature were determined using CRISON MM40 portable multimeter probe. The multimeter probe was calibrated before use with the buffer solutions at pH 4 and 7 respectively. The probe was also rinsed with deionized water before and after each calibration and measurement. EC and TDS were calibrated before use and regularly during use with NIST standards at 1430 µS/cm.

3.3 Preparations of Bentonite clay samples

The required grams of raw bentonite samples were putted into beaker and washed by soaking in ultra-pure water (Millipore, USA) to a level of 1cm. The washed bentonite was then dried in Rotech model 50 oven for 24 hours at a temperature of 105°C. The dried samples were crushed into fine powders using Rosch miller, model RS 200 at 80 rotary per minutes.

© University of Venda

3.4 Modification of bentonite clay with Al^{3+} and Fe^{3+}

3.4.1 Modification of raw bentonite clay with Al^{3+} species

3.4.1.1 Adsorption of Al^{3+} onto bentonite clay lattice as a function of contact time

In this batch experiment, 1000 ppm stock solution of Al^{3+} was prepared by dissolving 12.35 g of $Al_2(SO_4)_3.18H_2O$ in 0.5 mmol of HCl. The mixture was topped to 1000 mL using ultra-pure water. From the prepared stock solution, 100 mg/L dilution was made by extracting 100 mL of 1000 mg/L Al^{3+} solution and pipetted into 1000 mL volumetric flask. The volumetric flask was topped-up to the mark using ultra-pure water. Thereafter, 9 samples of 100 mL of 100 mg/L Al^{3+} solution were pipetted into 9, 250 mL bottles and 1 g of bentonite clay added. The mixture was then agitated for 0, 1, 5, 10, 15, 30, 60, 180, and 360 minutes at 250 rpm using the Stuart reciprocating shaker. pH, Temp, EC, and TDS was measured by the CRISON multimeter probe (model MM40) before and after agitation. After equilibration, the mixture was filtered through a 0.45 µm pore nitrate cellulose filter membrane and acidified with two drops of concentrated HNO_3 acid to prevent aging and immediate precipitation of Al^{3+} ions. The samples were refrigerated at 4°C until analysis by FAAS (Perkin Elmer 600).

3.4.1.2 Adsorption of Al^{3+} onto bentonite clay as a function of adsorbent dosage

In this batch experiment, 1000 mg/L stock solution of Al^{3+} was prepared by dissolving 12.35 g of $Al_2(SO_4)_3.18H_2O$ in 0.05 mmol of HCl. The mixture was topped-up to 1000 mL using ultra-pure water. From the prepared stock solution, 100 mg/L dilution was made by extracting 100 mL of 1000 mg/L Al^{3+} solution and pipetted into 1000 mL volumetric flask. The volumetric flask was topped-up to the mark using ultra-pure water. Thereafter, 9, 100 mL solutions of 100 mg/L Al^{3+} solution were pipetted into 9, 250 mL bottles and varying mass of bentonite clay was added. The masses of bentonite clay were 0, 0.1, 0.3, 0.5, 1, 2, 3, 4, and 5 grams. The mixtures were agitated for 60 minutes at 250 rpm using the Stuart reciprocating shaker. Measurement of pH, Temp, EC, and TDS were done by CRISON multimeter MM40 probe before and after agitation. After equilibration, the mixtures were filtered through a 0.45 µm pore nitrate cellulose filter membrane and acidified with two drops of concentrated HNO_3 acid to prevent precipitation of Al^{3+} ions. The samples were refrigerated at 4°C until analysis by FAAS (Perkin Elmer 600).

© University of Venda

3.4.1.3 Adsorption of Al^{3+} onto bentonite clay as a function of adsorbate concentration

1000 mg/L stock solution of Al^{3+} was prepared by dissolving 12.35 g of $Al_2(SO_4)_3.18H_2O$ in 0.5 mmol of HCl. The mixture was topped to 1000 mL using ultra-pure water. From the prepared stock solution, a series of 10, 50, 80, 150, 200, 250, 300, 450, and 500 mg/L dilution of Al^{3+} solution was made respectively. Thereafter, 100 ml of each solution were pipetted into 9, 250 mL bottles and 3g of bentonite clay added. The mixture was then agitated for 60 minutes at 250 rpm using the Stuart reciprocating shaker. Measurement of pH, Temp, EC, and TDS was done by CRISON multimeter MM40 probe before and after agitation. After equilibration, the mixtures were filtered through a 0.45 µm pore nitrate cellulose filter membrane and acidified with two drops of concentrated HNO_3 acid to prevent aging and immediate precipitation of Al^{3+} ions. The samples were refrigerated at 4°C until analysis by FAAS (Perkin Elmer 600). The percentage adsorption was calculated by using the following expression.

$$\%\ Removal = \left(\frac{Co-Ce}{Co}\right) \times 100 \quad \text{.....(5)}$$

Where: Co = initial concentration and Ce = equilibrium metal ion concentration respectively.

3.4.1.4 Procedures for impregnating Al^{3+} onto bentonite clay crystal lattice

The optimum conditions for loading Al^{3+} polycations onto bentonite clay lattice were observed to be 60 minutes of contact time, 3 grams of adsorbent dosage and 100 ppm of adsorbate concentration. 10 gram of bentonite clay was transferred to 1000 mL container with 500 mL of 100 ppm Al^{3+}. The mixture was shaked for 60 minutes on a table shaker. Same experiment was repeated for 25 times to make up a total of 250 grams of adsorbent.

© University of Venda

3.4.2 Modification of raw bentonite clay with Fe^{3+} cations

3.4.2.1 Adsorption of Fe^{3+} onto bentonite clay as a function of contact time

In this batch experiment, 1000 mg/L stock solution of Fe^{3+} was prepared by dissolving 3.74g of $Fe_2(SO_4)_3.H_2O$ in 0.5 mmol of HCl. The mixture was topped to 1000 mL using ultra-pure water. From the prepared stock solution, 100 mg/L dilution was made by extracting 100 mL of the Fe^{3+} solution and pipetted into 1000 mL volumetric flask. The volumetric flask was topped-up to the mark using ultra-pure water. Thereafter, 9 samples of 100 ml of 100 mg/L Fe^{3+} solution were pipetted into 9, 250 mL bottles and 1g of bentonite clay added. The mixture was then agitated for 0, 1, 5, 10, 15, 30, 60, 180, and 360 minutes at 250 rpm using the Stuart reciprocating shaker. pH, Temp, EC, and TDS was measured by the CRISON multimeter MM40 before and after agitation. After equilibration, the mixture was filtered through a 0.45 µm pore nitrate cellulose filter membrane and acidified with two drops of concentrated HNO_3 acid to prevent aging and immediate precipitation of Fe^{3+} ions. The samples were refrigerated at 4°C until analysis by FAAS (Perkin Elmer 600).

3.4.2.2 Adsorption of Fe^{3+} onto bentonite clay as a function of adsorbent dosage

In this batch experiment, 1000 mg/L stock solution of Fe^{3+} was prepared by dissolving 3.74g of $Fe_2(SO_4)_3.H_2O$ in 0.5 mmol of HCl. The mixture was topped to 1000 mL using ultra-pure water. From the prepared stock solution, 100 mg/L dilution was made by extracting 100 mL of the Fe^{3+} solution and pipetted into 1000 mL volumetric flask. The volumetric flask was topped-up to the mark using ultra-pure water. Thereafter, 9 samples of 100 ml of the 100 mg/L Fe^{3+} solution were pipetted into 9, 250 mL bottles and 0g, 0.1g, 0.3g, 0.5g, 1g, 2g, 3g, 4g and 5g of bentonite clay were added to each flask. The mixture was then agitated for 15 minutes at 250 rpm using the Stuart reciprocating shaker. Measurement of pH, Temp, EC, and TDS were done by CRISON multimeter port MM40 probe before and after agitation. After equilibration, the mixture was filtered through a 0.45 µm pore nitrate cellulose filter membrane and acidified with two drops of concentrated HNO_3 acid to prevent aging and immediate precipitation of Fe^{3+} ions. The samples were refrigerated at 4°C until analysis by FAAS (Perkin Elmer 600).

© University of Venda

3.4.2.3 Adsorption of Fe^{3+} onto bentonite clay as a function of adsorbate concentration

In this batch experiment, 1000 mg/L stock solution of Fe^{3+} was prepared by dissolving 3.74g of $Fe_2(SO_4)_3.H_2O$ in 0.5 mmol of HCl. The mixture was topped to 1000 mL using ultra-pure water. From the prepared stock solution, 8 samples of 100 ml of 10, 50, 80, 150, 200, 250, 300, 450 and 500 mg/L Fe^{3+} solution were prepared and pipetted into 9, 250ml Erlenmeyer plastic bottles and 1g of bentonite clay added to each. The mixture was then agitated for 15 minutes at 250 rpm using the Stuart reciprocating shaker. Measurement of pH, Temp, EC, and TDS were done by CRISON multimeter MM40 probe before and after agitation. After equilibration, the mixture was filtered through a 0.45 µm pore size nitrate cellulose filter membrane and acidified with two drops of concentrated HNO_3 acid to prevent aging and immediate precipitation of Fe^{3+} ions. The samples were refrigerated at 4°C until analysis by FAAS (Perkin Elmer 600). The percentage of adsorption was calculated by using the following expression.

$$\%\ Removal = \left(\frac{Co-Ce}{Co}\right) \times 100 \quad \text{.....(6)}$$

Where: Co = initial concentration and Ce = equilibrium metal ion concentration respectively

3.4.2.4 Procedures for impregnating Fe^{3+} onto bentonite clay crystal lattice

The optimum conditions for loading Fe^{3+} polycations onto bentonite clay lattice were observed to be 30 minutes of contact time, 2 grams of adsorbent dosage and 100 mg/L of adsorbate concentration. 10 gram of bentonite clay was transferred to 1000 mL container with 500 mL of 100 mg/L Fe^{3+}. The mixture was shaked for 15 minutes on a table shaker. Same experiment was repeated for 25 times to make up a total of 250 grams of adsorbent.

3.5 Physicochemical characterization of bentonite clay and coal fly ash leachates

Analysis of aqueous samples, synthetic and coal fly ash leachates for metal species, measurement of pH, EC, TDS and Temperature were initially performed at University of Venda laboratory using Atomic Adsorption Spectrometer (AAS), Graphite furnace Atomic adsorption spectrometer (FAAS) and CRISON multimeter probe. Further analyses of aqueous and solids

© University of Venda

was undertaken at University of Stellenbosch, University of Pretoria and Cape Town using XRF, XRD, BET and ICP-OES.

3.5.1 Determination of Cation Exchange Capacity (CEC)

The cation exchange capacity of raw and modified bentonite clay was determined using ammonium acetate method according to Chapman (1962).

3.5.1.1 Preparation of ammonium acetate

To prepare 1 M solution of ammonium acetate, 144ml of glacial acetic was added to a 2000ml volumetric flask. This was then diluted with ultrapure water to a volume of 1000ml. 138ml of concentrated ammonium hydroxide was then added. The volumetric flask was then topped with ultrapure water to a volume of 2000ml. A few drops of acetic acid were added until a pH of 7.4 was achieved. Same procedures were repeated to achieve a pH of 5.4.

3.5.1.2 CEC determination

CEC was determined using the ammonium acetate method at pH 5.4 and pH 7.4. Three 0.5 g of bentonite clay was extracted using 25 mL aliquots of 1 M ammonium acetate. The samples were equilibrated for 15 min using a table shaker. After agitation, the samples were centrifuged at 3000 rpm for 15 min. After centrifuging, the supernatant was decanted in a 100 mL bottle. This procedure was repeated for a total of four times for each sample. The cumulative extract was brought to 100 mL. To remove the suspended solids, the cumulative extracts were then filtered through 0.45µm pore cellulose acetate filter membranes. The filtrate was acidified by adding three drops of nitric acid and stored in the refrigerator until analysis by the Atomic Absorption Spectrometer (AAS). The samples were analyzed for the availability of base cations K^+, Na^+, Mg^{2+} and Ca^{2+}.

3.5.2 Determination of elemental composition of modified and raw clays

For determination of elemental composition of raw and modified bentonite clay, the samples were milled in a tungsten-carbide milling pot to achieve particle sizes of <75micron.The samples were then dried at 100°C and roasted at 1000°C to determine Loss On Ignition (LOI).1g sample

© University of Venda

of bentonite clay was mixed with 6g Lithiumteraborate flux and fused at 1050°C to make a stable fused glass bead. For trace element analyses, the sample was mixed with a PVA binder and pressed into a pellet using a 10 ton press. The Thermo Fisher ARL9400 XP+ Sequential XRF with WinXRF software was used for analysis.

3.5.3 Determination of surface area

The surface area and pore size distribution of raw and modified bentonite clay were determined using the Brunnet- Emmett- Teller method of analysis using a Micromeritics Accelerated Surface Area and Porosimetry (ASAP) 2010 system (Brunauer, 1943). Nitrogen adsorption isotherms were obtained at liquid nitrogen temperature. Prior to the determination of the adsorption isotherm, the samples were degassed and approximately 10 grams of raw and modified bentonite clay were subjected to degassing at 120 °C for 24 hours. The degassing process was meant to remove adsorbed gases and moisture. The raw and modified bentonite clay was then placed in a N_2 stream and the mass change of the solid due to gas adsorbed was measured relatively to the change in partial pressure of N_2.

3.5.4 Determination of water holding capacity

Triplicate 10g of bentonite was weighed in a weighing boat and put in a beaker. 100 mL of water was measured using a measuring cylinder. The water was then added into the beaker and left to stand for 24 hours. After 24 hours, the excess water was poured back into the measuring cylinder. The water absorbed by bentonite was calculated using the following formula:

Water Holding Capacity (WHC) = Total volume of water added – excess water (remaining water)

3.5.5 Determination of point of zero charge (PZC)

The surface charge and point of zero charge (PZC_{ZPC}) of raw and Al^{3+}/Fe^{3+} modified bentonite clay were determined using solid addition method as described by Kumar et al. (2011). 40 ml of 0.1 M KCl was transferred to a series of 100 ml bottles. The initial pH ($pH_{initial}$) of the solutions was adjusted between the range of 2.0-12.0 by adding 0.1 M HCl and 0.1 M NaOH solutions. The total volume of the solution in each tube was adjusted exactly to 50 ml by adding 0.1 KCl.

© University of Venda

Further, 0.5 g of Bentonite clay was added to all tubes and the suspensions were then equilibrated for 48 hrs. After completion of equilibration time, the solution was filtered and the final pH values (pH_{final}) of the filtrate were measured again. The difference between initial and final pH (pH_f) values ($\Delta pH = pH_i - pH_f$) was plotted against pH_i. The point of intersection of the resulting curve with abscissa (the co-ordinate that gives the distance along the horizontal axis), at which $\Delta pH=0$, was an indication of the point of zero charge. Same procedures were employed to determined 0.01 M and 0.001 M KCl solution.

3.5.6 Determination of the mineralogical composition of modified and raw bentonite clay

Mineralogical composition of raw and Al^{3+}/Fe^{3+} modified bentonite clay was determined by using a back loading preparation method. They were analyzed using a PANalytical X'Pert Pro powder diffractometer with X'Celerator detector and variable divergence- and receiving slits with Fe filtered Co-Kα radiation. The phases were identified using X'Pert Highscore plus software. The relative phase amounts (weights %) were estimated using the Rietveld method (Autoquan Program). Errors are on the 3 sigma level in the column to the right of the amount. A Venier was used to measure the d spacing of the peaks which were then compared with those in the Hanawalt index.

3.6 Generation of coal fly ash leachates

Coal fly ash leachates was generated by mixing 1 gram of coal fly ash with 100 mL of ultra-pure water at 1/100 S/L ratio (Gitari et al., 2009). The mixture was equilibrated for 60 minutes at 250 rpm on a table shaker. The generated leachates were filtered through 0.45µm cellulose membrane filter and acidified with three drops of nitric acid until analysis by ICP-MS.

© University of Venda

3.7 Removal of As, B, Cr, Mo and Se by raw and Al^{3+} Modified clay

3.7.1 Adsorption of As, B, Cr, Mo and Se onto bentonite clay as a function of contact time

1000 mg/L standard solutions were used to prepare the working solutions. From the stock solution, 10 ppm solution was prepared by extracting 10 mL of synthetic oxyanions and transferred into 1000 mL volumetric flask. The volumetric flask was topped to the mark by adding ultra-pure water. Thereafter, 7 samples of 100 mL of 10 mg/L As, B, Cr, Mo and Se solution was pipetted into 7, 250 mL bottles and 1g of Al^{3+} bentonite clay was added. The mixture was then agitated for 0, 1, 5, 10, 15, 30, and 30 minutes at 250 rpm using the Stuart reciprocating shaker. Measurement of pH, Temp, EC, and TDS was done by CRISON multimeter MM40 probe before and after agitation. After equilibration, the mixtures were filtered through 0.45 µm pore nitrate cellulose filter membrane and acidified with two drops of concentrated HNO_3 acid to prevent aging and immediate precipitation of oxyanions. The samples were refrigerated at 4°C until analysis by ICP-OES.

3.7.2 Adsorption of As, B, Cr, Mo and Se onto bentonite clay as a function of dosage

1000 mg/L standard solutions were used to prepare the working solutions. From the prepared stock solution, 10 mg/L solution was prepared by extracting 10 mL of synthetic oxyanions and transferred into 1000 mL volumetric flask. The volumetric flask was topped to the mark by adding ultra-pure water. Thereafter, 7, 100 mL solutions of 10 mg/L As, B, Cr, Mo and Se solution were pipetted into five, 250 mL bottles and varying masses of bentonite clay were added. The masses of bentonite clay were 0, 0.5, 1, 2, 3, 4, and 5 grams. The mixtures were agitated for 30 minutes at 250 rpm using the Stuart reciprocating shaker. Measurements of pH, Temp, EC, and TDS were done by CRISON multimeter MM40 probe before and after agitation. After equilibration, the mixtures were filtered through a 0.45 µm pore nitrate cellulose filter membrane and acidified with two drops of concentrated HNO_3 acid to prevent aging and immediate precipitation of As, B, Cr, Mo and Se. The samples were refrigerated at 4°C until analysis by ICP-OES.

© University of Venda

3.7.3 Adsorption of As, B, Cr, Mo and Se onto bentonite clay as a function of concentration

1000 mg/L standard solutions of As, B, Cr, Mo and Se was used to prepare 0.5, 1, 3, 5, 10 and 15 mg/L solutions. 0.5 mg/L was prepared by extracting 0.5 mL from the 1000 mg/L standard solution, 1 mg/L was prepared by extracting 1 mL from the standard solution, 3 mg/L was prepared by extracting 3 mL of the standard solution, 5 mg/L was prepared by extracting 5 mL of the prepared solution, 10 mg/L was prepared by extracting 10 mL of the standard solution, and 15 mg/L was prepared by extracting 15 mL of the prepared solution. The mixture was topped to 1000 ml using ultra-pure water. Thereafter, 100 mL of the solution were pipetted into 7, 250 mL bottles and 4 grams of adsorbent added. The mixture was then agitated for 30 minutes at 250 rpm using the Stuart reciprocating shaker. Measurement of pH, Temp, EC, and TDS were determined by CRISON multimeter MM40 probe before and after agitation. After equilibration, the mixtures were filtered through a 0.45 µm pore nitrate cellulose filter membrane and acidified with two drops of concentrated HNO_3 acid to prevent aging and immediate precipitation of As, B, Cr, Mo and Se. The samples were refrigerated at 4°C until analysis by ICP-OES. The percentage adsorption was calculated by using the following expression:

$$\%\ Removal = \left(\frac{Co-Ce}{Co}\right) \times 100 \quad \text{.....(8)}$$

Where: Co = initial concentration and Ce = equilibrium metal ion concentration respectively

3.7.4 Adsorption of As, B, Cr, Mo and Se onto bentonite clay as a function of pH

1000 mg/L standard solutions of As, B, Cr, Mo and Se was used to prepare 10 mg/L adsorbate concentration of each. 10 mg/L was prepared by extracting 10 mL of stock solution and transferred to the volumetric flask. The 1000 mL volumetric flask was topped to the mark using ultra-pure water. Thereafter, 100 mL solution was pipetted into each of the 6, 250mL bottles. The pH of the solution was adjusted to 2, 4, 6, 8, 10 and 12 using 0.1 M of HCl and 0.1 M NaOH. 4 grams of adsorbent dosage was added. The mixture was then agitated for 30 minutes using reciprocating shaker at 250 rpm. Initial and final pH, Temp, EC, and TDS was measured by the CRISON multimeter MM40 probe before and after agitation. After equilibration, the mixtures were filtered through 0.45 µm pore nitrate cellulose filter membrane and acidified with

© University of Venda

two drops of concentrated HNO_3 acid to prevent aging and immediate precipitation of As, B, Cr, Mo and Se ions. The samples were refrigerated at 4°C until analysis by ICP-OES.

3.8 Interaction of coal fly ash leachates with raw and Al^{3+} modified bentonite clay under natural conditions

100 mL of coal fly ash leachates was transferred into 250 mL container and 4 grams of bentonite clay was added. The mixtures were equilibrated for 60 minutes using a reciprocating shaker. After shaking, the mixture was filtered through 0.45 µm cellulose membrane. The filtrate was acidified with three drops of nitric acid and stored in the refrigerator until analysis for As, B, Cr, Mo and Se using ICP-OES.

3.9 Interaction of coal fly ash leachates with raw and Al^{3+} modified bentonite clay under optimized conditions

100 mL of coal fly ash leachates was transferred into 250 mL container and 4 grams of bentonite clay was added. The mixtures were equilibrated for 60 minutes using a reciprocating shaker. After shaking, the mixture was filtered through 0.45 µm cellulose membrane. The filtrate was acidified with three drops of nitric acid and stored in the refrigerator until analysis for As, B, Cr, Mo and Se using ICP-OES.

3.10 Removal of As, B, Cr, Mo and Se onto raw and Fe^{3+} Modified clay

3.10.1 Adsorption of As, B, Cr, Mo and Se onto bentonite clay as a function of contact time

1000 mg/L standard solutions were used to prepare the working solutions. From the stock solution, 10 mg/L solution was prepared by extracting 10 ml of synthetic oxyanions and transferred into 1000 mL volumetric flask. The volumetric flask was topped to the mark by adding ultra-pure water. Thereafter, 7 samples of 100 mL each of 10 mg/L As, B, Cr, Mo and Se solution was pipetted into 7, 250 mL bottles and 1g of Fe^{3+} bentonite clay added. The mixture was then agitated for 0, 1, 5, 10, 15, 30, and 60 minutes at 250 rpm using the Stuart reciprocating shaker. Measurement of pH, Temp, EC, and TDS were done by CRISON multimeter MM40 probe before and after agitation. After equilibration, the mixture was filtered through 0.45 µm pore nitrate cellulose filter membrane and acidified with two drops of concentrated HNO_3 acid to

© University of Venda

prevent aging and immediate precipitation of oxyanions. The samples were refrigerated at 4°C until analysis by ICP-OES.

3.10.2 Adsorption of As, B, Cr, Mo and Se onto bentonite clay as a function of adsorbent dosage

In this batch experiment, 1000 mg/L stock solutions of As, B, Cr, Mo and Se were used to prepare 10 mg/L of the aforementioned species respectively. 10 mg/L dilution was made by extracting 10 mL of As, B, Cr, Mo, and Se solutions and pipetted into 1000 mL volumetric flask. The volumetric flask was topped to the mark using ultra-pure water. Thereafter, 7, 100 mL solution each of 10 mg/L As, B, Cr, Mo and Se solutions were pipetted into 7, 250 mL bottles and varying mass of Fe^{3+} bentonite clay added. The masses of bentonite clay were 0, 0.5, 1, 2, 3, 4, and 5 grams. The mixtures were then agitated for 30 minutes at 250 rpm using the Stuart reciprocating shaker. Measurement of pH, Temp, EC, and TDS were done by CRISON multimeter port MM40 probe before and after agitation. After equilibration, the mixtures were filtered through a 0.45 µm pore nitrate cellulose filter membrane and acidified with two drops of concentrated HNO_3 acid to prevent aging and immediate precipitation of As, B, Cr, Mo and Se. The samples were refrigerated at 4°C until analysis by ICP-OES.

3.10.3 Adsorption of As, B, Cr, Mo and Se onto bentonite clay as a function of adsorbate concentration

1000 mg/L stock solutions of As, B, Cr, Mo and Se was used to prepare 0.5, 1, 3, 5, 10 and 15 ppm solutions. 0.5 mg/L was prepared by extracting 0.5 mL from the 1000 mg/L standard solution, 1 mg/L was prepared by extracting 1 mL from the standard solution, 3 mg/L was prepared by extracting 3 mL of the standard solution, 5 mg/L was prepared by extracting 5 mL of the prepared solution, 10 mg/L was prepared by extracting 10 mL of the standard solution, and 15 mg/L was prepared by extracting 15 mL of the prepared solution. All solutions were pippeted into 1000 mL volumetric flask. The mixture was topped to 1000 mL using ultra-pure water. Thereafter, 100 mL of the solution were pipetted into 7, 250 mL bottles and 4 grams of adsorbent added. The mixture was then agitated for 30 minutes at 250 rpm using the Stuart reciprocating shaker. Measurement of pH, Temp, EC, and TDS were determined by CRISON multimeter

© University of Venda

MM40 probe before and after agitation. After equilibration, the mixtures were filtered through a 0.45 µm pore nitrate cellulose filter membrane and acidified with two drops of concentrated HNO_3 acid to prevent aging and immediate precipitation of As, B, Cr, Mo and Se. The samples were refrigerated at 4°C until analysis by ICP-OES. The percentage adsorption was calculated by using the following expression:

$$\% \, Removal = \left(\frac{Co - Ce}{Co}\right) \times 100 \quad \text{.....(9)}$$

Where: Co = initial concentration and Ce = equilibrium metal ion concentration respectively

3.10.4 Adsorption of As, B, Cr, Mo and Se onto bentonite clay as a function of pH

1000 mg/L standard solutions of As, B, Cr, Mo and Se was used to prepare 10 mg/L adsorbate concentration of each. 10 mg/L was prepared by extracting 10 mL of stock solution and transferred to the volumetric flask. The 1000 mL volumetric flask was topped to the mark using ultra-pure water. Thereafter, 100 mL of each solution was pipetted into 6, 250 mL bottles. The pH of the solution was adjusted to 2, 4, 6, 8, 10 and 12 using 0.1 M of HCl and 0.1 M NaOH. 4 grams of adsorbent dosage was added. The mixture was then agitated for 30 minutes using reciprocating shaker at 250 rpm. Initial and final pH, Temp, EC, and TDS was measured by the CRISON multimeter MM40 probe before and after agitation. After equilibration, the mixtures were filtered through 0.45 µm pore nitrate cellulose filter membrane and acidified with two drops of concentrated HNO_3 acid to prevent aging and immediate precipitation of As, B, Cr, Mo and Se ions. The samples were refrigerated at 4°C until analysis by ICP-OES.

3.11 Interaction of coal fly ash leachates with raw and Fe^{3+} modified bentonite clay under natural conditions

100 mL of coal fly ash leachates was transferred into 250 mL container and 4 grams of bentonite clay was added. The mixtures were equilibrated for 30 minutes using a reciprocating shaker. After shaking, the mixture was filtered through 0.45 µm cellulose membrane. The filtrate was acidified with three drops of nitric acid and stored in the refrigerator until analysis for As, B, Cr, Mo and Se using ICP-OES.

© University of Venda

3.12 Interaction of coal fly ash leachates with raw and Fe^{3+} modified bentonite clay under optimized condition

100 mL of coal fly ash leachates was transferred into 250 mL container and 4 grams of bentonite clay was added. The mixtures were equilibrated for 30 minutes using a reciprocating shaker. After shaking, the mixture was filtered through 0.45 µm cellulose membrane. The filtrate was acidified with three drops of nitric acid and stored in the refrigerator until analysis for As, B, Cr, Mo and Se using ICP-OES. The experiment was done in triplicate

3.13 Calculation of adsorption capacity of the synthesized adsorbent

The amount of As, B, Cr, Mo and Se adsorbed per unit mass of adsorbent (q) was calculated using the following equation:

$$q = \frac{(C_i - C_e)V}{m} \quad \text{.....(10)}$$

Where: C_i = Initial As, B, Cr, Mo and Se concentration (ppm)

C_e = As, B, Cr, Mo and Se concentration at equilibrium (ppm)

V = Volume of As, B, Cr, Mo and Se solution (L)

m = Weight of bentonite clay (adsorbent)

The % metals removal by raw and modified bentonite clay was determined by the following equation:

$$\%\ Removal = \left(\frac{Co - Ce}{Co}\right) \times 100 \quad \text{.....(11)}$$

Where: Co = initial concentration and Ce = equilibrium metal ion concentration respectively

3.14 Equilibrium adsorption models

Adsorption isotherms are models which are used to describe the relation between equilibrium concentration of the adsorptive and the quantity of adsorbate on the surface at constant

© University of Venda

temperature. Mainly, they are employed to describe mechanisms and intensity of adsorption. The two commonly used isotherms are Langmuir and Freundlich adsorption isotherms (Sparks, 1997).

3.14.1 The Langmuir Isotherm

The Langmuir isotherm is valid for monolayer sorption due to a surface with finite number of identical sites (Singh et al., 2010) and it is expressed in the following linear form:

$$\frac{Ce}{Qe} = \frac{1}{Qmb} + \frac{Ce}{Qm} \quad \text{.....(12)}$$

Where, Ce = Equilibrium concentration (mg/L)

Qe = Amount adsorbed at equilibrium (mg/g)

Qm = Langmuir constants related to adsorption capacity

b = Langmuir constants related to energy of adsorption (L/mg)

A plot of Ce/Qe versus Ce should be linear if the data is described by the Langmuir isotherm. The value of Qm and b will be determined from the slope and the intercept of the plot and will be determining whether the adsorbent has high adsorption capacity or the adsorption is taking place at high or low energy.

Langmuir adsorption isotherm can also be expressed in terms of R_L, a dimensionless factor known as separation factor. It is used to determine whether the reaction was favorable or not.

$$R_L = \frac{1}{(1 + bCo)} \quad \text{.....(13)}$$

Where, Co = initial concentration. If R_L is between 0 and 1, the adsorption is favorable (Langmuir, 1918).

3.14.2 The Freundlich Isotherm

Freundlich adsorption isotherm describes the heterogeneous surface energy by multilayer adsorption and is expressed in linear form:

© University of Venda

$$\log Qe = \frac{1}{n}\log C_e + \log K_f \quad \text{.....(14)}$$

Where Ce = Equilibrium concentration (mg/L)

Qe = Amount adsorbed at equilibrium (mg/g)

Kf = Partition Coefficient

n = Intensity of adsorption

The linear plot of log Qe versus log Ce shows the applicability of Freundlich adsorption isotherm. The value of Kf implies that the energy of adsorption on a homogeneous surface is independent of surface coverage and n is an adsorption constants which reveals the rate at which adsorption is taking place. Those two constants are determined from the slope (Freundlich, 1906).

© University of Venda

University of Venda
Creating Future Leaders

CHAPTER FOUR

Physicochemical characterization of raw and modified bentonite clay

4.0 Introduction

The chemical and physical properties of bentonite clay play an important role in determining the behavior at which the clay interacts and interchanges ions with aqueous solution. In this chapter, cation exchange capacity (CEC), point of zero charge (PZC), Surface area, water holding capacity, elemental and mineralogical composition were evaluated as the principal physicochemical parameters which determine and influence the ability and efficiency of bentonite clay for adsorption of inorganic species from aqueous media. Also, the characterization of coal fly ash leachates was determined in an attempt to configure the constituents and concentration of South African coal fly ash leachates. The feasibility of loading Al^{3+} and Fe^{3+} on bentonite clay is also reported.

4.1 Modification of raw bentonite clay with Al^{3+} polycations

4.1.1 Adsorption of Al^{3+} onto bentonite clay as a function of contact time

The effects of contact time on reaction kinetics of Al^{3+} and bentonite clay was evaluated at 1g adsorbent dosage and 100 mg/L Al^{3+} concentration. The effects of contact time on adsorption of Al^{3+} onto bentonite clay was investigated for six hours at the interval of 1, 5, 10, 15, 30, 60, 180 and 360 minutes (Table A4). Fig 4.1, 4.2, and 4.3 shows the variation of pH, EC, TDS and Al^{3+} concentration with agitation time.

© University of Venda

University of Venda
Creating Future Leaders

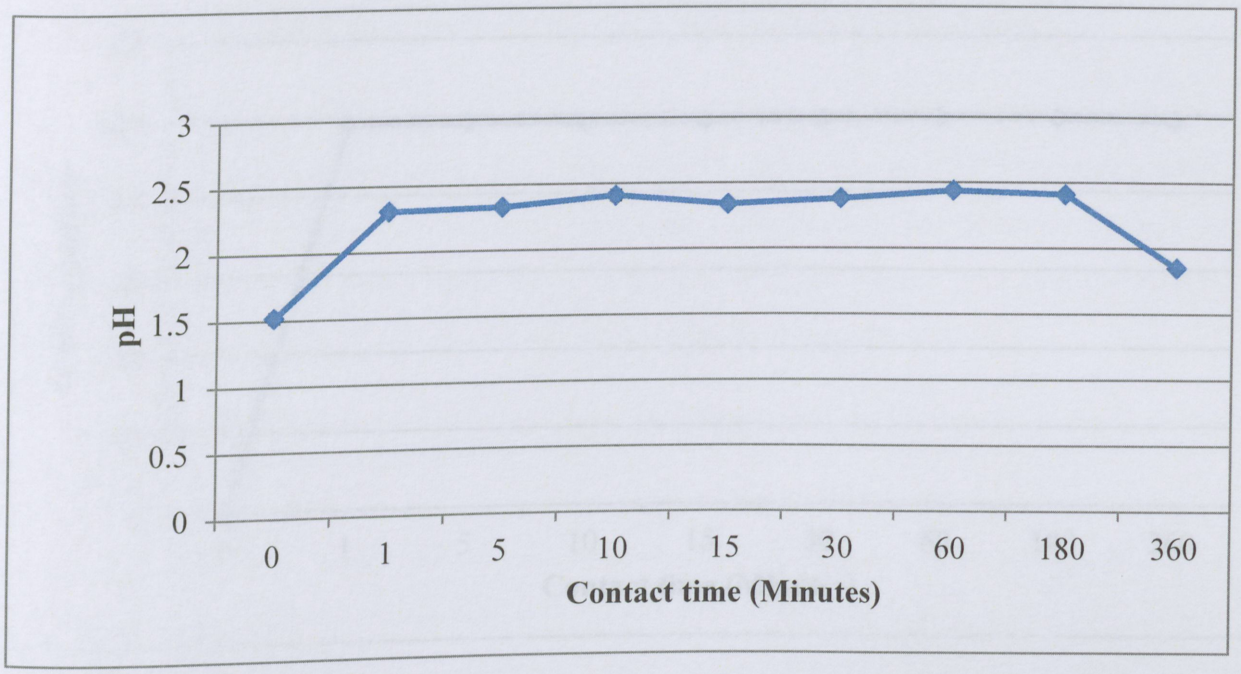


Figure 4.1: Variation of pH on adsorption of Al^{3+} onto bentonite clay as a function of contact time (1 gram of adsorbent dosage, 100 mg/L adsorbate concentration, 26°C and 1g/100 mL S/L ratios).

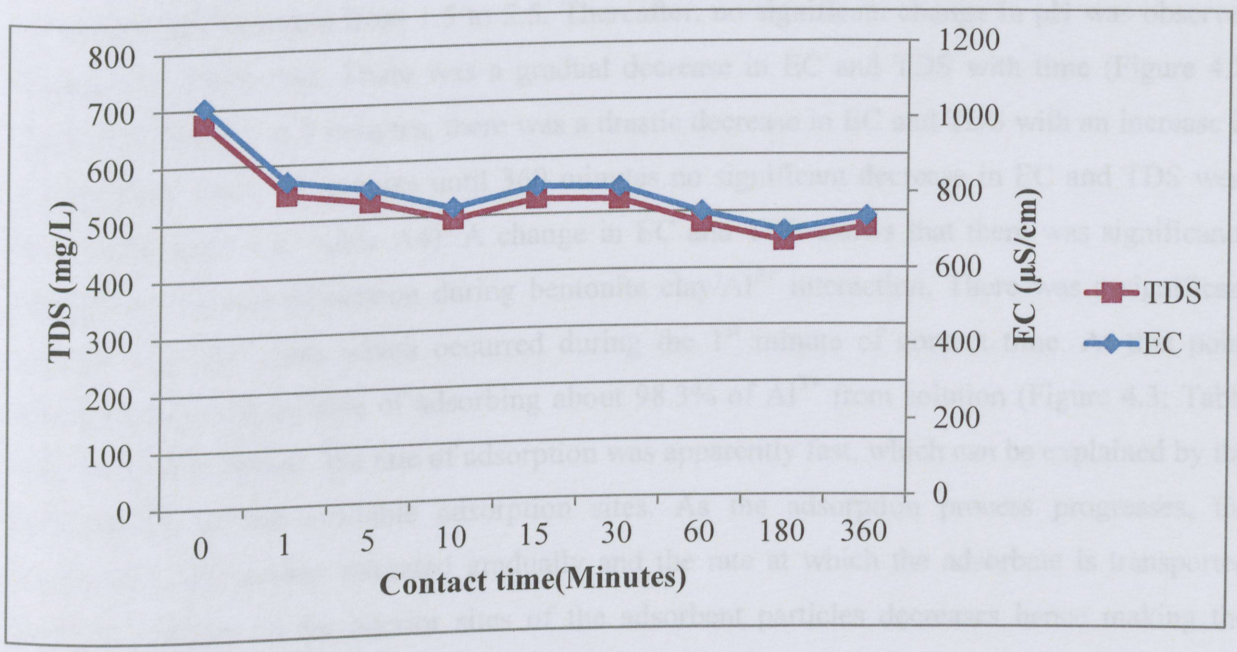


Figure 4.2: Variation of TDS and EC on adsorption of Al^{3+} onto bentonite clay lattices as a function of contact time (1 gram of adsorbent dosage, 100 mg/L adsorbate concentration, 26°C and 1g/100 mL S/L ratios).

UNIVERSITY OF VENDA
LIBRARY

© University of Venda

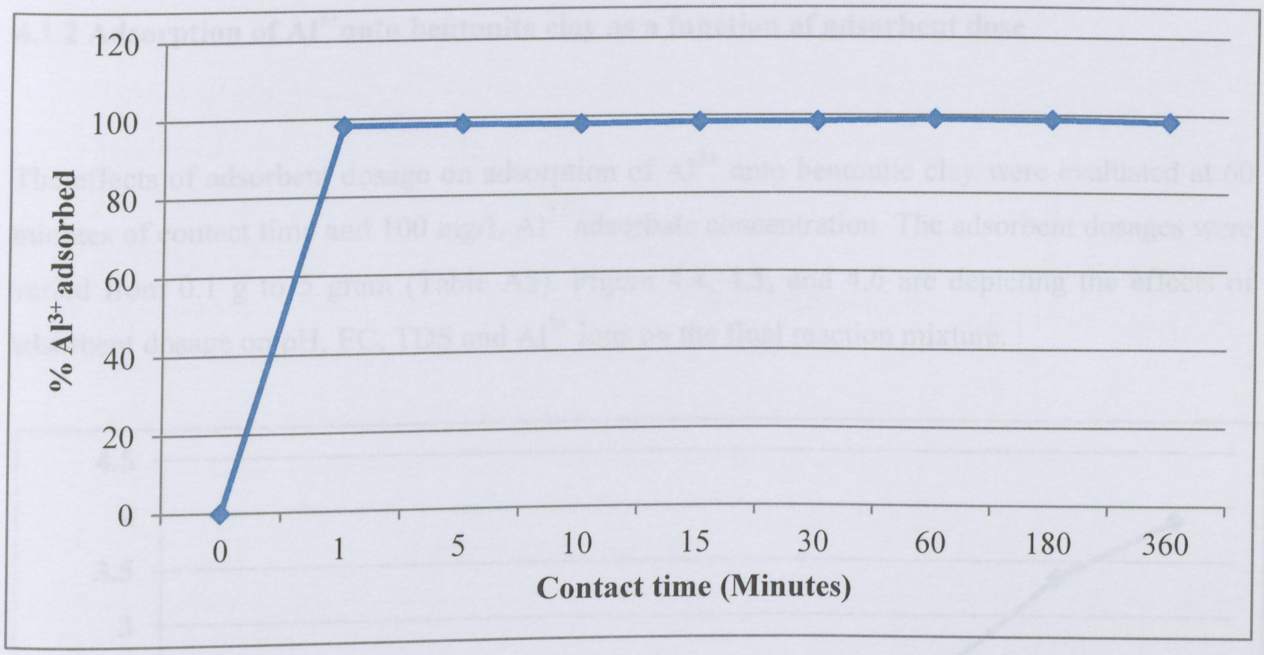


Figure 4.3: Variation of Al^{3+} adsorbed onto bentonite clay with an increase in contact time (1 gram bentonite clay, 100 mg/L Al^{3+}, 26 °C and 1g/100 mL S/L ratios).

There was a slight increase in with contact time (Figure 4.1; Table A4). From the first minute of interaction pH increased from 1.5 to 2.5. Thereafter, no significant change in pH was observed (Figure 4.1; Table A4). There was a gradual decrease in EC and TDS with time (Figure 4.2; Table A4). From 1 to 5 minutes, there was a drastic decrease in EC and TDS with an increase in contact time. From 10 minutes until 360 minutes no significant decrease in EC and TDS were observed (Figure 4.2; Table A4). A change in EC and TDS shows that there was significance proportion of metal adsorption during bentonite clay/Al^{3+} interaction. There was a significant adsorption of Al^{3+} ions which occurred during the 1st minute of contact time. At that point bentonite clay was capable of adsorbing about 98.3% of Al^{3+} from solution (Figure 4.3; Table A4). In the first minute, the rate of adsorption was apparently fast, which can be explained by the high density of the available adsorption sites. As the adsorption process progresses, the adsorption sites became saturated gradually and the rate at which the adsorbate is transported from the exterior to the interior sites of the adsorbent particles decreases hence making the adsorption process to become much slower hence indicating that the reaction has attained equilibrium. As such, 60 minutes of contact time was taken as the optimum time for loading Al^{3+} onto bentonite clay interlayers.

© University of Venda

4.1.2 Adsorption of Al^{3+} onto bentonite clay as a function of adsorbent dose

The effects of adsorbent dosage on adsorption of Al^{3+} onto bentonite clay were evaluated at 60 minutes of contact time and 100 mg/L Al^{3+} adsorbate concentration. The adsorbent dosages were varied from 0.1 g to 5 gram (Table A5). Figure 4.4, 4.5, and 4.6 are depicting the effects of adsorbent dosage on pH, EC, TDS and Al^{3+} ions on the final reaction mixture.

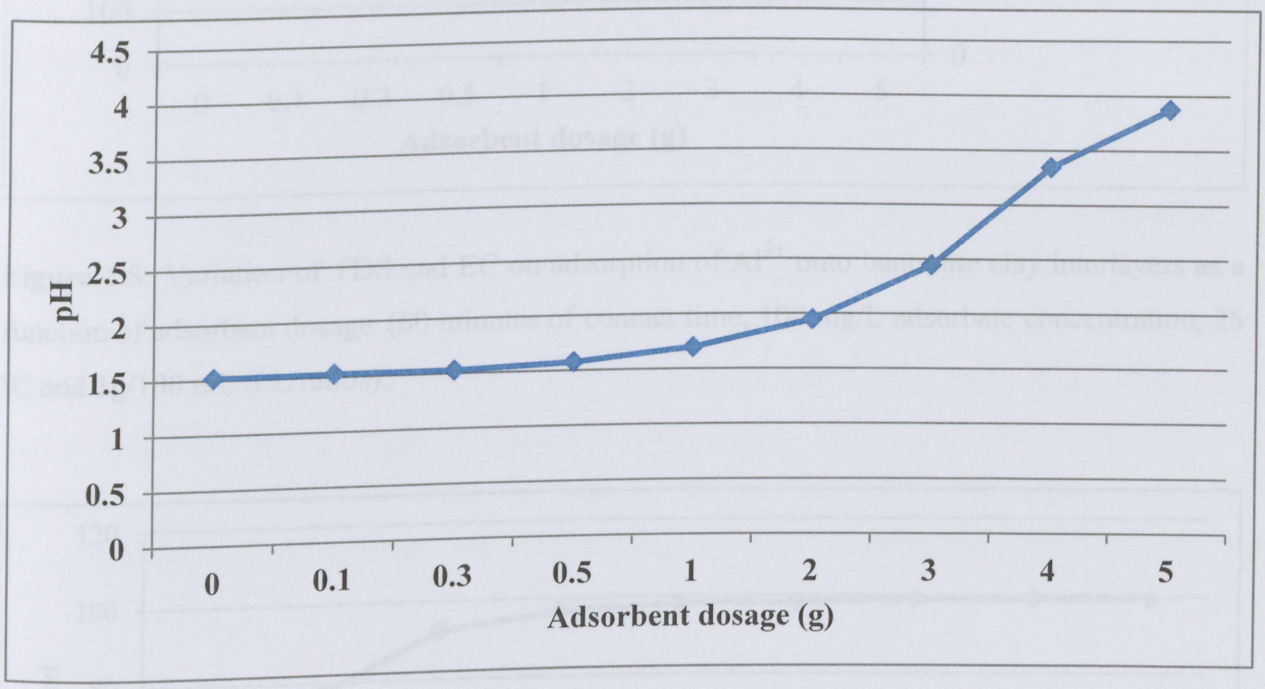


Figure 4.4: Variation of pH profile on adsorption of Al^{3+} onto bentonite clay with an increase in adsorbent dosage (60 minutes of contact time, 100 mg/L adsorbate concentration, 26 °C and 1g/100 mL S/L ratios).

© University of Venda

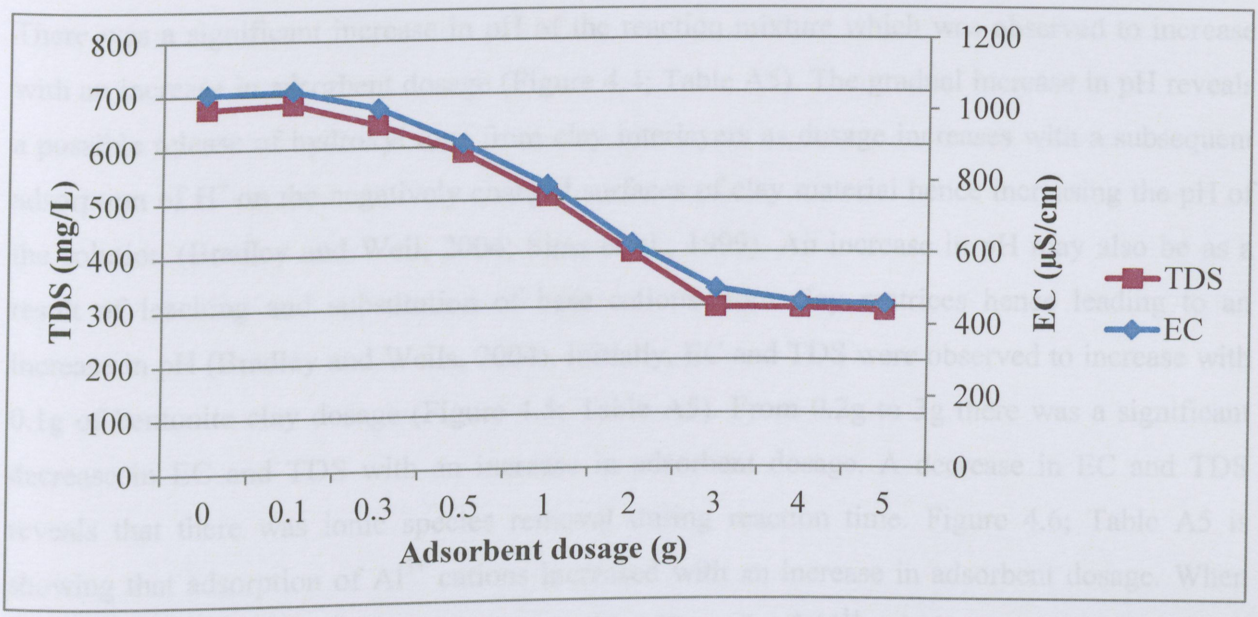


Figure 4.5: Variation of TDS and EC on adsorption of Al^{3+} onto bentonite clay interlayers as a function of adsorbent dosage (60 minutes of contact time, 100 mg/L adsorbate concentration, 26 °C and 1g/100 mL S/L ratios).

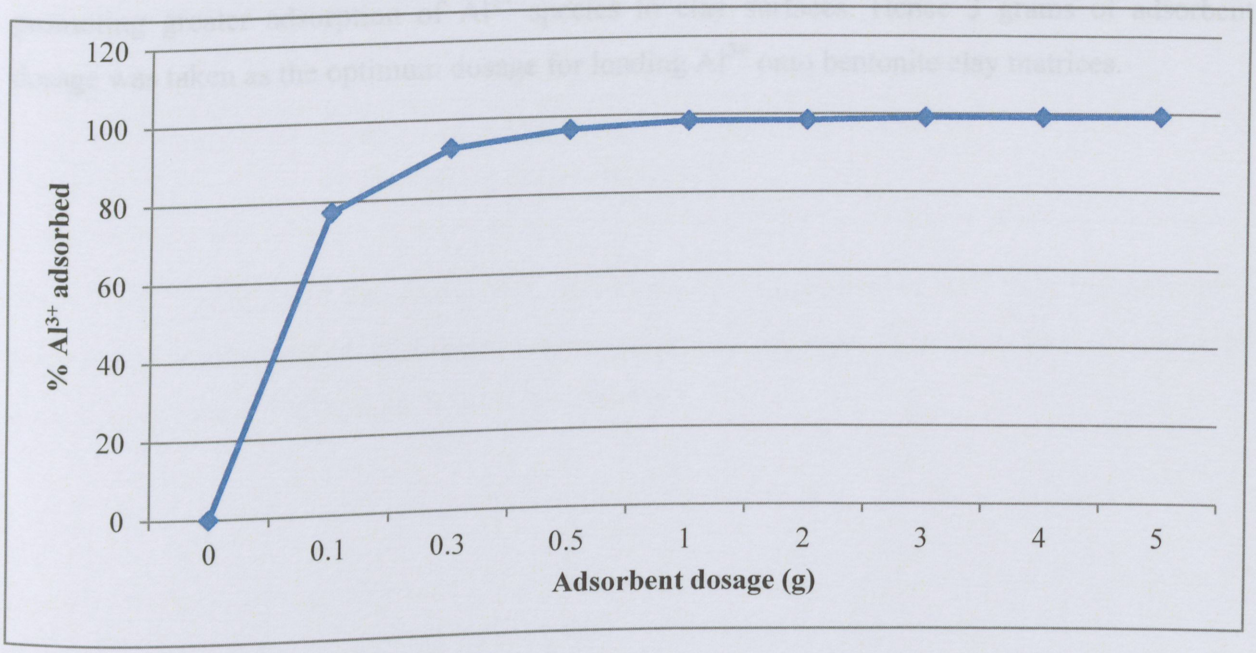


Figure 4.6: Variation of Al^{3+} concentration adsorbed onto bentonite clay lattice with an increase in adsorbent dosage (60 minutes of contact time, 100 mg/L of adsorbate concentration, and 26 °C).

© University of Venda

There was a significant increase in pH of the reaction mixture which was observed to increase with an increase in adsorbent dosage (Figure 4.4; Table A5). The gradual increase in pH reveals a possible release of hydroxyl ions from clay interlayers as dosage increases with a subsequent adsorption of H^+ on the negatively charged surfaces of clay material hence increasing the pH of the solution (Bradley and Weil, 2004; Sims et al., 1999). An increase in pH may also be as a result of leaching and substitution of base cations from clay matrices hence leading to an increase in pH (Bradley and Weils, 2004). Initially, EC and TDS were observed to increase with 0.1g of bentonite clay dosage (Figure 4.5; Table A5). From 0.2g to 3g there was a significant decrease in EC and TDS with an increase in adsorbent dosage. A decrease in EC and TDS reveals that there was ionic species removal during reaction time. Figure 4.6; Table A5 is showing that adsorption of Al^{3+} cations increased with an increase in adsorbent dosage. When 0.1 grams of bentonite clay was interacted with 100 mg/L of Al^{3+} solution, greater than 80% of Al^{3+} were adsorbed to clay interlayers hence depicting that small dose is effective for removal of Al^{3+} ions. A drastic adsorption of Al^{3+} ions was observed from 0.1 to 1g with the percentage adsorption reaching 98.41 % but from 3 to 5g no change in adsorption was been observed. This was an indication that as adsorbent dosage increases the adsorption sites also increases hence promoting greater adsorption of Al^{3+} species to clay surfaces. Hence 3 grams of adsorbent dosage was taken as the optimum dosage for loading Al^{3+} onto bentonite clay matrices.

© University of Venda

4.1.3 Adsorption of Al^{3+} onto bentonite clay as a function of adsorbate concentration

The effects of concentration on adsorption kinetics of Al^{3+} onto bentonite clay were evaluated at 60 minutes of contact time, 3g of adsorbent dosage, 26 °C and 3g/100 mL S/L ratio. The concentrations were varied from 10, 50, 80, 150, 200, 250, 300, 450, and 500 mg/L (Table A7). Figure 4.7, 4.8, 4.9 and 4.10 are depicting the effects of adsorbent dosage on pH, EC, TDS and Al^{3+} ions

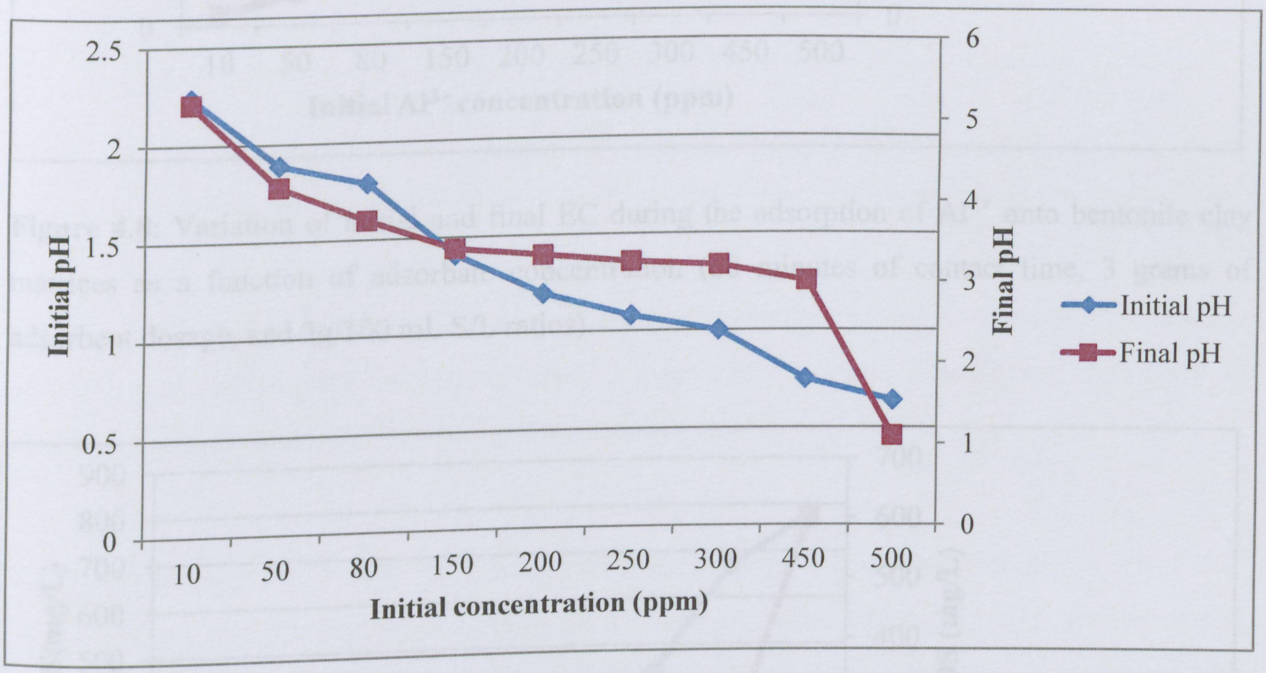


Figure 4.7: Variation of initial and final pH during the adsorption of Al^{3+} onto bentonite clay matrices as a function of adsorbate concentration (60 minutes of contact time, 3 grams of adsorbent dosage, 26 °C and 3g/100 mL S/L ratios).

© University of Venda

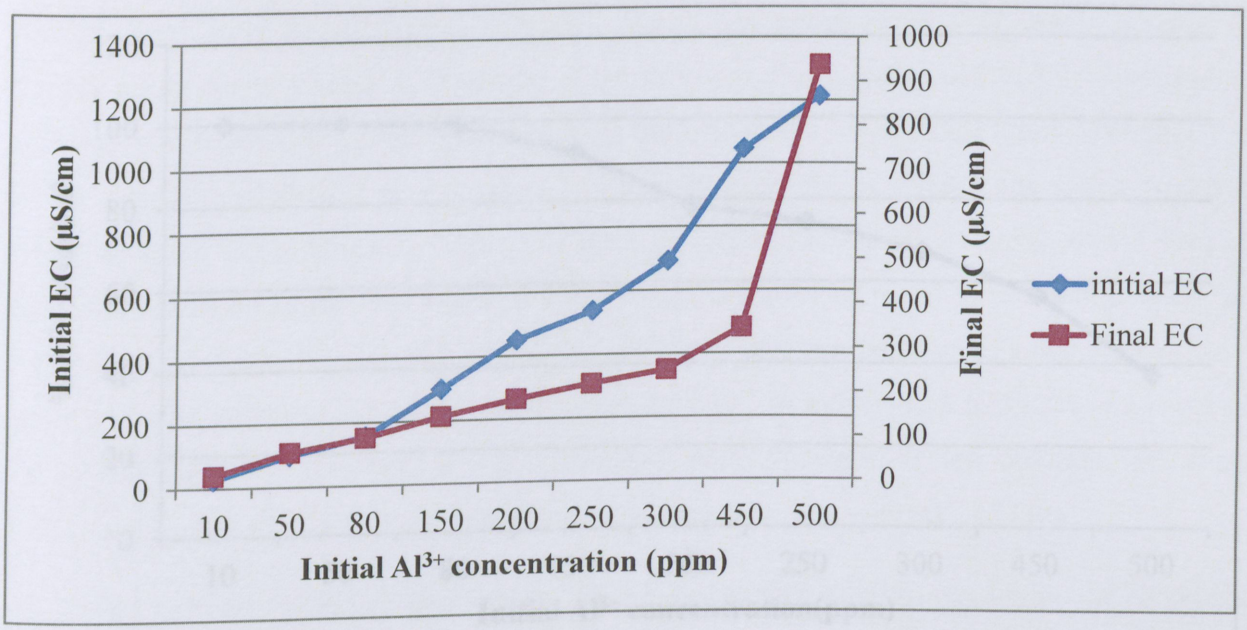


Figure 4.8: Variation of initial and final EC during the adsorption of Al^{3+} onto bentonite clay matrices as a function of adsorbate concentration (60 minutes of contact time, 3 grams of adsorbent dosage, and 3g/100 mL S/L ratios).

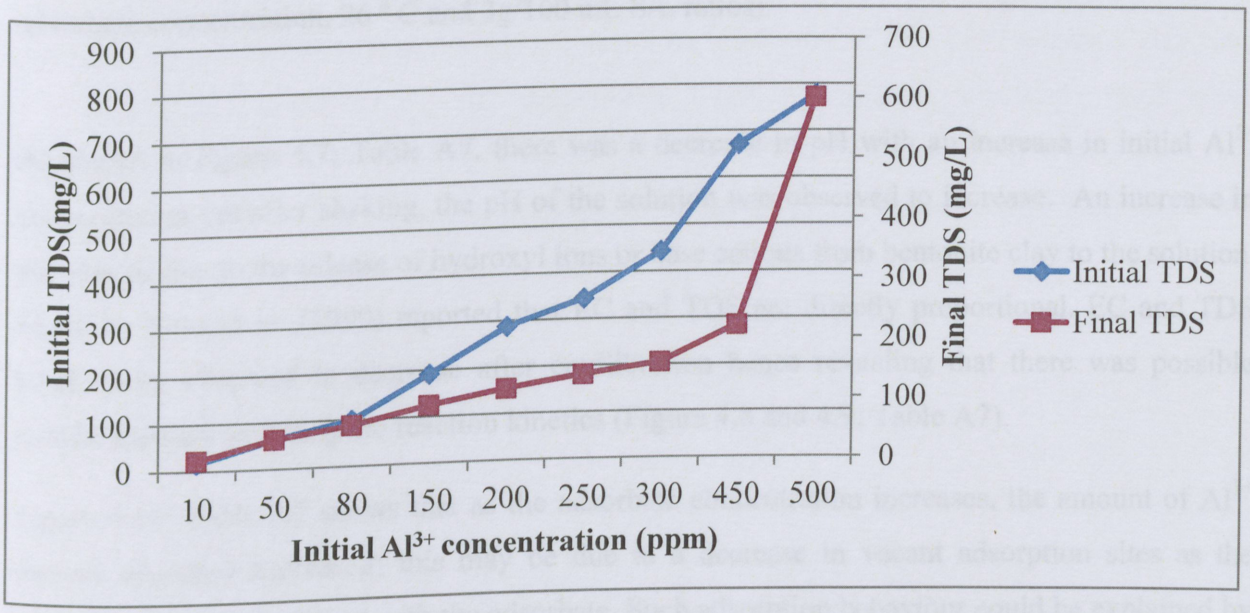


Figure 4.9: Variation of initial and final TDS during the adsorption of Al^{3+} onto bentonite clay matrices as a function of adsorbate concentration (60 minutes of contact time, 3 grams of adsorbent dosage, 26 °C and 3g/100 mL S/L ratios).

© University of Venda

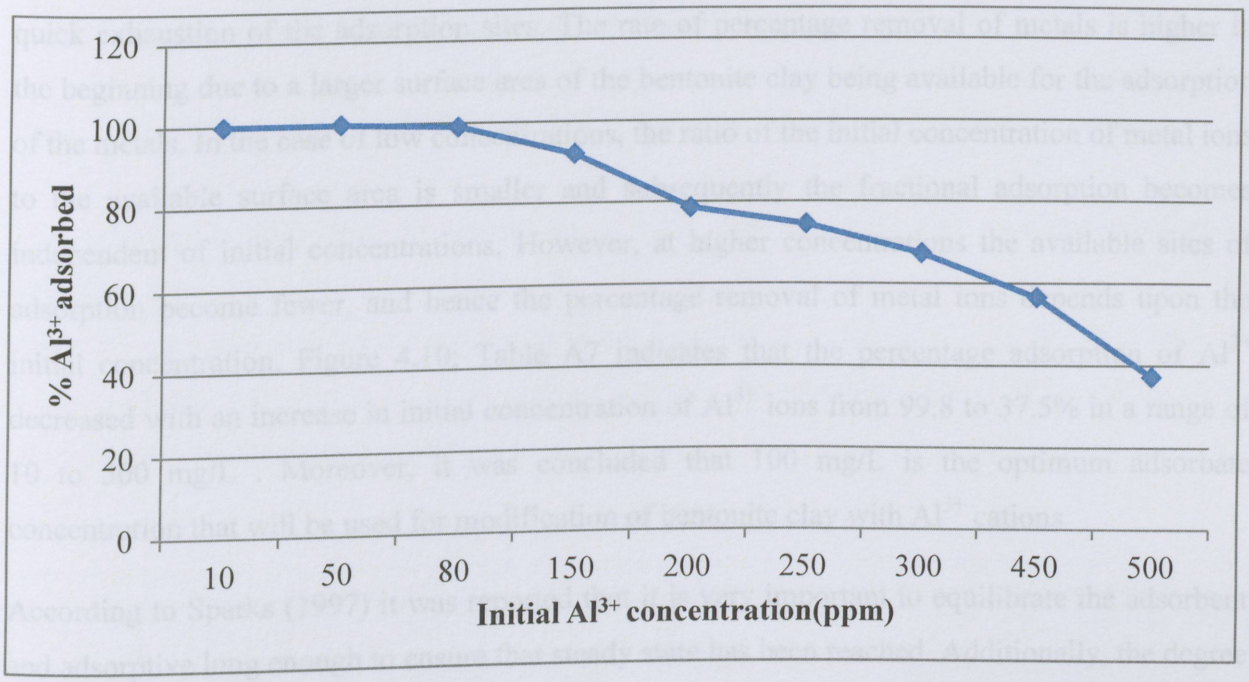


Figure 4.10: Variation of % Al^{3+} adsorbed onto bentonite clay as a function of adsorbate concentration (60 minutes of contact time, 3 grams of adsorbent dosage, and 100 mg/L of adsorbate concentration, 26 ° C and 3g/100 mL S/L ratios).

As shown in Figure 4.7; Table A7, there was a decrease in pH with an increase in initial Al^{3+} concentration but after shaking, the pH of the solution was observed to increase. An increase in pH may be due to the release of hydroxyl ions or base cations from bentonite clay to the solution. Study by Sims et al. (1999) reported that EC and TDS are directly proportional. EC and TDS levels were observed to decrease after equilibration hence revealing that there was possible metals attenuation during the reaction kinetics (Figure 4.8 and 4.9; Table A7).

Figure 4.10; Table A7 shows that as the adsorbate concentration increases, the amount of Al^{3+} cations adsorbed decreased; this may be due to a decrease in vacant adsorption sites as the adsorbent becomes covered with the adsorbate. Such adsorption behaviour could be explained by the high affinity of the adsorbent for the adsorptive at low concentrations, which then decreases as concentration increases (Spark, 1997). Moreover, it can also be stated that as the adsorbate concentration increases the rate of percentage removal becomes almost insignificant due to a

© University of Venda

quick exhaustion of the adsorption sites. The rate of percentage removal of metals is higher in the beginning due to a larger surface area of the bentonite clay being available for the adsorption of the metals. In the case of low concentrations, the ratio of the initial concentration of metal ions to the available surface area is smaller and subsequently the fractional adsorption becomes independent of initial concentrations. However, at higher concentrations the available sites of adsorption become fewer, and hence the percentage removal of metal ions depends upon the initial concentration. Figure 4.10; Table A7 indicates that the percentage adsorption of Al^{3+} decreased with an increase in initial concentration of Al^{3+} ions from 99.8 to 37.5% in a range of 10 to 500 mg/L . Moreover, it was concluded that 100 mg/L is the optimum adsorbate concentration that will be used for modification of bentonite clay with Al^{3+} cations

According to Sparks (1997) it was reported that it is very important to equilibrate the adsorbent and adsorptive long enough to ensure that steady state has been reached. Additionally, the degree of agitation used in the equilibration process should be forceful enough to effect good mixing but not so vigorous that adsorbent modification occurs (Sparks, 1997). From these experiments, it was concluded that the optimum conditions for impregnating polycations of Al^{3+} onto bentonite clay lattice is 60 minutes of contact time, 3 grams of adsorbent dosage, 100 mg/L of adsorbate concentration and 3/100 S/L ratios. Effects of pH on adsorption of Al^{3+} onto bentonite clay were not evaluated due to the fact that Al^{3+} precipitates at pH> 4. This study produced a result which is consistent with the findings of Ramesh et al. (2007) who found that loading of polymeric Al^{3+} onto bentonite clay occurs within 60 minutes of contact time, 3 grams of adsorbent dosage, 100 mg/L of adsorbate concentration and 26 °C.

© University of Venda

4.2 Modification of bentonite clay with Fe^{3+} polycations

4.2.1 Adsorption of Fe^{3+} onto bentonite clay as a function of contact time

The effect of contact time on adsorption of Fe^{3+} onto bentonite clay was evaluated at 1g adsorbent dosage and 100 mL solution with 100 mg/L Fe^{3+} concentration. The uptake of Fe^{3+} on bentonite clay was evaluated for 8 hours at the intervals of 1, 5, 10, 15, 30, 60, 180, and 360 minutes (Table A8). Fig 4.11, 4.12, and 4.13 shows the variation of pH, EC, TDS and Fe^{3+} concentration with agitation time.

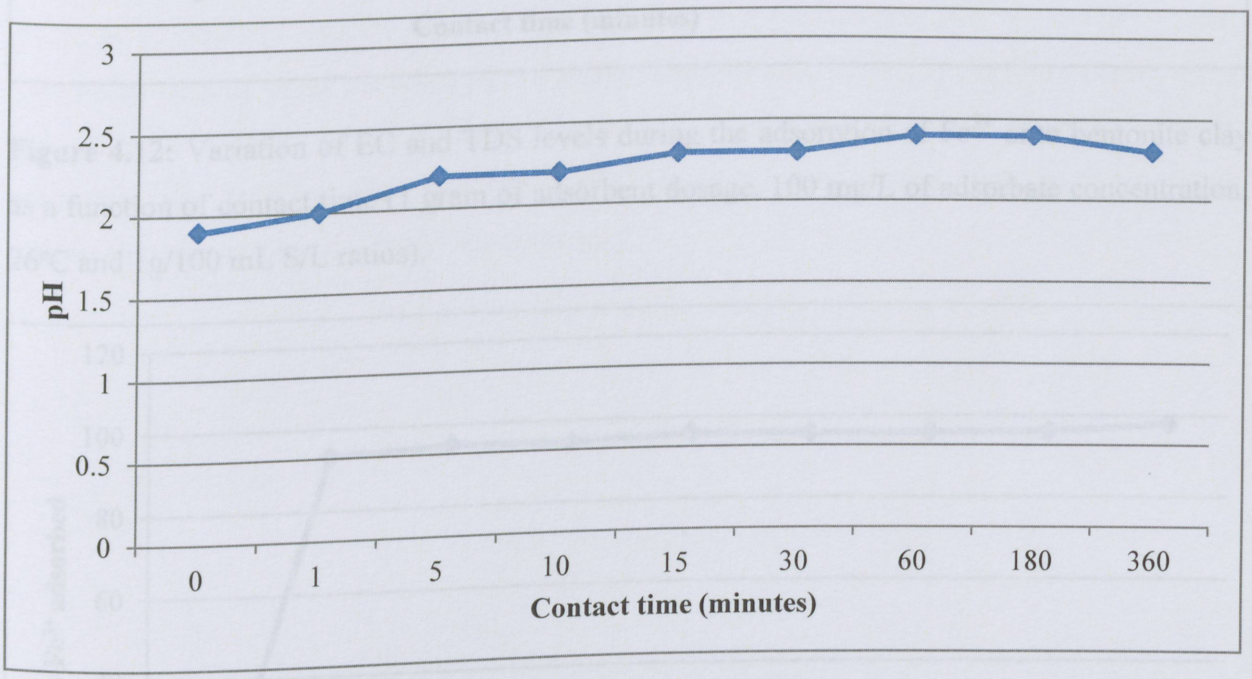


Figure 4.11: Variation of pH profile during the adsorption of Fe^{3+} cations onto bentonite clay matrices as a function of contact time (1 gram of adsorbent dosage, 100 mg/L of adsorbate concentration, 26°C and 1g/100 mL S/L ratios).

© University of Venda

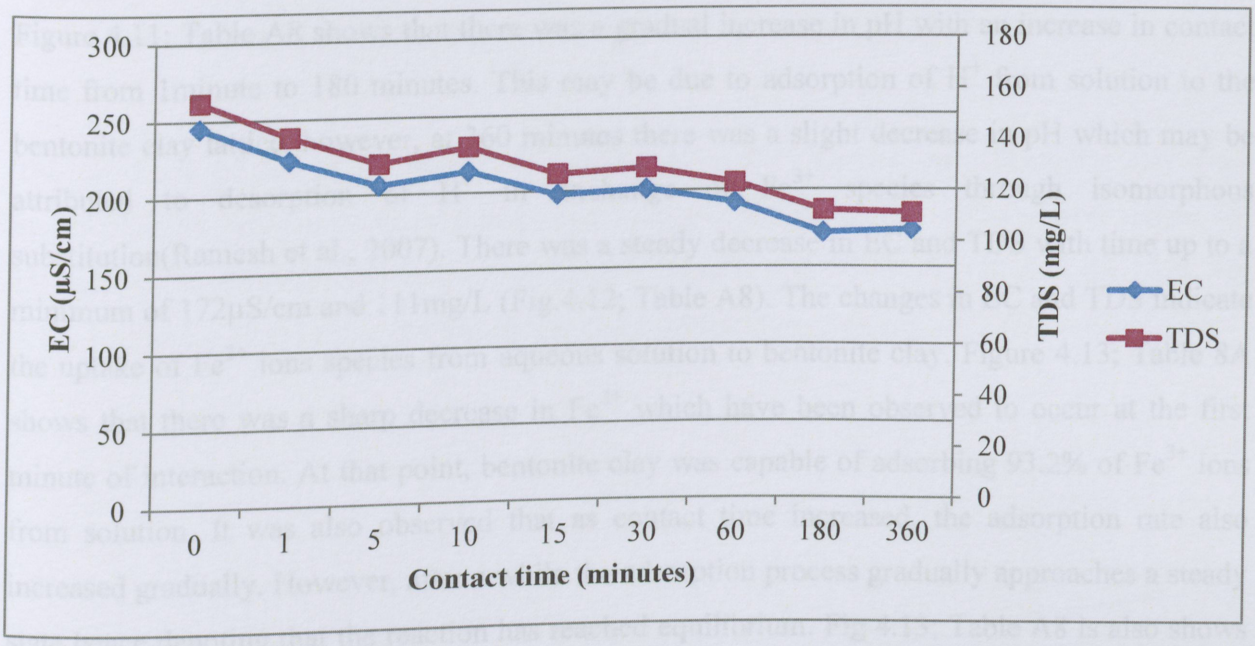


Figure 4.12: Variation of EC and TDS levels during the adsorption of Fe^{3+} onto bentonite clay as a function of contact time (1 gram of adsorbent dosage, 100 mg/L of adsorbate concentration, 26°C and 1g/100 mL S/L ratios).

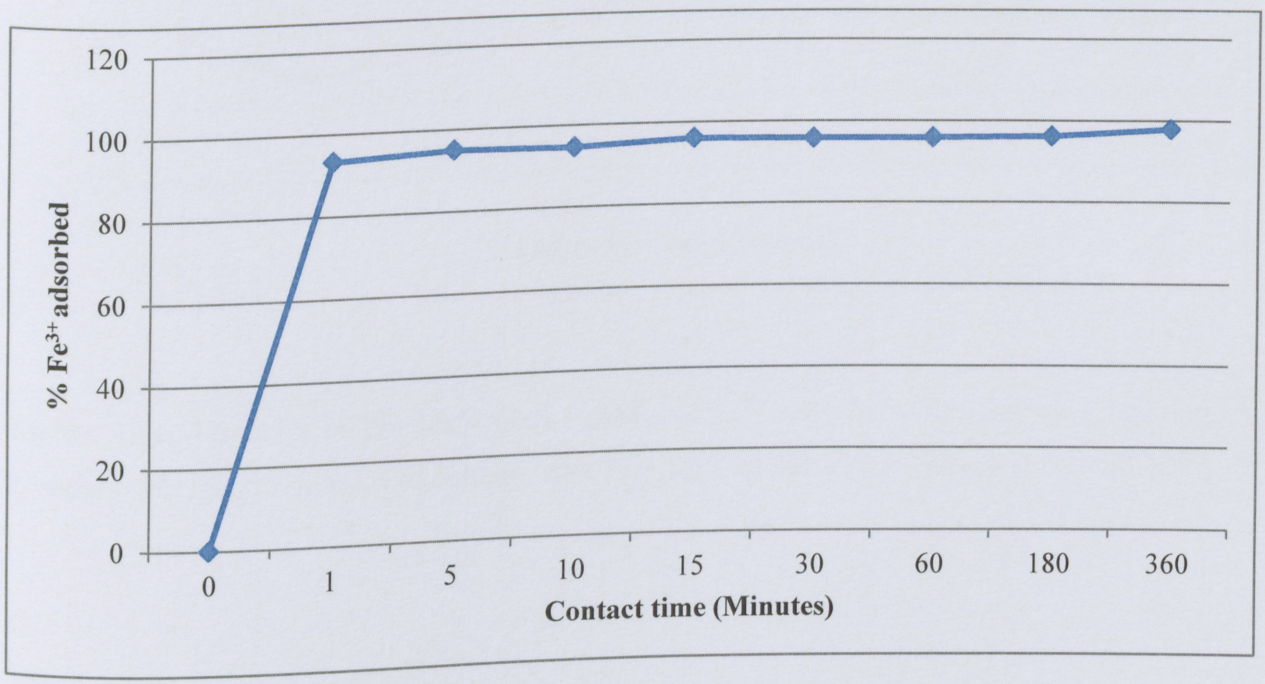


Figure 4.13: Variation of Fe^{3+} adsorbed onto bentonite clay surfaces with an increase in contact time (1 gram of adsorbent dosage, 100 mg/L of adsorbate concentration, 26°C and 1g/100 mL S/L ratios)

© University of Venda

Figure 4.11; Table A8 shows that there was a gradual increase in pH with an increase in contact time from 1minute to 180 minutes. This may be due to adsorption of H^+ from solution to the bentonite clay lattice, however, at 360 minutes there was a slight decrease in pH which may be attributed to desorption of H^+ in exchange of Fe^{3+} species through isomorphous substitution(Ramesh et al., 2007). There was a steady decrease in EC and TDS with time up to a minimum of 172µS/cm and 111mg/L (Fig.4.12; Table A8). The changes in EC and TDS indicate the uptake of Fe^{3+} ions species from aqueous solution to bentonite clay. Figure 4.13; Table 8A shows that there was a sharp decrease in Fe^{3+} which have been observed to occur at the first minute of interaction. At that point, bentonite clay was capable of adsorbing 93.2% of Fe^{3+} ions from solution. It was also observed that as contact time increased, the adsorption rate also increased gradually. However, after a while the adsorption process gradually approaches a steady state hence denoting that the reaction has reached equilibrium. Fig 4.13; Table A8 is also shows that after 15 minutes no significant change in Fe^{3+} concentration was observed with the adsorption rate reaching approximately 100%. Hence 15 minute was taken as the optimum contact time for loading Fe^{3+} onto bentonite clay.

© University of Venda

4.1.2.2 Adsorption of Fe^{3+} onto bentonite clay as a function of adsorbent dosage

The influence of adsorbent dosage on adsorption of Fe^{3+} species onto bentonite clay were investigated by varying adsorbent dosage in the range of 0.1 to 5g. The mixtures were shaken for 15 minutes, at the adsorbate concentration of 100 mg/L and 1/100 S/L ratios (Table A9). Fig 4.14, 4.15 and 4.16 are depicting the effects of adsorbent dosage on pH, EC, TDS and Fe^{3+} ions

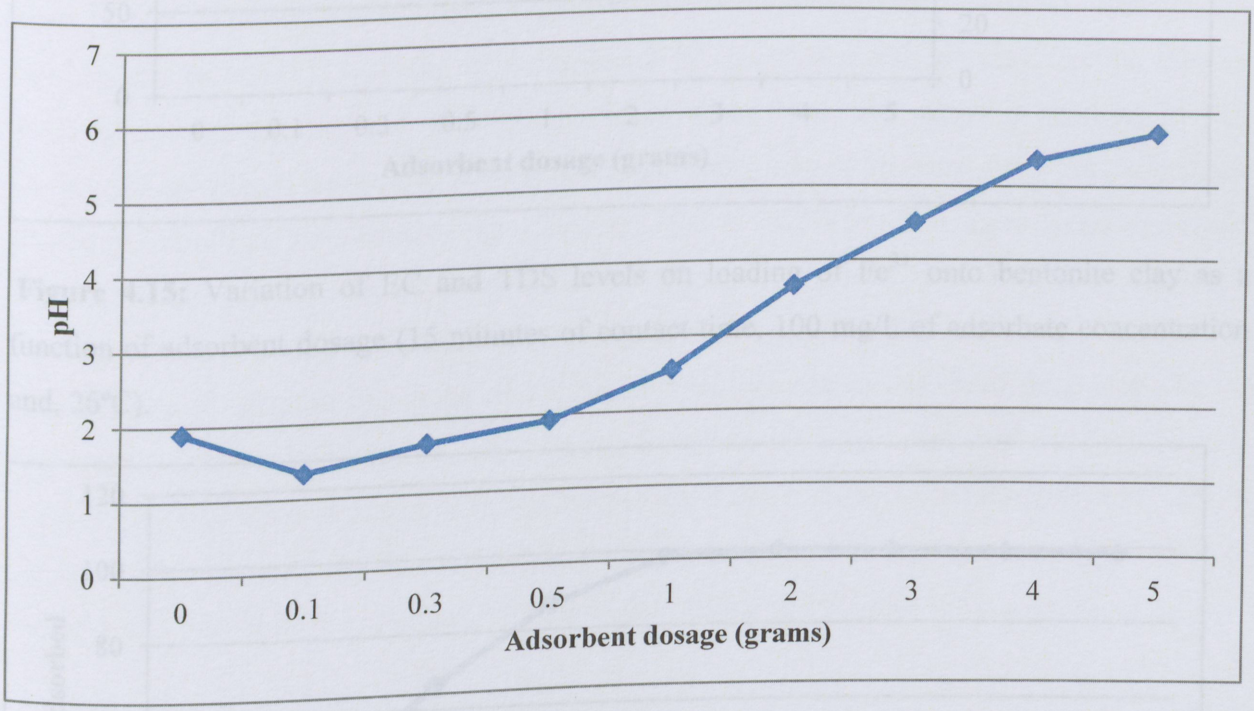


Figure 4.14: Variation of pH profiles on loading of Fe^{3+} onto bentonite clay as a function of adsorbent dosage (15 minutes of contact time, 100 mg/L of adsorbate concentration, and 26°C).

© University of Venda

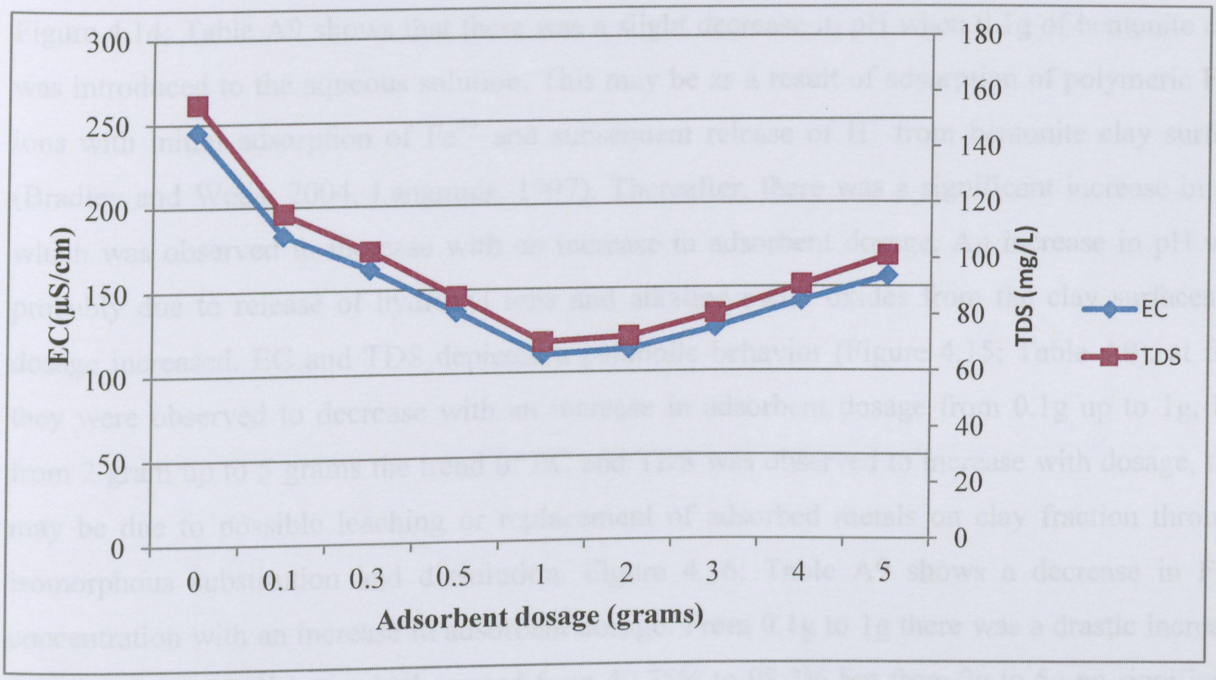


Figure 4.15: Variation of EC and TDS levels on loading of Fe^{3+} onto bentonite clay as a function of adsorbent dosage (15 minutes of contact time, 100 mg/L of adsorbate concentration and, 26°C).

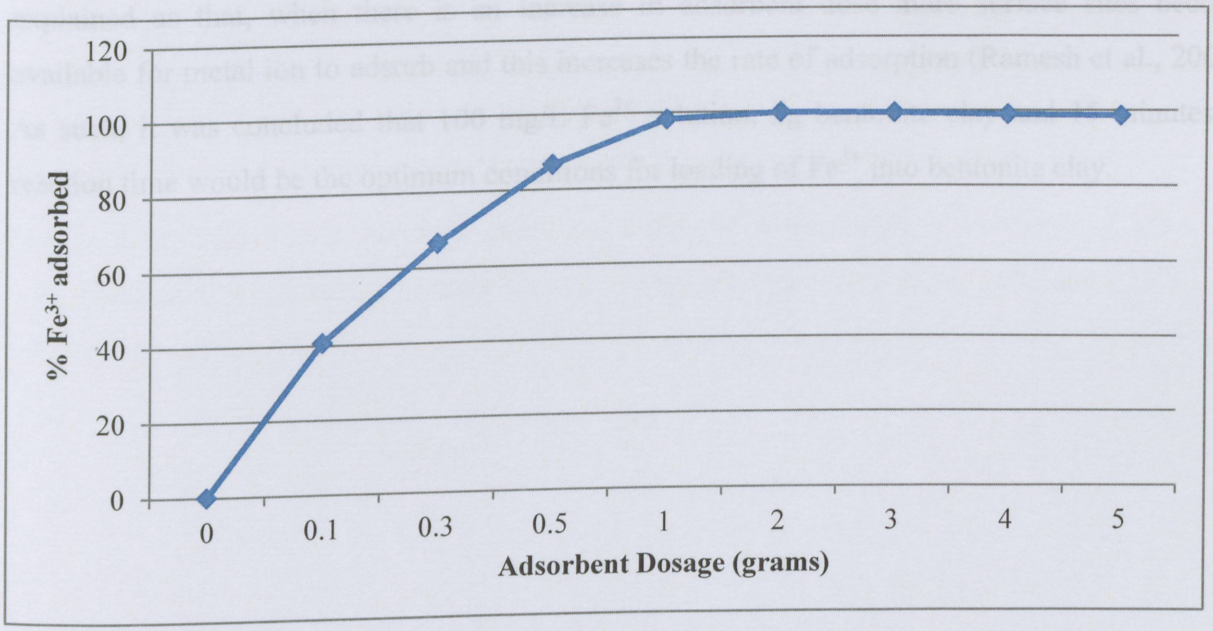


Figure: 4.16: Variation of Fe^{3+} concentration adsorbed onto bentonite clay as a function of adsorbent dosage (15 minutes of contact time, 100 mg/L of adsorbate concentration and, 26°C).

© University of Venda

Figure 4.14; Table A9 shows that there was a slight decrease in pH when 0.1g of bentonite clay was introduced to the aqueous solution. This may be as a result of adsorption of polymeric Fe^{3+} ions with initial adsorption of Fe^{3+} and subsequent release of H^{+} from bentonite clay surface (Bradley and Weils, 2004, Langmuir, 1997). Thereafter, there was a significant increase in pH which was observed to increase with an increase in adsorbent dosage. An increase in pH was probably due to release of hydroxyl ions and alkaline metal oxides from the clay surfaces as dosage increased. EC and TDS depicted a parabolic behavior (Figure 4.15; Table A9), at first they were observed to decrease with an increase in adsorbent dosage from 0.1g up to 1g, but from 2 gram up to 5 grams the trend of EC and TDS was observed to increase with dosage, this may be due to possible leaching or replacement of adsorbed metals on clay fraction through isomorphous substitution and dissolution. Figure 4.16; Table A9 shows a decrease in Fe^{3+} concentration with an increase in adsorbent dosage. From 0.1g to 1g there was a drastic increase in adsorption of Fe^{3+} ions which ranged from 40.75% to 98.2% but from 2g to 5g no significant variation in adsorption was observed hence indicating that greater than 3 gram of adsorbent provided enough adsorption sites for 100 mg/L Fe^{3+} solution (Ramesh et al., 2007). The phenomenon of increase in uptake of Fe^{3+} ions with increase in adsorbent dose may also be explained as that, when there is an increase in adsorbent dose more surface sites become available for metal ion to adsorb and this increases the rate of adsorption (Ramesh et al., 2007). As such, it was concluded that 100 mg/L Fe^{3+} solution, 2g bentonite clay and 15 minutes of reaction time would be the optimum conditions for loading of Fe^{3+} into bentonite clay.

© University of Venda

4.1.2.3 Adsorption of Fe^{3+} onto bentonite clay as a function of adsorbate concentration

The effects of concentration on adsorption process of Fe^{3+} onto bentonite clay were carried out under the optimized conditions of 15 minutes of contact time and 2g of adsorbent dosage. The initial concentrations ranged from 10, 50, 80, 150, 200, 250, 300, 450, and 500 mg/L (Table A11). Figure 4.17, 4.18, 4.19 and 4.20 shows initial and final pH, EC, TDS and Fe^{3+} concentration before and after equilibration.

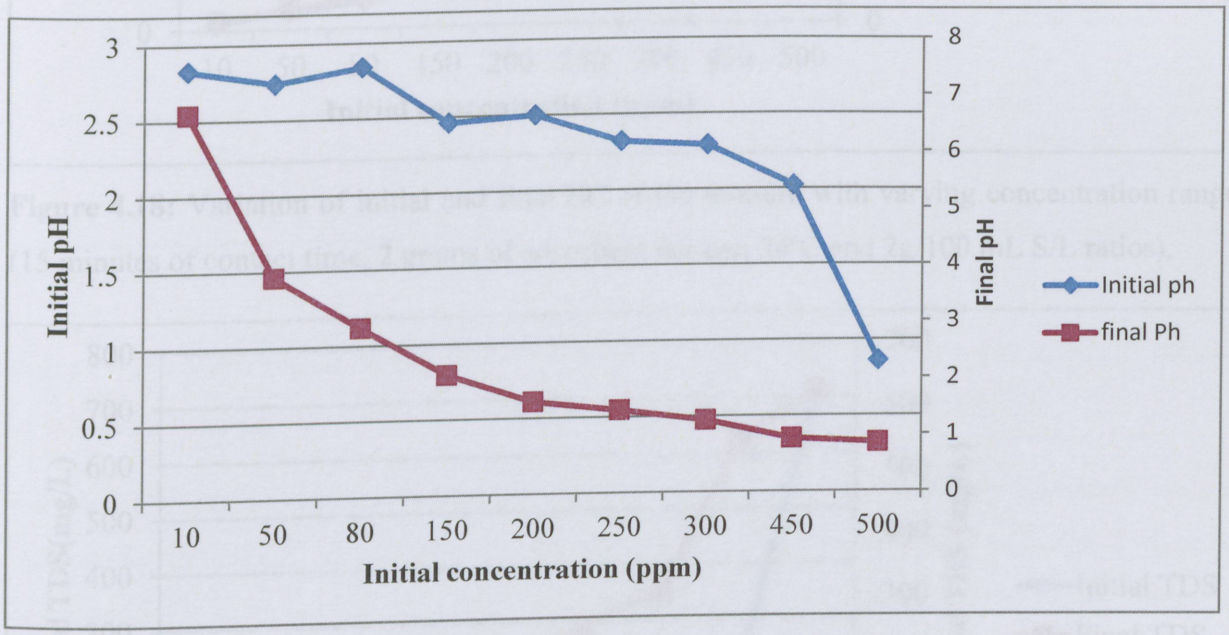


Figure 4.17: Variation in between initial and final pH of the solution with varying adsorbate concentration (15 minutes of contact time, 2 grams of adsorbent dosage, 26°C and 2g/100 mL S/L ratios).

© University of Venda

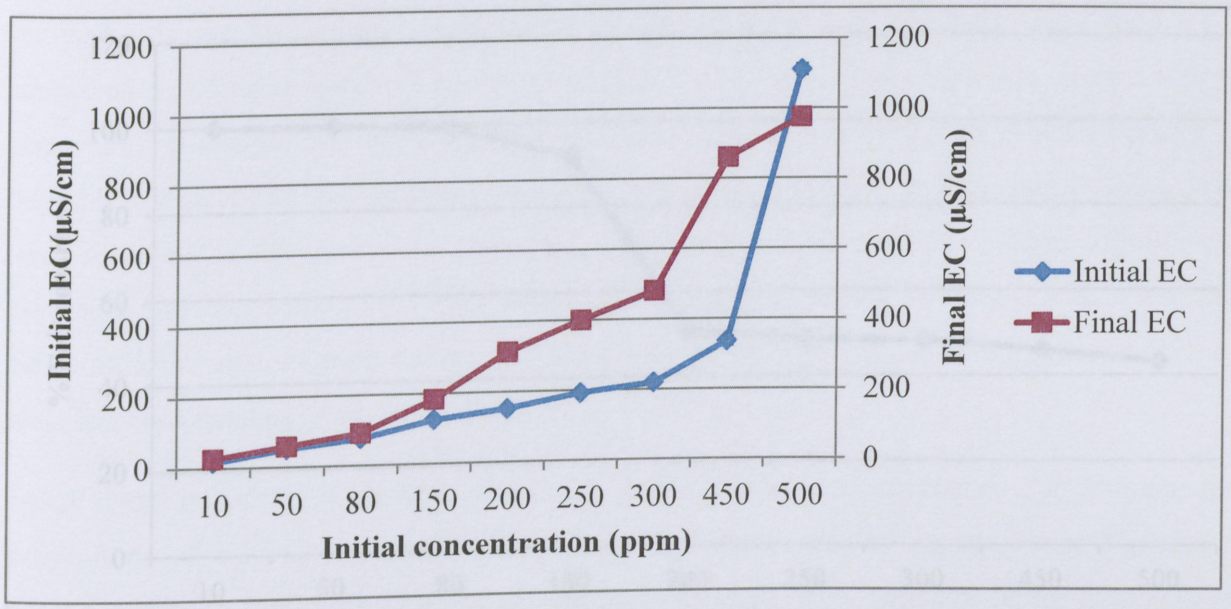


Figure 4.18: Variation of initial and final EC of the mixture with varying concentration ranges (15 minutes of contact time, 2 grams of adsorbent dosage, 26°C and 2g/100 mL S/L ratios).

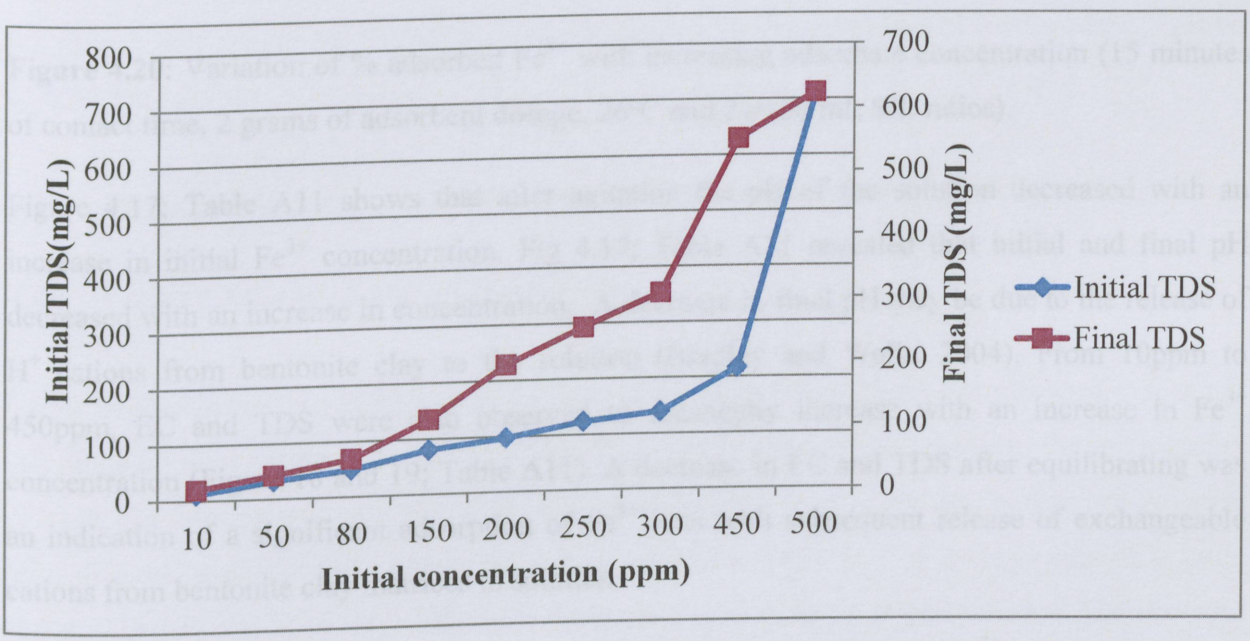


Figure 4.19: Variation of initial and final TDS of the mixture with varying adsorbate concentration (15 minutes of contact time, 2 grams of adsorbent dosage and 2g/100 mL S/L ratios).

© University of Venda

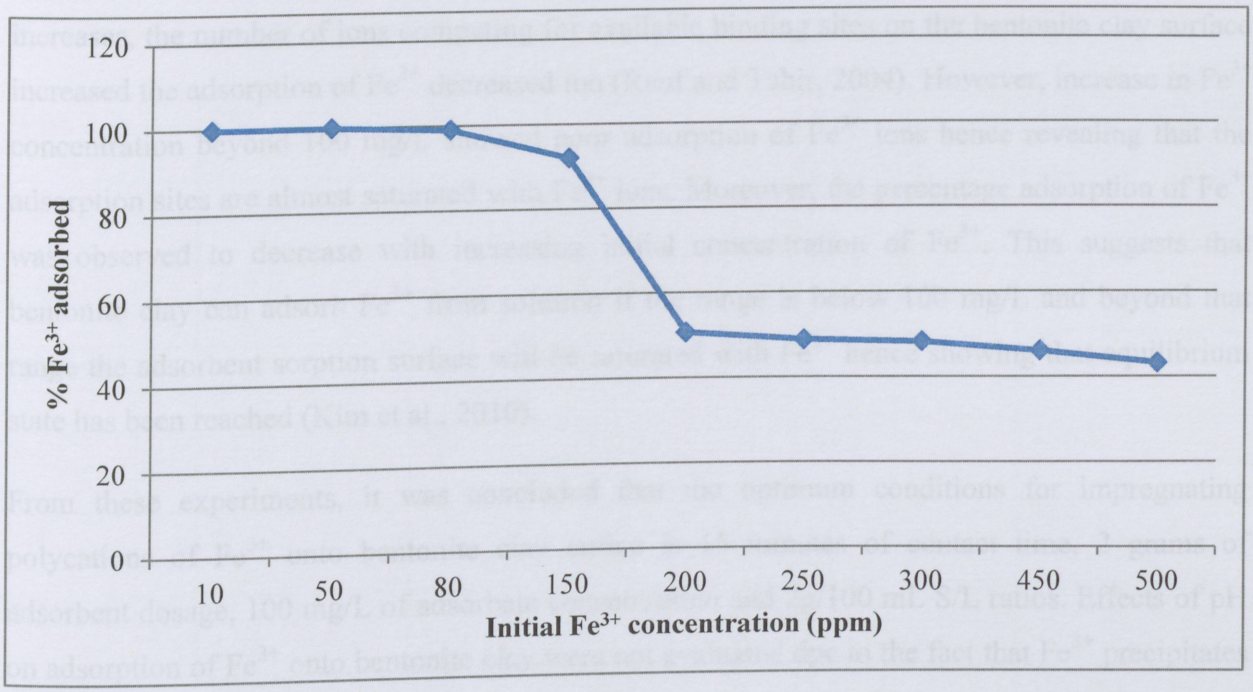


Figure 4.20: Variation of % adsorbed Fe^{3+} with increasing adsorbate concentration (15 minutes of contact time, 2 grams of adsorbent dosage, 26°C and 2g/100 mL S/L ratios).

Figure 4.17; Table A11 shows that after agitation the pH of the solution decreased with an increase in initial Fe^{3+} concentration. Fig 4.17; Table A11 revealed that initial and final pH decreased with an increase in concentration. A decrease in final pH may be due to the release of H^+ cations from bentonite clay to the solution (Bradley and Weils, 2004). From 10ppm to 450ppm, EC and TDS were also observed to drastically increase with an increase in Fe^{3+} concentration (Figure 18 and 19; Table A11). A decrease in EC and TDS after equilibrating was an indication of a significant adsorption of Fe^{3+} ions with subsequent release of exchangeable cations from bentonite clay matrices to solution.

Fig 4.20; Table A11 shows the effect of initial metal concentration on Fe^{3+} adsorption. It was observed that adsorption of Fe^{3+} decreased from 99.8% to 43.2% with an increase in metal concentration from 10-500 mg/L. At higher concentrations, most of the Fe^{3+} ions are left unabsorbed due to saturation of adsorption sites. As the ratio of sorptive surface to ion concentration decreased with increasing metal ion concentration and so metal ion removal was reduced. At low initial concentration more binding sites are available, but as the concentration

© University of Venda

increases, the number of ions competing for available binding sites on the bentonite clay surface increased the adsorption of Fe^{3+} decreased too (Rauf and Tahir, 2004). However, increase in Fe^{3+} concentration beyond 100 mg/L showed poor adsorption of Fe^{3+} ions hence revealing that the adsorption sites are almost saturated with Fe^{3+} ions. Moreover, the percentage adsorption of Fe^{3+} was observed to decrease with increasing initial concentration of Fe^{3+}. This suggests that bentonite clay can adsorb Fe^{3+} from solution if the range is below 100 mg/L and beyond that range the adsorbent sorption surface will be saturated with Fe^{3+} hence showing that equilibrium state has been reached (Kim et al., 2010).

From these experiments, it was concluded that the optimum conditions for impregnating polycations of Fe^{3+} onto bentonite clay lattice is 15 minutes of contact time, 2 grams of adsorbent dosage, 100 mg/L of adsorbate concentration and 2g/100 mL S/L ratios. Effects of pH on adsorption of Fe^{3+} onto bentonite clay were not evaluated due to the fact that Fe^{3+} precipitates beyond pH> 3. The results corroborate the findings of Rauf and Tahir. (2004) who found that optimum conditions of adsorbing Fe^{3+} onto bentonite clay is 15 minutes of contact time, 3 grams of adsorbent dosage

4.2 Physico-chemical characterization of raw and modified bentonite clay

4.2.1 Cation Exchange Capacity (CEC)

Cation exchange capacity (CEC) refers to the total quantity of positively charged species that soil can retain on their surfaces at a given pH by electrostatic force. It also measures the soil capacity to exchange cations with soil solutions. CEC is dependent on soil organic matter and it varies with different types of soil. Sandy soils have low CEC because they are not rich in organic matter whereas clay soils have high CEC because they are rich in organic matter. The clay and organic matter of the soil supplies the negative charges at their edge and surfaces, opposite charges attract each other, as such, negatively charged species will attract electro positive species that are in a solution and loosely hold them on their surfaces (Chapman, 1962). However, those cations are held in an exchangeable state and they can be replaced through isomorphous substitution (Bradley and Weils, 2004). Table 4.1 shows the content of exchangeable base cations that are adsorbed on the raw and modified bentonite clay interlayers.

© University of Venda

Table 4.1: CEC of raw and modified bentonite clay in Milli-Equivalent (meq/100g)

Raw	**Na^+**	**K^+**	**Ca^{2+}**	**Mg^{2+}**	**CEC(meq/100g)**
5.4	115.2	3.3	57.1	86.4	262
7.4	117.7	3.7	56.2	87.9	265.5
Al-Bentonite					
5.4	45.1	2.6	57.1	82.1	186.9
7.4	44	2.5	57.8	79	183.3
Fe-Bentonite					
5.4	49.2	2.8	57.8	85.7	195.5
7.4	46.6	2.6	56.8	82.9	188.9

The exchangeable cations identified in bentonite clay were Na^+, Ca^{2+}, Mg^{2+} and K^+. The concentrations of the exchangeable cations were measured in milli-equivalent per 100g (meq/100g). Before modification, bentonite clay was having a very high CEC with Na significantly present at relatively high concentration amongst the other base cations at both pH, followed by Mg, Ca and K. The higher Na content on bentonite is a good indication that the bentonite clay used in this study is sodium-type bentonite clay. Moreover, the CEC results obtained at different pH reveals that CEC is not a function of pH since it was relatively equal at both pH values. This study corroborated a study conducted by Foth (1951) which states that the CEC of expendable clay is independent of pH. After modification, there was a drastic decrease in Na content on bentonite clay hence revealing that the monovalence Na is the element which is exchanged within bentonite clay interlayers during impregnation of Al^{3+}/Fe^{3+} hence enhancing its ability and affinity to adsorb inorganic contaminants from the solution.

© University of Venda

4.2.2 Elemental composition of raw and modified bentonite clays

The concentration of major and trace elements in bentonite clay are shown in Tables 4.4 and 4.5.

Table 4.2: XRF analysis of raw and modified bentonite clay

% Composition	Raw bentonite clay	Al^{3+} bentonite clay	Fe^{3+} bentonite clay
SiO_2	66.51	66.01	67.26
TiO_2	0.14	0.14	0.13
Al_2O_3	16.81	17.22	16.99
Fe_2O_3	3.26	3.28	3.76
MnO	0.13	0.12	0.13
MgO	3.12	3.03	3.12
CaO	1.43	1.30	1.33
Na_2O	1.17	0.46	0.43
K_2O	0.54	0.51	0.46
P_2O_5	0.03	0.03	0.03
Cr_2O_3	*<0.01*	*<0.01*	*<0.01*
NiO	*<0.01*	*<0.01*	*<0.01*
V_2O_5	*<0.01*	*<0.01*	*<0.01*
ZrO_2	0.02	0.02	0.02
CuO	*<0.01*	*<0.01*	*<0.01*
LOI	7.19	7.55	6.96
TOTAL	**100.35**	**99.68**	**100.62**

© University of Venda

Table 4.3: Trace elements in raw and modified bentonite clay

Concentration(ppm)	Raw bentonite clay	Al^{3+} bentonite clay	Fe^{3+} bentonite clay
As	6.25	12.51	12.21
Cu	2.00	2.76	2.00
Ga	11.01	12.33	9.20
Mo	1.00	1.00	1.00
Nb	2.00	2.00	2.00
Ni	3.00	3.00	3.00
Pb	15.15	21.72	13.09
Rb	2.00	2.00	2.00
Sr	14.58	18.08	5.52
Th	3.00	3.00	3.00
U	3.00	3.00	3.00
W*	6.00	6.00	6.00
Y	3.00	4.07	3.00
Zn	30.15	34.39	27.65
Zr	75.36	83.60	55.19
Cl*	7.58	7.58	7.58
Co	2.36	2.36	2.36
Cr	6.84	6.84	6.84
F*	100.00	100.00	100.00
S*	16.00	612.59	16.00
Sc	6.05	6.53	7.24
V	16.81	16.81	16.81
Cs	36.64	35.72	28.68
Ba	353.18	395.94	407.26
La	41.94	49.18	50.34
Ce	82.34	89.62	86.50

© University of Venda

University of Venda
Creating Future Leaders

XRF results revealed that raw bentonite clay contains a high concentration of SiO_2 and Al_2O_3. Low concentration of Fe_2O_3, MgO, CaO, Na_2O, K_2O, P_2O_5 and ZrO_2 are also available and indicate variable cation contents, which could contribute to adsorption capacity (Silva, 2011). The availability of P_2O_5 suggests the presence of phosphate minerals (Alloways, 1995). The obtained XRF results also show the presence of a wide range of minor elements that are available on clay fractions (Table 4.5). After modification, the results revealed that the contents of Al^{3+} and Fe^{3+} increased from 16.81 to 17.22 and 3.26 to 3.76 respectively, whereas the content of NaO decreased drastically from 1.17 to 0.46 and 0.43. This implies that during the impregnation process the cation exchanged to a greater extent was Na^{+}.

4.2.3 Surface area of raw and modified bentonite clay

Specific surface area of soil is the sum of total surface area of soil particles per unit mass. It is expressed in m^2/g. Specific surface area can also be expressed as the measure of exposed surface area that can be covered by ionic soil solution. Specific surface area of mineral is an essential parameter to quantify interaction processes at the liquid-solid interface because it influences the adsorption of molecules and many other physical and chemical processes that takes place in the soil surfaces (Bohn et al., 1979). Surface area is a surface phenomenon and it is dependent upon soil particle size, the smaller the soil particle size the higher the surface area and the bigger the soil particle size the smaller the surface area. In contrast to sand, clay minerals have the smallest particle size which contributes to large surface area. The large specific surface area of soil provides sites in which molecules from soil solution can bind through weak van der Waal forces. Clay soils consists of charged colloid fractions which contain electrostatic surface charge, a property which accounts for adsorption, binding, and exchange of ions and molecules on particle surface (WHO, 2005). Table 4.6 shows the surface areas of raw and modified bentonite clay

Table 4.4: BET specific surface area and micro-pore area of raw and modified bentonite clay

Surface area	Raw bentonite	Al^{3+} Modified bentonite	Fe^{3+} Modified bentonite
BET (Total)	16	44.3	50
External surface area	11.09	33.1	37.4
Micro-pore area	4.9	11.2	12.5

© University of Venda

The surface area of a clay material is one of the most significant properties that influence adsorption of alien species to clay fractions. The calculated surface area of bentonite clay was 16 m^2/g, but when Al^{3+} and Fe^{3+} polycations were introduced the surface area increased to 44.3 m^2/g for Al^{3+} bentonite and 50 m^2/g for Fe^{3+} bentonite. An increase in surface area is due to an increase in micro-pore area in the interlayers of modified bentonite clay hence enhancing and increasing the efficiency of bentonite clay to scavenge negatively charged species from solutions. The relatively greater surface area obtained in this study indicates that the bentonite understudy is capable of holding more water thereby promoting higher chemical reactivity between bentonite surfaces and soil solution. In addition, the higher surface area also indicates that the modified bentonite clay can present large surface area that can be covered by toxic pollutants present in a solution. The higher surface area in bentonite clay is evident of the higher CEC as well as higher water holding capacity results obtained in this study. This correlates to study conducted by Chapman (1962) which observed that the higher the surface area, the higher the CEC and the higher the water holding capacity.

4.2.4 Water holding capacity

Water holding capacity (WHC) refers to the ability of a particular type of soil to hold water against the force of gravity. Different types of soil have different water holding capacities. For example, sandy soil has low water holding capacity as compared to clay soil. The nature of soil, composition of soil, amount of organic matter, surface area and soil particle size plays a significant role in maintaining the ability of soil to retain water. Principally, the availability of organic matters and clay minerals enhances the sorption ability of soil because they provide the soil with high CEC and surface area. High CEC and surface area allows soil to attract polar substances such as water molecules and hold them closely to individual soil particle by the force of cohesion induced by the charges embedded within soil colloids. Research studies have shown that bentonite clay can absorb water and expand by 30 percent its original size. This enables the percolating solution to have sufficient time to exchange ions with clay fractions (WHO, 2005).

From the present study, the obtained results revealed that out of 100 % of water added, Bentonite clay managed to retain 42.7 % of water in its matrix. This physical ability of bentonite clay to absorb and retain water in its matrix enables it to have more time to react and scavenge the

© University of Venda

contaminants that are in a solution hence purifying the water bodies and setting them free from pollutants. Higher water holding capacity of bentonite clay is an attribute of high surface area, high CEC and swelling properties of bentonite clay. These good physicochemical properties of bentonite clay allow it to attract water molecules and retain it on their surfaces due to weak Vander Waal forces (Bradley and Weils, 2004). The higher water holding capacity also provides greater opportunity for toxic ionic species that are in a solution to react with charged species that are embedded on clay matrices so as to remove the contaminants. This statement was also supported by Bhattacharyhya and Gupta, (2008).

4.2.5 Point of zero charge (PZC) of raw and modified bentonite clay

PZC refers to the suspension pH where the clay has zero net charges on the surfaces (Sparks, 1997). Above the PZC, the clay is negatively charged and below PZC the clay is positively charged (Bohn et al., 1979). Figure 4.21, 4.22 and 4.23 shows the point of zero charge of raw and modified bentonite clay.

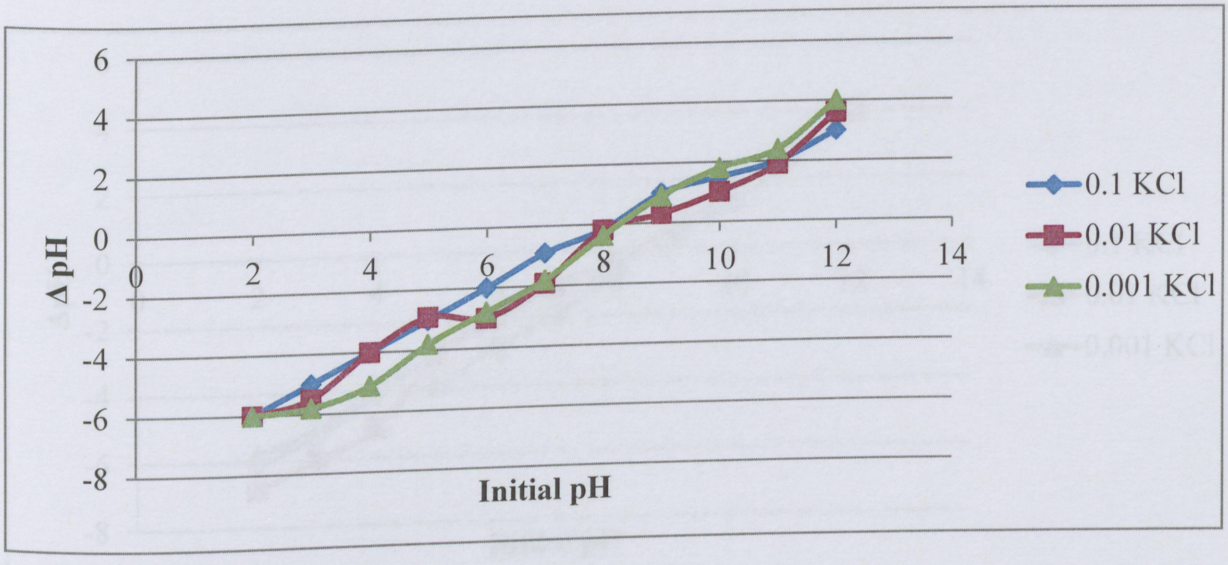


Figure 4.21: PZC of Raw bentonite clay

© University of Venda

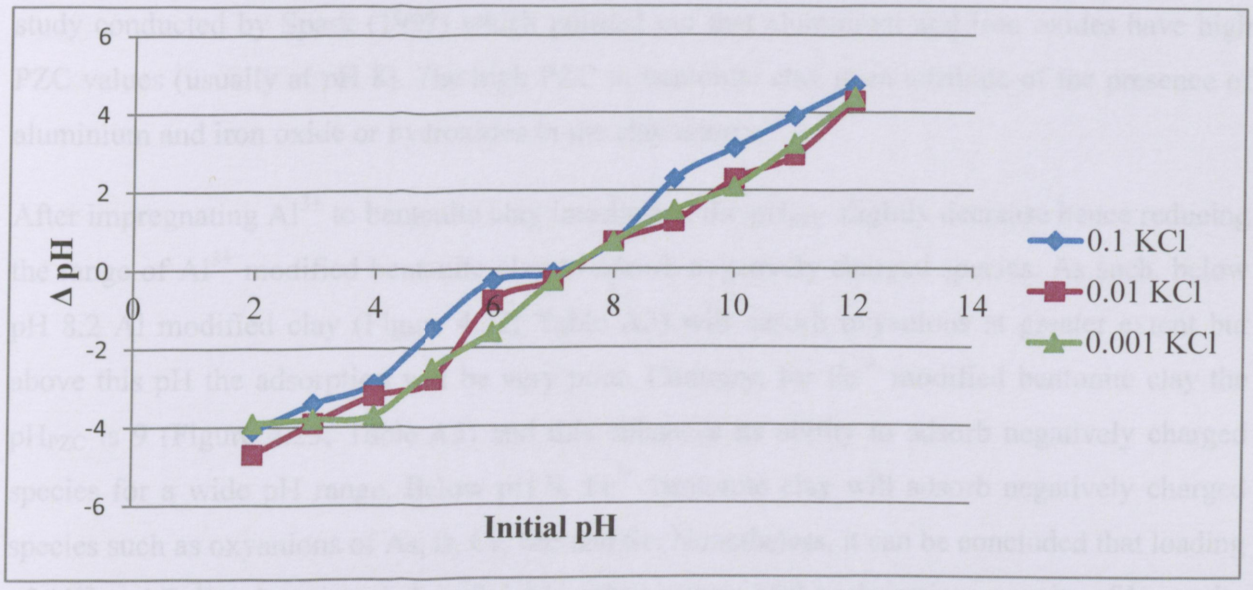


Figure 4.22: PZC of Al^{3+} bentonite clay

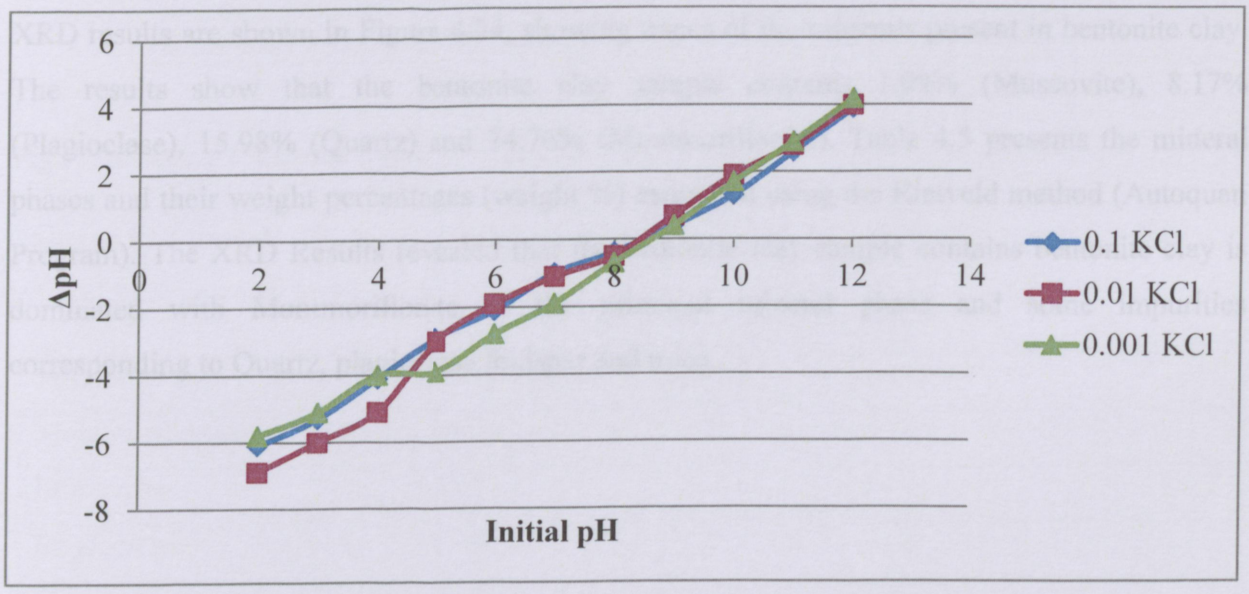


Figure 4.23: PZC of Fe^{3+} bentonite clay

The obtained results shows that the materials understudy have PZC at pH 8.0 for raw bentonite clay (Figure 4.21; Table A1), 8.2 for Al^{3+} modified bentonite clay (Figure 4.22; Table 2A) and 9 for Fe^{3+} modified bentonite clay (Figure 4.23; Table 3A). This collaborate findings in a research

© University of Venda

study conducted by Spark (1997) which pointed out that aluminium and iron oxides have high PZC values (usually at pH 8). The high PZC in bentonite clay is an attribute of the presence of aluminium and iron oxide or hydroxides in the clay matrix.

After impregnating Al^{3+} to bentonite clay interlayers, the pH_{PZC} slightly decrease hence reducing the range of Al^{3+} modified bentonite clay to adsorb negatively charged species. As such, below pH 8.2 Al modified clay (Figure 4.22; Table A2) will adsorb oxyanions at greater extent but above this pH the adsorption will be very poor. Contrary, for Fe^{3+} modified bentonite clay the pH_{PZC} is 9 (Figure 4.23; Table A3) and this enhances its ability to adsorb negatively charged species for a wide pH range. Below pH 9, Fe^{3+} bentonite clay will adsorb negatively charged species such as oxyanions of As, B, Cr, Mo and Se. Nonetheless, it can be concluded that loading of Al^{3+} and Fe^{3+} polycations is beneficial in enhancement of the adsorption capacity of bentonite clay for negatively charged chemical species.

4.2.6 Mineralogical composition of bentonite clay

XRD results are shown in Figure 4.24, showing traces of the minerals present in bentonite clay. The results show that the bentonite clay sample contains 1.09% (Muscovite), 8.17% (Plagioclase), 15.98% (Quartz) and 74.76% (Montmorillonite). Table 4.5 presents the mineral phases and their weight percentages (weight %) estimated using the Rietveld method (Autoquan Program). The XRD Results revealed that the bentonite clay sample contains bentonite clay is dominated with Montmorillonite as the principal mineral phase and some impurities corresponding to Quartz, plagioclase feldspar and mica.

© University of Venda

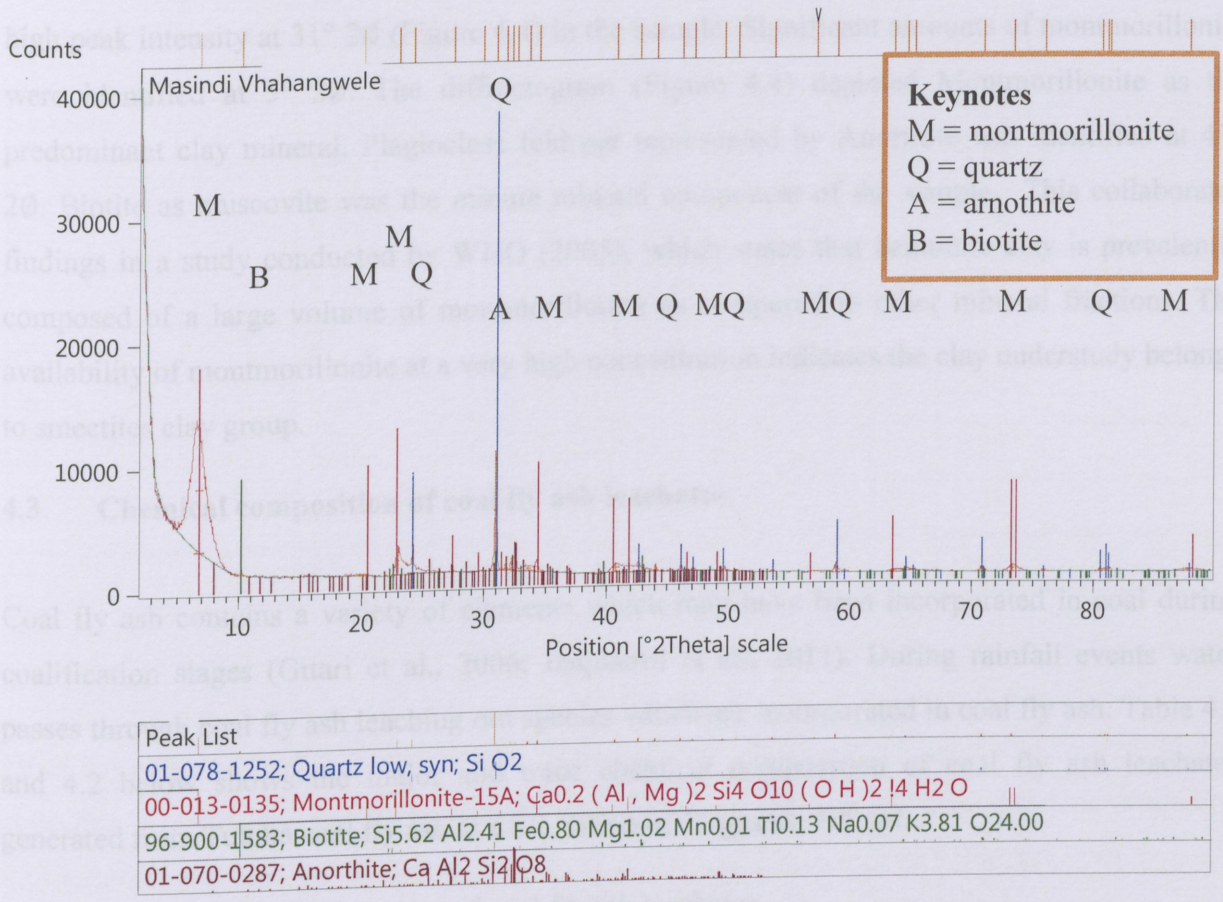


Figure 4.24: XRD diffractogram of bentonite clay.

Table 4.5: Minerals phases and their percentages (weight %) estimated using the Rietveld method (Autoquan Program).

Mineral	Weight %	3 σ error
Montmorillonite	74.76	1.08
Muscovite	1.09	0.42
Plagioclase	8.17	0.84
Quartz	15.98	0.66

The observed mineralogical assemblages in bentonite clay are muscovite, plagioclase, quartz and Montmorillonite as the major mineral phase amongst the others. The results showed that bentonite clay is dominated by Montmorillonite (Table 4.5). Abundant quartz was identified by

© University of Venda

high peak intensity at 31° 2Ø (Figure 4.4) in the sample. Significant amounts of montmorillonite were identified at 5° 2Ø. The diffractogram (Figure 4.4) depicted Montmorillonite as the predominant clay mineral. Plagioclase feldspar represented by Anorthite was identified at 49° 2Ø. Biotite as muscovite was the minute mineral component of the sample. This collaborates findings in a study conducted by WHO (2005), which states that bentonite clay is prevalently composed of a large volume of montmorillonite as compared to other mineral fractions. The availability of montmorillonite at a very high concentration indicates the clay understudy belongs to smectites clay group.

4.3 Chemical composition of coal fly ash leachates

Coal fly ash contains a variety of elements which may have been incorporated in coal during coalification stages (Gitari et al., 2006; Iziquierol et al., 2011). During rainfall events water passes through coal fly ash leaching out species which are incorporated in coal fly ash. Table 4.6 and 4.2 below shows the major and trace chemical composition of coal fly ash leachates generated from Tutuka coal fly ash at a S/L ration of 10 grams: 100 mL.

Table 4.6: Major chemical species of coal fly ash leachates

Element	Concentration (mg/L)	Element	Concentration (mg/L)
Al	8.6	Mn	0.01
B	1.73	Na	2.0
Ba	0.7	Ni	0.002
Ca	311.9	P	0.2
Fe	0.1	Si	1.6
K	0.7	Sr	4.4
Mg	0.1	Ti	0.01

© University of Venda

Table 4.7: Minor chemical species of coal fly ash leachates

Element	Concentration (µg/L)	Element	Concentration (µg/L)
Li	231.3	Mo	165
Be	0.04	Pd	0.18
V	13.8	Cd	0.01
Cr	271	Sn	0.01
Co	0.2	Pt	0.001
Cu	8.3	Au	0.09
Zn	2.2	Hg	0.01
As	53	Pb	0.04
Se	170		

N = 3 ± SD

From the obtained results, it was observed that coal fly ash leachates are enriched with higher concentrations of Ca as compared to the other leached elements which are available. Furthermore, it is also enriched with a wide range of other major and trace elements which might have been partitioned within coal fly ash during the ashing process. Moreover, As, B, Cr, Mo, and Se were also observed to be present in concentration which is above the DWAF prescribed standards (DWAF, 1996) hence dictating that leaching of those species from coal fly ash can pose detrimental impacts to living organisms that thrives or utilizes surface and underground water bodies. Insignificant impurities in coal fly ash were also observed but in very low concentrations.

© University of Venda

University of Venda
Creating Future Leaders

CHAPTER FIVE

Adsorption of As, B, Cr, Mo and Se onto Al^{3+} modified bentonite clay: optimization of adsorption conditions and application for coal fly ash leachates remediation

5.0 Introduction

In this chapter, factors which influence the adsorption of As, B, Cr, Mo and Se onto Al^{3+} modified bentonite clay were evaluated in attempt to determine the optimum condition for removal of As, B, Cr, Mo and Se from coal fly ash leachates. The optimization conditions were determined using synthetic solutions consisting As, B, Cr, Mo and Se at various concentrations.

5.1 Adsorption of oxyanions As, B, Cr, Mo and Se using Al^{3+} modified bentonite clay

5.1.1 Adsorption of As, B, Cr, Mo, Se as a function of contact time

Effects of contact time on the adsorption of As, B, Cr, Mo and Se by Al^{3+} modified bentonite clay and raw bentonite clay (Initial concentration of 10 mg/L, adsorbent dosage of 1g/100 mL, 26°C and 250 rpm). The uptake of As, B, Cr, Mo and Se onto modified and raw bentonite clay was evaluated for three hours at the intervals of 1, 5, 10, 15, 30, 60, and 180 minutes (Table A12 and A17) . Figure 5.1, 5.2, 5.3 and 5.4 shows the variation of As, B, Cr, Mo, Se, pH, EC and TDS with an increase in contact time.

© University of Venda

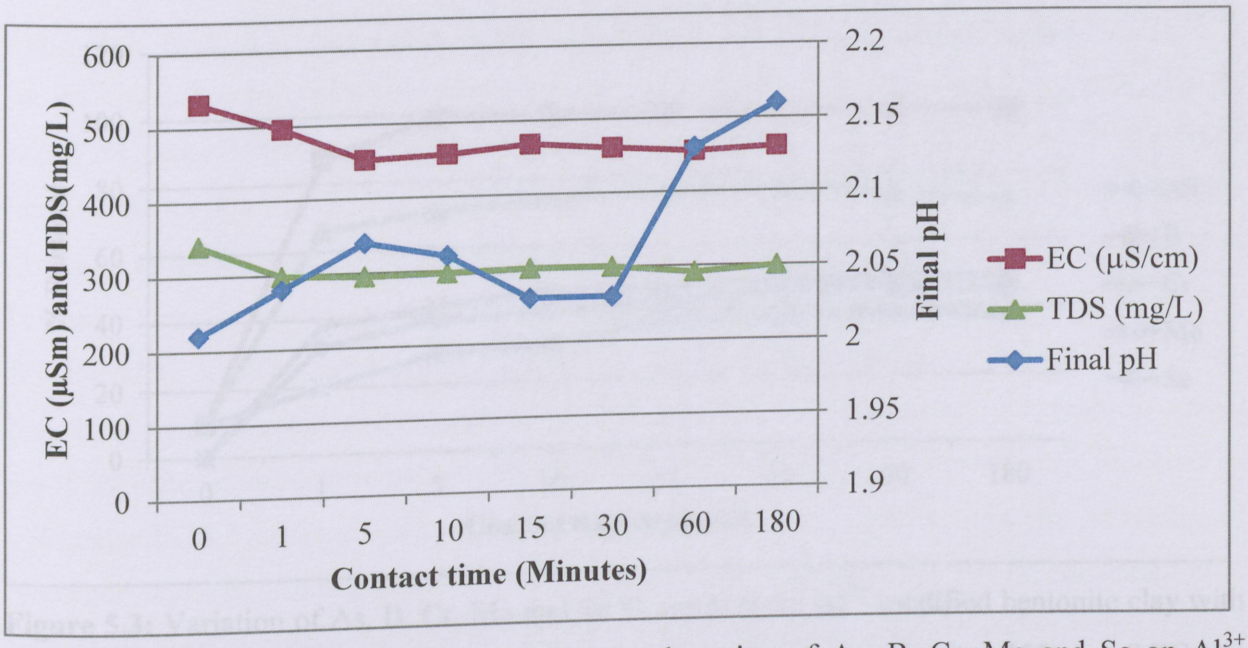


Figure 5.1: Variation of pH, EC and TDS on adsorption of As, B, Cr, Mo and Se on Al^{3+} modified bentonite clay with contact time (1 gram of adsorbent dosage, 10 mg/L adsorbate concentrations, 26°C and 1g/100 mL S/L ratio).

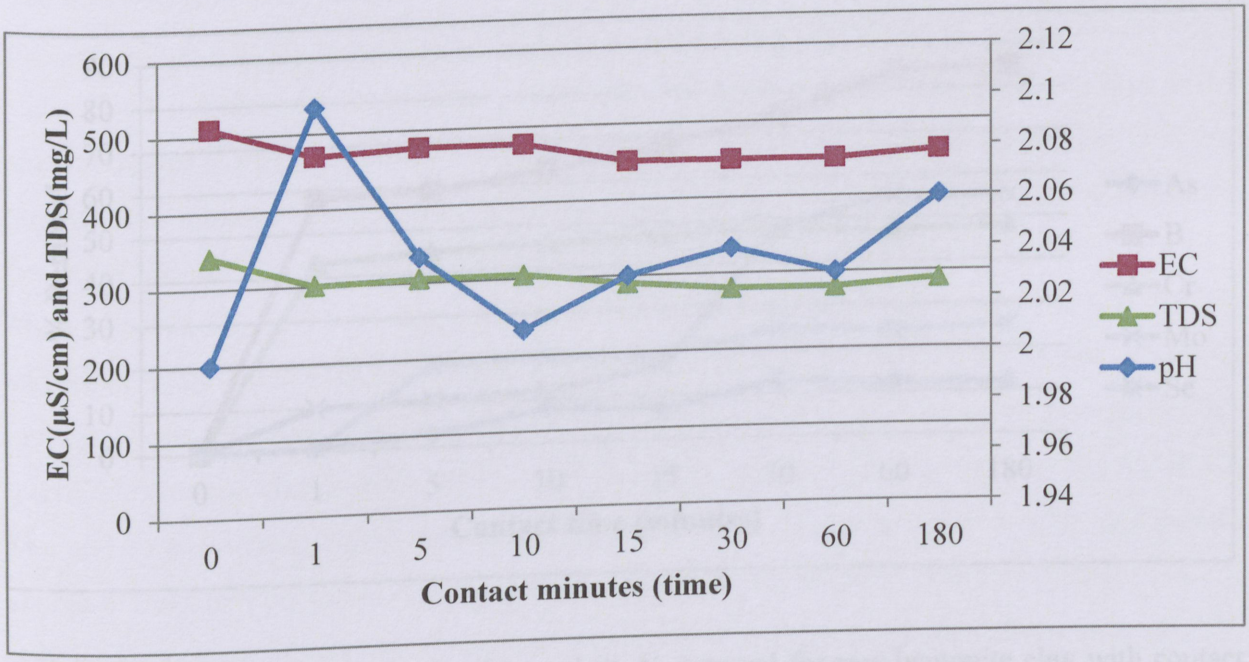


Figure 5.2: Variation of pH, EC and TDS on adsorption of As, B, Cr, Mo and Se on raw bentonite clay with contact time (1 gram of adsorbent dosage, 10 mg/L adsorbate concentrations, 26°C and 1g/100 mL S/L ratio).

© University of Venda

University of Venda
Creating Future Leaders

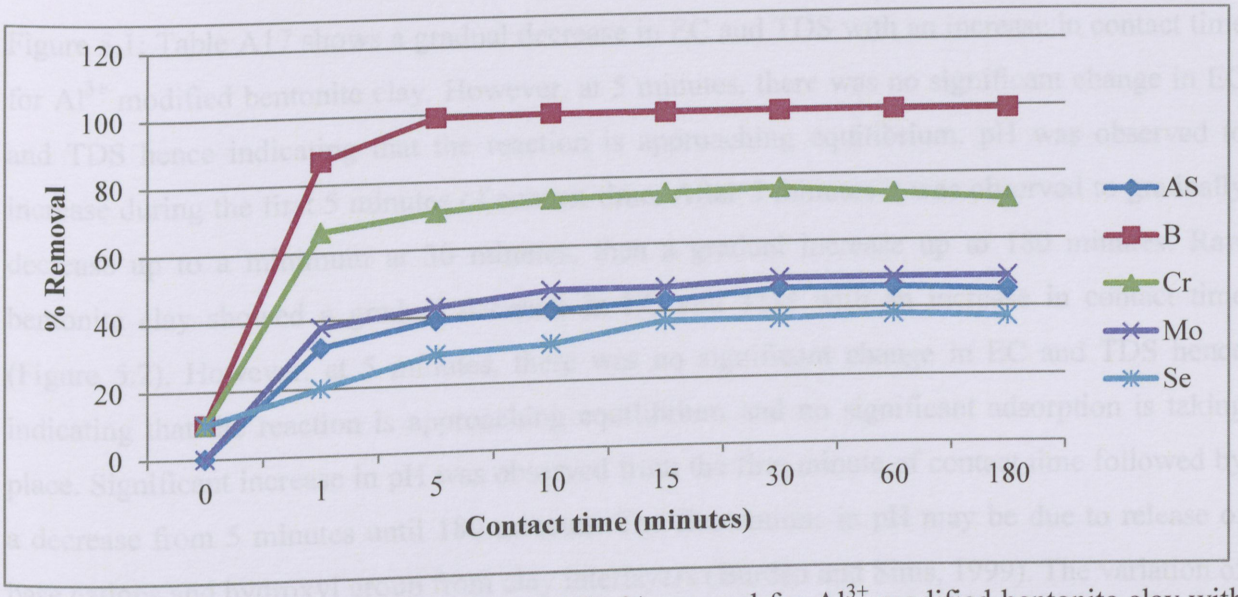


Figure 5.3: Variation of As, B, Cr, Mo and Se % removal for Al^{3+} modified bentonite clay with contact time (1 gram of adsorbent dosage, 10 mg/L adsorbate concentration, 250 rpm, 26°C and 1g/100 mL S/L ratio).

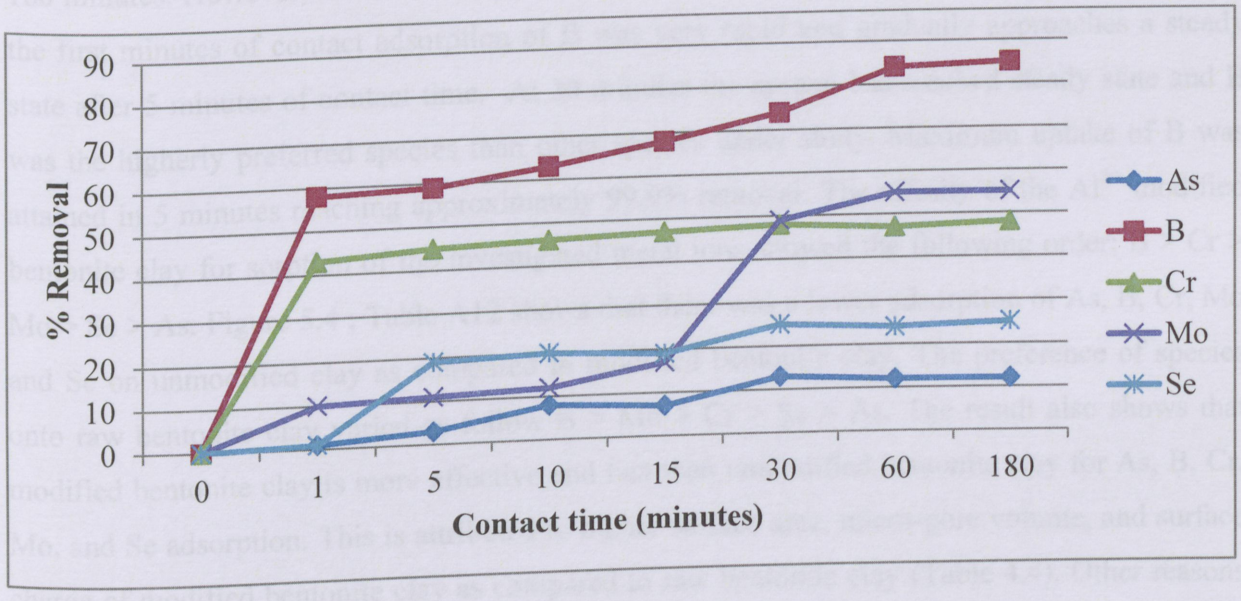


Figure 5.4: Variation of As, B, Cr, Mo and Se % removal for raw bentonite clay with contact time (1 gram of adsorbent dosage, 10 mg/L adsorbate concentration, 26°C and 1g/100 mL S/L ratio).

UNIVERSITY OF VENDA
LIBRARY

© University of Venda

Figure 5.1; Table A17 shows a gradual decrease in EC and TDS with an increase in contact time for Al^{3+} modified bentonite clay. However, at 5 minutes, there was no significant change in EC and TDS hence indicating that the reaction is approaching equilibrium. pH was observed to increase during the first 5 minutes of contact time. After 5 minutes it was observed to gradually decrease up to a minimum at 30 minutes, then a gradual increase up to 180 minutes. Raw bentonite clay showed a gradual decrease in EC and TDS with an increase in contact time (Figure 5.2). However, at 5 minutes, there was no significant change in EC and TDS hence indicating that the reaction is approaching equilibrium and no significant adsorption is taking place. Significant increase in pH was observed from the first minute of contact time followed by a decrease from 5 minutes until 180 minutes. The fluctuations in pH may be due to release of base cations and hydroxyl group from clay interlayers (Burden and Sims, 1999). The variation of percentage uptake of the selected ions as a function of contact time is indicated in figure 5.3 and 5.4; Table A17 and A12. From figure 5.3 is showing that the sorption of As, B, Cr, Mo and Se onto Al^{3+} bentonite clay increases with an increase in contact time to reach a steady state at 15 to 180 minutes. However, the time of equilibration varies with chemical species. It is clear, that in the first minutes of contact adsorption of B was very rapid and gradually approaches a steady state after 5 minutes of contact time. At 30 minutes the system has reached steady state and B was the higherly preferred species than other species under study. Maximum uptake of B was attained in 5 minutes reaching approximately 99.9% removal. The affinity of the Al^{3+} modified bentonite clay for sorption of the investigated metal ions showed the following order: B > Cr > Mo > Se > As. Figure 5.4 ; Table A12 shows that there was a lower adsorption of As, B, Cr, Mo and Se on unmodified clay as compared to modified bentonite clay. The preference of species onto raw bentonite clay varied as follow B > Mo > Cr > Se > As. The result also shows that modified bentonite clay is more effective and fast than unmodified bentonite clay for As, B, Cr, Mo, and Se adsorption. This is attributed to higher surface area, micro-pore volume, and surface charge of modified bentonite clay as compared to raw bentonite clay (Table 4.4). Other reasons may be an increase in density of sorption site which is enhanced by polycations such as Al^{3+}. Based on the obtained results, 30 minutes of contact time was observed to be the optimum adsorption conditions for removing As, B, Cr, Mo and Se from aqueous media using Al^{3+} modified bentonite clay. Raw bentonite clay revealed that 60 minutes of contact time will be the optimum contact time for removing those chemical species from aqueous media.

© University of Venda

5.1.2 Adsorption of As, B, Cr, Mo, Se as a function of adsorbent dosage

Effects of adsorbent dosage on the adsorption of As, B, Cr, Mo and Se by Al^{3+} modified bentonite clay and raw bentonite clay was evaluated at an initial concentration of 10 mg/L, 30 minutes of contact time, 250 rpm and 26°C . The uptake of As, B, Cr, Mo and Se onto modified and raw bentonite clay was evaluated by varying the adsorbent dosage from 0.5, 1, 2, 3, 4, and 5 grams (Table A13 and A18). Figure 5.5, 5.6, 5.7 and 5.8 shows the variation of As, B, Cr, Mo, Se, pH, EC and TDS with an increase in adsorbent dosage.

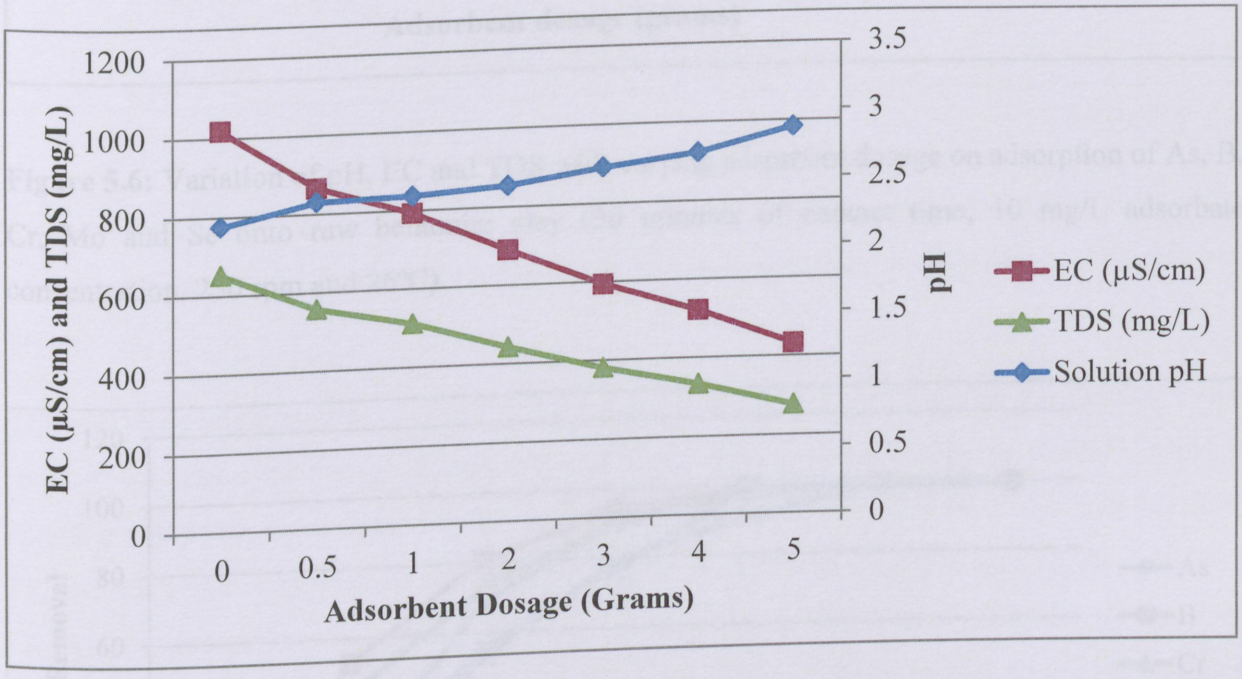


Figure 5.5: Variation of pH, EC and TDS with varying adsorbent dosage on adsorption of As, B, Cr, Mo and Se onto Al^{3+} modified bentonite clay (30 minutes of contact time, 10 mg/L adsorbate concentration, 250 rpm and 26°C).

© University of Venda

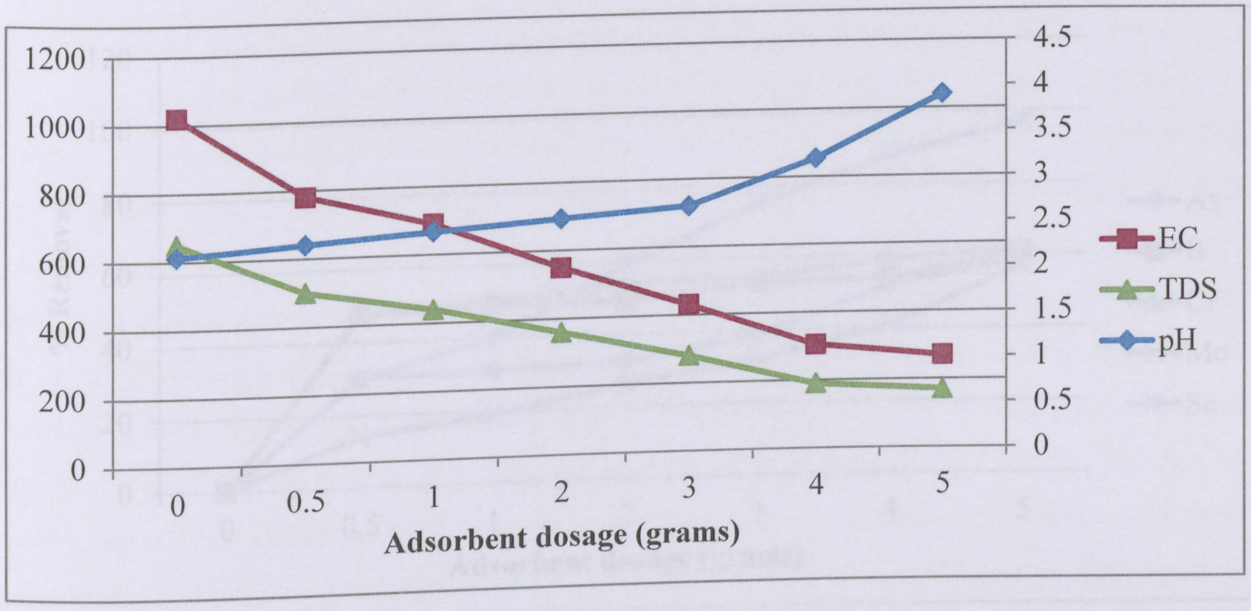


Figure 5.6: Variation of pH, EC and TDS with varying adsorbent dosage on adsorption of As, B, Cr, Mo and Se onto raw bentonite clay (30 minutes of contact time, 10 mg/L adsorbate concentration, 250 rpm and 26°C).

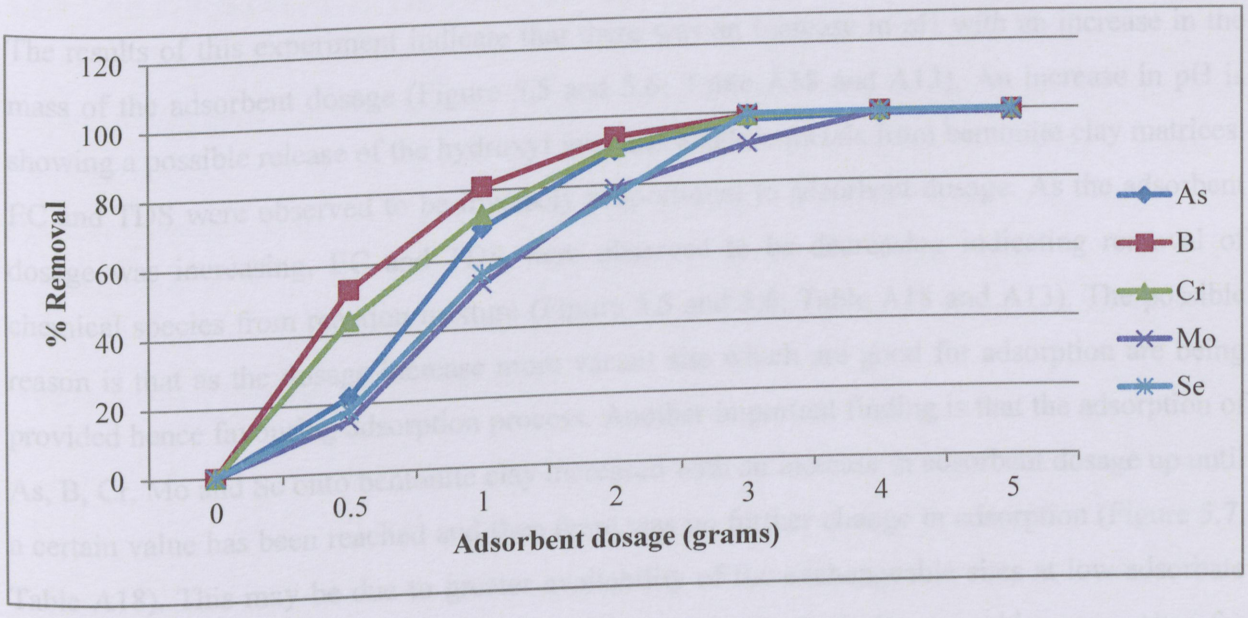


Figure 5.7: Variation of As, B, Cr, Mo and Se % adsorption for Al^{3+} bentonite as a function of adsorbent dosage (30 minutes of contact time, 10 mg/L adsorbate concentration, 250 rpm and 26°C).

© University of Venda

University of Venda
Creating Future Leaders

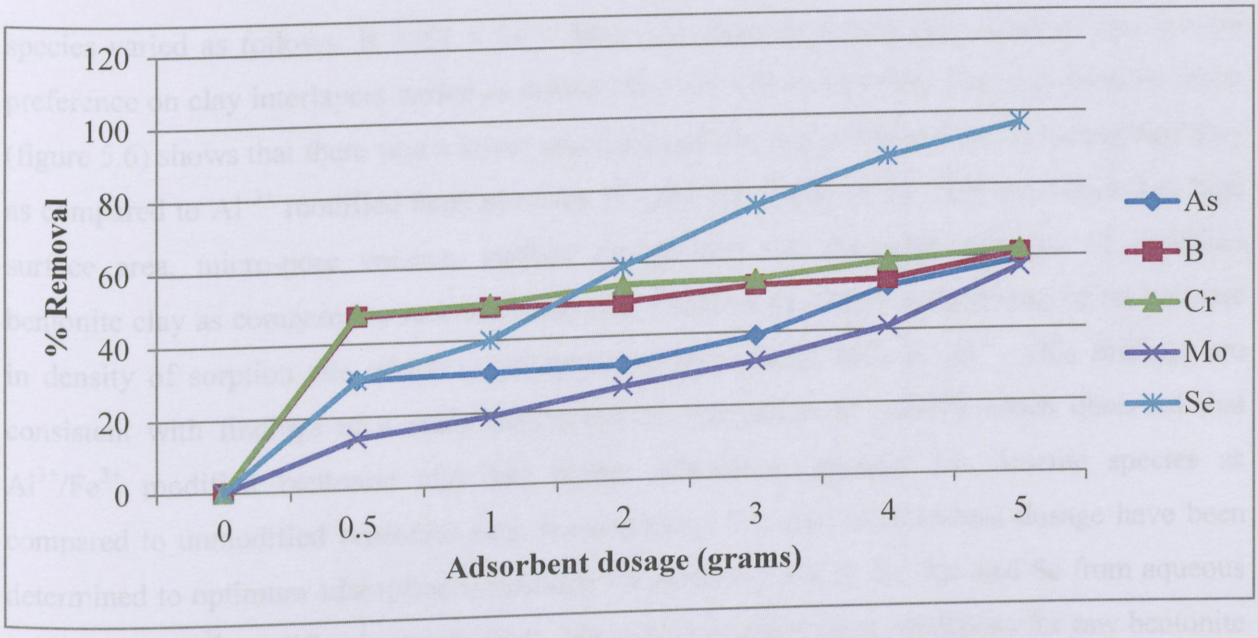


Figure 5.8: Variation of As, B, Cr, Mo and Se % adsorption for raw bentonite as a function of adsorbent dosage (30 minutes of contact time, 10 mg/L adsorbate concentration, 250 rpm and 26°C).

The results of this experiment indicate that there was an increase in pH with an increase in the mass of the adsorbent dosage (Figure 5.5 and 5.6; Table A18 and A13). An increase in pH is showing a possible release of the hydroxyl ions and alkaline metals from bentonite clay matrices. EC and TDS were observed to be inversely proportional to adsorbent dosage. As the adsorbent dosage was increasing, EC and TDS were observed to be decreasing indicating removal of chemical species from reaction mixture (Figure 5.5 and 5.6; Table A18 and A13). The possible reason is that as the dosage increase more vacant site which are good for adsorption are being provided hence favouring adsorption process. Another important finding is that the adsorption of As, B, Cr, Mo and Se onto bentonite clay increased with an increase in adsorbent dosage up until a certain value has been reached and then there was no further change in adsorption (Figure 5.7; Table A18). This may be due to greater availability of the exchangeable sites at low adsorbate concentration and high adsorbent dosage. Increase of adsorbent dose provides more sites for adsorption. As seen from figure 5.5, 4g/100 mL of Al^{3+} modified bentonite clay was enough for quantitative adsorption of As, B, Cr, Mo and Se whereas 4 grams was not enough for quantitative analysis in raw bentonite clay. The adsorption affinity for modified clay for various

© University of Venda

species varied as follows: B > Cr > Se = Mo > As. Raw bentonite clay revealed that species preference on clay interlayers varied as follow: Se > Cr > B > As > Mo. The experimental result (figure 5.6) shows that there was a lower adsorption of As, B, Cr, Mo and Se on unmodified clay as compared to Al^{3+} modified bentonite clay (Figure 5.8; Table A13). This is attributed to high surface area, micro-pore volume, surface charge and ion exchange capacity of modified bentonite clay as compared to raw bentonite clay (Table 4.6). Other reasons may be an increase in density of sorption site which is enhanced by polycations such as Al^{3+}. This findings are consistent with findings of a study conducted by Ramesh et al. (2007) which observed that Al^{3+}/Fe^{3+} modified bentonite clay has higher adsorption capacity for Arsenic species as compared to unmodified bentonite clay, consequently, 4 grams of adsorbent dosage have been determined to optimum adsorption conditions for removing As, B, Cr, Mo and Se from aqueous media using Al^{3+} modified bentonite clay. The optimum adsorption conditions for raw bentonite clay were determined to be 5 grams for effective adsorption of those chemical species from the solution.

5.1.3 Adsorption of As, B, Cr, Mo, Se as a function of adsorbate concentration

Effects of adsorbate concentration on the adsorption of As, B, Cr, Mo and Se by Al^{3+} modified bentonite clay and raw bentonite clay was evaluated at a contact time of 30 minutes ,4 grams of adsorbent dosage, 250 rpm, 26°C and 4g/100 mL S/L ratios (Table A15 and A20). The concentrations of As, B, Cr, Mo and Se were varied from 0.1 to 15 mg/L. Figure 5.9, 5.10, 5.11, 5.12, 5.13 and 5.14 shows the variation of As, B, Cr, Mo, Se, initial and final pH, EC and TDS with an increase in adsorbate concentration.

© University of Venda

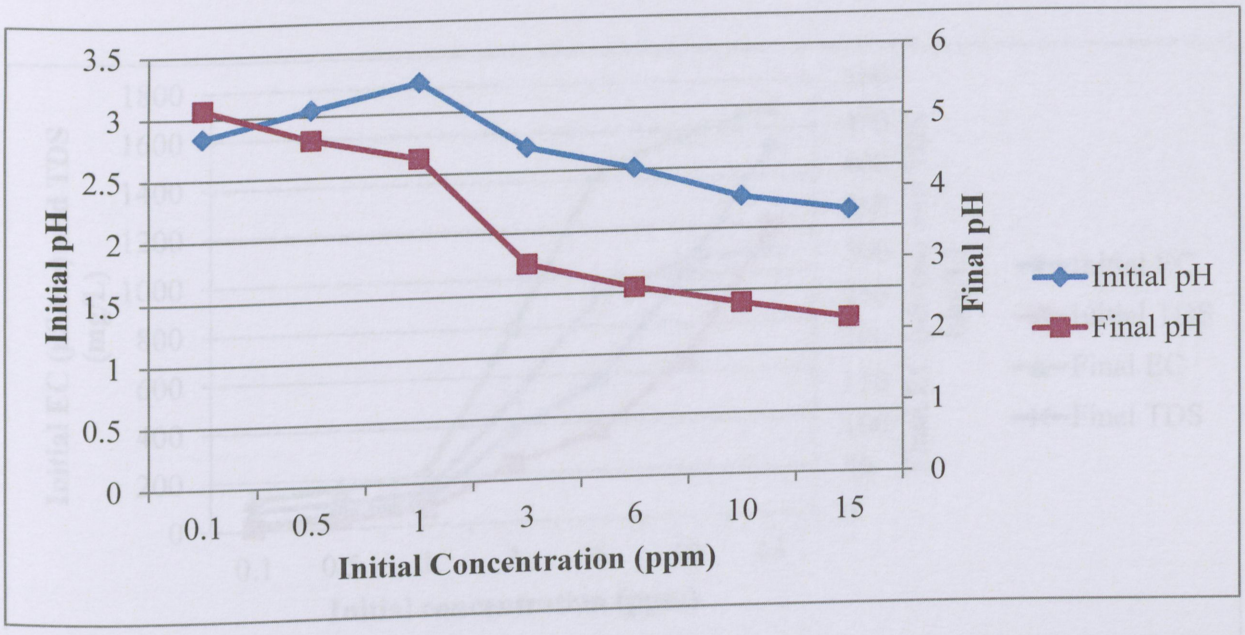


Figure 5.9: Variation of initial and final pH profiles with an increase in adsorbate concentration for Al^{3+} modified bentonite clay (30 minutes of contact time, 4 grams of adsorbent dosage, 250 rpm, 26°C and 4g/100 mL S/L ratios).

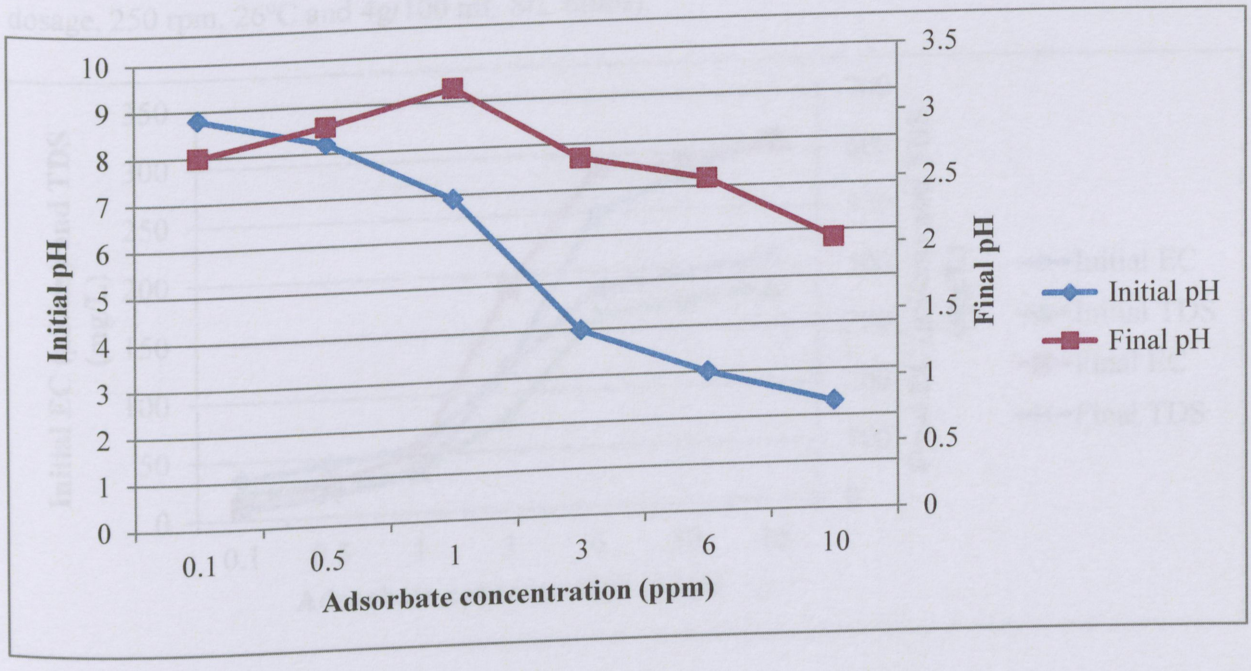


Figure 5.10: Variation of initial and final pH profiles with an increase in adsorbate concentration for raw bentonite clay (30 minutes of contact time, 4 grams of adsorbent dosage, 250 rpm, 26°C and 4g/100 mL S/L ratios).

© University of Venda

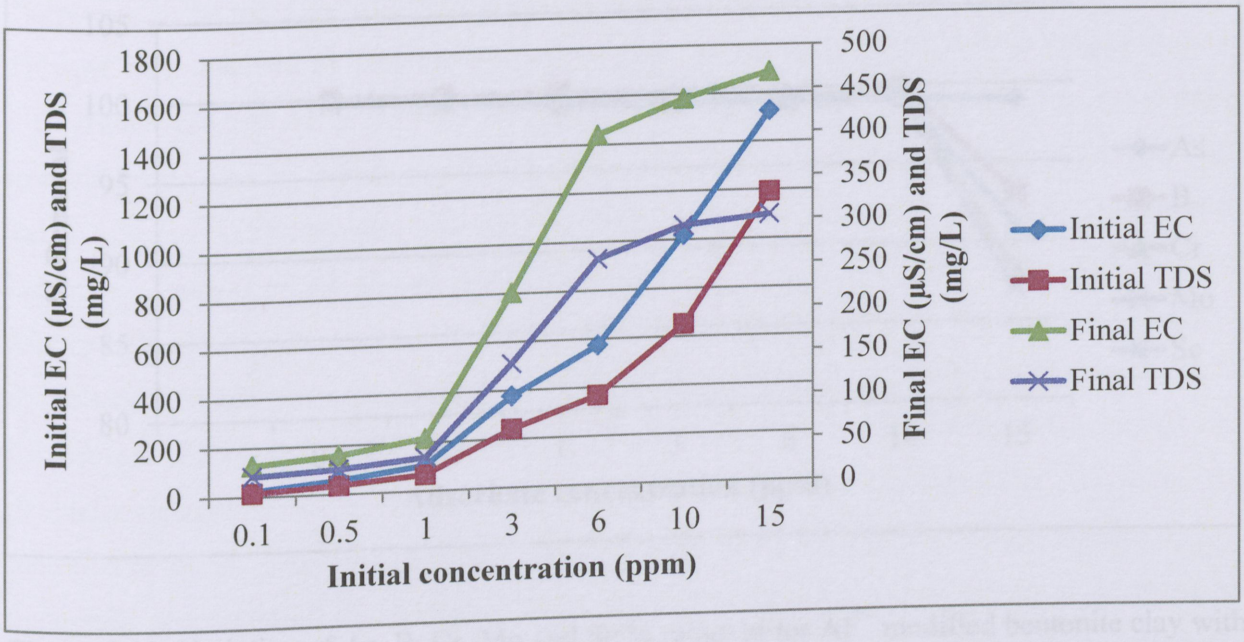


Figure 5.11: Variation of initial and final EC and TDS with an increase in adsorbate concentration for Al^{3+} modified bentonite clay (30 minutes of contact time, 4 grams of adsorbent dosage, 250 rpm, 26°C and 4g/100 mL S/L ratios).

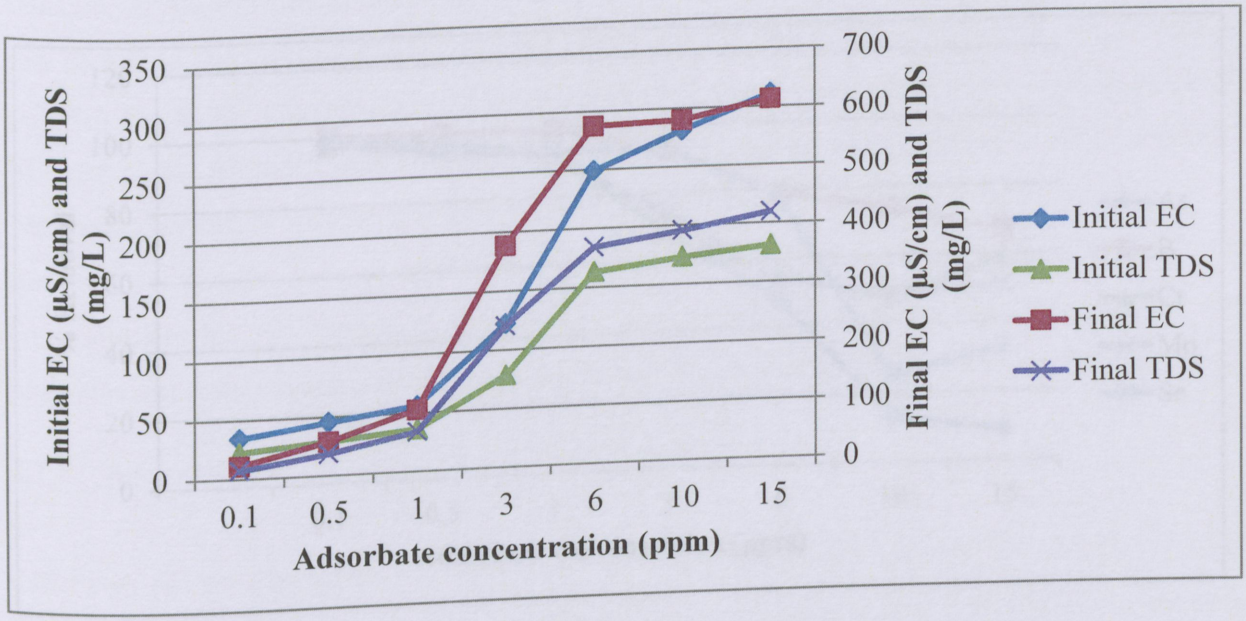


Figure 5.12: Variation of initial and final EC and TDS with an increase in adsorbate concentration for raw bentonite clay (30 minutes of contact time, 4 grams of adsorbent dosage, 250 rpm, 26°C and 4g/100 mL S/L ratios).

© University of Venda

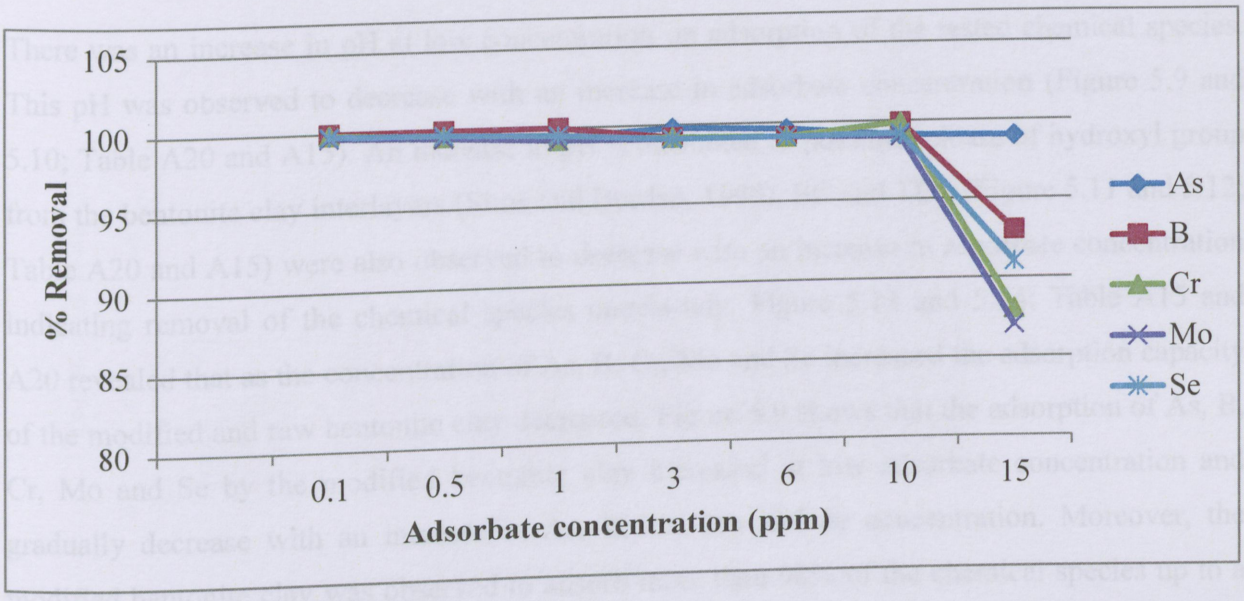


Figure 5.13: Variation of As, B, Cr, Mo and Se % removal for Al^{3+} modified bentonite clay with an increase in adsorbate concentration clay (30 minutes of contact time, 4 grams of adsorbent dosage, 250 rpm, 26°C and 4g/100 mL S/L ratios).

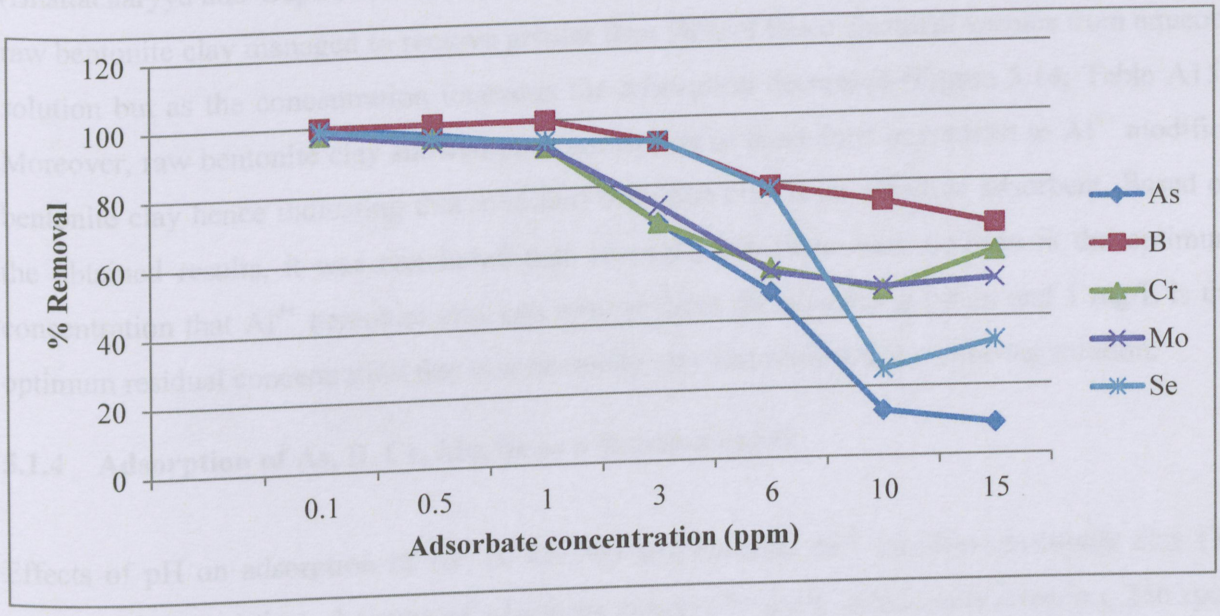


Figure 5.14: Variation of As, B, Cr, Mo and Se % removal for raw bentonite clay with an increase in adsorbate concentration clay (30 minutes of contact time, 4 grams of adsorbent dosage, 250 rpm, 26°C and 4g/100 mL S/L ratios).

© University of Venda

There was an increase in pH at low concentration on adsorption of the tested chemical species. This pH was observed to decrease with an increase in adsorbate concentration (Figure 5.9 and 5.10; Table A20 and A15). An increase in pH is attributed to possible release of hydroxyl group from the bentonite clay interlayers (Sims and Burden, 1999). EC and TDS (Figure 5.11 and 5.12; Table A20 and A15) were also observed to decrease with an increase in adsorbate concentration indicating removal of the chemical species understudy. Figure 5.13 and 5.14; Table A15 and A20 revealed that as the concentration of As, B, Cr, Mo and Se increased the adsorption capacity of the modified and raw bentonite clay decreased. Figure 5.9 shows that the adsorption of As, B, Cr, Mo and Se by the modified bentonite clay increased at low adsorbate concentration and gradually decrease with an increase in As, B, Cr, Mo and Se concentration. Moreover, the modified bentonite clay was observed to adsorb more than 98% of the chemical species up to a maximum concentration of 10 mg/L but its adsorption capacity was observed to decrease for concentrations greater than 10 mg/L but was still greater than 80 %. At low concentration, the adsorption sites are plenty and the uptake tends to be very high but as the concentration increases the adsorption sites become limited hence resulting in poor adsorption at higher concentration (Bhattacharyya and Gupta, 2008; Singh et al., 2010; Nassef and Eltaweel, 2012). Below 1 mg/L, raw bentonite clay managed to remove greater than 98% of those chemical species from aqueous solution but as the concentration increases the adsorption decreased (Figure 5.14; Table A15). Moreover, raw bentonite clay showed poor adsorption of those ions in contrast to Al^{3+} modified bentonite clay hence indicating that modified bentonite clay is an effective adsorbent. Based on the obtained results, it was concluded that 10 mg/L adsorbate concentration is the optimum concentration that Al^{3+} bentonite clay can remove from the aqueous solution and 1 mg/L is the optimum residual concentration that raw bentonite clay can remove from aqueous solution.

5.1.4 Adsorption of As, B, Cr, Mo, Se as a function of pH

Effects of pH on adsorption of As, B, Cr, Mo and Se onto Al^{3+} modified bentonite clay (30 minutes of contact time, 4 grams of adsorbent dosage, 10 mg/L metals concentration, 250 rpm, 26°C and 4g/100 mL S/L ratios) (Table A21). Figure 5.15, 5.16, 5.17, 5.18, 5.19 and 5.20 shows variation in As, B, Cr, Mo, Se, final pH, EC and TDS with varying pH ranges.

© University of Venda

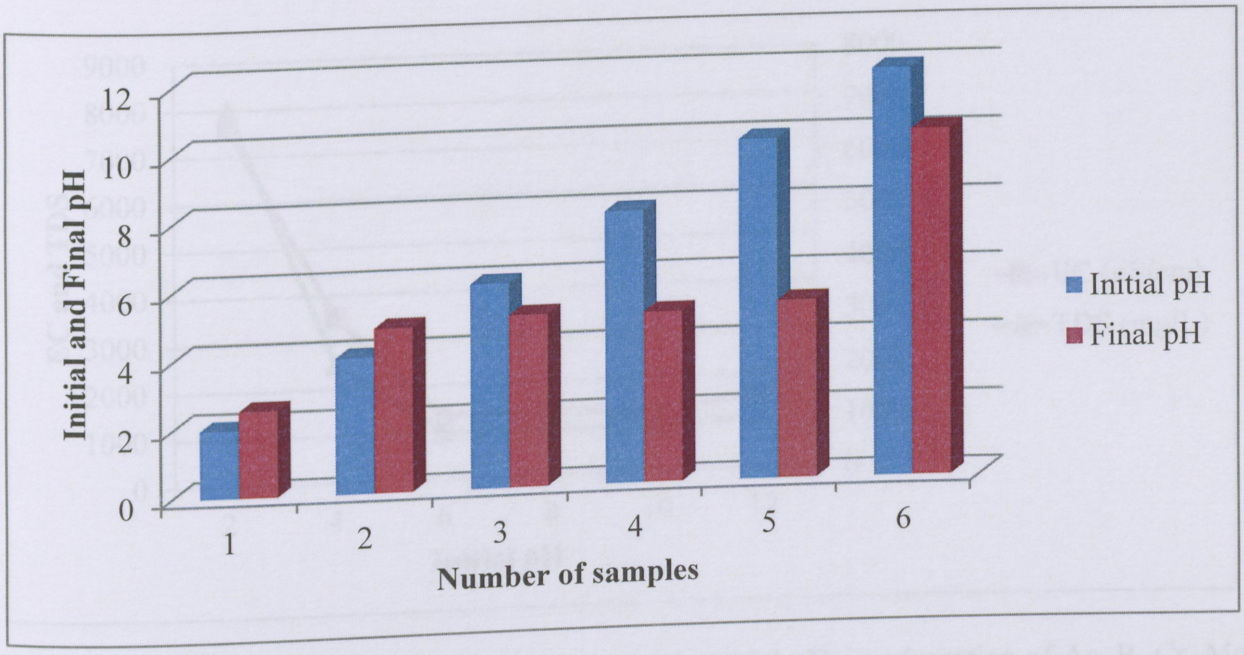


Figure 5.15: Variation of final pH at varying initial pH on adsorption of As, B, Cr, Mo and Se onto Al^{3+} modified bentonite clay (30 minutes of contact time, 4 grams of adsorbent dosage, 10 mg/L metals concentration, 250 rpm, 26°C and 4g/100 mL S/L ratios).

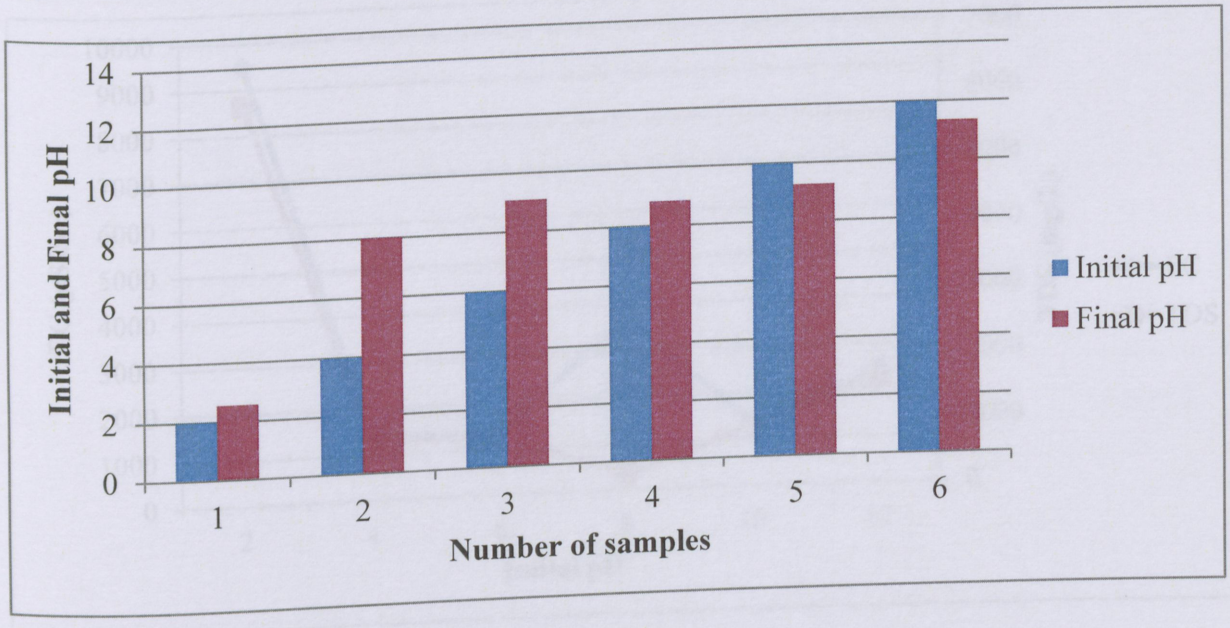


Figure 5.16: Variation of final pH at varying initial pH on adsorption of As, B, Cr, Mo and Se onto raw bentonite clay (30 minutes of contact time, 4 grams of adsorbent dosage, 10 mg/L metals concentration, 250 rpm, 26°C and 4g/100 mL S/L ratios).

© University of Venda

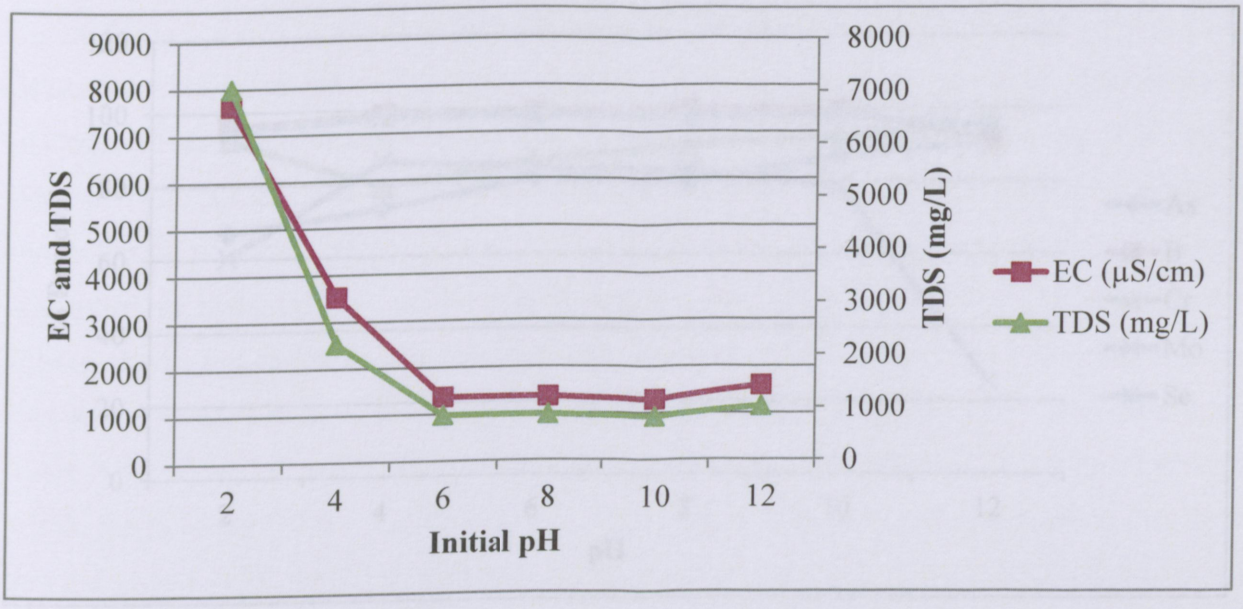


Figure 5.17: Variation of EC and TDS with varying initial pH on adsorption of As, B, Cr, Mo and Se onto Al^{3+} modified bentonite clay (30 minutes of contact time, 4 grams of adsorbent dosage, 10 mg/L metals concentration, 250 rpm, 26°C and 4g/100 mL S/L ratios).

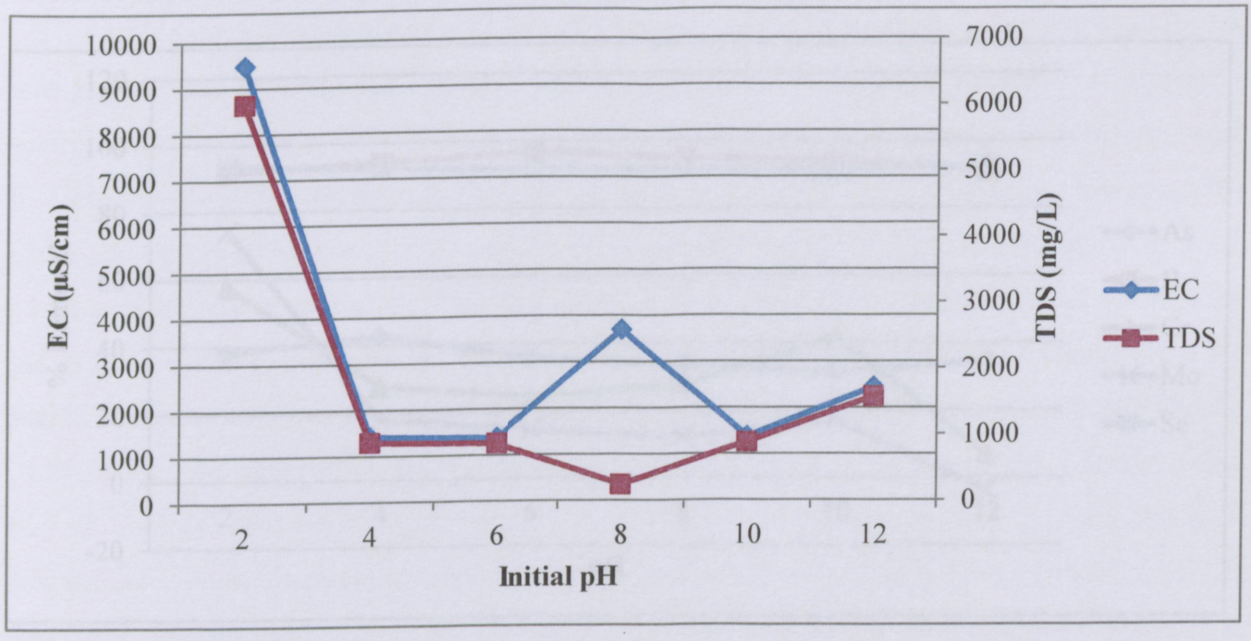


Figure 5.18: Variation of EC and TDS with varying initial pH on adsorption of As, B, Cr, Mo and Se onto raw bentonite clay (30 minutes of contact time, 4 grams of adsorbent dosage, 10 mg/L metals concentration, 250 rpm, 26°C and 4g/100 mL S/L ratios).

© University of Venda

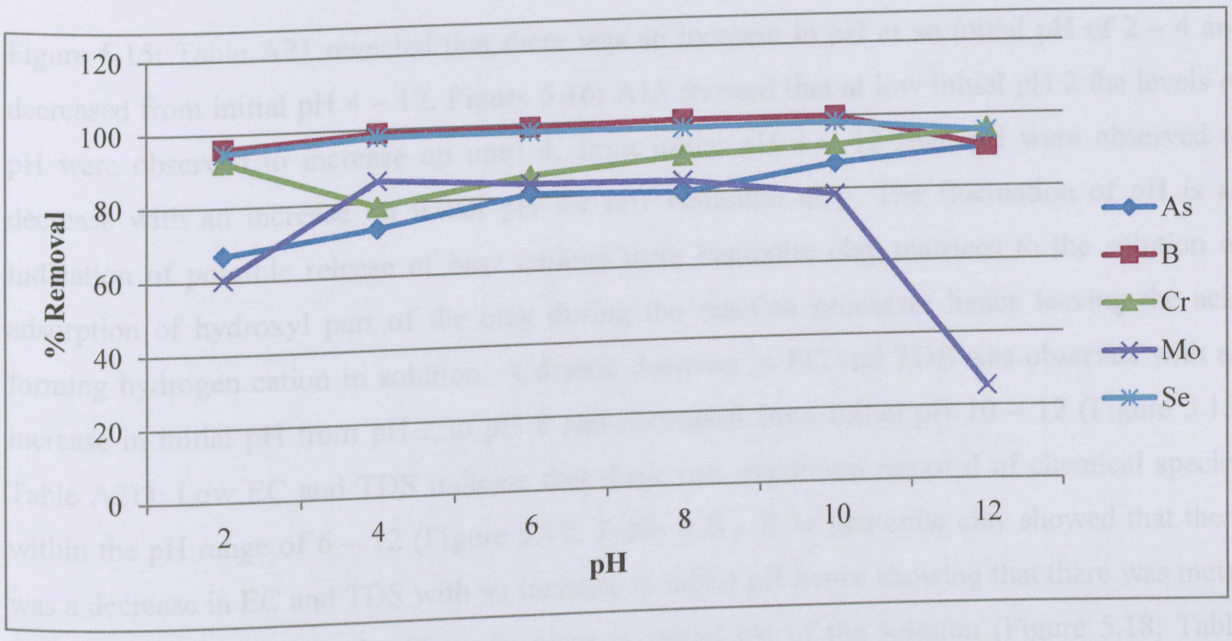


Figure 5.19: Variation of As, B, Cr, Mo and Se % removal with varying pH on interaction with Al^{3+} modified bentonite clay (30 minutes of contact time, 4 grams of adsorbent dosage, 10 mg/L metals concentration, 250 rpm, 26°C and 4g/100 mL S/L ratios).

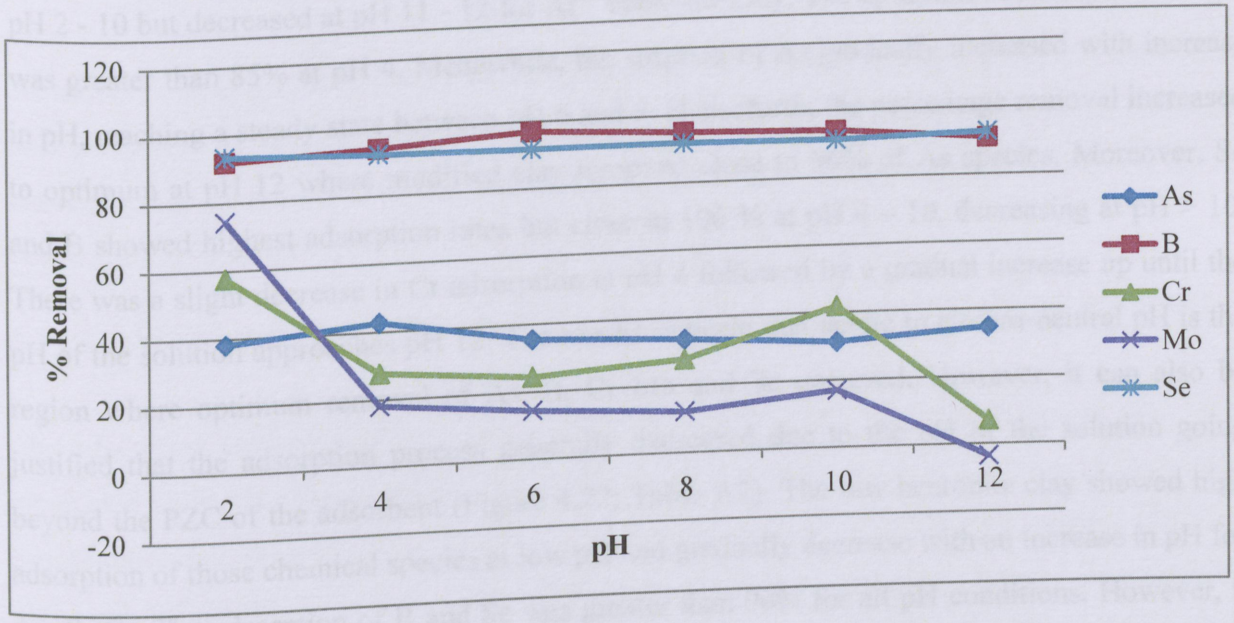


Figure 5.20: Variation of As, B, Cr, Mo and Se % removal with varying pH on interaction with raw bentonite clay (30 minutes of contact time, 4 grams of adsorbent dosage, 10 mg/L metals concentration, 250 rpm, 26°C and 4g/100 mL S/L ratios).

© University of Venda

Figure 5.15; Table A21 revealed that there was an increase in pH at an initial pH of 2 – 4 and decreased from initial pH 4 – 12. Figure 5.16; A15 showed that at low initial pH 2 the levels of pH were observed to increase up until 4, from initial pH 4 – 12 final pH were observed to decrease with an increase on initial pH for raw bentonite clay. The fluctuation of pH is an indication of possible release of base cations from bentonite clay matrices to the solution or adsorption of hydroxyl part of the clay during the reaction processes hence leaving the acid forming hydrogen cation in solution. A drastic decrease in EC and TDS was observed with an increase in initial pH from pH 2 to pH 8 and decreased from initial pH 10 – 12 (Figure 5.15; Table A21). Low EC and TDS indicate that there was maximum removal of chemical species within the pH range of 6 – 12 (Figure 5.17; Table A21). Raw bentonite clay showed that there was a decrease in EC and TDS with an increase in initial pH hence showing that there was metal adsorption which increased with an increase in initial pH of the solution (Figure 5.18; Table A16). Figure 5.19; Table A21 shows the effect of varying the pH on the uptake (% removal) of As, B, Cr, Mo and Se for Al^{3+} bentonite clay. Generally, it is clear that the percentage uptake of these chemical species increases with increasing pH except for Mo which initially increased at pH 2 - 10 but decreased at pH 11 - 12 for Al^{3+} bentonite clay. The optimum % adsorption for Mo was greater than 85% at pH 4. Meanwhile, the sorption of As gradually increased with increase in pH, reaching a steady state between pH 6 and 8. Henceforth, the percentage removal increased to optimum at pH 12 where modified clay removed close to 96% of As species. Moreover, Se and B showed highest adsorption rates but close to 100 % at pH 4 – 10, decreasing at pH > 10. There was a slight decrease in Cr adsorption at pH 4 followed by a gradual increase up until the pH of the solution approaches pH 12. The results indicate that acidic to circum-neutral pH is the region where optimum removal of As, B, Cr Mo and Se occurred. However, it can also be justified that the adsorption process generally decreased due to the pH of the solution going beyond the PZC of the adsorbent (Figure 4.22; Table A2). The raw bentonite clay showed high adsorption of those chemical species at low pH and gradually decrease with an increase in pH for As, B, Cr. The adsorption of B and Se was greater than 90% for all pH conditions. However, it can be concluded that raw bentonite clay showed poor adsorption of those chemical species as compared to Al^{3+} modified bentonite clay.

© University of Venda

5.2 Adsorption capacity of raw and modified bentonite clay

Table 5.1: Adsorption capacities of Al^{3+} modified and raw bentonite clay for As, B, Cr, Mo and Se

	Adsorption Capacity (mg/g)									
	Aluminium modified bentonite clay					Raw Bentonite				
Co (mg/L)	As	B	Cr	Mo	Se	As	B	Cr	Mo	Se
0.1	0.002	0.002	0.002	0.002	0.002	0.002	0.002	0.000	0.002	0.001
0.5	0.012	0.012	0.012	0.012	0.012	0.005	0.012	0.003	0.008	0.005
1	0.024	0.025	0.025	0.025	0.025	0.008	0.023	0.005	0.015	0.010
3	0.073	0.075	0.075	0.074	0.074	0.023	0.057	0.018	0.033	0.038
6	0.141	0.149	0.149	0.148	0.148	0.038	0.110	0.038	0.043	0.095
10	0.227	0.248	0.248	0.246	0.245	0.063	0.178	0.120	0.058	0.153
15	0.335	0.372	0.372	0.368	0.367	0.078	0.248	0.218	0.078	0.218

As shown in table 5.1, as the concentration of species in solution increases, the amount adsorbed also increases. At low concentrations, the limiting factor on the adsorption is the adsorbate concentration. Table 5.1 shows that the adsorption capacity of raw bentonite clay is low at higher concentration as compared to the Al^{3+} modified bentonite clay.

5.3 Adsorption isotherms for As, B, Cr, Mo and Se onto Al^{3+} modified bentonite clay

The adsorption isotherms of As, B, Cr, Mo and Se onto Al^{3+} modified bentonite clay were conducted by varying the initial As, B, Cr, Mo and Se concentration between 0.1 - 15 mg/L. The adsorption condition were 30 minutes of contact time, 4 grams of adsorbent dosage, 250 rpm, 26°C and 4g/100 mL S/L ratios. Two widely used adsorption isotherms, namely the Langmuir (Langmuir, 1918; Ramesh et al., 2007; Bhati and Singh, 2012) and Freundlich (Freundlich, 1906; Ramesh et al., 2007; Bhati and Singh, 2012) were used to describe the adsorption data. The Langmuir isotherm is valid for monolayer sorption due to a surface with finite number of identical sites (Singh et al., 2010) and it is expressed in the following linear form:

© University of Venda

$$\frac{Ce}{Qe} = \frac{1}{Qmb} + \frac{Ce}{Qm} \quad \text{.....(15)}$$

Where, Ce = Equilibrium concentration (mg/L)

Qe = Amount adsorbed at equilibrium (mg/g)

Qm = Langmuir constants related to adsorption capacity

b = Langmuir constants related to energy of adsorption (L/mg)

A plot of Ce/Qe versus Ce should be linear if the data is described by the Langmuir isotherm. The value of Qm and b will be determined from the slope and the intercept of the plot and are used to assess whether the adsorbent has high adsorption capacity or the adsorption is taking place at high or low energy.

Langmuir adsorption isotherm can also be expressed in terms of R_L, a dimensionless factor known as separation factor. It is used to determine whether the reaction was favorable or not.

$$R_L = \frac{1}{(1 + bCo)} \quad \text{.....(16)}$$

Where, Co = initial concentration. If R_L is between 0 and 1, the adsorption is favorable (Langmuir, 1918). Figure 5.15, 5.16, 5.17, 5.18 and 5.19 shows Langmuir adsorption isotherm for chemical species understudy.

© University of Venda

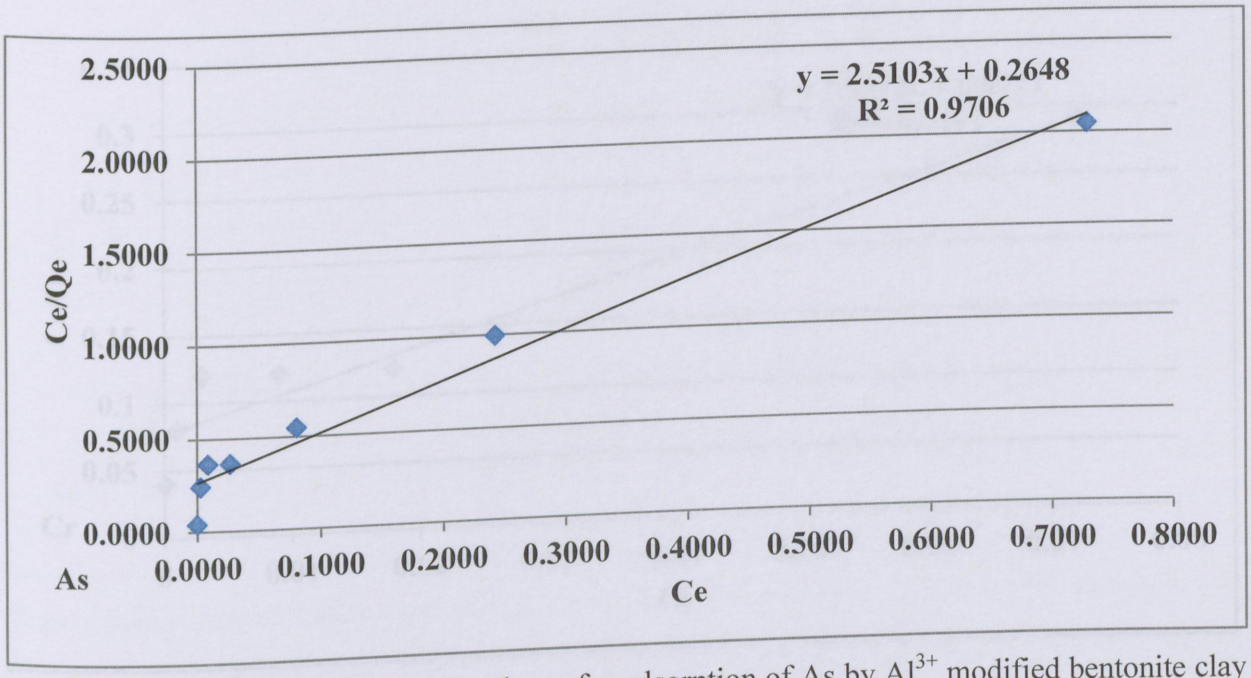


Figure 5.21: Langmuir adsorption isotherm for adsorption of As by Al^{3+} modified bentonite clay (30 minutes of contact time, 4 grams of adsorbent dosage, 250 rpm, 26°C and 4g/100 mL S/L ratios).

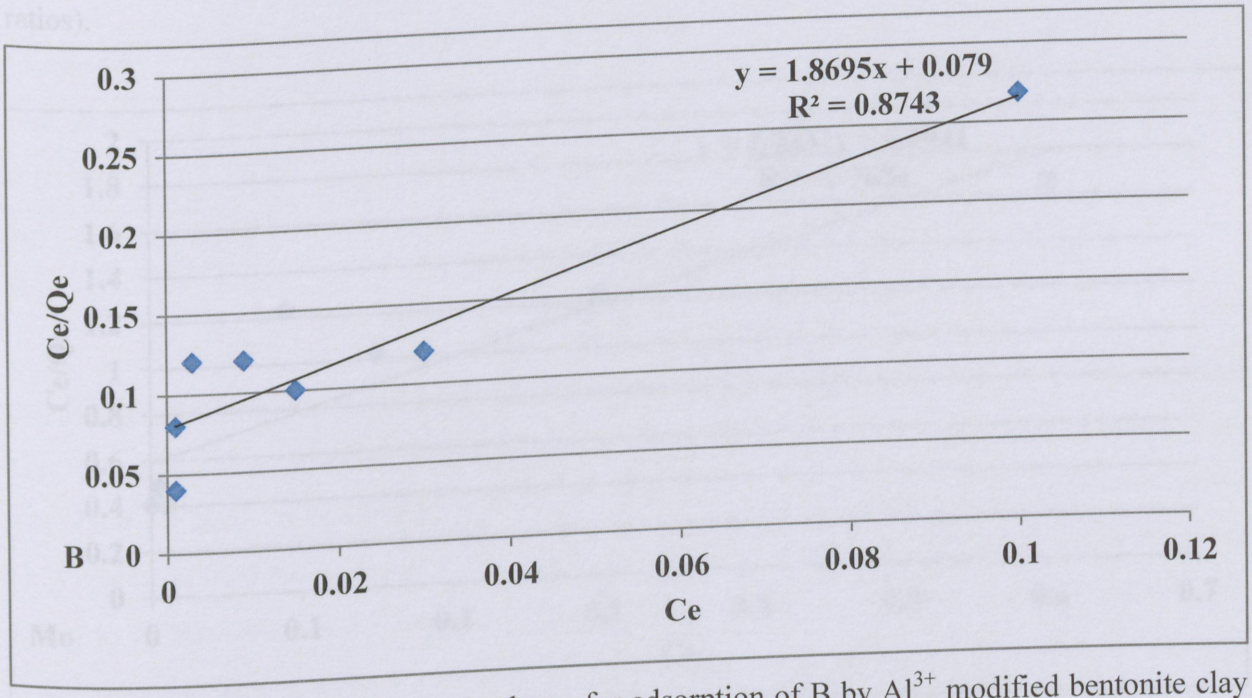


Figure 5.22: Langmuir adsorption isotherm for adsorption of B by Al^{3+} modified bentonite clay (30 minutes of contact time, 4 grams of adsorbent dosage, 250 rpm, 26°C and 4g/100 mL S/L ratios).

© University of Venda

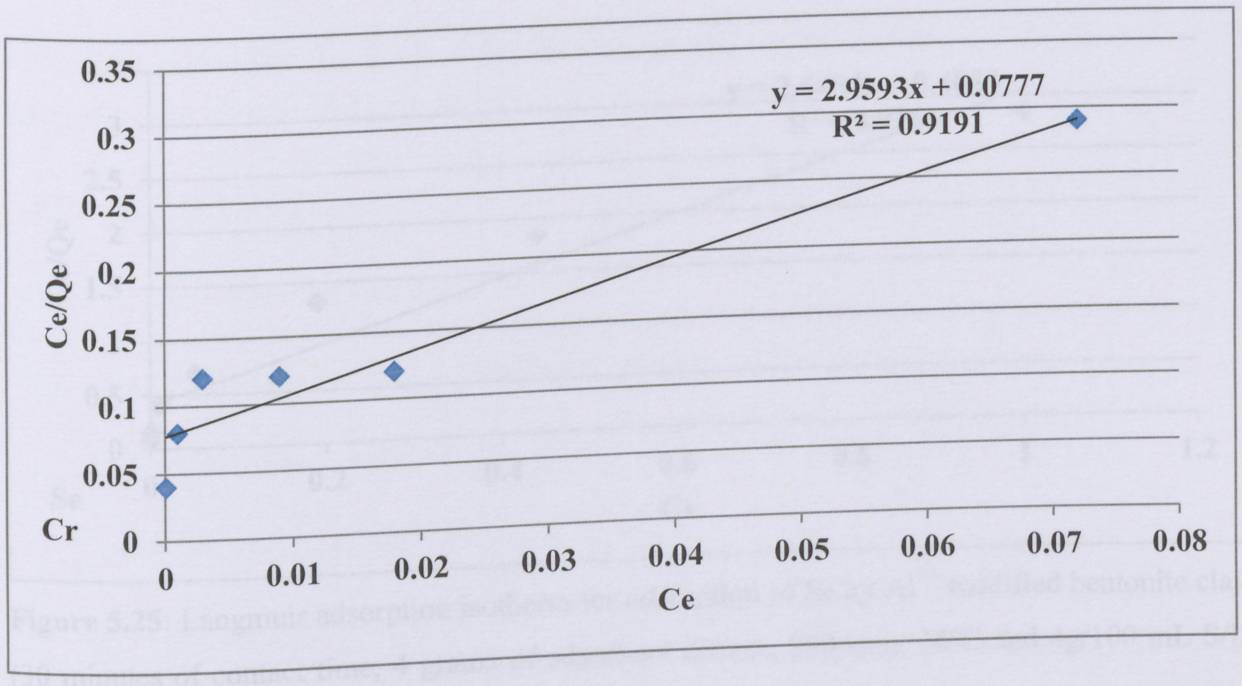


Figure 5.23: Langmuir adsorption isotherm for adsorption of Cr by Al^{3+} modified bentonite clay (30 minutes of contact time, 4 grams of adsorbent dosage, 250 rpm, 26°C and 4g/100 mL S/L ratios).

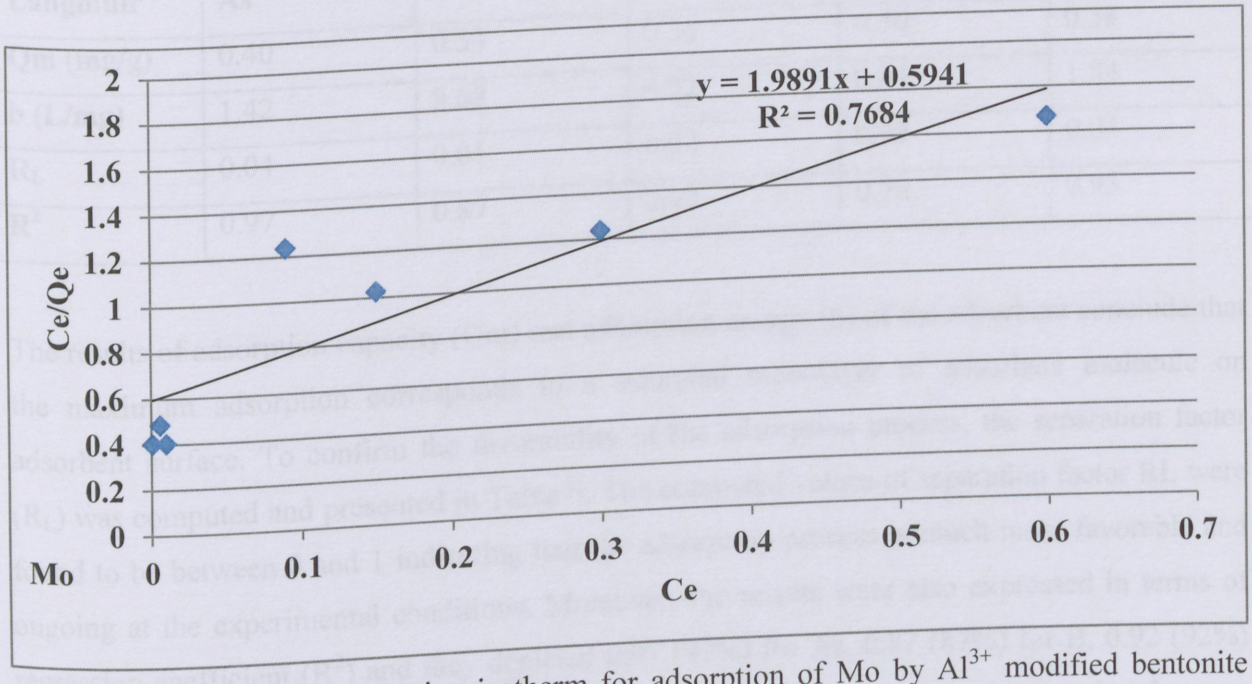


Figure 5.24: Langmuir adsorption isotherm for adsorption of Mo by Al^{3+} modified bentonite clay (30 minutes of contact time, 4 grams of adsorbent dosage, 250 rpm, 26°C and 4g/100 mL S/L ratios).

© University of Venda

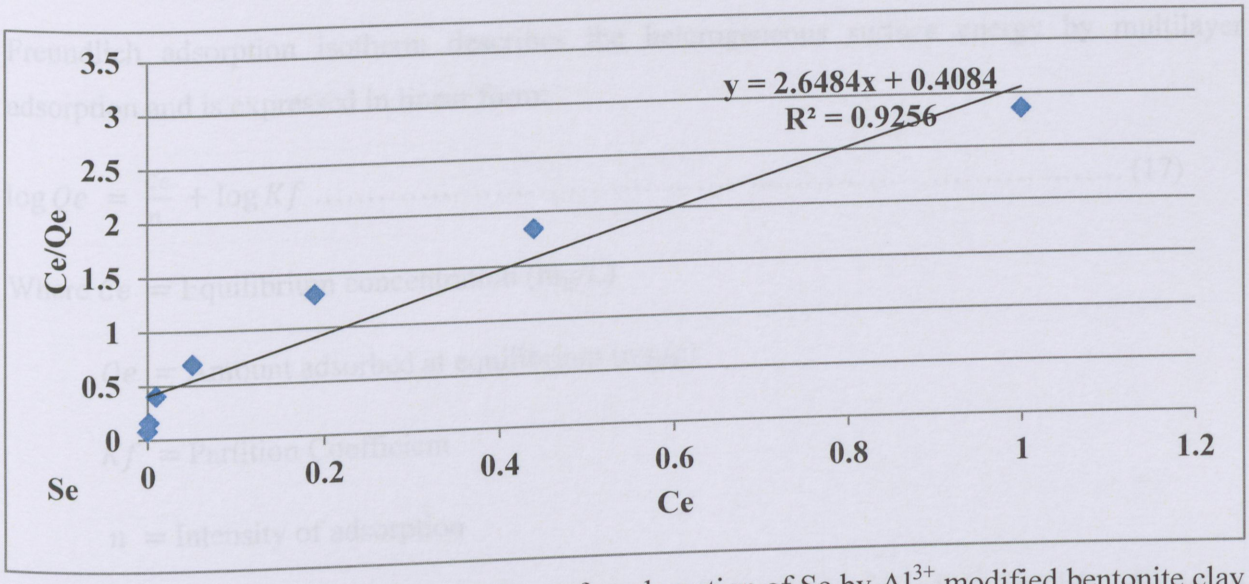


Figure 5.25: Langmuir adsorption isotherm for adsorption of Se by Al^{3+} modified bentonite clay (30 minutes of contact time, 4 grams of adsorbent dosage, 250 rpm, 26°C and 4g/100 mL S/L ratios).

Table 5.2: Langmuir adsorption isotherm constant for adsorption of As, B, Cr, Mo and Se onto Al^{3+} modified bentonite clay

Langmuir	As	B	Cr	Mo	Se
Qm (mg/g)	0.40	0.53	0.34	0.50	0.38
b (L/mg)	1.42	8.68	4.32	0.84	1.84
R_L	0.04	0.01	0.02	0.07	0.04
R^2	0.97	0.87	0.92	0.76	0.93

The results of adsorption capacity (Qm) and adsorption energy (b) of the adsorbent conclude that the maximum adsorption corresponds to a saturated monolayer of adsorbate molecule on adsorbent surface. To confirm the favorability of the adsorption process, the separation factor (R_L) was computed and presented in Table 5. The computed values of separation factor RL were found to be between 0 and 1 indicating that the adsorption process is much more favorable and ongoing at the experimental conditions. Moreover, the results were also expressed in terms of regression coefficient (R^2) and they depicted 0.97 (97%) for As, 0.87 (87%) for B, 0.92 (92%) for Cr, 0.76 (76%) for Mo and 0.93 (93%) for Se, indicating a positive, very good and strong mathematical fit.

© University of Venda

Freundlich adsorption isotherm describes the heterogeneous surface energy by multilayer adsorption and is expressed in linear form:

$$\log Qe = \frac{Ce}{n} + \log Kf \quad \ldots\ldots\ldots\

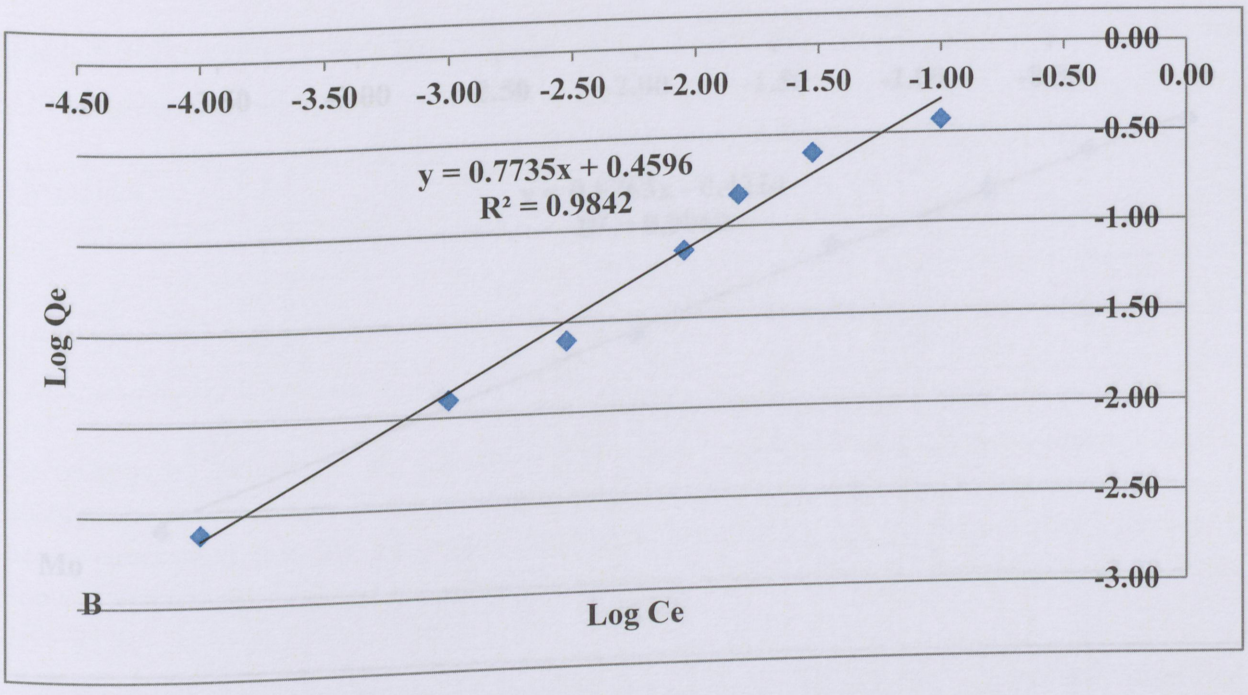


Figure 5.27: Freundlich adsorption isotherm for adsorption of B by Al^{3+} modified bentonite clay (30 minutes of contact time, 4 grams of adsorbent dosage, 250 rpm, 26°C and 4g/100 mL S/L ratios).

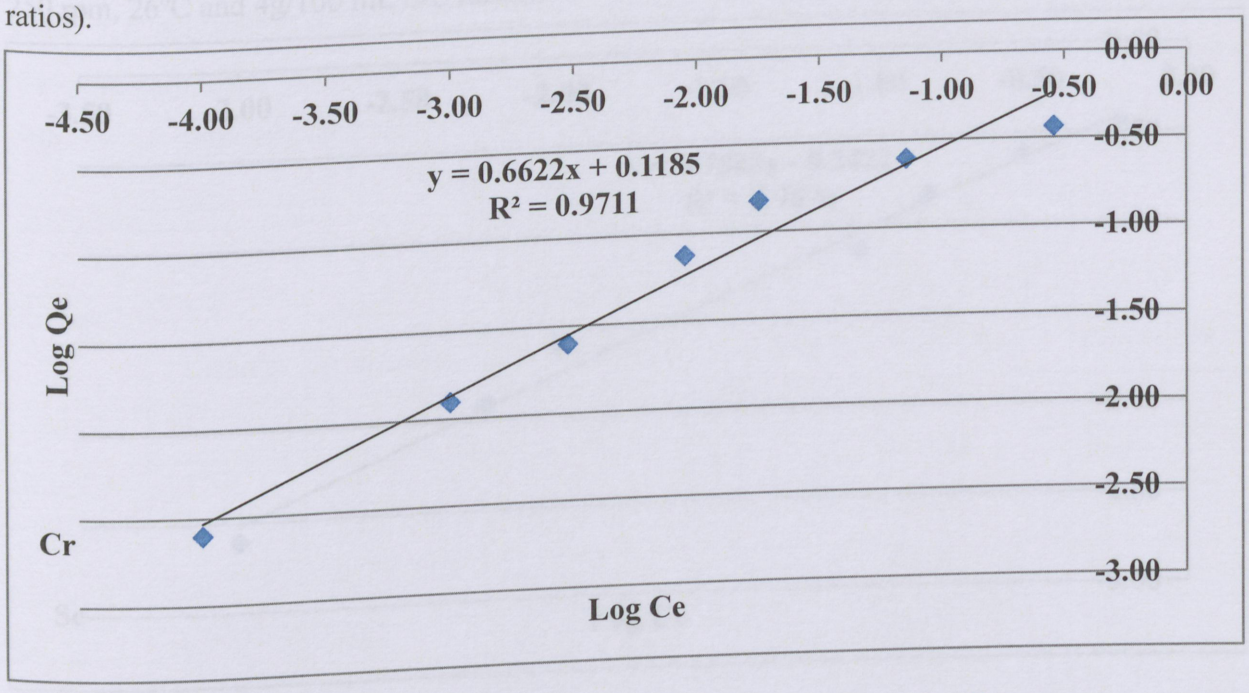


Figure 5.28: Freundlich adsorption isotherm for adsorption of Cr by Al^{3+} modified bentonite clay (30 minutes of contact time, 4 grams of adsorbent dosage, 250 rpm, 26°C and 4g/100 mL S/L ratios).

© University of Venda

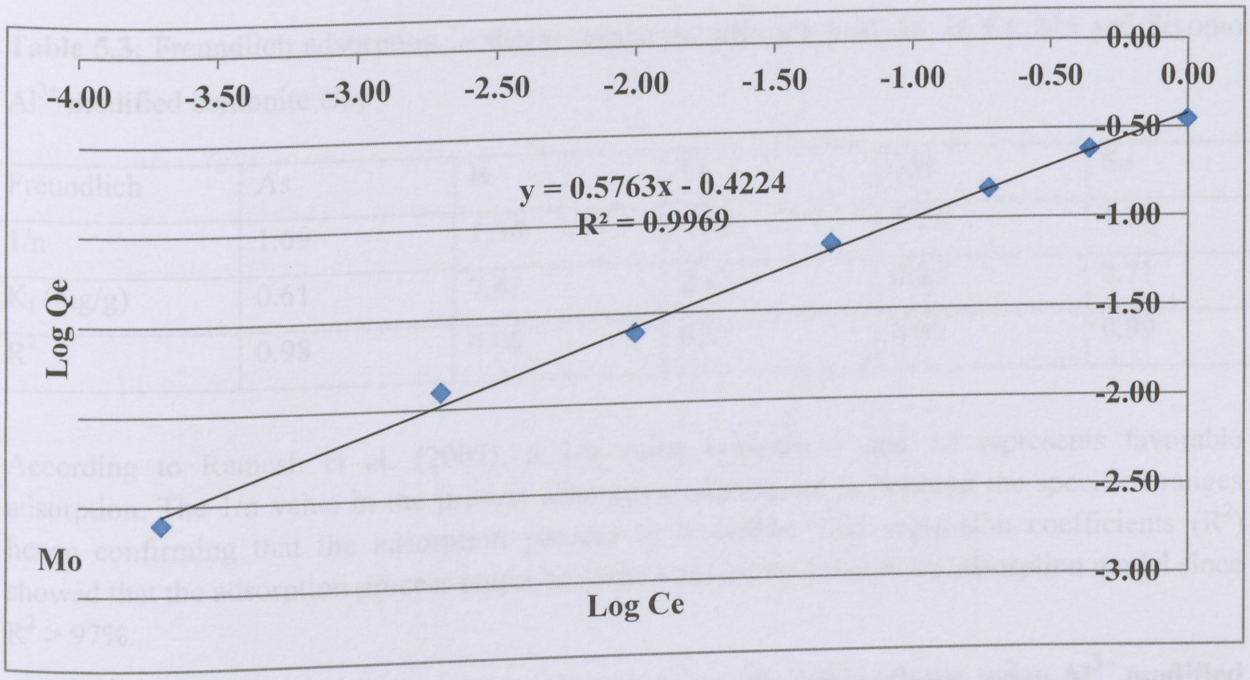


Figure 5.29: Freundlich adsorption isotherm for Freundlich adsorption isotherm for adsorption of Mo by Al^{3+} modified bentonite clay (30 minutes of contact time, 4 grams of adsorbent dosage, 250 rpm, 26°C and 4g/100 mL S/L ratios).

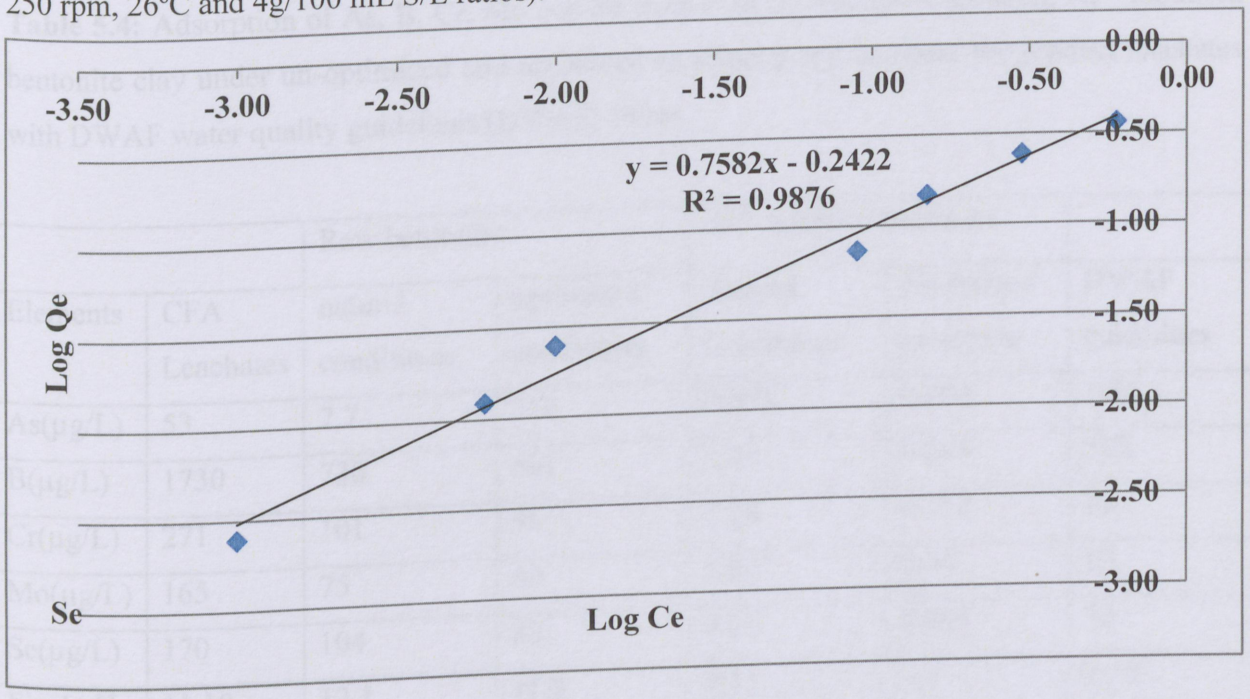


Figure 5.30: Freundlich adsorption isotherm for Freundlich adsorption isotherm for adsorption of Se by Al^{3+} modified bentonite clay (30 minutes of contact time, 4 grams of adsorbent dosage, 250 rpm, 26°C and 4g/100 mL S/L ratios).

© University of Venda

Table 5.3: Freundlich adsorption isotherm results on adsorption of As, B, Cr, Mo and Se onto Al^{3+} modified bentonite clay

Freundlich	As	B	Cr	Mo	Se
1/n	1.69	1.30	1.52	1.72	1.32
K_f (mg/g)	0.61	7.41	2.43	0.35	0.71
R^2	0.98	0.98	0.97	0.99	0.99

According to Ramesh et al. (2007), a 1/n value between 1 and 10 represents favorable adsorption. The 1/n value in the present adsorption experiment is between the specified ranges hence confirming that the adsorption process is favorable. The regression coefficients (R^2) showed that the adsorption process could be described best by Freundlich adsorption model since $R^2 > 97\%$.

5.4 Adsorption of As, B, Cr, Mo and Se from coal fly ash leachates using Al^{3+} modified bentonite clay under un-optimized and optimized conditions

Table 5.4: Adsorption of As, B, Cr, Mo and Se from coal fly ash leachates using Al^{3+} modified bentonite clay under un-optimized and optimized conditions and compare the product leachates with DWAF water quality guidelines (DWAF, 1996).

		Raw bentonite		Al^{3+}modified bentonite		
Elements	CFA Leachates	natural conditions	optimized conditions	Natural Conditions	Optimized condition	DWAF guidelines
As(µg/L)	53	7.7	7.3	0.073	0.004	100
B(µg/L)	1730	730	501	1.45	0.018	500
Cr(µg/L)	271	101	99	1.38	0.153	10
Mo(µg/L)	165	75	69	1.89	0.09	10
Se(µg/L)	170	104	83	0.01	0.001	20
Final pH	11.10	12.1	11.8	9.11	8.9	6 - 9

Table 5.1 shows the adsorption of As, B, Cr, Mo and Se from coal fly ash leachates onto raw and Al^{3+} modified bentonite clay. As shown in Table 5.1, for raw bentonite, the adsorption of As, B,

© University of Venda

Cr, Mo and Se were observed to be high at optimum condition as compared to natural conditions. In the optimized conditions raw bentonite clay did not remove the concentration of chemical species understudy to the prescribed DWAF standard whereas for optimized conditions, it managed for As and B. Al^{3+} modified bentonite clay showed good adsorption of those chemical species for both natural and optimized conditions, reducing the concentration of these chemical species to below the DWAF water quality guidelines. Based on that, it can be concluded that Al^{3+} modified bentonite clay is an effective adsorbent for As, B, Cr, Mo and Se from coal fly ash leachates. This also implies that Al^{3+} modified bentonite clay can be used as a liner or reactive barrier in ash retention ponds trapping the oxyanionic species.

© University of Venda

University of Venda
Creating Future Leaders

CHAPTER SIX

Adsorption of As, B, Cr, Mo and Se onto Fe^{3+} modified bentonite clay: Optimization of adsorption conditions and application for coal fly ash leachates remediation

6.0 Introduction

In this chapter, results on parameters and conditions which plays a significant role on the adsorption of As, B, Cr, Mo and Se onto Fe^{3+} modified bentonite clay were evaluated in an attempt to determine the optimum condition for removal of As, B, Cr, Mo and Se from coal fly ash leachates. The optimization conditions were determined using synthetic solutions containing As, B, Cr, Mo and Se.

6.1 Adsorption of oxyanions of As, B, Cr, Mo and Se using Fe^{3+} modified bentonite clay

6.1.1 Adsorption of As, B, Cr, Mo, Se as a function of contact time

Effects of contact time on the adsorption of As, B, Cr, Mo and Se by Fe^{3+} modified bentonite clay and raw bentonite clay was evaluated at an initial concentration of 10 mg/L, adsorbent dosage of 1 gram, 250 rpm, 26°C and 1g/100 mL S/L. The uptake of As, B, Cr, Mo and Se onto modified and raw bentonite clay was evaluated for three hours at the intervals of 1, 5, 10, 15, 30, 60, and 180 minutes (Table A27). Figure 6.1, 6.2, 6.3 and 6.4 shows the variation of pH, EC, TDS, As, B, Cr, Mo and Se levels with contact time on the interaction of As, B, Cr, Mo and Se solution with raw and Fe^{3+} modified bentonite clay.

© University of Venda

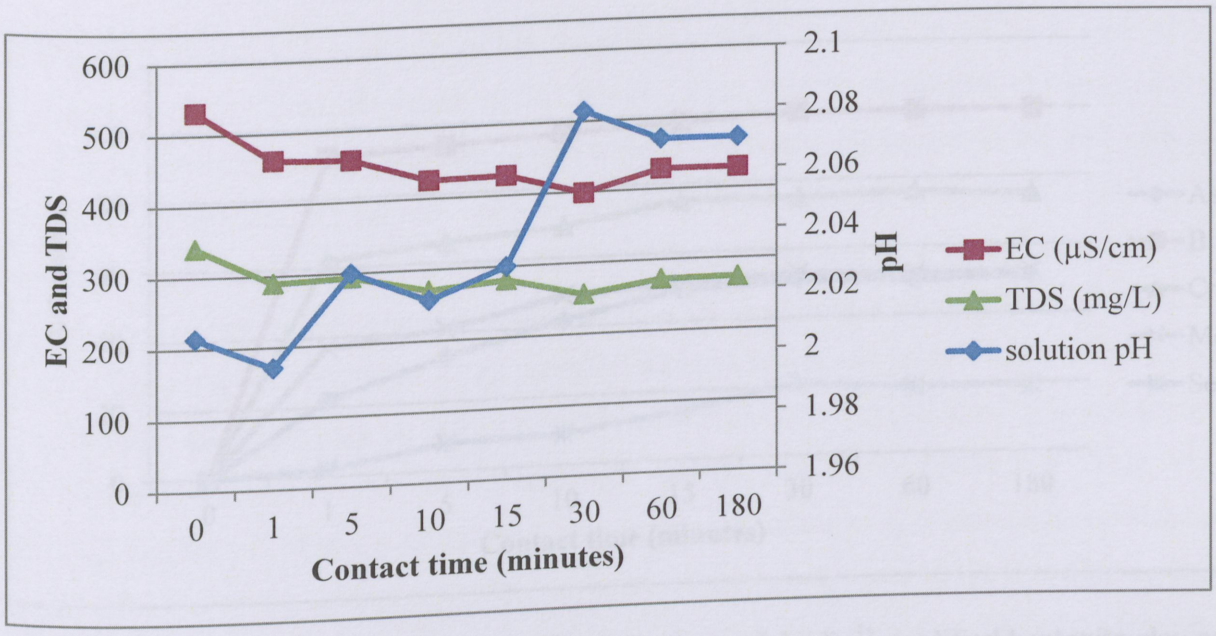


Figure 6.1: Variation of pH, EC and TDS with adsorption of As, B, Cr, Mo and Se by Fe^{3+} bentonite clay as a function of contact time (1 gram of adsorbent dosage, 10 mg/L of adsorbate concentration, 250 rpm, 26°C and 1g/100 mL S/L ratios) the mixtures were shaked for 3 hours.

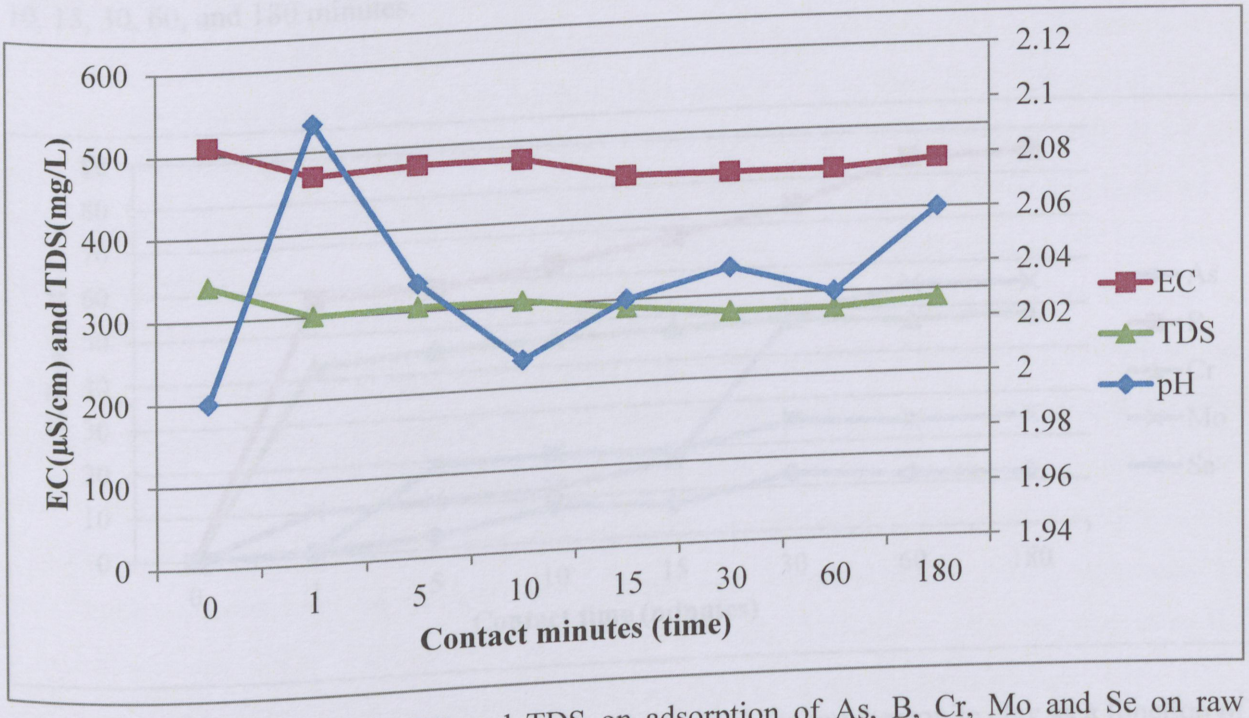


Figure 6.2: Variation of pH, EC and TDS on adsorption of As, B, Cr, Mo and Se on raw bentonite clay with contact time (1 gram of adsorbent dosage, 10 mg/L adsorbate concentrations, 26°C and 1g/100 mL S/L ratio).

© University of Venda

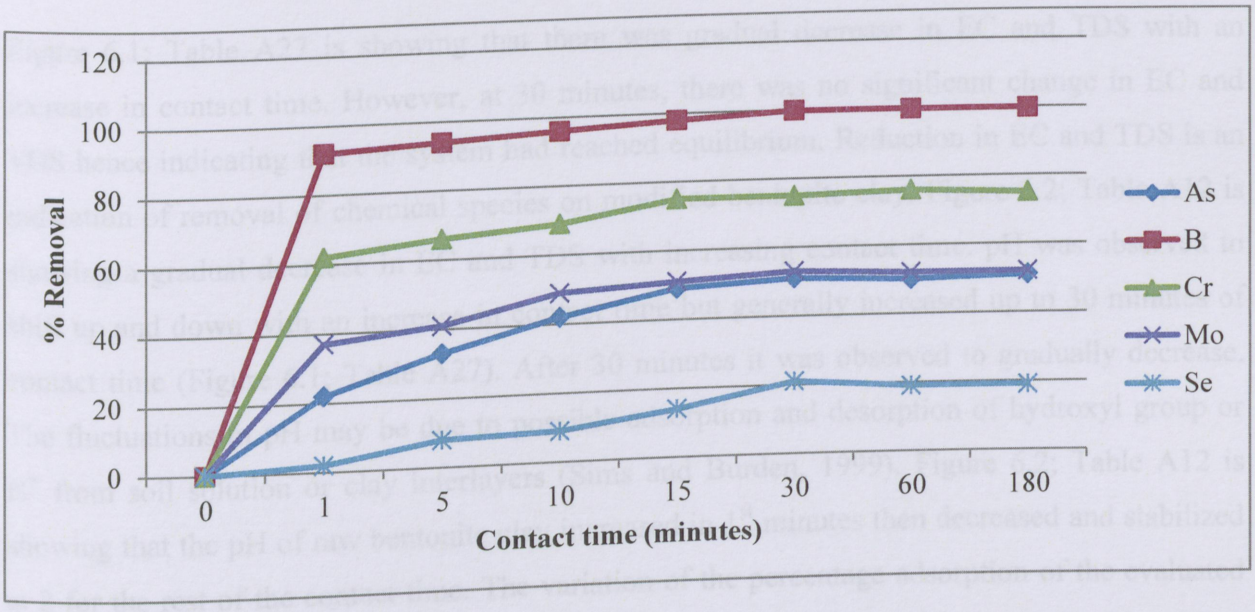


Figure 6.3: Variation of As, B, Cr, Mo and Se % removal for Fe^{3+} modified bentonite clay as a function of contact time (1 gram of adsorbent dosage, 10 mg/L of adsorbate concentration, 250 rpm, 26°C and 1g/100 mL S/L ratios) the mixtures were shaked for 3 hours at the interval of 1, 5, 10, 15, 30, 60, and 180 minutes.

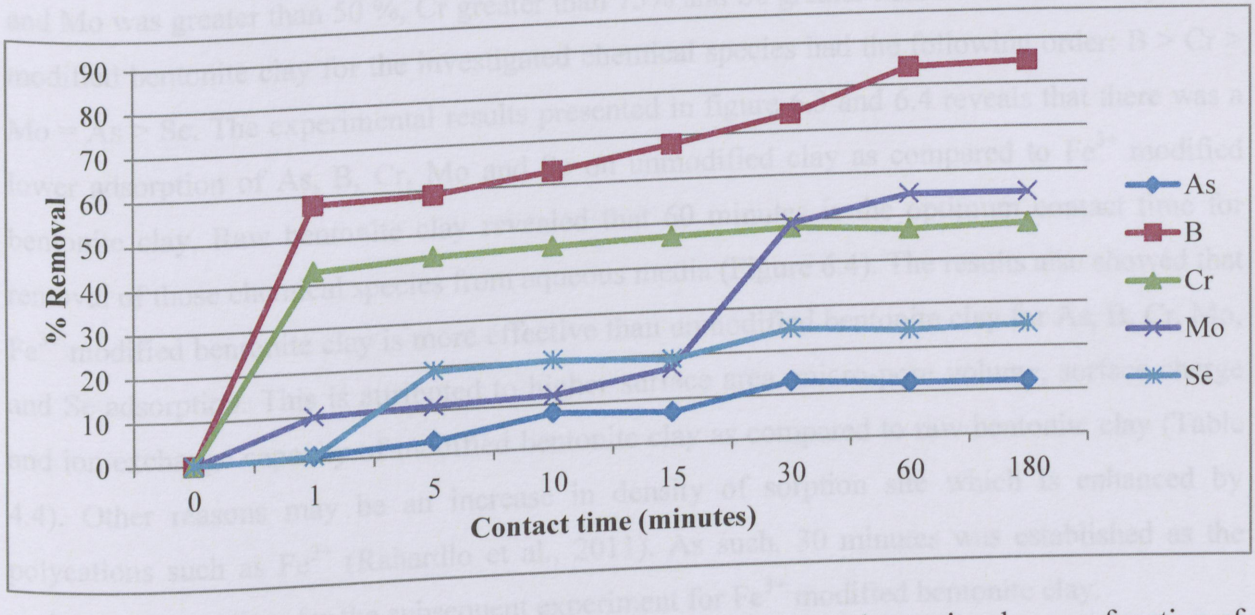


Figure 6.4: Variation of As, B, Cr, Mo and Se % removal for raw bentonite clay as a function of contact time (1 gram of adsorbent dosage, 10 mg/L of adsorbate concentration, 250 rpm, 26°C and 1g/100 mL S/L ratios) the mixtures were shaked for 3 hours.

© University of Venda

University of Venda
Creating Future Leaders

Figure 6.1; Table A27 is showing that there was gradual decrease in EC and TDS with an increase in contact time. However, at 30 minutes, there was no significant change in EC and TDS hence indicating that the system had reached equilibrium. Reduction in EC and TDS is an indication of removal of chemical species on modified bentonite clay. Figure 6.2; Table A12 is showing a gradual decrease in EC and TDS with increasing contact time. pH was observed to shift up and down with an increase in contact time but generally increased up to 30 minutes of contact time (Figure 6.1; Table A27). After 30 minutes it was observed to gradually decrease. The fluctuations in pH may be due to possible adsorption and desorption of hydroxyl group or H^+ from soil solution or clay interlayers (Sims and Burden, 1999). Figure 6.2; Table A12 is showing that the pH of raw bentonite clay increased in 1st minutes then decreased and stabilized at 2 for the rest of the contact time. The variation of the percentage adsorption of the evaluated species is indicated in figure 6.3; Table A27. It is clear that the sorption of As, B, Cr, Mo and Se increases with contact time until it reaches equilibrium. It is clear, that the in the first minutes of contact adsorption was very rapid and gradually approaches a steady state after 5 minutes of contact time. At 30 minutes the adsorbent is saturated, B exhibits highest sorption rates than other species. B adsorption occurred in 5 minutes reaching a maximum of 99.9%. Sorption of As and Mo was greater than 50 %, Cr greater than 75% and Se greater than 20%. The affinity of the modified bentonite clay for the investigated chemical species had the following order: B > Cr > Mo = As > Se. The experimental results presented in figure 6.3 and 6.4 reveals that there was a lower adsorption of As, B, Cr, Mo and Se on unmodified clay as compared to Fe^{3+} modified bentonite clay. Raw bentonite clay revealed that 60 minutes is the optimum contact time for removal of those chemical species from aqueous media (Figure 6.4). The results also showed that Fe^{3+} modified bentonite clay is more effective than unmodified bentonite clay for As, B, Cr, Mo, and Se adsorption. This is attributed to higher surface area, micro-pore volume, surface charge and ion exchange capacity of modified bentonite clay as compared to raw bentonite clay (Table 4.4). Other reasons may be an increase in density of sorption site which is enhanced by polycations such as Fe^{3+} (Rahardlo et al., 2011). As such, 30 minutes was established as the optimum contact time for the subsequent experiment for Fe^{3+} modified bentonite clay.

UNIVERSITY OF VENDA
LIBRARY

© University of Venda

6.1.2 Adsorption of As, B, Cr, Mo, Se as a function of adsorbent dosage

Effects of adsorbent dosage on the adsorption of As, B, Cr, Mo and Se by Fe^{3+} modified bentonite clay and raw bentonite clay was evaluated at 10 mg/L adsorbate concentration and 30 minutes contact time, 250 rpm and 26°C). The adsorbent dosage was varied from 0.5, 1, 2, 3, 4, to 5 grams (Table A28). Figure 6.5, 6.6, 6.7 and 6.8 shows variation of As, B, Cr, Mo, Se, pH, EC, and TDS with adsorbent dosage.

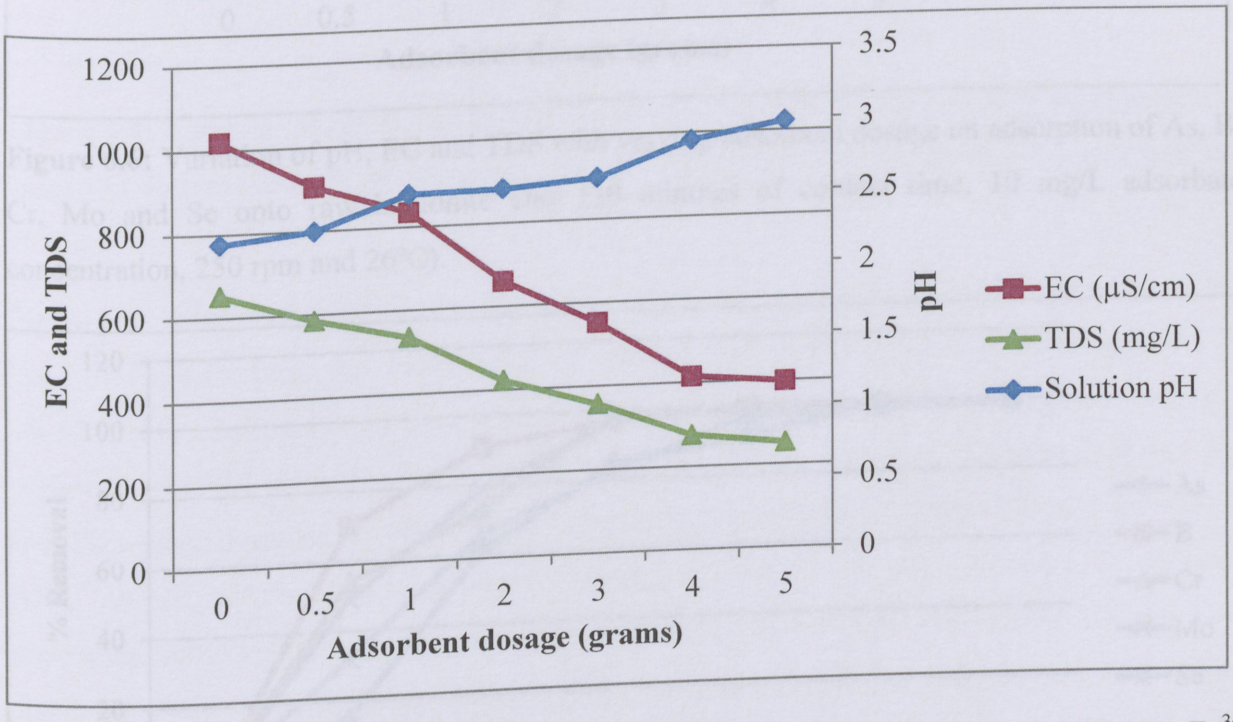


Figure 6.5: Variation of pH, EC and TDS on adsorption of As, B, Cr, Mo and Se onto Fe^{3+} modified bentonite clay with varying adsorbent dosage (30 minutes of contact time, 10 mg/L of adsorbate concentration and 26°C). The dosages were varied from 0.5, 1, 2, 3, 4, and 5 grams.

© University of Venda

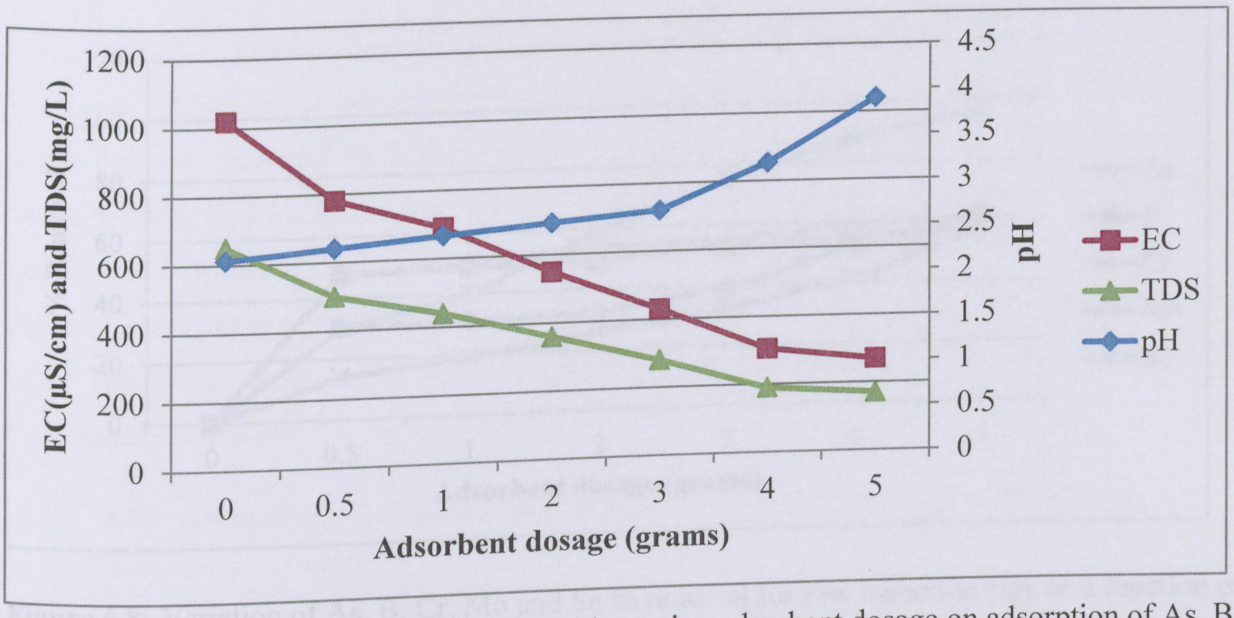


Figure 6.6: Variation of pH, EC and TDS with varying adsorbent dosage on adsorption of As, B, Cr, Mo and Se onto raw bentonite clay (30 minutes of contact time, 10 mg/L adsorbate concentration, 250 rpm and 26°C).

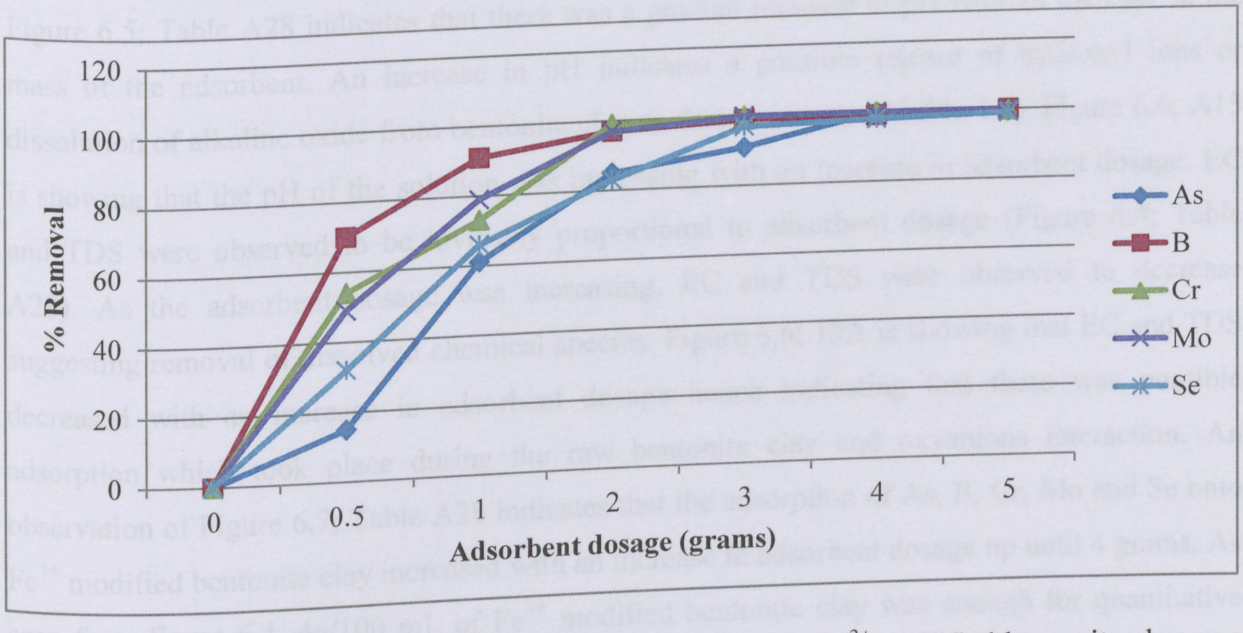


Figure 6.7: Variation of As, B, Cr, Mo and Se % removal for Fe^{3+} modified bentonite clay as a function of adsorbent dosage (30 minutes of contact time, 10 mg/L of adsorbate concentration, 250 rpm and 26°C).

© University of Venda

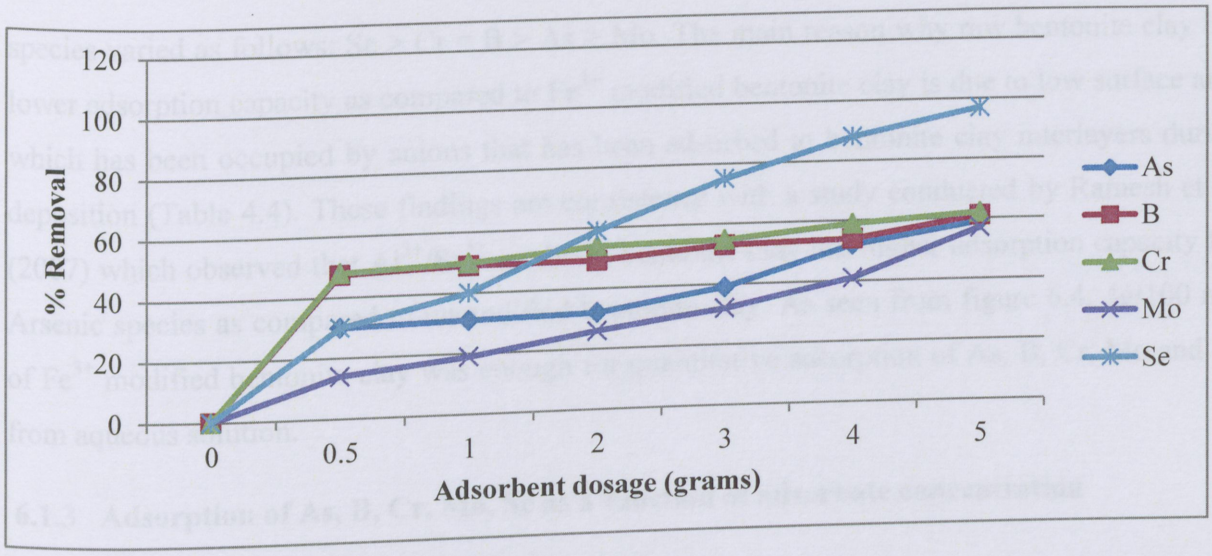


Figure 6.8: Variation of As, B, Cr, Mo and Se % removal for raw bentonite clay as a function of adsorbent dosage (30 minutes of contact time, 10 mg/L of adsorbate concentration, 250 rpm and 26°C).

Figure 6.5; Table A28 indicates that there was a gradual increase in pH with an increase in the mass of the adsorbent. An increase in pH indicates a possible release of hydroxyl ions or dissolution of alkaline oxide from bentonite clay as dosage increase (Table 4.2). Figure 6.6; A13 is showing that the pH of the solution was increasing with an increase in adsorbent dosage. EC and TDS were observed to be inversely proportional to adsorbent dosage (Figure 6.4; Table A28). As the adsorbent dosage was increasing, EC and TDS were observed to decrease suggesting removal of dissolved chemical species. Figure 6.6; 13A is showing that EC and TDS decreased with an increase in adsorbent dosage hence indicating that there was possible adsorption which took place during the raw bentonite clay and oxyanions interaction. An observation of Figure 6.7; Table A28 indicates that the adsorption of As, B, Cr, Mo and Se onto Fe^{3+} modified bentonite clay increased with an increase in adsorbent dosage up until 4 grams. As seen from figure 6.4, 4g/100 mL of Fe^{3+} modified bentonite clay was enough for quantitative adsorption of As, B, Cr, Mo and Se. The adsorption affinity of the modified clay for the tested chemical species varied as follows: B > Cr = Mo > As = Se. Increased adsorbent dose provides more sites for adsorption (Karthikeyan et al., 2005). The experimental results obtained from figure 6.8 revealed that there was a lower adsorption of As, B, Cr, Mo and Se on unmodified clay as compared to modified bentonite clay. The affinity of raw bentonite clay for the chemical

© University of Venda

species varied as follows: Se > Cr = B > As > Mo. The main reason why raw bentonite clay has lower adsorption capacity as compared to Fe^{3+} modified bentonite clay is due to low surface area which has been occupied by anions that has been adsorbed to bentonite clay interlayers during deposition (Table 4.4). These findings are consistence with a study conducted by Ramesh et al. (2007) which observed that Al^{3+}/Fe^{3+} modified bentonite clay has higher adsorption capacity for Arsenic species as compared to unmodified bentonite clay. As seen from figure 6.4, 4g/100 mL of Fe^{3+} modified bentonite clay was enough for quantitative adsorption of As, B, Cr, Mo and Se from aqueous solution.

6.1.3 Adsorption of As, B, Cr, Mo, Se as a function of adsorbate concentration

Effects of adsorbate concentration on the adsorption of As, B, Cr, Mo and Se by Fe^{3+} modified bentonite clay and raw bentonite clay was evaluated at the contact time of 30 minutes, adsorbent dosage of 4 grams, 250 rpm and 26°C (Table A30). The concentrations of As, B, Cr, Mo and Se were varied from 0.1 to 15 mg/L. Figure 6.9, 6.10, 6.11, 6.12, 6.13 and 6.14 shows the variation of As, B, Cr, Mo, Se, initial and final pH, EC and TDS with an increase in adsorbate concentration for raw and modified bentonite clay.

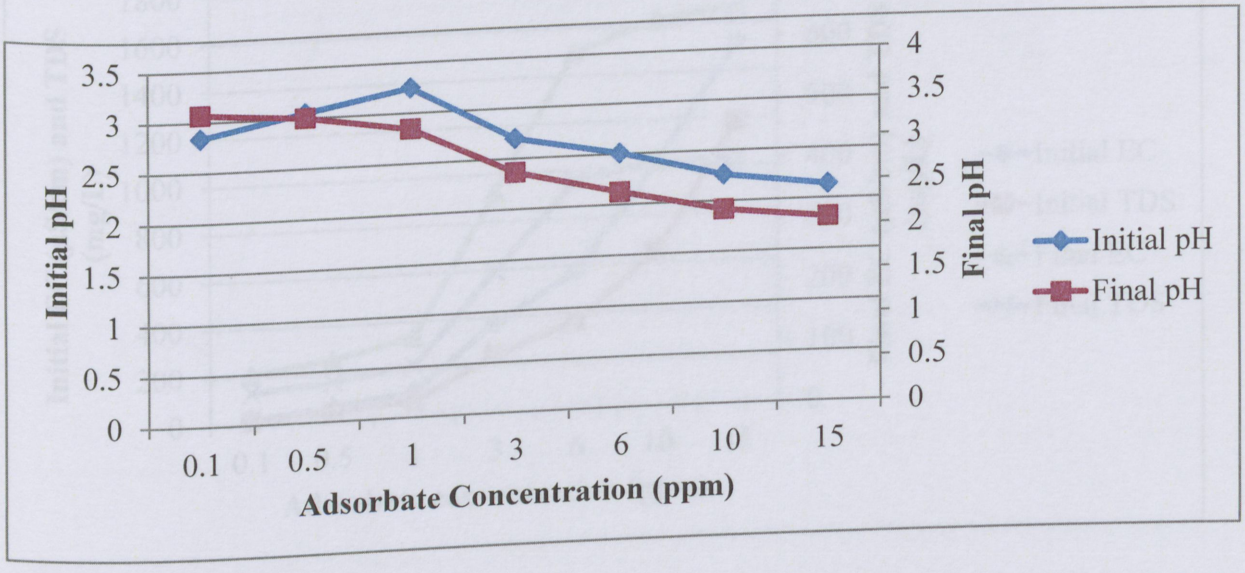


Figure 6.9: Variation of initial and final pH profiles for adsorption of As, B, Cr, Mo and Se by Fe^{3+} modified bentonite clay with an increase in adsorbate concentration (contact time of 30 minute, adsorbent dosage of 4 grams, 250 rpm, 26°C, and 4g/100 mL S/L ratios). The concentration was varied from 0.1, 0.5, 1, 3, 6, 10, and 15 mg/L.

© University of Venda

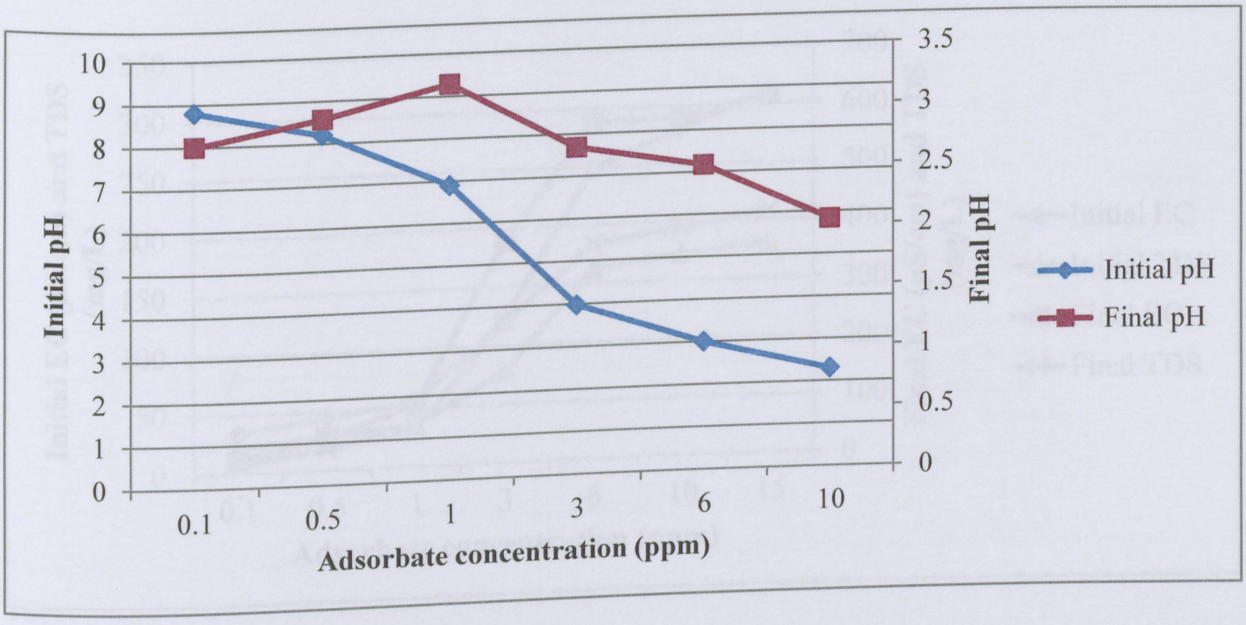


Figure 6.10: Variation of initial and final pH profiles with an increase in adsorbate concentration for raw bentonite clay (30 minutes of contact time, 4 grams of adsorbent dosage, 250 rpm, 26°C and 4g/100 mL S/L ratios).

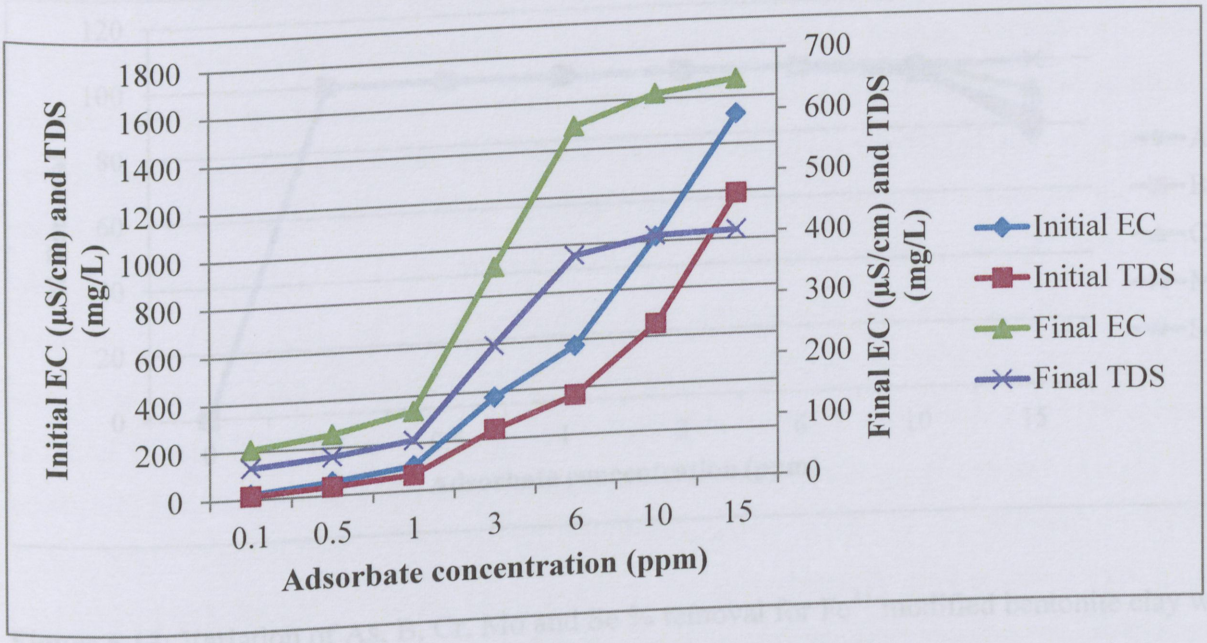


Figure 6.11: Variation of initial and final EC and TDS levels on adsorption of As, B, Cr, Mo and Se by Fe^{3+} modified bentonite clay with an increase in adsorbate concentration (contact time of 30 minute, adsorbent dosage of 4 grams, 26°C, 4g/100 mL S/L ratios, concentration varied 0.1, 0.5, 1, 3, 6, 10, and 15 mg/L).

© University of Venda

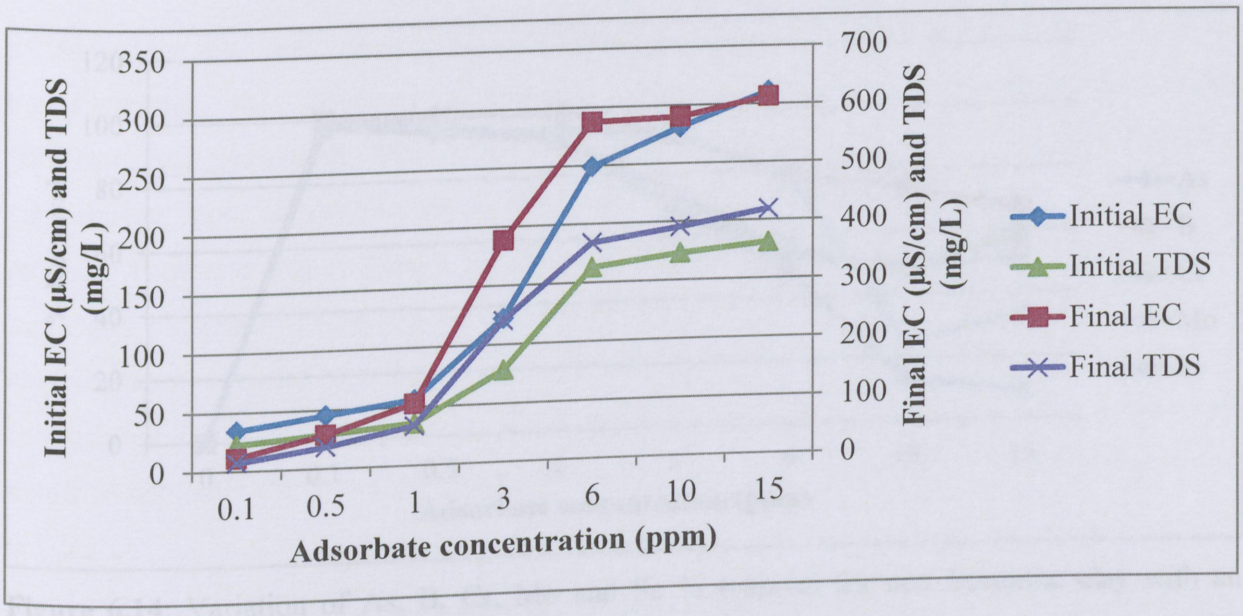


Figure 6.12: Variation of initial and final EC and TDS with an increase in adsorbate concentration for raw bentonite clay (30 minutes of contact time, 4 grams of adsorbent dosage, 250 rpm, 26°C and 4g/100 mL S/L ratios).

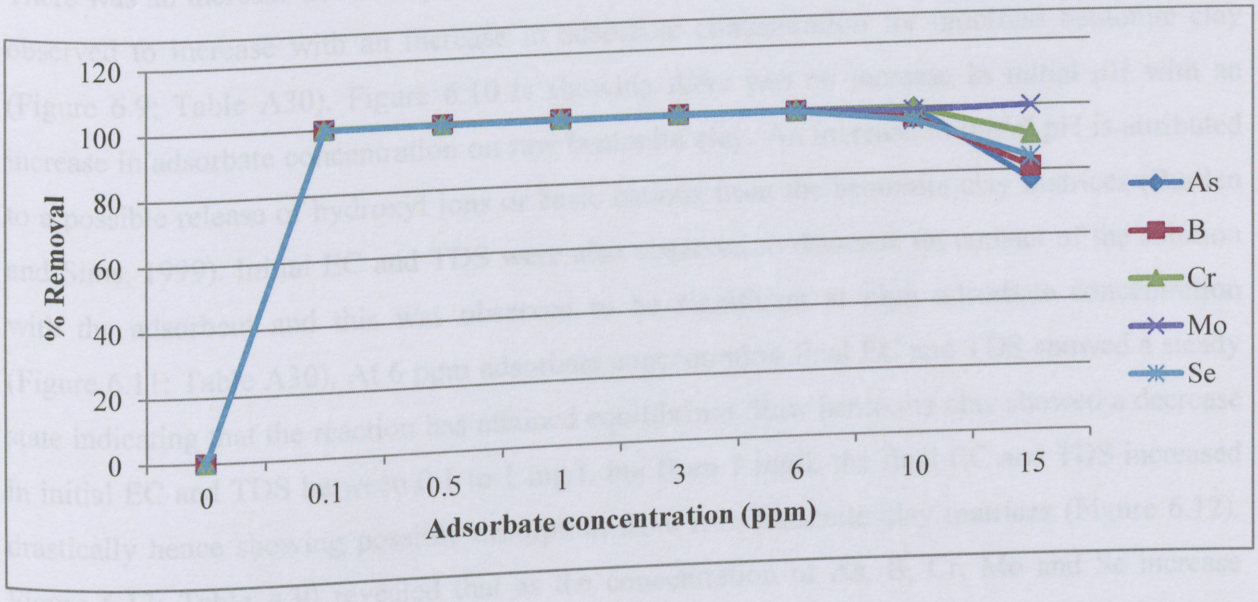


Figure 6.13: Variation of As, B, Cr, Mo and Se % removal for Fe^{3+} modified bentonite clay with an increase in adsorbate concentration (contact time of 30 minute, adsorbent dosage of 4 grams, 250 rpm, 26°C, 4g/100 mL S/L ratios, concentration varied from 0.1, 0.5, 1, 3, 6, 10, and 15 mg/L).

© University of Venda

University of Venda
Creating Future Leaders

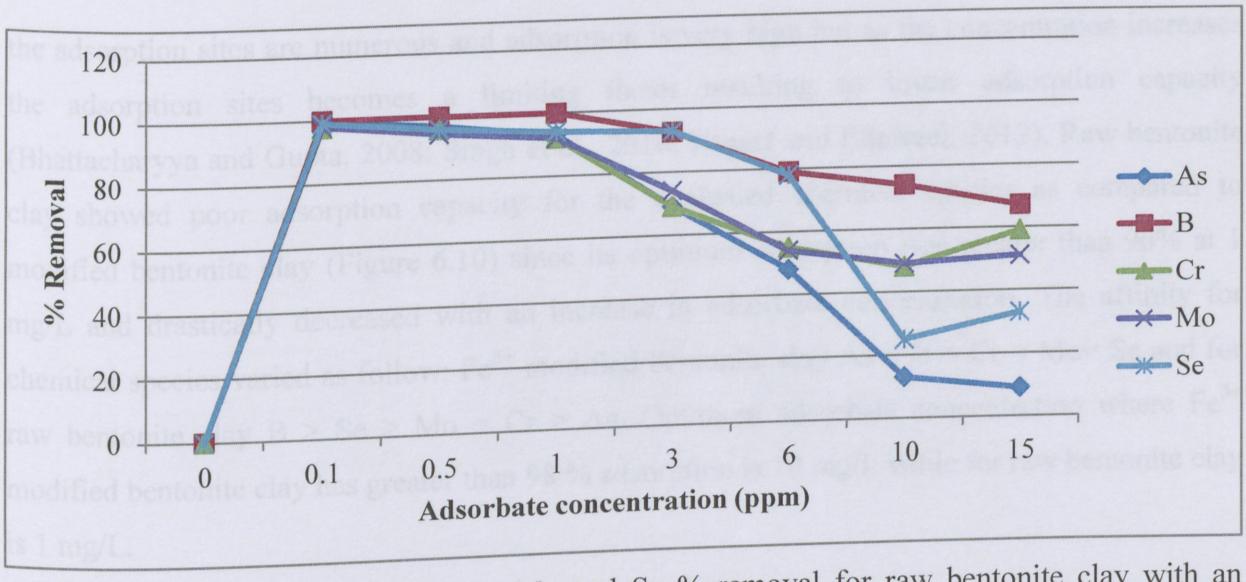


Figure 6.14: Variation of As, B, Cr, Mo and Se % removal for raw bentonite clay with an increase in adsorbate concentration (contact time of 30 minute, adsorbent dosage of 4 grams, 250 rpm, 26°C, 4g/100 mL S/L ratios, concentration varied from 0.1, 0.5, 1, 3, 6, 10, and 15 mg/L).

There was an increase in initial pH in the reaction mixture at low concentration which was then observed to increase with an increase in adsorbate concentration for modified bentonite clay (Figure 6.9; Table A30). Figure 6.10 is showing there was an increase in initial pH with an increase in adsorbate concentration on raw bentonite clay. An increase in initial pH is attributed to a possible release of hydroxyl ions or basic cations from the bentonite clay matrices (Burden and Sims, 1999). Initial EC and TDS were also observed to decrease on contact of the solution with the adsorbent and this was observed to be significant at high adsorbate concentration (Figure 6.11; Table A30). At 6 ppm adsorbate concentration final EC and TDS showed a steady state indicating that the reaction has attained equilibrium. Raw bentonite clay showed a decrease in initial EC and TDS between 0.1 to 1 mg/L but from 1 mg/L the final EC and TDS increased drastically hence showing possible desorption from raw bentonite clay matrices (Figure 6.12). Figure 6.13; Table A30 revealed that as the concentration of As, B, Cr, Mo and Se increase beyond 10 mg/L for Fe^{3+} modified bentonite clay and approximately greater than 1 ppm for raw bentonite clay, the adsorption capacity of those chemical species from aqueous media decreased. Figure 6.13; Table A30 also showed that the adsorption of As, B, Cr, Mo and Se by the Fe^{3+} modified bentonite clay was high at low adsorbate concentration and gradually decreased with an increase in adsorbate concentration. The modified bentonite clay adsorbed greater than 98% of the evaluated chemical species at concentration range of 0.1 to 10 mg/L. At low concentration,

© University of Venda

the adsorption sites are numerous and adsorption is very high but as the concentration increases the adsorption sites becomes a limiting factor resulting to lower adsorption capacity (Bhattacharyya and Gupta, 2008; Singh et al., 2010; Nassef and Eltaweel, 2012). Raw bentonite clay showed poor adsorption capacity for the evaluated chemical species as compared to modified bentonite clay (Figure 6.10) since its optimum adsorption was greater than 90% at 1 mg/L and drastically decreased with an increase in adsorbate concentration. The affinity for chemical species varied as follow: Fe^{3+} modified bentonite clay As = B = Cr = Mo= Se and for raw bentonite clay B > Se > Mo = Cr > As. Optimum adsorbate concentration where Fe^{3+} modified bentonite clay has greater than 98 % adsorption is 10 mg/L while for raw bentonite clay is 1 mg/L.

6.1.4 Adsorption of As, B, Cr, Mo, Se as a function of pH

Effects of pH on adsorption of As, B, Cr, Mo and Se onto Fe^{3+} modified bentonite clay was evaluated for 30 minutes of contact time, 4 grams of adsorbent dosage, 10 mg/L metals concentration, 250 rpm, 26°C and 4g/100 mL S/L ratios) (Table A31). Figure 6.15, 6.16, 6.17, 6.18, 6.19 and 6.20 shows variation in As, B, Cr, Mo, Se, final pH, EC and TDS with varying initial pH ranges

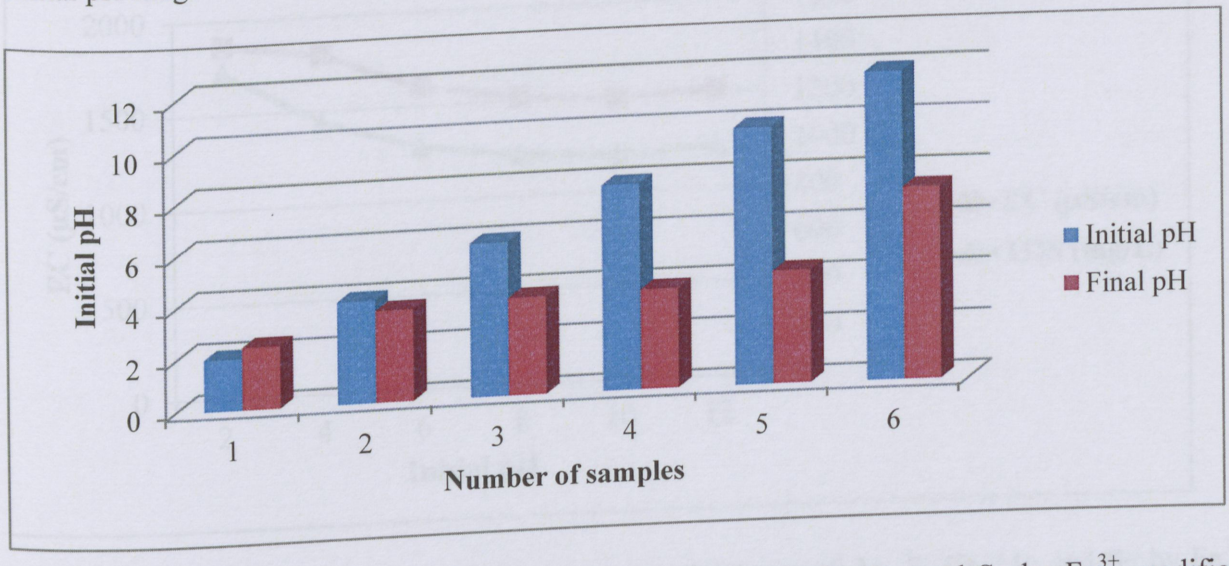


Figure 6.15: Variation of final pH on adsorption of As, B, Cr, Mo and Se by Fe^{3+} modified bentonite clay with varying initial pH (30 minutes of contact time, 4 grams of adsorbent dosage, 10 mg/L metals concentration, 26°C and 4g/100 mL S/L ratios).

© University of Venda

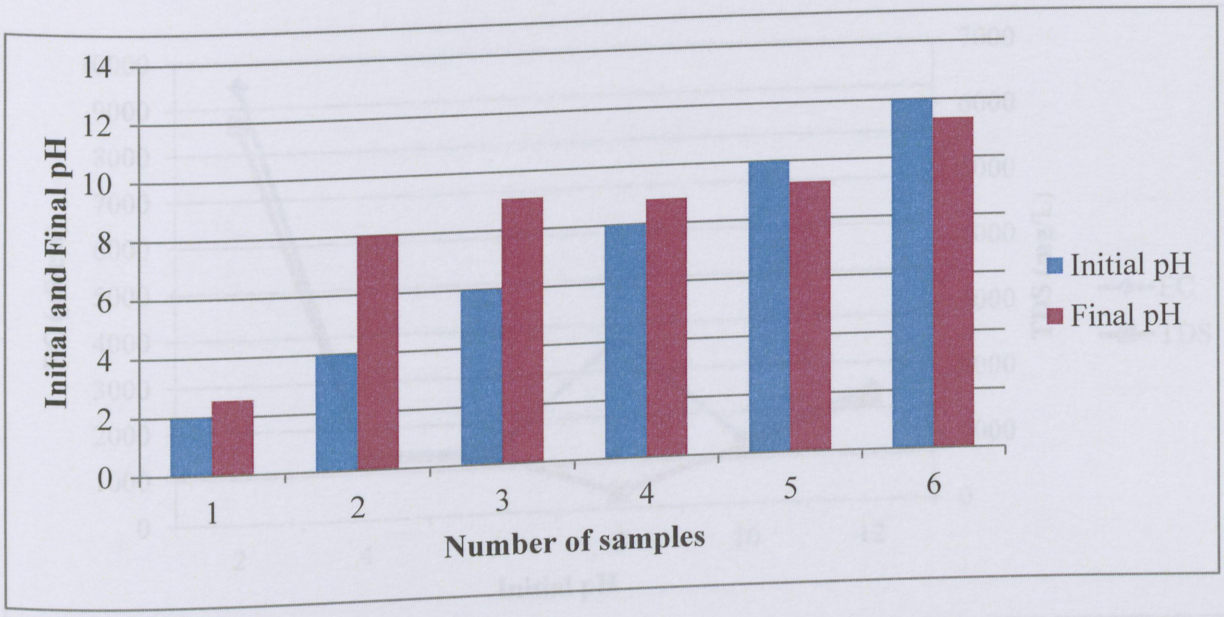


Figure 6.16: Variation of final pH at varying initial pH on adsorption of As, B, Cr, Mo and Se onto raw bentonite clay (30 minutes of contact time, 4 grams of adsorbent dosage, 10 mg/L metals concentration, 250 rpm, 26°C and 4g/100 mL S/L ratios).

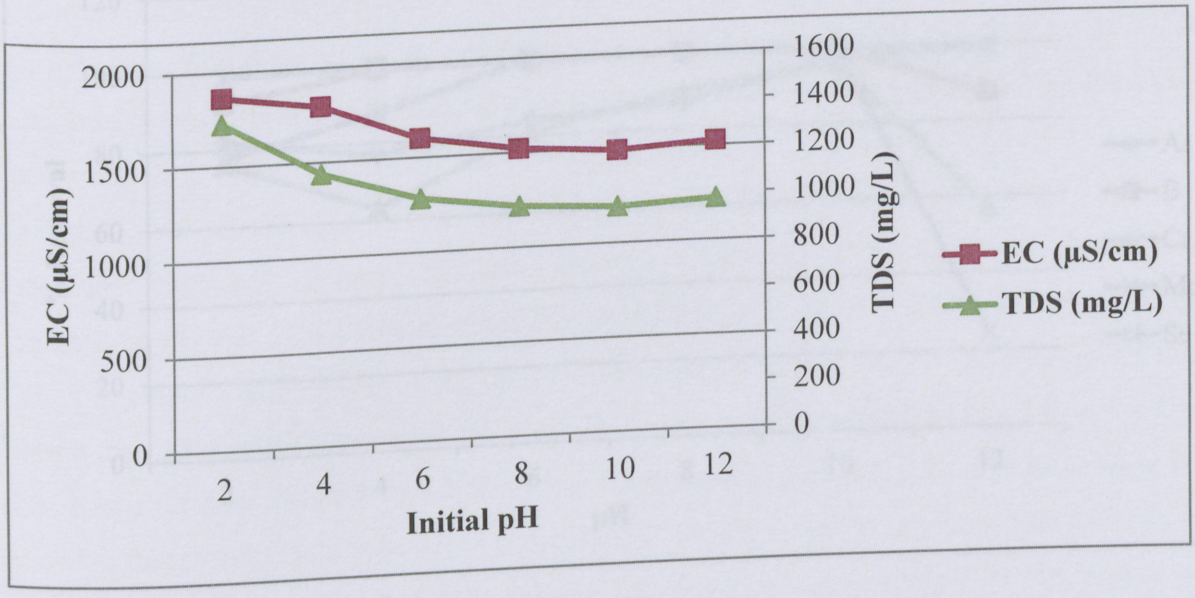


Figure 6.17: Variation of EC and TDS levels on adsorption of As, B, Cr, Mo and Se by Fe^{3+} modified bentonite clay with varying initial pH (30 minutes of contact time, 4 grams of adsorbent dosage, 10 mg/L metal concentration, 250 rpm, 26°C and 4g/100 mL S/L ratios).

© University of Venda

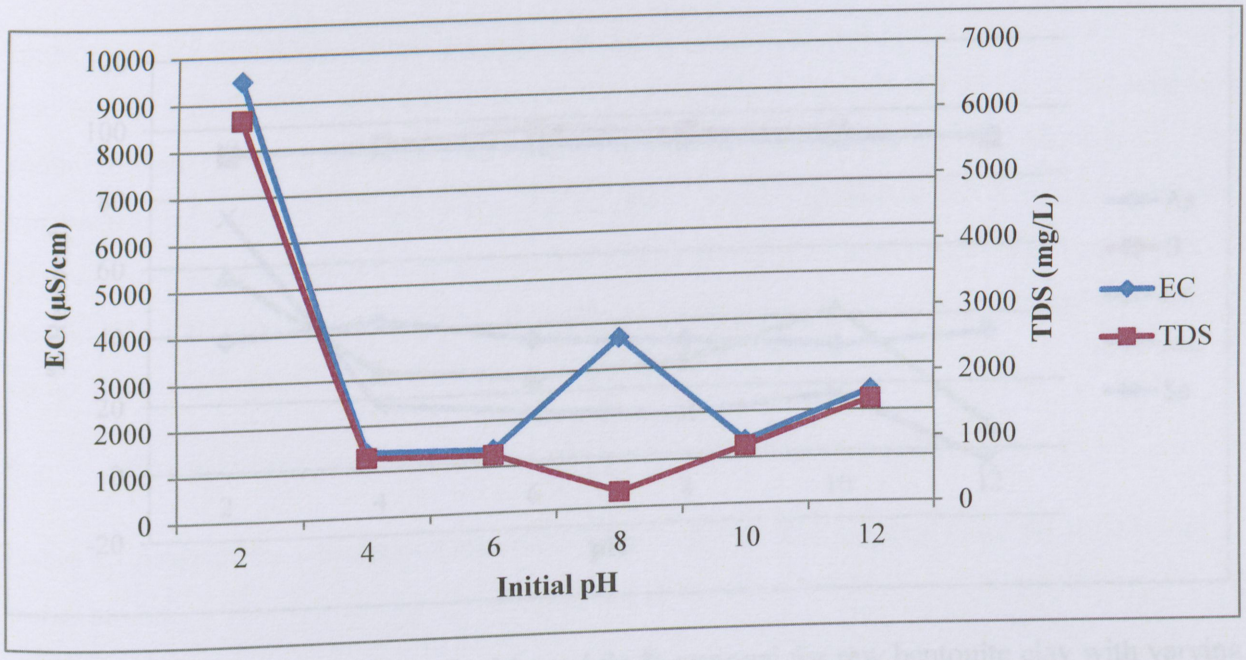


Figure 6.18: Variation of EC and TDS with varying initial pH on adsorption of As, B, Cr, Mo and Se onto raw bentonite clay (30 minutes of contact time, 4 grams of adsorbent dosage, 10 mg/L metals concentration, 250 rpm, 26ºC and 4g/100 mL S/L ratios).

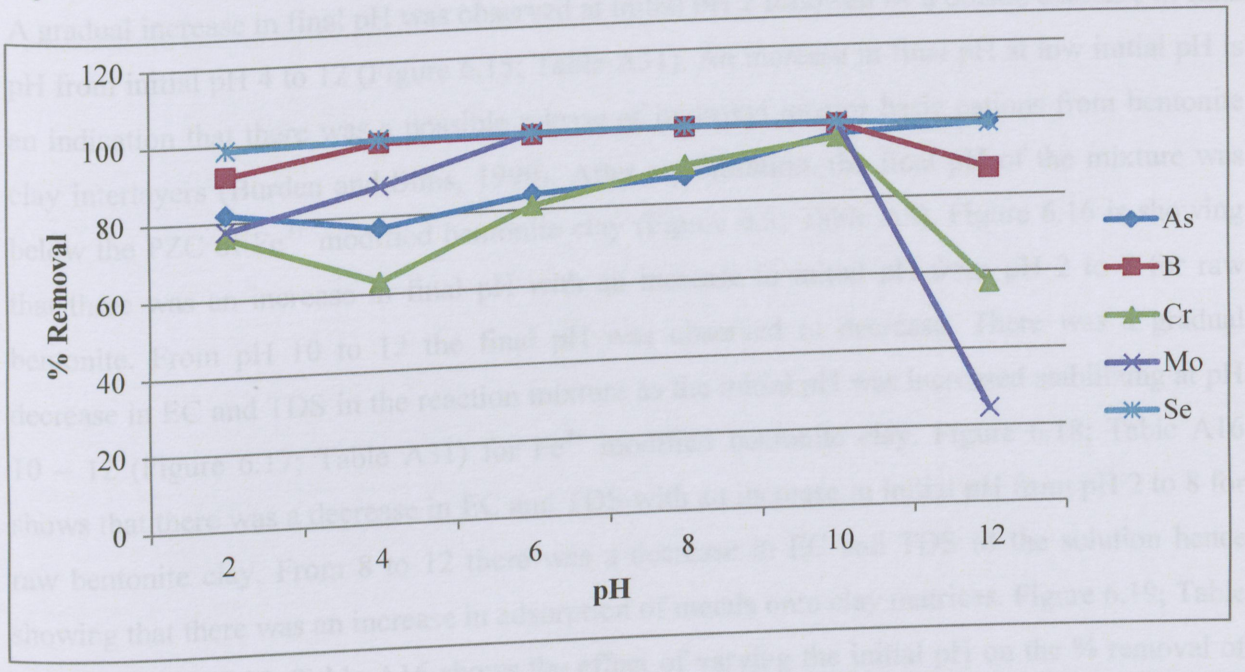


Figure 6.19: Variation of As, B, Cr, Mo and Se % removal for Fe^{3+} modified bentonite clay with varying pH ranges (30 minutes of contact time, 4 grams of adsorbent dosage, 10 mg/L metals concentration, 250 rpm, 26ºC and 4g/100 mL S/L ratios).

© University of Venda

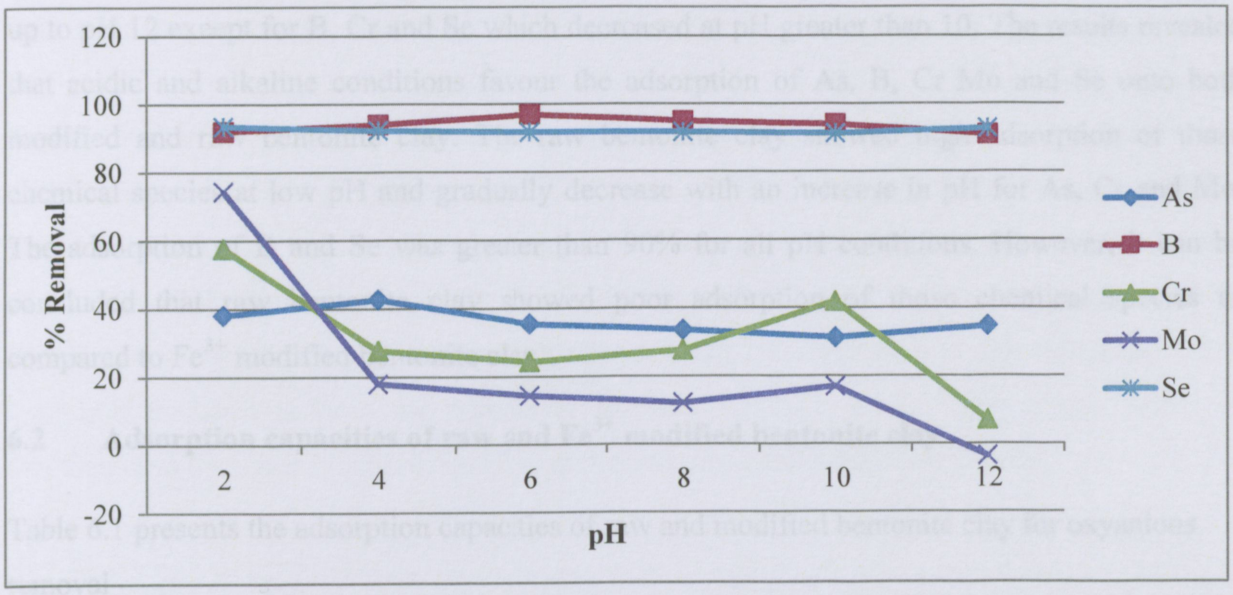


Figure 6.20: Variation of As, B, Cr, Mo and Se % removal for raw bentonite clay with varying pH ranges (30 minutes of contact time, 4 grams of adsorbent dosage, 10 mg/L metals concentration, 250 rpm, 26°C and 4g/100 mL S/L ratios).

A gradual increase in final pH was observed at initial pH 2 followed by a drastic decrease in final pH from initial pH 4 to 12 (Figure 6.15; Table A31). An increase in final pH at low initial pH is an indication that there was a possible release of hydroxyl ions or basic cations from bentonite clay interlayers (Burden and Sims, 1999). After equilibration, the final pH of the mixture was below the PZC of Fe^{3+} modified bentonite clay (Figure 4.3; Table A3). Figure 6.16 is showing that there was an increase in final pH with an increase in initial pH from pH 2 to 8 for raw bentonite. From pH 10 to 12 the final pH was observed to decrease. There was a gradual decrease in EC and TDS in the reaction mixture as the initial pH was increased stabilizing at pH 10 – 12 (Figure 6.17; Table A31) for Fe^{3+} modified bentonite clay. Figure 6.18; Table A16 shows that there was a decrease in EC and TDS with an increase in initial pH from pH 2 to 8 for raw bentonite clay. From 8 to 12 there was a decrease in EC and TDS of the solution hence showing that there was an increase in adsorption of metals onto clay matrices. Figure 6.19; Table A31 and figure 6.20; Table A16 shows the effect of varying the initial pH on the % removal of As, B, Cr, Mo and Se for Fe^{3+} modified bentonite clay. The percentage removal of the evaluated chemical species increased on increasing the pH except for As and Cr which initially decreased at pH 2 to 4 for modified bentonite clay. Thereafter, adsorption increased for all chemical species

© University of Venda

up to pH 12 except for B, Cr and Se which decreased at pH greater than 10. The results revealed that acidic and alkaline conditions favour the adsorption of As, B, Cr Mo and Se onto both modified and raw bentonite clay. The raw bentonite clay showed high adsorption of those chemical species at low pH and gradually decrease with an increase in pH for As, Cr and Mo. The adsorption of B and Se was greater than 90% for all pH conditions. However, it can be concluded that raw bentonite clay showed poor adsorption of those chemical species as compared to Fe^{3+} modified bentonite clay.

6.2 Adsorption capacities of raw and Fe^{3+} modified bentonite clay

Table 6.1 presents the adsorption capacities of raw and modified bentonite clay for oxyanions removal

Table 6.1: Adsorption capacities (mg/g) of raw and Fe^{3+} modified bentonite clay for oxyanions of As, B, Cr, Mo and Se

Adsorption Capacity (mg/g)										
	Iron modified bentonite clay					**Raw Bentonite**				
Co (mg/L)	As	B	Cr	Mo	Se	As	B	Cr	Mo	Se
0.1	0.002	0.002	0.002	0.002	0.002	0.002	0.002	0.000	0.002	0.001
0.5	0.012	0.012	0.012	0.012	0.012	0.005	0.012	0.003	0.008	0.005
1	0.025	0.025	0.025	0.025	0.025	0.008	0.023	0.005	0.015	0.010
3	0.074	0.075	0.075	0.074	0.075	0.023	0.057	0.018	0.033	0.038
6	0.149	0.149	0.150	0.149	0.149	0.038	0.110	0.038	0.043	0.095
10	0.247	0.247	0.249	0.248	0.249	0.063	0.178	0.120	0.058	0.153
15	0.370	0.370	0.373	0.373	0.373	0.078	0.248	0.218	0.078	0.218

As shown in table 6.1, as the concentration of species in solution increases, the amount adsorbed also increases. At low concentrations, the limiting factor on adsorption is the adsorbate concentration. It is clear that the adsorption capacity of raw bentonite clay is low as compare to Fe^{3+} modified bentonite clay.

© University of Venda

6.3 Adsorption isotherms

The adsorption isotherms of Fe^{3+} onto bentonite clay lattice were investigated at the contact time of 30 minute, adsorbent dosage of 4 grams, 250 rpm, 26°C, 4g/100 mL S/L ratios, concentration varied from 0.1, 0.5, 1, 3, 6, 10, and 15 mg/L. Two adsorption isotherms, namely the Langmuir (Langmuir, 1918; Ramesh et al., 2007; Bhati and Singh, 2012) and Freundlich (Freundlich, 1906; Ramesh et al., 2007; Bhati and Singh, 2012) were used to describe the adsorption data. The Langmuir isotherm is valid for monolayer sorption due to a surface with finite number of identical sites (Singh et al., 2010) and it is expressed in the following linear form:

$$\frac{Ce}{Qe} = \frac{1}{Qmb} + \frac{Ce}{Qm} \quad \text{..... (18)}$$

Where, Ce = Equilibrium concentration (mg/L)

Qe = Amount adsorbed at equilibrium (mg/g)

Qm = Langmuir constants related to adsorption capacity

b = Langmuir constants related to energy of adsorption (L/mg)

A plot of Ce/Qe versus Ce should be linear if the data is described by the Langmuir isotherm. The value of Qm and b will be determined from the slope and the intercept of the plot and will be determining whether the adsorbent has high adsorption capacity or the adsorption is taking place at high or low energy.

Langmuir adsorption isotherm can also be expressed in terms of R_L, a dimensionless factor known as separation factor. It is used to determine whether the reaction was favorable or not.

$$R_L = \frac{1}{(1 + bCo)} \quad \text{..... (19)}$$

Where, Co = initial concentration. If R_L is between 0 and 1, the adsorption is favorable (Langmuir, 1918). Figures 6.11, 12, 13, 14 and 15 shows the Langmuir adsorption isotherm for As, B, Cr, Mo and Se.

© University of Venda

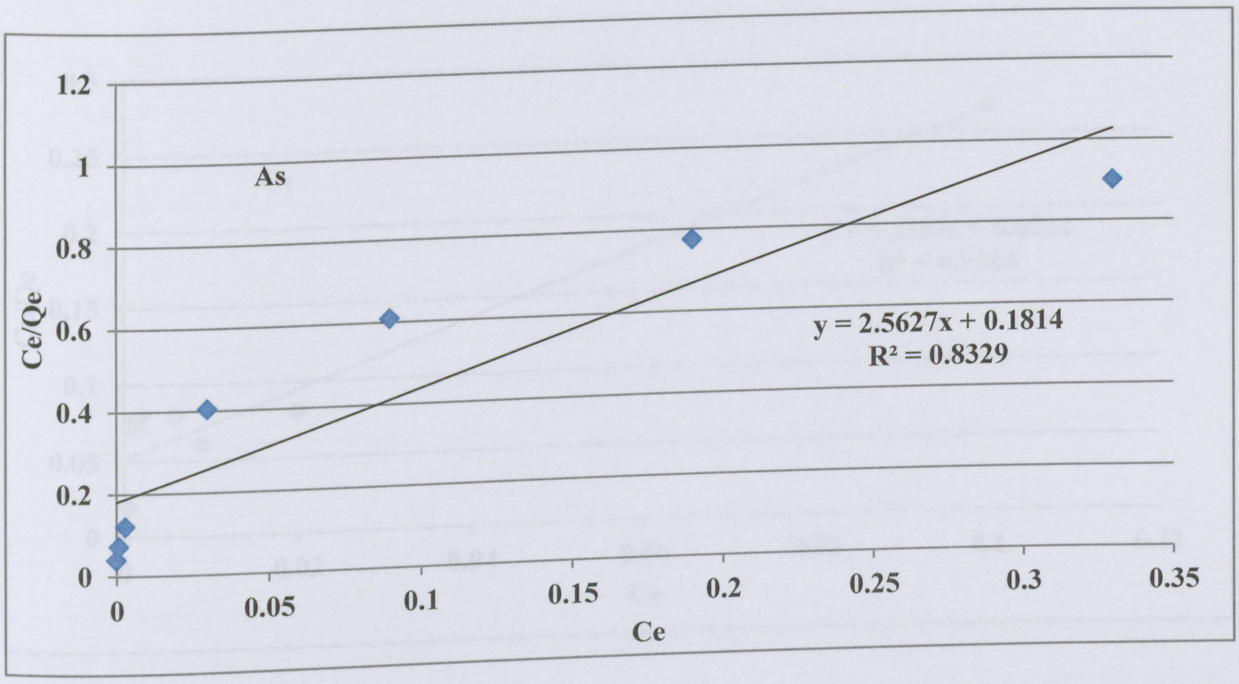


Figure 6.21: Langmuir adsorption isotherm for adsorption of As by Fe^{3+} modified bentonite clay (30 minutes of contact time, 4 grams of adsorbent dosage, 250 rpm, 26°C and 4g/100 mL S/L ratios).

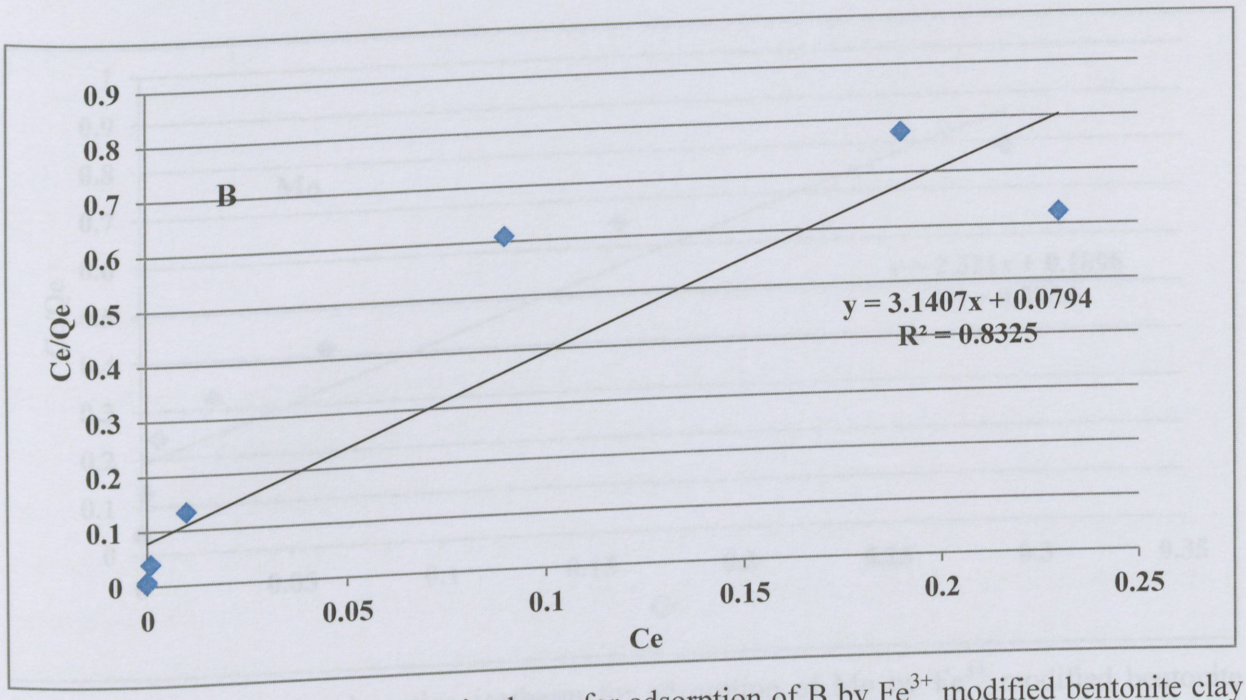


Figure 6.22: Langmuir adsorption isotherm for adsorption of B by Fe^{3+} modified bentonite clay (30 minutes of contact time, 4 grams of adsorbent dosage, 250 rpm, 26°C and 4g/100 mL S/L ratios).

© University of Venda

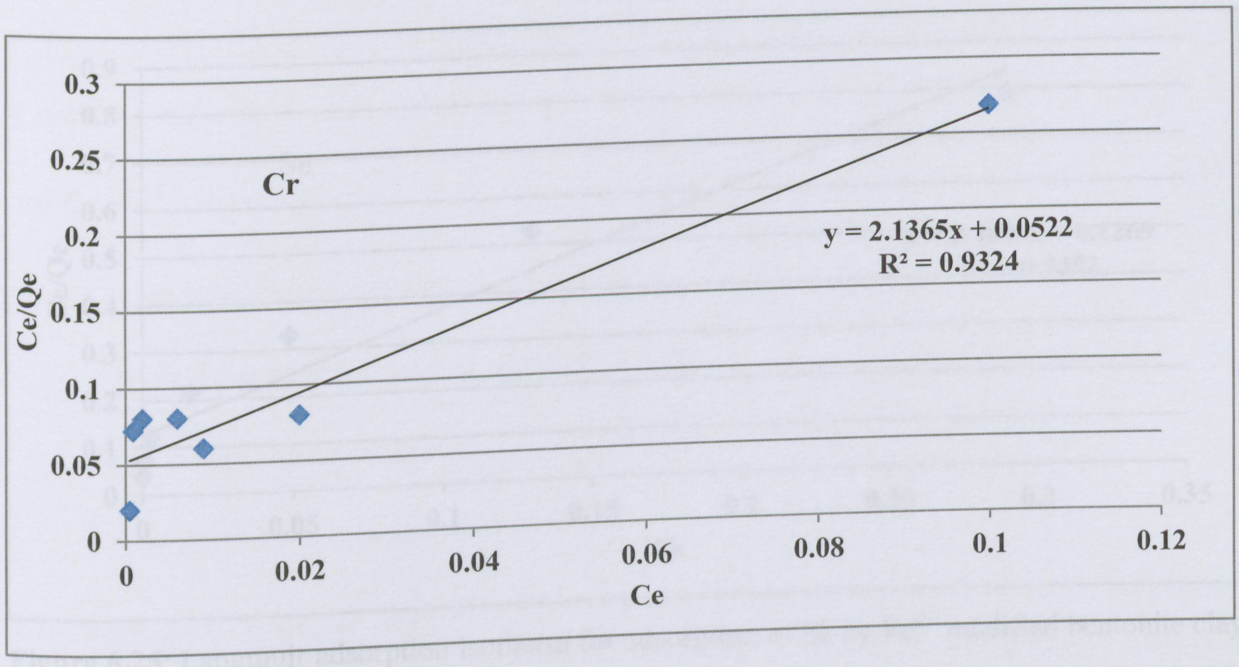


Figure 6.23: Langmuir adsorption isotherm for adsorption of Cr by Fe^{3+} modified bentonite clay (30 minutes of contact time, 4 grams of adsorbent dosage, 250 rpm, 26°C and 4g/100 mL S/L ratios).

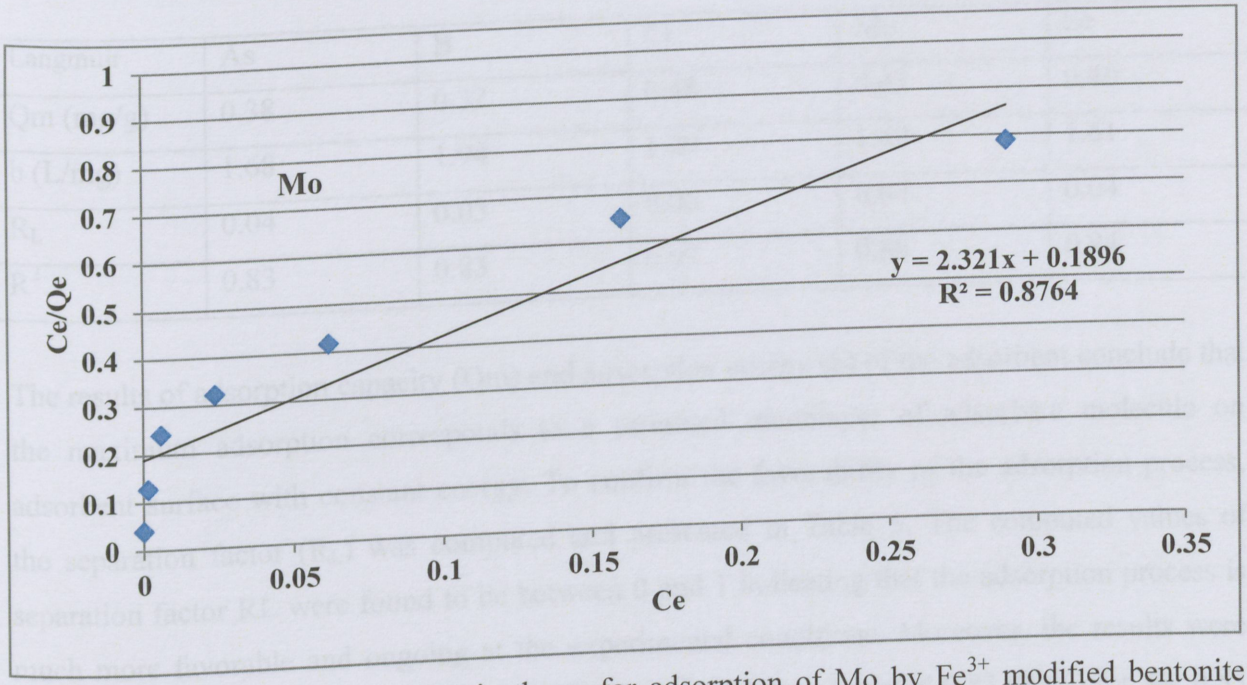


Figure 6.24: Langmuir adsorption isotherm for adsorption of Mo by Fe^{3+} modified bentonite clay (30 minutes of contact time, 4 grams of adsorbent dosage, 250 rpm, 26°C and 4g/100 mL S/L ratios).

© University of Venda

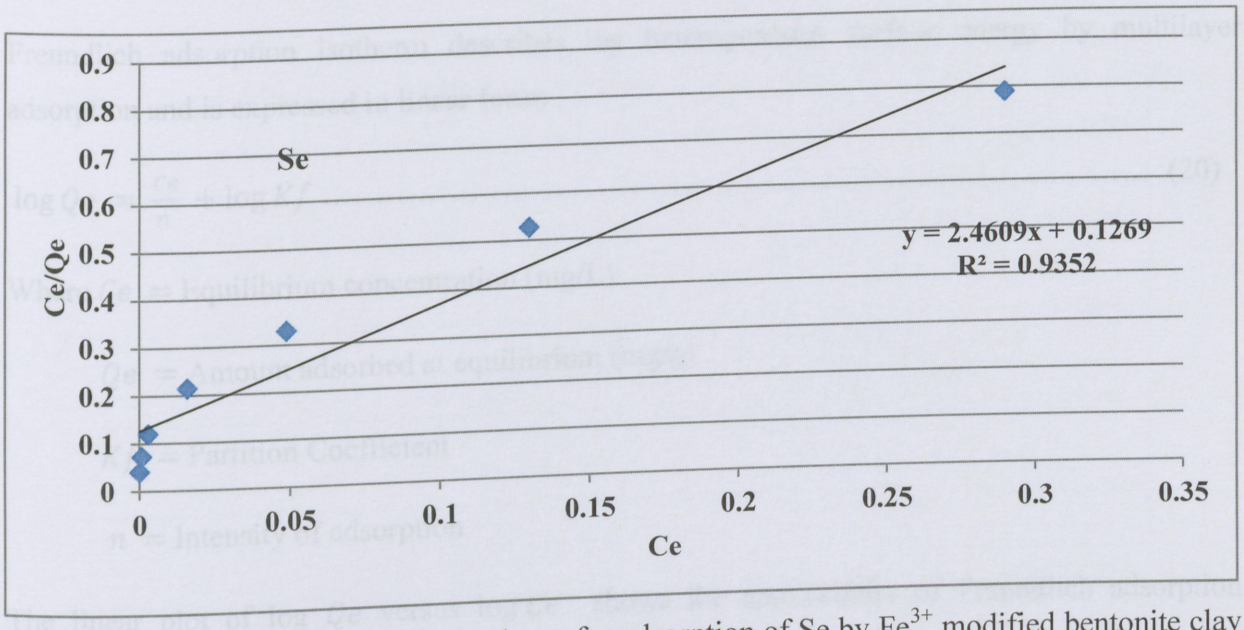


Figure 6.25: Langmuir adsorption isotherm for adsorption of Se by Fe^{3+} modified bentonite clay (30 minutes of contact time, 4 grams of adsorbent dosage, 250 rpm, 26°C and 4g/100 mL S/L ratios).

Table 6.2: Langmuir adsorption isotherms constants for adsorption of As, B, Cr, Mo and Se onto Fe^{3+} modified bentonite clay

Langmuir	As	B	Cr	Mo	Se
Qm (mg/g)	0.38	0.32	0.48	0.43	0.40
b (L/mg)	1.68	1.94	1.29	1.49	1.61
R_L	0.04	0.03	0.05	0.04	0.04
R^2	0.83	0.83	0.93	0.88	0.94

The results of adsorption capacity (Qm) and adsorption energy (b) of the adsorbent conclude that the maximum adsorption corresponds to a saturated monolayer of adsorbate molecule on adsorbent surface with constant energy. To confirm the favorability of the adsorption process, the separation factor (R_L) was computed and presented in Table 5. The computed values of separation factor RL were found to be between 0 and 1 indicating that the adsorption process is much more favorable and ongoing at the experimental conditions. Moreover, the results were also expressed in terms of regression coefficient (R^2) and they depicted 0.83 (83%) for As, 0.83 (83%) for B, 0.93 (93%) for Cr, 0.88 (88%) for Mo and 0.94 (94%) for Se, indicating a positive, very good and strong mathematical fit.

© University of Venda

Freundlich adsorption isotherm describes the heterogeneous surface energy by multilayer adsorption and is expressed in linear form:

$$\log Qe = \frac{Ce}{n} + \log Kf \quad \text{..... (20)}$$

Where Ce = Equilibrium concentration (mg/L)

Qe = Amount adsorbed at equilibrium (mg/g)

Kf = Partition Coefficient

n = Intensity of adsorption

The linear plot of $\log Qe$ versus $\log Ce$ shows the applicability of Freundlich adsorption isotherm. The value of Kf implies that the energy of adsorption on a homogeneous surface is independent of surface coverage and n is an adsorption constants which reveals the rate at which adsorption is taking place. Those two constants are determined from the slope (Freundlich, 1906). Figure 6.26, 6.27, 6.28, 6.29, and 6.30 shows the Freundlich adsorption isotherm for As, B, Cr, Mo and Se.

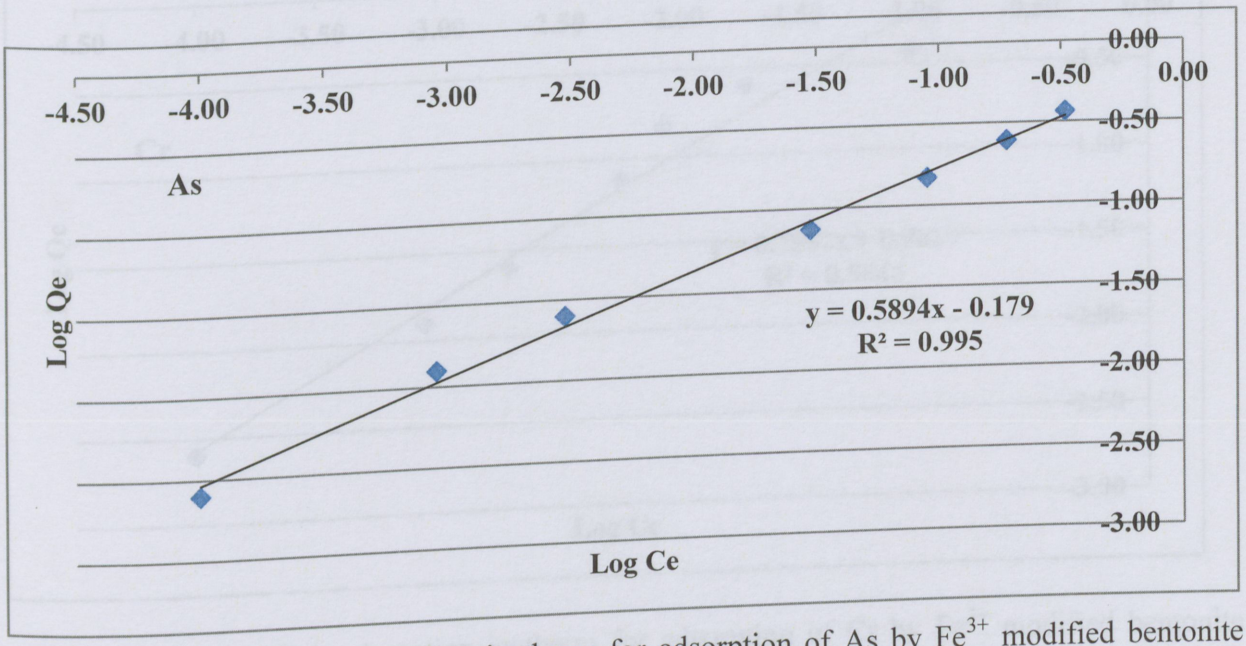


Figure 6.26: Freundlich adsorption isotherm for adsorption of As by Fe^{3+} modified bentonite clay (30 minutes of contact time, 4 grams of adsorbent dosage, 250 rpm, 26°C and 4g/100 mL S/L ratios).

© University of Venda

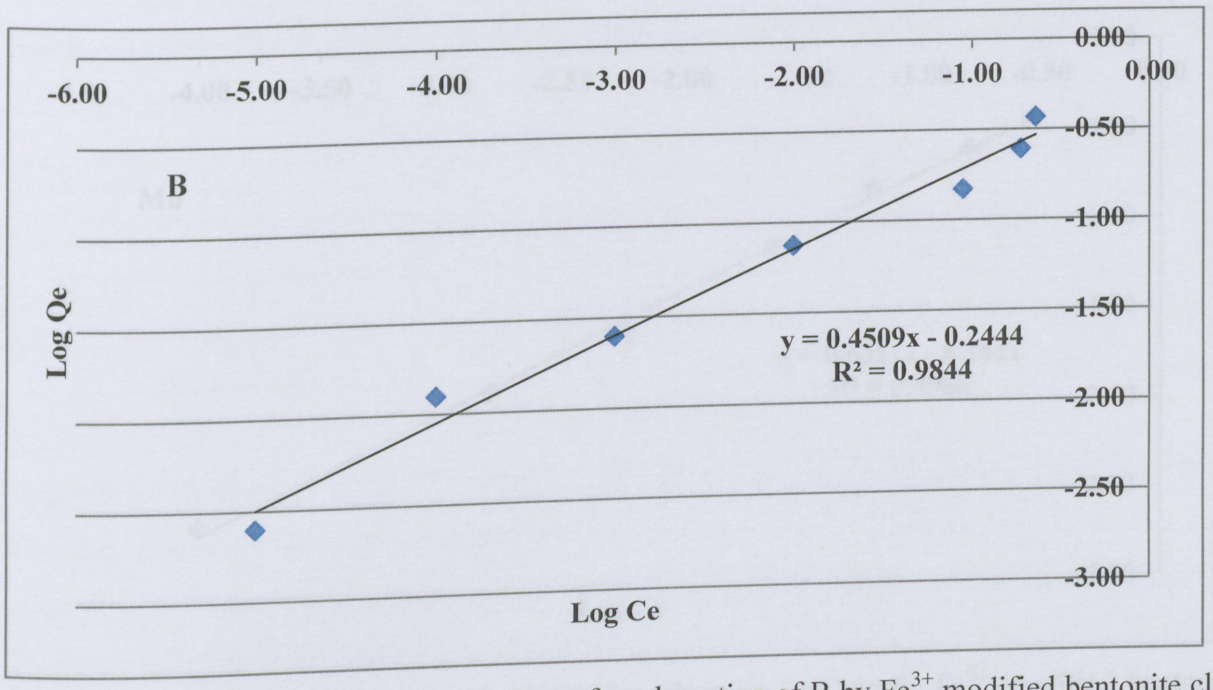


Figure 6.27: Freundlich adsorption isotherm for adsorption of B by Fe^{3+} modified bentonite clay (30 minutes of contact time, 4 grams of adsorbent dosage, 250 rpm, 26°C and 4g/100 mL S/L ratios).

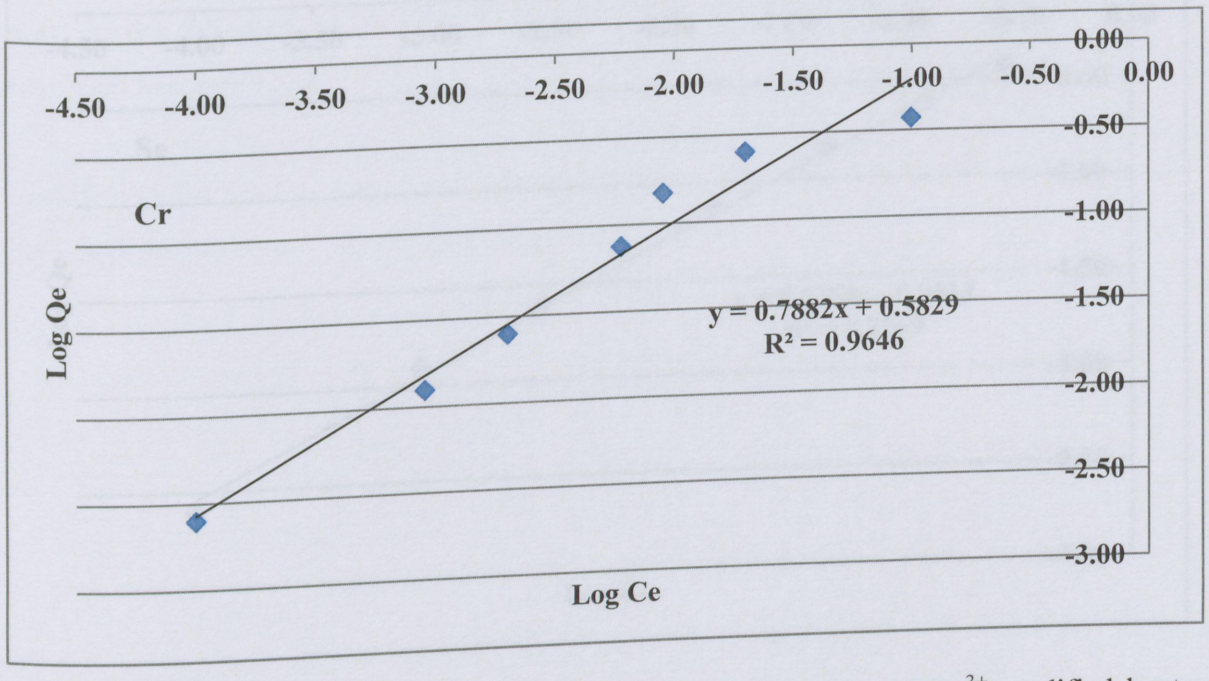


Figure 6.28: Freundlich adsorption isotherm for adsorption of Cr by Fe^{3+} modified bentonite clay (30 minutes of contact time, 4 grams of adsorbent dosage, 250 rpm, 26°C and 4g/100 mL S/L ratios).

© University of Venda

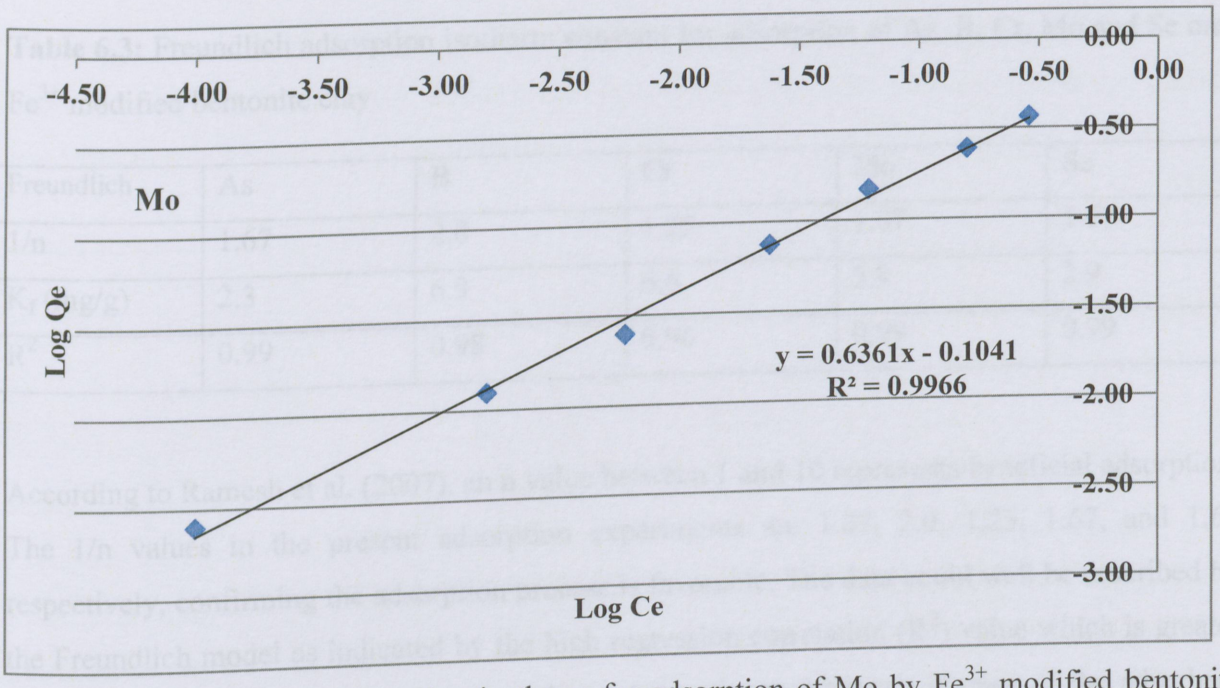


Figure 6.29: Freundlich adsorption isotherm for adsorption of Mo by Fe^{3+} modified bentonite clay (30 minutes of contact time, 4 grams of adsorbent dosage, 250 rpm, 26°C and 4g/100 mL S/L ratios).

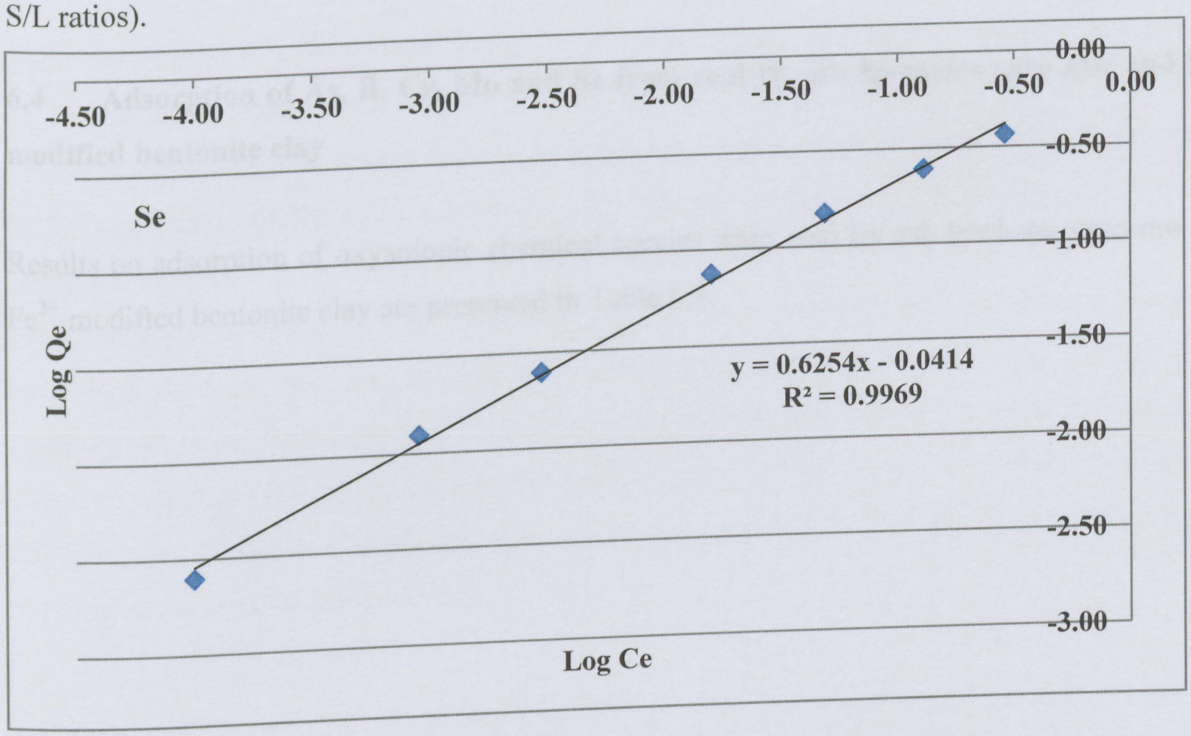


Figure 6.10: Freundlich adsorption isotherm for adsorption of Se by Fe^{3+} modified bentonite clay (30 minutes of contact time, 4 grams of adsorbent dosage, 250 rpm, 26°C and 4g/100 mL S/L ratios).

© University of Venda

Table 6.3: Freundlich adsorption isotherm constant for adsorption of As, B, Cr, Mo and Se onto Fe^{3+} modified bentonite clay

Freundlich	As	B	Cr	Mo	Se
1/n	1.67	2.0	1.25	1.67	1.67
K_f (mg/g)	2.3	6.9	6.6	2.9	2.9
R^2	0.99	0.98	0.96	0.99	0.99

According to Ramesh et al. (2007), an n value between 1 and 10 represents beneficial adsorption. The 1/n values in the present adsorption experiments are 1.67, 2.0, 1.25, 1.67, and 1.67 respectively, confirming the adsorption process is favorable. The data could well be described by the Freundlich model as indicated by the high regression correlation (R^2) value which is greater than 96%. This indicates that the adsorption process is a multilayer coverage of the adsorbent surface.

6.4 Adsorption of As, B, Cr, Mo and Se from coal fly ash leachates onto raw and Fe^{3+} modified bentonite clay

Results on adsorption of oxyanionic chemical species from coal fly ash leachates onto raw and Fe^{3+} modified bentonite clay are presented in Table 6.4.

UNIVERSITY OF VENDA
LIBRARY

© University of Venda

Table 6.4: Adsorption of As, B, Cr, Mo and Se from coal fly ash leachates using Fe^{3+} modified and raw bentonite clay under natural and optimized conditions and compared the product leachates to DWAF water quality guidelines (DWAF, 1996).

		Raw bentonite clay		Fe^{3+} modifiedbentonite clay		
Elements	Coal fly ash Leachates	natural conditions	optimized conditions	Natural Conditions	Optimized condition	DWAF guidelines
As(µg/L)	53	7.7	7.3	0.087	0.013	100
B(µg/L)	1730	630	501	1.49	0.034	500
Cr(µg/L)	271	101	99	9	0.009	10
Mo(µg/L)	165	75	79	3	0.03	10
Se(µg/L)	170	104	83	0.05	0.001	20
Final pH	11.10	12.3	7.9	8.3	9.1	6 - 9

N = 3

Table 6.4 shows the adsorption of As, B, Cr, Mo and Se from coal fly ash leachates onto raw and Fe^{3+} modified bentonite clay. As shown in Table 6.4, for raw bentonite, the adsorption of As, B, Cr, Mo and Se were observed to be high at optimum condition as compared to natural conditions. In the optimized conditions raw bentonite clay did not remove the concentration of chemical species understudy to the prescribed DWAF standard except for As and B. Fe^{3+} modified bentonite clay showed good adsorption of these chemical species at both natural and optimized conditions reducing the concentration of these chemical species to below the DWAF water quality guidelines. Based on that, it can be concluded that Fe^{3+} modified bentonite clay is an effective adsorbent for As, B, Cr, Mo and Se from coal fly ash leachates. This also implies that Fe^{3+} modified bentonite clay can be used as a liner or reactive barrier in ash retention ponds for trapping of these oxyanionic species.

© University of Venda

CHAPTER SEVEN

Conclusions and recommendations

7.1 Conclusion

This study was designed in an attempt to answer the following questions regarding the application of Al^{3+}/Fe^{3+} modified bentonite clay for adsorption of oxyanions of As, B, Cr, Mo and Se from coal fly ash leachates.

- What is the feasibility of modifying South African bentonite clay by introducing Al^{3+}/Fe^{3+} into the lattice?
- What are the physicochemical properties of raw and modified bentonite i.e. Cation Exchange Capacity (CEC), surface area, point of zero charge (PZC), water holding capacity, Elemental composition, and Mineralogical composition of bentonite clay?
- What are the adsorption capacities and mechanisms of modified bentonite clay for the oxyanions of As, B, Cr, Mo and Se in coal fly ash leachates?
- What is the efficiency of modified Bentonite clay for oxyanions adsorption in coal fly ash leachates as compared to DWAF water quality guidelines?

Therefore the following discussion will attempt to evaluate and elucidate more on the success and drawbacks of the study with regard to each of the above questions and also give recommendations on the future research prospective.

© University of Venda

7.1.1 Modification of raw bentonite clay with Al^{3+}/Fe^{3+} polycations

Modification of raw bentonite clay with polycations of Al^{3+} and Fe^{3+} revealed that 60 minutes of contact time, 3 grams of adsorbent dosage and 100 mg/L adsorbate concentration are the feasible optimum condition for loading polymeric Al^{3+} ions onto bentonite clay lattice and 15 minutes of contact time, 2 grams of adsorbent dosage and 100 mg/L of adsorbate concentration are the feasible optimum conditions for impregnating Fe^{3+} cations onto bentonite clay interlayers.

7.1.2 Physicochemical characterization of raw and modified bentonite clay

CEC results showed that South African bentonite clay is characterized by high CEC of 262 meq/100g at pH 5.4 and 265.5 meq/100g at pH 7.4 which decreased to 186.9 meq/100g at pH 5.4 and 183.3 meq/100g at pH 7.4 on introducing Al^{3+} onto bentonite clay interlayers and 195.5 meq/100g at pH 5.4 and 188.9 meq/100g at pH 7.4 on introducing Fe^{3+} onto bentonite clay interlayers. The results show that CEC is independent of pH. BET results indicated that the loading of Al^{3+} onto bentonite clay interlayers increased the surface area from 16 m^2/g to 44.3 m^2/g and 50 m^2/g for Fe^{3+}, external surface area from 11.1 m^2/g to 33.1 m^2/g for Al^{3+} and 37.4 m^2/g for Fe^{3+}, micro-pore area from 4.9 m^2/g to 11.2 m^2/g for Al^{3+} and 12.5 m^2/g for Fe^{3+}. There was a slight difference in pH_{PZC} of Al^{3+} modified bentonite clay (8.2) as compared to raw bentonite (8.0). For Fe^{3+} modified bentonite clay, the pH_{PZC} was observed to increase from 8.0 for raw bentonite clay to 9.0. An increase in pH_{PZC} shows that modification will favour adsorption of anions from aqueous media. WHC of bentonite clay was determined to be 42.7%. Elemental composition by XRF showed SiO_2, Al_2O_3, Fe_2O_3 , CaO, Na_2O, K_2O and MgO as the major chemical species. XRF results also confirmed that bentonite clay is an aluminosilicate material. XRD results showed that bentonite clay is dominated by montmorillonite (≅ 74.76) as the main mineral phase followed by Quartz (≅ 15.98) > Plagioclase (≅ 8.17) > Muscovite (≅ 1.09). Modification of bentonite clay with polycations of Al^{3+}/Fe^{3+} improved the physiochemical properties of bentonite clay. Characterization of fly ash leachates revealed that coal fly ash leachates contain 53 µg/L of As, 1730 µg/L of B, 271 µg/L of Cr, 165 µg/L of Mo and 170 µg/L of Se.

© University of Venda

7.1.3 Adsorption capacities and mechanisms of raw and Al^{3+}/Fe^{3+} modified bentonite clay for oxyanions of As, B, Cr, Mo and Se

Adsorption of As, B, Cr, Mo and Se onto Al^{3+} modified bentonite clay revealed that 30 minutes of contact time, 4 grams of adsorbent dosage, 10 mg/L of adsorbate concentration and pH 10 are the optimum conditions for removing those species from aqueous media. The adsorption affinity of those species obeyed the following order: B = Se > Mo = Cr > As. Adsorption of As, B, Cr, Mo and Se onto Fe^{3+} modified bentonite clay revealed that 30 minutes of contact time, 4 grams of adsorbent dosage, 10 mg/L of adsorbate concentration and pH 10 are the optimum conditions for removing those species from aqueous media. The adsorption affinity of those species obeyed the following order: B = Se > Mo > Cr = As. The adsorption capacity of raw and modified bentonite clay increased with an increase in adsorbate concentration. Modified bentonite clay showed greater adsorption capacity as compared to raw bentonite clay hence indicating that modification of bentonite clay increases the adsorption capacity of bentonite clay. The data fitted well to both Langmuir and Freundlich adsorption isotherm hence showing that the adsorption is energetically favourable. The unmodified clay showed poor adsorption for these chemical species.

Both Al^{3+} and Fe^{3+} modified bentonite clay successfully removed As, B, Cr, Mo and Se from generated coal fly ash leachates to below DWAF water quality guidelines at the optimized conditions. This shows that Al^{3+} or Fe^{3+} modified bentonite clay is an effective adsorbent for removal of oxyanionic species of As, B, Cr, Mo and Se from coal fly ash leachates and could be applied as a reactive barrier or liner in ash retention ponds. This study successfully proved that As, B, Cr, Mo and Se can be adsorbed from aqueous media in significant amounts by Al^{3+}/Fe^{3+} modified bentonite clay as compared to raw bentonite clay.

© University of Venda

University of Venda
Creating Future Leaders

7.2 Recommendations

There are many different issues which the work has brought out which can be further investigated.
These include:

(a) Evaluation of the regeneration mechanisms for Al^{3+}/Fe^{3+} modified bentonite clay that have been used to adsorb metal ions. This will encourage re-usability of the residue generated, reduce disposal costs and increase the economic viability of the developed technology.

(b) Evaluation of the ability of raw and modified bentonite clay to remove other negatively charged chemical species from coal fly ash leachates

(c) Geochemical modeling of the lifespan of the clay liner and the appropriate thickness of the reactive barrier for effective adsorption.

(d) This study also proposes the use of basic solution such as KOH and NaOH for washing of raw bentonite to remove anions adsorbed during deposition processes hence activating the adsorbent and enhancing its efficiency to adsorb oxyanions from aqueous medium.

UNIVEN LIBRARY
Library Item : 20132631

© University of Venda

University of Venda
Creating Future Leaders

REFERENCES

Abbott, D. E., Essington, M. E., Mullen, M. D., Ammons, J.T., 2001. Fly ash and lime-stabilized bio-solid mixtures in mine spoil reclamation: Simulated weathering. *Journal of Environmental Quality*, 30 (2), pp. 608-616.

Adriano, D.C., Page A.L., Chang, A.C., Straughan, I., 1980. Utilization and disposal of fly ash and other coal residues in terrestrial ecosystem: A review. *Journal of Environmental Quality*, 9, pp. 333-344.

Agnello, V.N., 2004. Bentonite, Pyrophyllite and Talc in the republic of South Africa. Mineral Economics, Mineralia centre. Pretoria. www.dme.gov.za/publications/

Ahmaruzzaman, M., 2010. A review on the utilization of fly ash. *Progress in Energy and Combustion Science*, 36, pp. 327- 363.

Alloways, B.J. 1995. *Heavy metals in soils*. 2nd edition. Blackie academic and professional. London.

Alper, B., Gulbin, G., Fatma S., 2010. Leaching characteristics of fly ash from fluidized bed combustion thermal power plant: Case study: Çan (Çanakkale-Turkey). *Fuel Processing Technology*, 91, pp. 1073-1090.

American Coal Ash Association., 2008. website: http://www.acaa-usa.org.

American Society for Testing and Materials (ASTM)., 1993. Standard speciation for fly ash and raw or calcined natural pozzolan for use as a mineral admixture in Portland cement concrete. Annual Book of ASTM Standards, C 618. ASTM, Philadelphia, PA.

© University of Venda

Baba, G., Gurdal, F., Sengunalp, O. O., 2008. Effects of leachant temperature and pH on leacheability of metals from fly ash: case study: Çan Thermal Power Plant, province of Çanakkale, Turkey, *Environmental Monitoring Assessment*, 139 (1-3), pp. 287–298.

Barker, O.B., 1999. A techno-economic and historical review of the South African coal industry in the 19th and 20th centuries. In: PINHEIRO, H.J. (Ed.) Bulletin 113, South African Bureau of Standards, *Coal and Mineral Services*, pp. 1-63 20.

Besq, A., Malfoy, C., Pantet, A., Monnet, P., Righi, D., 2003. Physiochemical characterization and flow properties of some bentonite muds. *Applied Clay Science*, 23, pp. 275-286.

Bhatnagar, A., Kumar, E., Sillanpaa, M., 2011. Flouride removal from water by adsorption: a review. *Chemical Engineering Journal*.

Bhattacharyya, K. G., Gupta, S. S., 2008. Adsorption of a few heavy metals on natural and modified kaolinite and montmorillonite: A review. *Advance in Colloid and Interface Science*, 140, pp. 114-131.

Binay, K. D., Khanra, S., Durjoy, M., 2009. Leaching of element from coal fly ash: assessment of its potential for use in filling abandoned coal mines. *Fuel*, 88, pp. 1314-1323.

Boggs, S. Jr., 1995. *Principles of sedimentology and stratigraphy*. 2nd ed. Prentice Hall, New Jersey: USA.

Bohn, H. L., McNeal, B. L., O'Connor, G., 1979. *Soil chemistry*. A wiley- interscience publication. John wiley and sons. New York.

Booth, C.A., Spears, D.A., Krause, P., Cox, A.G., 1999. The determination of low level trace elements in coals by laser ablation-inductively coupled plasma-mass spectrometry. *Fuel*, 78, pp. 1665– 1670.

© University of Venda

Bradley G., Weils, D.H., 2004. *Elements of nature*. 5th edition. Blackies and sons. USA

Brunauer, S., 1943. *The adsorption of gases and vapours*. Volume 1: Physical adsorption Princeton University press, Princeton, U.S.A.

Burden, D. S, Sims, J. L. 1999. Fundamentals of soil science as applicable to management of hazardous waste. EPA/540/5-98/500.

Campbell, A.E., 1999. Chemical, Physical and mineralogical properties associated with hardening of some South Africa fly ashes. Unpublished MSc Thesis, University of Cape Town, S.A.

Carlson, C.L., Adrian, D.C., 1993. Environmental impacts of coal combustion residues. *Journal of Environmental Quality*, 22, pp. 227-247.

Chang, A. C., Lund, L.J., Pange, A.L., Warneke, J.E., 1977. Physical properties of fly ash amended soils. *Journal of Environmental Quality*, 6(3),267-270.

Chang, A., Lund, L., Page, A., Warneke, J., 1977. Physical Properties of Fly Ash- Amended Soils, *Journal of Environmental Quality* v.6, n.3:267.

Chapman, H.D., 1962. *Cation Exchange Capacity*. In: C. A. Black (ed.) Methods of soil analysis - Chemical and microbiological properties. Agronomy 9: 891-901.

Cheremisinoff, P., 1988. Coal Fly ash: Power Plant Waste or By-Product? Power Engineering, v.92, n.7:40.

© University of Venda

Choi S. K., Lee Song Y. K., Moon H. S., 2002. Leaching characteristics of selected Korean fly ashes and its implications for the groundwater composition near the disposal mound. *Fuel*, 81, pp. 1083-1090. 21.

Christidis, G. E., 1998. Physical and chemical properties of some bentonite deposits of kimolos island, Greece. *Applied Science Clay*, 13, 79-98.

Collins, R., 1988. A Comparison Between Coal Ash and Incinerator Ash," in Proceedings of the First International Conference on Municipal Solid Waste Combustor Ash Utilization, Philadelphia, Pa., p.99 - 108.

Cunningham, W.P., Saigo, B.W., 1990. Environmental Science, A global concern, 336-340, Wm. C. Brown Publishers.

Dar, B.A., Tahir, A., Arif, M., Wani, A., Faroogui, M., 2012. Lawn grass: An excellent and low cost sorbent for the removal of Ni(II) ions from wastewater. *Electronic Journal of Environmental, Agricultural and Food Chemistry*. ISSN 1579-4377.

Davidson, R.L., Natusch, D.F.S., Wallace, J.R., Evans Jr., C.A., 1974. *Environmental Science technology*, 8, pp. 1107.

Dilip, T., Sadhana, R., Raju, K., Siddharth, M., Subrt, J., Nitin, L., 2010. Magnesium incorporated bentonite clay for deflourization of drinking water. *Journal of Hazardous Materials*, 180, pp. 122-130.

Dutta, B. K., Khanra, S., Mallick, D., 2009. Leaching of elements from coal fly ash: Assessment of its potential for use in filling abandoned coal mines. *Fuel*, 88, 1314-1323.

DWAF., 1996. South African water quality guidelines. 2nd ed. Vol 4: agricultural use: irrigation.

DWAF., 2002. National water management strategies. Proposed 1st ed. Department of water affairs and forestry, South Africa.

© University of Venda

University of Venda
Creating Future Leaders

El-Mogazi, E., Lisk, D., Weinstein, L., 1988. A Review of Physical, Chemical, and Biological Properties of Fly Ash and Effects on Agricultural Ecosystems. *The Science of the Total Environment*, v. 74:1.

Eary, L.E., Dhunpat R. D., Mattigod, S.V and Ainsworth, C.C., 1990. Geochemical factors controlling the mobilization of inorganic constituents from fossil fuel combustion residues:vol: II. Review of the minor elements. *Journal of Environmental Quality*, 19, pp. 202-214.

Electric Power Research Institute (EPRI)., 1986. Mobilization and Attenuation of Trace Elements in an Artificially Weathered Fly Ash, EPRI EA-4747, Project 2485-1.

ESKOM Annual Report., 2001 www.eskom.co.za

ESKOM annual report., 2010. www.eskom.co.za

Evangelou, V. P., 1998. *Environmental soil and water chemistry*. Principles and applications. A wiley-interscience publication. John wiley and sons inc. Toronto.

Fatoba O.O., 2008. The chemical composition and leaching behavior of some South African fly ashes. VDM Verlag Dr Muller Aktiengesellschaft and Co.Kg USA.

Fisher, G., Prentice, B., Silberman, D., Ondov, J., Biermann, A., Bagaini, R., McFarland, A., 1978. Physical and Morphological Studies of Size-Classified Coal Fly Ash, *Environmental Science and Technology*, v.12, n.4:447.

Foth, H. D., 1951. *Fundamentals of soil sciences*. 8th edition. John and Willey and sons press. Singapore.

Freundlich, H., 1906. Uber die adsorption in losungen, Z. *Physical. Chemistry*. 57, 387-470.

© University of Venda

University of Venda
Creating Future Leaders

Furr, A., Parkinson, T., 1977. National Survey of Elements and Radioactivity in Fly Ashes, Adsorption of Elements by Cabbage Grown in Fly Ash-Soil Mixtures, *Environmental Science and Technology*, v.11, n.13:1194.

Furr, A.K., T.F., Parkinson, W.H., Gutenmann, I.S., Pakkala, and D.J., Lisk., 1978. Elemental content of vegetables, grains, and forages field-grown on fly ash-amended soil. *J. Agricultural. Food Chemistry,* 26, pp. 847-851.

Fytianos, K., Tsaniklidi, B., Voudrias, E., 1998. Leachability of heavy metals in greek fly ash from coal combustion. *Environmental International*, vol. 24, 4, pp. 477-486.

Geert, C., Johnson, C. A., Gerven, T. V., Vandecasteele, C., 2008. Leaching mechanisms of Oxyanionic metalloid and metal species in alkalinesolid wastes: A review. *Applied Geochemistry*, 23, 955-976.

George, E. C., 1998. Physical and chemical properties of some bentonite deposits of kimolos island, Greece. *Applied Clay Science*, 13, pp. 79-98. 22

Gitari, M. W., Petrik, L. F., Etchebes O., Key, D. L., Iwuoha E., and Okujeni C., 2006. Treatment of acid mine drainage with fly ash, removal of major contaminants and trace elements. Journal environmental science health *.A Toxicology Hazard Substances Environmental Engineering*, 41(8), pp. 1729-47.

Gitari, W. M., Fatoba, O. O., Leslie, F. P., and Vadapalli, V. R. K., 2009. Leaching characteristics of selected South African fly ashes: effect of pH on th e release of major and trace species. *Journal of Environmental Science and Health part A,* 44, pp. 206-220.

Gitari, W. M., Leslie, F. P., Key, D. L., Okujeni, C., 2010. Partitioning of major and trace inorganic contaminants in fly ash acid mine drainage derived solid residues. *International Journal Environmental Science Technology*, 7 (3), pp. 519-534.

© University of Venda

Golden, D., 1983. Water Pollution Arising from Solid Waste (Coal, Fly Ash, Slag) Disposal, and Measures to Prevent Water Pollution, *Water Science and Technology*, v.15:1.

Goodarzi, F., 2002. Mineralogy, elemental composition and modes of occurrence of elements in Canadian feed-coals. *Fuel*, 81, pp. 1199– 1213.

Gottlieb, B., Gilbert, G. S., Evans, G. L., 2010. Coal ash: The toxic threat to our health and environment. A report from physician for social responsibility and earth justice.

Grygar, T., Hradil, D., Bezdicka, P., Dousava, B., Capek, L., Schneeweiss, O., 2007. Fe(III) modified montmorillonite and bentonite clay: Synthesis, chemical and UV-VIS spectral characterization, Arsenic sorption and catalysis of oxidative dehydrogenation of propane. *Clays and Clay Minerals*, vol 55, No: 2, 165-176.

Guo, L., Lian, L, Wang, A., 2009. Use of CaCl2 modified bentonite clay for removal of congo red dye from aqueous solutions. *Desalination,* 249, pp. 797- 801.

Gupta, U. C. 1997. *Molybdenum in Agriculture*. Cambridge university press. USA

Haghseresht, F., Wang, S., Do, D. D., 2009. A novel lanthanum- modified bentonite clay, phoslock, for phosphate removal from wastewaters. *Applied Clay Science*, 46, pp. 369- 375.

Hareeparsad, S., Tiruta- Barna, L., Brouckaert, C. J., Buckley, C. A., 2011. Quantative geochemical modeling using leaching tests: application for coal ashes produced by two South African thermal processes. *Journal of Hazardous Materials*, 186, 1163-1173.

Heebink, L. V., Hassett, D. J., 2001. Coal fly ash trace elements mobility in soil. International ash utilization symposium.

Hill, C., Paolo, F., 1997. *Deposition and Stability of Silicate Minerals*. Cave Minerals of the World. 2nd Ed. National Speleological Society. pp. 177. ISBN 1-879961-07-5.

© University of Venda

University of Venda
Creating Future Leaders

Hodgson, D.R., Holiday, R., 1966. The agronomic properties of pulverized fuel ash, Chemical Industry, May, 785-790.

Huggins, F.E., 2002. Overview of analytical methods for inorganic constituents in coal. *International Journal of Coal Geology* , 50, pp. 169– 214.

Hyks, J., Astrup, T., Christensen, T. H., 2009. Long- term leaching from MSWI air pollution control residues: leaching characterization and modeling. *Journal of Hazardous Materials* 162 80-91

Iyer R., 2002. The surface chemistry of leaching coal fly ash. *Journal of Hazardous Materials,* B93, pp. 321-329. 23

Iziquiezdo, M., Querol, X., 2011. Leaching behavior of elements from coal combustion fly ash: An overview. *International Journal of Coal Geology*.

Jankowski, J., Ward, C. R., French, D., Groves, S., 2006. Mobility of trace elements from selected Australian fly ashes and its potential impact on aquatic ecosystems. *Fuel* 85 243-256.

Jiuhui, Q. U., 2008. Research progress of novel adsorption processes in water purification: A review.*Journal of Environmental science*. 20, 1-13.

Johnson, C.A., Brandenberger, S., Baccini, P., 1995. Acid neutralizing capacity of municipal waste incinerator bottom ash. *Environmental Science Technology*, 29, 142-147.

Jones, D.R., 1995. Environmental aspects of trace elements in coal. Dordrecht: Kluwer; [chapter 12].

Joubert, A., 2003 . Personal communication, Directorate: communication. Department of water affairs and forestry, Pretoria, South Africa.

© University of Venda

UNIVERSITY OF VENDA LIBRARY

University of Venda
Creating Future Leaders

Kalibantonga, P.D., 2005. Adsorption of heavy metals from solution by South African industrial clay. Published Masters thesis. Tswane University of Technology.

Kamble, S., Dixit, P., Rayalu, S.S., Labhsetwar, N.K., 2009. Magnesium incorporated bentonite clay for deflourization of drinking water, *Desalination*, 249, pp. 687-693.

Kara, M., Yuzer, H., Sabah, E., Celik, M.S., 2003. adsorption of cobalt from aqueous solution onto sepiolite. *Water Resource*, 37, pp. 224-232.

Karthikeyan, G.; Pius, A.; Alagumuthu, G., 2005. Fluoride adsorption studies of montmorillonite clay. *Indian Journal of Chemical Technology*, Volume 12, pp. 263-272.

Katsumata, H., Kaneco, S., Inomata, K., Itoh, K., Funasaka, K., Masyama, K., Suzuki, T., Ohta, K., 2003. Removal of heavy metals in rinsing wastewater from plating factory by adsorption with economical viable materials. *Journal of Environmental Management*. 69, pp. 187-191.

Kearsley, E. P., Mahlaba, J.S., Kruger, R. A., 2011. Physical, chemical and mineralogical characterization of hydraulically disposed fine coal ash from SASOL synfuels. *Fuel*, 90, 2491-2500.

Kim, J. S., and Keane, M.A., 2002. The removal of iron and cobalt from aqueos solutions by ion exchange with Na- Y- Zeolite batch, semibatch and continuous operation. *Journal of Chemical Biotechnology*, 77, pp. 633-640.

Koukouzas, N., Ketikidis, C., Itskos, G., 2011. Heavy metal characterization of CFB- derived coal fly ash. *Fuel Processing Technology*, 92, 441-446.

Krebs, J., Belevi, H., Baccini, P., 1988. Long-term behavior of bottom ash landfills, in: Andersen, L. (Ed.) ISWA 88: proc. Fifth international solid waste conference, vol 1, September 11-16, Copenhagen, *Academic Press*, pp. 371-376.

© University of Venda

Krishna, G. B and Susmita, S. G., 2008. Adsorption of a few heavy metals on natural and modified kaolinite and montmorillonite: a review. *Advances in Colloid and Interface Science*, 140, 114-131.

Kuhn, E. M. R., 2005. Microbiology of fly ash-acid mine drainage co-disposal processes. Published master's thesis, university of Western Cape.

Kumar, E.; Bhatnagar, A.; Kumar, U.; Sillanpaa, M., 2011. Defluoridation from aqueous solution by nano-alumina: Characterization and sorption studies. *Journal of Hazardous Materials*, 186, 1042- 1049.

Kumpiene J., Lagerkvist, A. Christian Maurice., 2006. Stabilization of Pb- and Cu- contaminated soil using coal ash and peat. Environmental pollution, XX: 1-9.

Kutchko, B. G. and Kim, A. G., 2006. Fly ash characterization by SEM-EDS. *Fuel*, 85, pp. 2537-2544.

Lagaly G., 1995. Surface and interlayer reactions: bentonites as adsorbents. pp. 137–144, in Churchman, G.J., Fitzpatrick, R.W., Eggleton R.A. Clays Controlling the Environment. Proceedings of the 10th International Clay Conference, Adelaide, Australia. CSIRO Publishing, Melbourne, ISBN 0643055363.

Langmuir, D., 1997. *Aqueous environmental geochemistry*. Prentice-Hall, Inc. Upper Saddle River: New Jersey 07458. 24

Langmuir, I., 1918. The adsorption of gases on plane surface of glass, mica and platinum, Journal of Am. Chem. Soc. 40, 1361-1368

Lian, L., Guo, L., Wang, A., 2009. Use of $CaCl_3$ modified bentonite clay for removal of congo red dye from aqueous solutions. *Desalination*, 249, 797-801.

© University of Venda

Mahlaba, J. S., Kearsley, P. E., Kruger, R. A., 2011. Physical, chemical and mineralogical characterization of hydraulically disposed fine coal ash from SASOL Synfuels. *Fuel*, 90 2491-2500.

Manahan E.S., 1984. Environmental chemistry forth edition, Willard grant press, PWS publishers

Manohar, D. M., Noeline, B. F., Anirudhan, T. S., 2006. Adsorption performance of Al- pillared bentonite clay for the removal of cobalt (ii) from aqueous phase. *Applied Clay Science*, 31, pp. 194-206.

Manohar, D. M., Noeline, B. F., Anirudhan, T.S, 2006. Adsorption performance of Al-pillared bentonite clay for removal of Cobalt(II) from aqueous phase, *Applied Clay Science,* 31, 194-206.

Manoharan, V., Yunusa, I. A. M. and Lawrie, R., 2007. Influence of coal fly ash application on trace element mobility and distribution in soil, plant and leachate. World of coal ash (WOCA) 2007.

Manz, O. E., 1999. Coal fly ash: A retrospective and future look. *Fuel*, 78, 133-136.

Martens, D. C., M. G. Schnappinger and L. W. Zelazny., 1970. The Plant Availability of Potassium in Fly Ash. Soil Science Society of America Proc. 34:453-456.

Martinez-Tarazona, M. R., and Spears, D. A., 1996. The fate of trace elements and bulk minerals in pulverized coal combustion in a power station. *Fuel Processing Technology*, 47, 79-92.

Mattigod, S.V., Rai D., Eary L.E. and Ainsworth C.C., 1990. Geochemical factors controlling the mobilisation of inorganic constituents from fossil fuel combustion residues: I. Review of major elements. *Journal of Environmental Quality*, 19, pp. 188 – 201.

© University of Venda

University of Venda
Creating Future Leaders

Mishra, S. B., Langwenya, S. P., Mamba, B. B., Balakrishnan, M., 2010. Study on surface morphology and physiochemical properties of raw and activated south African coal and coal fly ash. *Physics and chemistry of Earth*, 35, 811-814.

Mittra, B. N., Karmaka, S., Swain, D. K., Ghosh, B. C., 2003. Fly ash- a potential source of soil amendment and a component of integrated plant nutrients supply system. International ash utilization symposium.

Moitsheki, L. J., Matjie, R. H., Baran, A., Mooketsi, O. I., Schobert, H. H., 2010. Chemical and mineralogical characterization of a South African bituminous coal and its ash, and effect on PH of ash transport. Mineral engineering 23 258-261.

Mulder, J and Cresser, M.S., 1994. *Soil and soil solution chemistry*. Biogeochemistry of small catchments. A tool for environmental research. Published by John and sons, LTD

Murarka, I.P., Rai, D., Ainsworth, C.C., 1991. Geochemical basis for predicting leaching of inorganic constituents from coal–combustion residues. ASTM STP 1075, Friedman D. Ed., American Society for Testing and Materials, pp. 279-288.

Muriithi, G. N, Gitari, W. M, Petrik, L. F, Ndungu, P. G., 2011. Carbonation of brine impacted fractioned coal fly ash: implication for CO2 sequestration. *Journal of Environmental Management*, 92, pp. 655-664.

Nameni, M., Alavi Moghadam, M. R., Arami, M., 2008. Adsorption of hexavalent chromium from aqueous solutions by wheat bran. Int. *Journal Environmental Science Technology*., 5 (2), pp. 161-168.

Nassef, E. and Eltaweel, Y., 2012. Adsorption of phenol from aqueous solution by local Egyptian bentonite. *Journal of American Science*, 8, 8.

© University of Venda

University of Venda
Creating Future Leaders

Natusch, D.F.S., Bauer, C.F., Matusiewicz, H., Evans, Jr. C.A., Barker, J., Loh, A., Linton, R.W., and Hopke, P.K., 1975. Characterization of trace elements in fly ash, 553-575. In: Hutchison, T.E (Ed.) Proceedings of International Conference On Heavy Metals in Environment, Toronto, Ontario, Canada, 27-31 October 1975, Volume 2, Part 2.

NEBRASKA department of environmental quality (NDEQ)., 2004. Beneficial use of coal combustion by-products steel manufacturing by-products and other similar materials

NRDC., 2007. Dangerous disposal: keeping coal combustion waste out of water supply. (www.nrdc.org/policy)

Openshaw, S.C., 1992. Utilization of coal fly ash, Published MSc thesis. University of Florida

Page, A.L., Elseewi, A. A and Straughan, I., 1979. Physical and chemical properties of fly ash from coal fired power plants with reference to environmental impacts. *Residual Review*, 71, pp. 83- 120.

Peffer, J., 1982. Fly Ash Disposal in a Limestone Quarry, Ground Water, v.20, n.3:267.

Pepper, I.L., Gerba, C.P., Brusseau, M.L. 1996. Pollution Science. Academic press. San Diego

Petrik L.F., White R.A., Klink M.J., Somerset S.V., Burgers L.C and Fey V.M., 2003. Utilization of South Africa fly ash to treat acid coal mine drainage, and production of high quality zeolites from the residual solids. International Ash Utilization symposium, Lexington, Kentucky, USA.

Petrik, L.F., White, R., Klink, M., Somerset, V., Key, D., Lwuoha, E., Burger, C., Fey, M.V., 2005. Utilization of fly ash for acid mine drainage remediation, water research commission report No. 1242/1/05, South Africa.

© University of Venda

Prahara, T., Powell, M. A., Hart, B. R., Tripathy, S., 2002. Leachability of elements from sub-bituminous coal fly ash from india. *Environment international*, 27, 609-615.

Prothero, D. R., 1996. *Sedimentary geology*, W. H. freeman and company: united states of America.

Pulles, W., Howie, D., Otto, D. and Eaton, J., 1996. A Manual on Mine Water Treatment and Management Practices in South Africa, Appendix to Water Research Commision Report No.527/1/96.

Querol, X., Umana, J. C., Alastuey, A., Ayora, C., Lopez-Soler, A., Plana, F., 2001. Extraction of soluble major and trace elements from fly ash in open and closed leaching system. *Fuel,* 80, pp. 801-813.

Rahardlo, A. K., Susanto, M. J. J., Kurniawan, A., Indraswati, N., Ismadji, S., 2011. Modified ponorogo bentonite for the removal of ampicillin from wastewater. *Journal of Hazardous Materials*, 190, pp. 1001-1008.

Ramasubramania, I., 2002. The surface chemistry of leaching coal fly ash. *Journal of Hazardous Materials*, B93, pp. 321- 329.

Ramesh, A., Hasegawa, H., Maki, T., Ueda, K., 2007. Adsorption of inorganic and organic arsenic from aqueous solution by polymeric Al/Fe modified montmorillonite. *Seperation and Purification Technology*, 56, 90-100.

Rauf, N., and Tahi, S. S., 2004. Removal of Fe(II) from wastewater of a galvanized pipe manufacturing industry by adsorption onto bentonite clay. *Journal of Environmental Management*, 73. 285-292.

© University of Venda

Reardon, E. J., Czank, C. A., Warren, C. J., Dayal, R., Johnson, H. M., 1995. Determining controls on element concentrations in fly ash leachate. *Waste Management. Resource*., 13 (5), pp.435-450.

Reash, R.J., Lohner, T.W., Wood, K.V., 2006. Selenium and other trace metals in fish inhabiting a fly ash stream: Implications for regulatory tissue thresholds

Robertson, H. S., 1986. Fuller's Earth. A History of calcium montmorillonite. Volturna, Press, U.K., ISBN 0856060704

Roy, W. R. and Griffin, R.A., 1984. Illinois basin coal fly ashes. 2. Equilibria relationships and quantitative modeling of ash-water reactions. *Environmental Science Technology*, 18, 10, 739-742.

Roy, W., Thiery, R., Schuller, R., Suloway,J., 1981. Coal Fly Ash: A Review of the Literature and Proposed Classification System with Emphasis on Environmental Impacts, Environmental Geology Notes, #96.

Sandhu, S., Mills, G., 1991. Mechanisms of Mobi:ization and Attenua of Inorganic Contaminants in coal Ash Basins, (ACS Emerging Thchnologies in Hazardous Waste Management II, New Jersey), Environmental Index: 91-07328.

Sanjay, P. K., Priyadarshini, D., Sadhana, S. R., Nitin, K. L., 2009. Deflourization of drinking water using chemical modified bentonite clay. *Desalination*, 249, pp. 687-693.

Sarkar, B., Xi, Y., Megharaj, M., Krishnamurti, G. S. R., Rajarathnam, D., Naidu, R., 2010. Remediation of hexavalent chromium through adsorption by bentonite based arquad 2HT-75 organoclays. *Journal of hazardous materials*, 183, 87-97.

Scheetz, B.E and Earl, R., 1998. Utilization of fly ash. *Current Opinion in Solid State and Mineral Science*. 3, pp. 510-520.

© University of Venda

University of Venda
Creating Future Leaders

Sear, L. K. A.; Weatherly, A. J.; Dawson, A., 2003. The environmental impacts of using coal fly ash- the UK producers perspective. International ash utilization symposium

Silva, M. G.C.; Kleinubing, S. J.; Bertagnolli, C., 2011. Preparation and characterization of a Brazilian bentonite clay for removal of copper in porous beds. *Applied clay science*, 53, 73-79.

Singh, D and Bhati, S., 2012. Adsorption of Cr (VI) metal ion fro aqueous solution on low cost adsorbent. *Biointerface Research in Applied Chemistry*, Volume 2, issue 2, 284-290.

Singh, G; Gupta S. K; Kumar R; Sunderarajan, M., 2007. Mathematical Modeling of Leachates from Ash Ponds of Thermal Power Plants Environ Monit Assess 130:173–185

Skodras, G., Grammelis, P., Prokopidou, M., Kakaras, E., Sakellaropoulos, G., 2009. Chemical, leaching and toxicity characteristics of CFB combustion residues. *Fuel,* 88, pp. 1201- 1209.

Smith, R.D., 1980. The trace element composition of coal during combustion and the emission from coal fired plants. *Progress in Energy and Combustion Science*, 6, 53-119.

Spark, D. L., 1997. *Environmental soil chemistry*. 2nd ed. Academic press: Amsterdam.

Spears, D. A., Lee, S., 2004. Geochemistry of leachates from coal ash, Geological Society, London. *Special publications*, 236, pp. 619-639. 26

Spears, D.A., and Martinez-Tarazona, M.R., 1996. The fate of trace elements and bulk minerals in pulverized coal combustion in a power station. *Fuel Processing Technology*, 47, 79-92.

Spencer, L., Drake, L., 1987. Hydrogeology of an Alkaline Fly Ash Landfill in Eastern Iowa, Ground Water, v.25, n.5:519.

© University of Venda

Stathi, P., Papadas, I.T., Tselepidou, A., Deligiannakis, Y., 2010. Heavy metal uptake by a high cation exchange capacity montmorillonite: The role of permanent charge sites. *Global NEST journal*, Volume 12, No: 3, pp 248-255.

Steenari B. M., Schelauder S., Lindqvist O., 1999. Chemical and leaching characteristics of ash from combustion of coal, peat and wood in a 12MW CFB – a comparative study. *Fuel*, 78, pp. 249-258.

Stylianou, M. A., Gkantzou, D., Loizidou, M. A., Inglezakis, V.J., 2007. Removal of Pb(II) from aqueous solution by using clinoptilolite and bentonite as adsorbent. *Desalination*, 210, 248-256.

Tahir, S. S. and Naseem, R. (2007). Removal of Cr(III) from tannery wastewater by adsorption onto bentonite clay. *Separation and Purification Technology*, 53, 312-321.

Taylor, E.M. Jr. and Schuman, G.E., 1988. Fly ash and lime amendment of an acidic coal spoil revegetation. *Journal of Environmental Quality*, 17, 120-124.

Thakre, D., Rayalu, S., Kawade, R., Meshram, S., Subrt, J., Labhsetwar, N., 2010. Magnesium incorporated bentonite clay for deflourization of drinking water. *Journal of Hazardous Materials*, 180, 122- 130.

Theis, T., Gardner, K., 1990. Environmental Assessment of Ash Disposal, Critical Reviews in Environmental Control, v.20, n.1:21.

Toor, M.K., 2010. Enhancing adsorption capacity of bentonite for dye removal: physiochemical modification and characterization. Published Masters of Engineering thesis. University of Aldelaide.

Tor, A., 2006. Removal of fluoride from an aqueous solution by using montmorillonite. *Desalination*, 201, 267-276.

© University of Venda

University of Venda
Creating Future Leaders

Treybal, E. R., 1981. Mass transfer operations. McGraw- Hill international editions. Singapore.

Tripathy, S., Praharaj, T., Powell, M. A., Hart, B. R., 2002. Leachability of elements from sub-bituminous coal fly ash from india. *Environment International*, 27, 609-615.

Tyler, G and Miller, J.R., 2007. *Living in the environment*, 5th, jack carey, Thomson learning academic resource centre, Canada.

U.S. Environmental Protection Agency, 2007. Human and Ecological Risk Assessment of Coal Combustion Wastes, RTI, Research Triangle Park.

Van den Berg, J.J., Cruywagen, L., De Necker, E. and Hodgson, F.D.I., 2001. The suitability and impact of power station fly ash for water quality control in coal opencastmine rehabilitation. Report to the Water Research Commission, WRS Report No.745/1/01. VINNICOMBO, D.A 2000: Acid Mine Drainage: Neutralisation, Conditioning and Partial.

Van der Hoek EE, Comans R. N J., 1994. In: Goumans JJJM, Van der Sloot HA, Aalbers ThG, editors. Environmental aspects of construction with waste materials. Amsterdam: Elsevier; p. 467–76.

Vinson, D. S., Mclntosh, J. C., Dwyer, G. S., Vengosh, A., 2011. Arsenic and other oxyanion forming trace elements in an alluvial basin aquifer: Evaluating sources and mobilization by isotopic tracers (Sr, B, S, O, H, Ra). *Applied geochemistry*, 26, 1364-1376.

Wagner, N. J. and Hlatshwayo, B., 2005. The occurance of potential hazardous trace elements in five Highveld coals, south Africa., *International Journal of Coal Geology*, 63, 228-246.

Wang, S. L., Ang, H. M., Tade, M. O., 2008. Novel application of red mud as coagulant, adsorbent and catalyst for environmentally benign processes. *Chemosphere*, 72, pp. 1621- 1635.

© University of Venda

University of Venda
Creating Future Leaders

Wasay, S.A., 1992. Leaching behaviour of trace toxic metals from fly ash, their seepage control to groundwater and utilization of fly ash. *Journal Environmental. Science Health*, A27, pp. 25-39.

Willis, J., 1999. Lectures given as part of the environmental geochemistry masters course, geological sciences, university of Cape Town.

Willis, J.P., 1987. Variation in the composition of South African fly ash. Ash– a valuable resource, 2-6, Council for Science and Industrial Research, vol. 3

Wong, M.; Wong, J., 1989. Germination and Seedling Growth of Vegetable Crops in Fly Ash-amended Soils," Agriculture. Ecosystems and Environment, v.26:23.

World Health Organisation., 2005. Bentonite, kaolinite, and selected clay minerals. Environmental health criteria 231.ISBN 92 4 157231 0.

www.eurelectric.org

www.worldcoal.org/coal/uses of coal/coal-electricity (EIA Report, 2010)

Young, S.C., 1993. Physical and Hydraulic properties of fly ash and other by-products from coal combustion. Electric Power Research Institute, Palo Alto, EPRI pp. 83.

Yunusa, I. A. M., Eamus, D., DeSilva, D. L., Murray B. R., Burchett, M. D., Skilbeck, G. C., Heidrich C., 2006. Fly-ash: An exploitatable resources for management of Australian agriculture soils. *Fuel*, 85: 2337-2344.

© University of Venda

University of Venda
Creating Future Leaders

Yurdakoc, M., Karahan, S., Seki, Y., Yurdokoc, K., 2006. Removal of boron from aqueous solution by clays and modified clays. *Journal of Colloid and Interface Science*, 293, 36-42.

Zhang, M and Reardon, E. J., 2003. Removal of B, Cr, Mo, and Se from wastewater by incorporation into hydrocalumite and ettringite. *Environmental Science Technology*, 37, pp. 2947- 2952.

Zipper, C., Haering, K., Stewart, B., Daniels, W.L., 2002. The potential for reuse of coal fly ash in south west Virginia mining environments. Reclamation guidelines. Virginia cooperative extention, publication 460-134

Zouboulis, A.I., and Tzimou-Tsitouridou, R., 1990. Fly ash utilization in environmental engineering the case of Greece, reclamation, treatment and utilization of coal mining wastes, Rainbow, Balkema, Rotterdam, pp. 493–499.

UNIVERSITY OF VENDA

© University of Venda

APPENDICES

Table A1: Change in pH for pH_{Pzc} determination for raw bentonite clay at 0.1, 0.01, 0.001 KCl concentration

pH	0.1 KCl	0.01 KCl	0.001 KCl
2	-6	-6	-6
3	-5	-5.5	-5.8
4	-4	-4	-5.12
5	-3	-2.9	-3.8
6	-2	-3	-2.8
7	-0.9	-1.9	-1.8
8	-0.18	-0.19	-0.38
9	1	0.3	0.9
10	1.5	1	1.8
11	2	1.9	2.4
12	3	3.6	4

© University of Venda

Table A2: Change in pH for pH_{Pzc} determination for Al^{3+} modified bentonite clay at 0.1, 0.01, 0.001 KCl concentration

pH	0.1 KCl	0.01 KCl	0.001 KCl
2	-4.1	-4.7	-3.9
3	-3.4	-3.9	-3.8
4	-2.9	-3.2	-3.7
5	-1.5	-2.8	-2.5
6	-0.3	-0.8	-1.6
7	-0.1	-0.3	-0.3
8	0.7	0.7	0.7
9	2.3	1.2	1.5
10	3.1	2.3	2.1
11	3.9	2.9	3.2
12	4.7	4.3	4.4

© University of Venda

Table A3: Change in pH for pH_{Pzc} determination for Fe^{3+} modified bentonite clay at 0.1, 0.01, 0.001 KCl concentration

pH	0.1 KCl	0.01 KCl	0.001 KCl
2	-6.1	-6.9	-5.8
3	-5.3	-6	-5.1
4	-4.1	-5.1	-4
5	-2.9	-3	-3.9
6	-2.1	-1.9	-2.8
7	-1	-1.1	-1.9
8	-0.4	-0.5	-0.7
9	0.4	0.7	0.4
10	1.3	1.9	1.7
11	2.6	2.8	2.9
12	3.9	4	4.2

© University of Venda

Table A4: Variation of pH, TDS, EC, Temp and Al^{3+} with agitation time (1 gram of adsorbent dosage, 100 mg/L of adsorbate concentration and 26ºC).

Contact time	pH±SD	EC(µS/cm)±SD	TDS(mg/L)±SD	Temp(◦C)±SD	Al^{3+} Conc (mg/L)±SD	% Al^{3+} Adsorbed
0	1.52±0.04	1055±9.07	676±2.6	21.7±0.05	100±0	0
1	2.31±0.02	855±5.81	547±4.1	21.0±0	1.71±0.03	98.29
5	2.33±0.01	828±11.3	530±6.6	20.2±0.2	1.6±0.19	98.4
10	2.41±0.04	773±4.25	495±2.8	20.6±0.2	1.9±0.15	98.11
15	2.34±0.02	823±3.82	527±2.5	21.1±0.05	1.54±0.22	98.46
30	2.38±0.02	818±10.6	524±6.0	21.8±0.05	1.48±0.04	98.52
60	2.44±0.03	750±2.47	481±1.6	22.4±0.05	0.95±0.02	99.05
180	2.41±0.01	699±2.46	448±1.7	23.1±0	1.11±0.06	98.89
360	1.85±0.02	736±7.09	473±3.5	23.0±0	1.57±0.11	98.43

Concentration reported as mean ± SD (n=3)

© University of Venda

Table A5: Variation of pH, EC, TDS, Temp and Al^{3+} with adsorbent dosage (60 minutes contact time, 100 mg/L adsorbate and 26°C)

Adsorbent dose(g)	pH±SD	EC(µS/cm)±SD	TDS(mg/L)±SD	Temp(◦C)±SD	Al^{3+} Conc (mg/L)±SD	% Al^{3+} Adsorbed
0	1.52±0.05	1055±2.1	676±0.22	21.7±0.05	100±0	0
0.1	1.53±0.09	1062±2.6	683±8.39	21.2±0.41	22.55±1.89	77.45
0.3	1.53±0.02	1011±13.8	643±3.13	22.1±0.68	7.33±0.46	92.67
0.5	1.58±0.02	911±2.12	590±1.81	21.3±0.79	3.36±0.14	96.64
1	1.70±0.03	792±2.12	507±1.35	21.3±0.95	1.59±0.09	98.41
2	1.95±0.01	626±2.12	401±6.65	21.2±0.98	1.54±0.02	98.46
3	2.45±0.17	500±10.2	298±2.51	22.3±0.35	0.84±0.14	99.16
4	3.35±0.02	462±3.05	297±4	22.3±0.26	0.79±0.04	99.21
5	3.88±0.17	458±6.02	293±2.3	22.5±0.11	0.56±0.04	99.44

Concentration reported as mean ± SD (n=3)

© University of Venda

Table A6: Initial pH, TDS (mg/L), EC (µS/cm), Temp (°C) before agitation as a function of Al^{3+} adsorbate concentration (60 minutes of contact time, 3 grams of adsorbate concentration, 26°C and 3g/100 mL S/L ratios).

Initial Concentration	pH± SD	EC± SD	TDS± SD	Temp± SD
10 mg/L	2.24±0.04	26.9±0.6	17.2±0.4	20.1±0.2
50 mg/L	1.89±0.11	100.1±0.5	64±0.7	20.1±0
80 mg/L	1.71±0.02	155.9±1.1	99.9±0.7	20.1±0.05
150 mg/L	1.41±0.04	300.6±1.5	192.2±0.9	20.1±0
200 mg/L	1.20±0.04	450.6±3.9	288.3±2.2	20.3±0.32
250 mg/L	1.08±0	538.6±1.9	344.7±0.9	20.3±0.1
300 mg/L	1±0.05	693.3±8.9	443.7±4.8	20.4±0.05
450 mg/L	0.75±0.01	1048±2.7	671.3±0.6	20.3±0.1
500 mg/L	0.65±0.03	1215.6±1.9	778.3±1.2	20.4±0.25

Concentration reported as mean ± SD (n=3)

© University of Venda

Table A7: Final pH, TDS, EC, Temp and Al^{3+} concentration with varying intial concentration ranges (60 minutes contact time, 3 grams , 250 rpm, 26°C and 3g/100 mL)

Initial Conc	pH±SD	EC(µS/cm)±SD	TDS(mg/L)±SD	Temp(◦C)±SD	Al^{3+} Conc (mg/L)±SD	% Al^{3+} Adsorbed
10	5.3±0.1	28.5±0.7	18.26±0.4	20.4±0	0.02±0.005	99.8
50	4.27±0.1	78.4±0.9	50.1±0.6	20.5±0.1	0.04±0.03	99.92
80	3.84±0.1	109±0.9	69.2±1	20.4±0	0.73±0.28	99.09
150	6.46±0	153±1.7	97.6±0.49	20.6±0.2	11.95±0.52	92.03
200	3.36±0	189±0.9	120.7±2.6	20.6±0.1	42.8±2.75	78.6
250	3.26±0	221±4.1	141.3±4.5	20.5±0.05	63.9±5.60	74.44
300	3.21±5.4	250±8.1	159.9±4.2	20.6±0	98±2.33	67.33
450	3.01±0	345±1.5	221.3±0.6	20.2±0.05	195.3±16.7	56.6
500	1.10±0	939±4.2	601.3±2.7	20.5±0.21	313.7±4.6	37.26

Concentration reported as mean ± SD (n=3)

© University of Venda

Table A8: Variation of pH, TDS (mg/L), EC (µS/cm), Temp (°C) and Fe^{3+} with agitation time (3 gram adsorbent dosage, 100 adsorbate concentration, 250 rpm, 26°C and 1g/100 mL S/L ratios).

Contact time (minutes)	pH±SD	EC(µS/cm)±SD	TDS(mg/L)±SD	Temp(◦C)±SD	Fe^{3+} Conc (mg/L)±SD	% Fe^{3+} Adsorbed
0	1.9±0.02	245±8.3	157±5.26	19.2±0	100±0	0
1	2.0±0.07	223±1.52	143±0.95	19.0±0	6.8 ±0.8	93.2
5	2.2±0.02	206±4.61	132±2.78	19.0±0	6.1 ±1.9	93.9
10	2.2±0.08	214±13.0	138±8.05	19.1±0.15	5.4 ±0.9	94.6
15	2.3±0.03	198±2.75	127±1.89	19.0±0	3.9 ±0.1	96.1
30	2.3±0.04	201±8.90	129±5.61	19.3±0.5	4.2 ±0.7	95.8
60	2.4±0.04	192±3.81	123±2.42	19.6±0.1	4.1 ±0.8	95.9
180	2.4±0.02	172±3.29	112±2.62	20.1±0.5	3.8 ±0.7	96.2
360	2.3±0.10	174±2.91	111±1.88	20.2±0.5	2.1 ±0.1	97.9

Concentration reported as mean ± SD (n=3)

© University of Venda

Table A9: Variation of pH, TDS (mg/L), EC(µS/cm), Temp(°C) and Fe^{3+} ions with adsorbent dosage (15 minutes of contact time, and 100 mg/L adsorbate concentration, 250 rpm and 26°C).

Dosage (g)	pH±SD	EC(µS/cm)±SD	TDS(mg/L)±SD	Temp(◦C)±SD	Remained Fe^{3+} Conc (mg/L)±SD	% Fe^{3+} Adsorbed
0	1.9 ±0.08	223 ±0.5	157 ±0.2	19.2 ±0	100 ±0	0
0.1	1.34 ±0.08	183.6 ±4.2	117.6 ±2.71	21.1 ±0.1	59.25 ±3.65	40.75
0.3	1.67 ±0.02	162.3 ±1.7	103.9 ±1.01	21.1 ±0.17	33.51 ±0.54	66.49
0.5	1.92 ±0.03	136.7 ±3.6	87.6 ±2.26	20.9 ±0	13.33 ±1.15	86.67
1	2.55 ±0.03	110.7 ±1.4	70.9 ±0.87	21.1 ±0.1	1.79 ±0.24	98.2
2	3.66 ±0.19	113.6 ±3.5	72.7 ±2.21	21.0 ±0	0.21 ±0.07	99.79
3	4.51 ±0.06	126 ±2.7	80.7 ±1.69	21.2 ±0.1	0.46 ±0.09	99.54
4	5.36 ±0.03	141.8 ±4	90.8 ±2.55	21.2 ±0.1	1.08 ±0.40	98.92
5	5.72 ±0.6	156.2 ±5	101 ±3.53	21.3 ±0.5	1.36 ±0.15	98.64

Concentration reported as mean ± SD (n=3)

© University of Venda

Table A10: Variation of pH, TDS, EC, Temp and Fe^{3+} with initial adsorbate concentration before agitation (15 minutes contact time, 2 grams adsorbent dosage, 250 rpm, 26°C and 2g/100 mL S/L ratios).

Initial Concentration	pH± SD	EC(µS/cm)± SD	TDS(mg/L)± SD	Temp(°C)± SD
10 mg/L	2.83±0.15	16.7±1.15	10.7±0.72	20.2±0
50 mg/L	2.74±0.55	51.5±4.25	32.4±2.75	19.9±0
80 mg/L	2.84±0.01	76.3±2.48	48.8±1.61	19.8±0.05
150 mg/L	2.46±0.01	125.4±6.02	80.2±3.5	19.5±0.1
200 mg/L	2.50±0.02	151.8±6.35	97.7±4.04	19.5±0
250 mg/L	2.32±0.02	192.5±7.63	123.4±5.03	19.4±0.05
300 mg/L	2.29±0.02	219.3±5.77	139.2±3.78	19.2±0
450 mg/L	2.02±0.02	336±13.0	216.3±7.57	18.4±0.05
500 mg/L	0.86±0.02	1111.7±15.6	710.7±9.6	21.2±0

Concentration reported as mean ± SD (n=3)

© University of Venda

Table A11: Final pH, TDS(mg/L), EC(µS/cm), Temp(°C) and Fe^{3+} ions with adsorbate concentration (15 minutes of agitation, 2 grams of adsorbent dosage, 26°C and 2g/100 mL S/L ratios).

Initial Conc (mg/L)	pH±SD	EC(µS/cm)±SD	TDS(mg/L)±SD	Temp(◦C)±SD	Fe^{3+} Concentration (mg/L)±SD	% Fe^{3+} Adsorbed
10	6.78±0.44	26.3±0.32	16.9±0.22	21.5±0.05	0.02±0.01	99.8
50	3.9±0.07	58.6±1.79	37.5±1.1	21.2±0.05	0.04±0.03	99.92
80	2.98±0.08	91.9±1.31	59.8±1.58	21.2±0.05	0.74±0.28	99.06
150	2.12±0.06	183.3±8.5	117.4±5.36	21.2±0.1	11.95±0.52	92.03
200	1.62±0.01	312.7±6.5	199.8±4.25	21.3±0.1	98.7±5.69	50.65
250	1.45±0.04	400±2.1	256.3±13.5	21.3±0.05	128±1.73	48.8
300	1.26±0.03	481.7±1.7	309±10.1	21.2±0.15	155.3±12.7	48.23
450	0.93±0.04	860.3±6.11	550.7±4.04	21.3±0.05	242.7±10.2	46.07
500	0.86±0.04	975±1.5	623.7±8.62	21.4±0.11	284±13.45	43.2

Concentration reported as mean ± SD (n=3)

© University of Venda

Table A12: % removal of As, B, Cr, Mo and Se, pH, EC and TDS as a function of contact time for raw bentonite clay (1 gram of adsorbent dosage, 10 mg/L of Adsorbate concentration, 250 rpm, 26°C and 1g/100 mL S/L ratios).

	% Removal							
Time(minutes)	As (mg/L)	B (mg/L)	Cr (mg/L)	Mo (mg/L)	Se (mg/L)	Solution pH	EC (µS/cm)	TDS (mg/L)
0	0	0	0	0	0	2.01	532	341
1	1	58	43	10	1	2.05	469	302
5	3	59	45	11	19	2.03	4.74	305
10	8	63	46	12	20	2.01	477	305
15	7	68	47	17	19	2.04	454	291
30	13	74	48	49	25	2.03	450	294
60	12	84	47	55	24	2.02	459	295
180	12	85	48	55	25	2.01	449	293

N = 3

Table A13: % removal of As, B, Cr, Mo and Se, pH, EC and TDS as a function of adsorbent dosage onto raw bentonite clay (30 minutes of contact time, 10 mg/L adsorbate concentration, 250 rpm and 26°C).

	% Removal							
Dosage (g)	As (mg/L)	B (mg/L)	Cr (mg/L)	Mo (mg/L)	Se (mg/L)	Solution pH	EC (µS/cm)	TDS (mg/L)
0	0	0	0	0	0	2.26	1019	652
0.5	30	47.4	48	14	30	2.43	783	501
1	31	49	49.9	19	40	2.52	690	447
2	32	49.2	54	26	59	2.69	559	359
3	39	53	54.7	32	75	2.84	433	277
4	52	54	59	41	88	3.28	310	190
5	59	61	62	57	97	3.85	277	170

N = 3

© University of Venda

Table A14: Initial pH, EC and TDS on adsorption of As, B, Cr, Mo and Se onto raw bentonite clay as a function of adsorbate concentration (30 minutes contact time, 4 grams adsorbate dosage, 250 rpm, 26°C and 4g/100 mL S/L ratios).

Initial concentration (ppm)	pH	EC (µS/cm)	TDS (mg/L)
0.1	2.84	21.9	14.04
0.5	3.05	57.6	36.8
1	3.25	105.7	67.7
3	2.70	377	241
6	2.51	575	368
10	2.26	1019	652
15	2.14	1526	1191

N = 3

Table A15: % removal of As, B, Cr, Mo and Se, pH, EC and TDS as a function of adsorbate concentration onto raw bentonite clay (30 minutes contact time, 4 grams adsorbate dosage, 250 rpm, 26°C and 4g/100 mL S/L ratios).

	% Removal							
Concentration (mg/L)	As (mg/L)	B (mg/L)	Cr (mg/L)	Mo (mg/L)	Se (mg/L)	Solution pH	EC (µS/cm)	TDS (mg/L)
0.1	99.8	100	97.7	98	99.1	8.9	34.1	21.6
0.5	97	100	96	94.5	96	8.29	45.3	29.0
1	93	99.9	92	92	94	6.90	56.0	35.9
3	69	92.7	69	74	93	4.01	122.3	78.3
6	48	79	55	54	78	2.97	256	168.4
10	13	74	48	49	25	2.3	501	309
15	9	67	37	39	11	2.09	689	433

N = 3

© University of Venda

Table A16: % removal of As, B, Cr, Mo and Se, pH, EC and TDS as a function of pH onto raw bentonite clay (30 minutes of contact time, 4 grams of adsorbent dosage, 10 mg/L of adsorbate concentration, 250 rpm, 26°C and 4g/100 mL S/L ratios).

	% Removal							
Initial pH	As (mg/L)	B (mg/L)	Cr (mg/L)	Mo (mg/L)	Se (mg/L)	Final pH	EC (µS/cm)	TDS (mg/L)
2	38.2	92	57.675	74.4	93.5	2.57	9480	6050
4	42.725	94	27.775	18.05	92.25	8.02	1415	906
6	35.5	97	24.425	14.4	91.75	9.09	1371	878
8	33.6	95	27.675	12.15	91.75	8.85	369	2.4
10	31.25	94	41.85	16.925	91.25	9.26	1375	880
12	34.65	91	7	3.6	92.75	11.35	2440	1568

N = 3

Table A17: % removal of As, B, Cr, Mo and Se, pH, EC and TDS as a function of contact time onto Al^{3+} modified bentonite clay (1 gram of adsorbent dosage, 10 mg/L of Adsorbate concentration, 26°C and 1/100 mL S/L ratios).

	% Removal							
Time (Minutes)	As (mg/L)	B (mg/L)	Cr (mg/L)	Mo (mg/L)	Se (mg/L)	Final pH	EC (µS/cm)	TDS (mg/L)
0	0	0	0	0	0	2.01	532	341
1	32	87	66	38	20	2.04	496	298
5	39	99.1	71	43	29	2.07	452	295
10	41	99.5	74	47	31	2.06	457	297
15	43	99.2	75	47	37	2.03	468	300
30	46	99.2	76	49	37	2.03	461	300
60	46	99.2	74	49	38	2.13	455	291
180	45	99.1	72	49	37	2.16	461	299

N = 3

© University of Venda

Table A18: % removal of As, B, Cr, Mo and Se, pH, EC and TDS as a function of adsorbent dosage onto Al^{3+} modified bentonite clay (30 minutes of contact time, 10 mg/L adsorbate concentration, 250 rpm, and 26°C).

	% Removal							
Dosage (g)	As (mg/L)	B (mg/L)	Cr (mg/L)	Mo (mg/L)	Se (mg/L)	Solution pH	EC (µS/cm)	TDS (mg/L)
0	0	0	0	0	0	2.26	1019	652
0.5	22	53	44	15	18	2.42	866	557
1	69	81	73	53	56	2.44	793	511
2	90	94	91	79	77	2.49	690	442
3	98	99.1	99.1	91	99.7	2.60	594	381
4	99.1	99.9	99.9	99.7	99.9	2.69	521	333
5	99.1	99.8	99.9	99.1	99.99	2.87	432	276

N = 3

Table A19: Initial pH, EC and TDS on adsorption of As, B, Cr, Mo and onto Al^{3+} modified bentonite clay as a function of adsorbate concentration (30 minutes contact time, 4 grams adsorbate dosage, 250 rpm, 26°C and 4g/100 mL S/L ratios).

Initial concentration (mg/L)	pH	EC (µS/cm)	TDS (mg/L)
0.1	2.84	21.9	14.04
0.5	3.05	57.6	36.8
1	3.25	105.7	67.7
3	2.70	377	241
6	2.51	575	368
10	2.26	1019	652
15	2.14	1526	1191

N = 3

© University of Venda

UNIVERSITY OF VENDA

Table A20: % removal of As, B, Cr, Mo and Se, pH, EC and TDS as a function of adsorbate concentration onto Al^{3+} modified bentonite clay (30 minutes contact time, 4 grams adsorbate dosage, 250 rpm, 26°C and 4g/100 mL S/L ratios).

	% Removal							
Concentration (mg/L)	As (mg/L)	B (mg/L)	Cr (mg/L)	Mo (mg/L)	Se (mg/L)	Solution pH	EC (µS/cm)	TDS (mg/L)
0.1	99.999	99.999	99.999	99.998	99.99	5.26	35.4	23.1
0.5	99.97	99.99	99.99	99.98	99.94	4.81	44.5	28.7
1	99.91	99.97	99.97	99.9	99.9	4.51	60.2	38.5
3	99.73	99.91	99.91	99.49	99.1	3.00	223	1424
6	99.19	99.85	99.82	98.1	98.5	2.64	400	258
10	97.57	99.7	99.28	95.6	97	2.39	439	294
15	92.7	99	97.12	90	94	2.16	469	305

N = 3

Table A21: % removal of As, B, Cr, Mo and Se, pH, EC and TDS as a function of pH onto Al^{3+} modified bentonite clay (30 minutes of contact time, 4 grams of adsorbent dosage, 10 mg/L of adsorbate concentration, 250 rpm, 26°C and 4g/100 mL S/L ratios).

	% Removal							
Initial pH	As (mg/L)	B (mg/L)	Cr (mg/L)	Mo (mg/L)	Se (mg/L)	Final pH	EC (µS/cm)	TDS (mg/L)
2	67	96	92.2	60.425	94.75	2.55	111	7110
4	73	99	79	86	97.925	4.82	3530	2250
6	81	99.2	86	83.775	97.925	5.06	1368	876
8	80	99.99	90	83.175	97.75	5.01	1365	874
10	87	99.9	92	78.45	98.25	5.23	1287	824
12	91	91	96	25.35	95.25	10.2	1596	1021

N = 3

© University of Venda

Table A22: Langmuir and Freundlich adsorption isotherms for Al^{3+} modified bentonite clay (30 minutes contact time, 4 grams adsorbate dosage, 250 rpm, and 1/100 S/L ratios) for As.

Initial Conc	**Final Conc**	**Langmuir Isotherm (As)**		**Freundlich Isotherm (As)**	
Co(mg/L)	Ce (mg/L)	Qe	Ce/Qe	log Ce	Log Qe
0.1	0.005	0.002	2.00	-2.3	-2.6
0.5	0.003	0.012	0.24	-2.5	-1.9
1	0.009	0.024	0.38	-2.0	-1.6
3	0.012	0.073	0.17	-1.9	-1.1
6	0.049	0.141	0.35	-1.3	-0.9
10	0.13	0.227	0.57	-0.9	-0.6
15	0.39	0.335	1.17	-0.4	-0.5

Table A23: Langmuir and Freundlich adsorption isotherms for Al^{3+} modified bentonite clay (30 minutes contact time, 4 grams adsorbate dosage, 250 rpm, and 1/100 S/L ratios) for B.

Initial Conc	**Final Conc**	**Langmuir Isotherm (B)**		**Freundlich Isotherm (B)**	
Co(mg/L)	Ce (mg/L)	Qe	Ce/Qe	log Ce	Log Qe
0.1	0.001	0.002	0.40	-3.0	-2.6
0.5	0.001	0.012	0.08	-3.0	-1.9
1	0.003	0.025	0.12	-2.5	-1.6
3	0.009	0.075	0.12	-2.0	-1.1
6	0.019	0.149	0.13	-1.7	-0.8
10	0.069	0.248	0.28	-1.2	-0.6
15	0.19	0.372	0.51	-0.7	-0.4

© University of Venda

Table A24: Langmuir and Freundlich adsorption isotherms for Al^{3+} modified bentonite clay (30 minutes contact time, 4 grams adsorbate dosage, 250 rpm, and 1/100 S/L ratios) for Cr.

Initial Conc	**Final Conc**	**Langmuir Isotherm (Cr)**		**Freundlich Isotherm (Cr)**	
Co (mg/L)	Ce (mg/L)	Qe	Ce/Qe	log Ce	Log Qe
0.1	0.001	0.002	0.40	-3.0	-2.6
0.5	0.001	0.012	0.08	-3.0	-1.9
1	0.003	0.025	0.12	-2.5	-1.6
3	0.007	0.075	0.09	-2.2	-1.1
6	0.009	0.149	0.06	-2.0	-0.8
10	0.019	0.248	0.08	-1.7	-0.6
15	0.21	0.372	0.56	-0.7	-0.4

Table A25: Langmuir and Freundlich adsorption isotherms for Al^{3+} modified bentonite clay (30 minutes contact time, 4 grams adsorbate dosage, 250 rpm, and 1/100 S/L ratios) for Mo.

Initial Conc	**Final Conc**	**Langmuir Isotherm (Mo)**		**Freundlich Isotherm (Mo)**	
Co (mg/L)	Ce (mg/L)	Qe	Ce/Qe	log Ce	Log Qe
0.1	0.008	0.002	3.20	-2.1	-2.6
0.5	0.009	0.012	0.72	-2.0	-1.9
1	0.013	0.025	0.52	-1.9	-1.6
3	0.047	0.074	0.63	-1.3	-1.1
6	0.091	0.148	0.61	-1.0	-0.8
10	0.13	0.246	0.53	-0.9	-0.6
15	0.28	0.368	0.76	-0.6	-0.4

© University of Venda

Table A26: Langmuir and Freundlich adsorption isotherms for Al^{3+} modified bentonite clay (30 minutes contact time, 4 grams adsorbate dosage, 250 rpm, and 1/100 S/L ratios) for Se.

Initial Conc	**Final Conc**	**Langmuir Isotherm (Se)**		**Freundlich Isotherm (Se)**	
Co (mg/L)	Ce (mg/L)	Qe	Ce/Qe	log Ce	Log Qe
0.1	0.009	0.002	3.63	-2.0	-2.6
0.5	0.009	0.012	0.73	-2.0	-1.9
1	0.019	0.025	0.77	-1.7	-1.6
3	0.045	0.074	0.61	-1.3	-1.1
6	0.099	0.148	0.67	-1.0	-0.8
10	0.29	0.245	1.18	-0.5	-0.6
15	0.47	0.367	1.28	-0.3	-0.4

Table A27: % removal of As, B, Cr, Mo and Se, pH, EC and TDS as a function of contact time onto Fe^{3+} bentonite clay (1 gram of adsorbent dosage, 10 mg/L of Adsorbate concentration, 250 rpm, 26°C and 1/100 S/L ratios).

	% Removal							
Time (Minutes)	As (mg/L)	B (mg/L)	Cr (mg/L)	Mo (mg/L)	Se (mg/L)	solution pH	EC (µS/cm)	TDS (mg/L)
0	0	0	0	0	0	2.01	532	341
1	22	92	62	37	2	2.0	462	290
5	33	94	66	41	8	2.03	459	294
10	42	96	69	49	9	2.02	426	271
15	49	98	75	51	14	2.03	428	281
30	51	99.9	75	53	21	2.08	399	256
60	50	99.8	76	52	19	2.07	429	273
180	51	99.7	75	52	19	2.07	429	274

N = 3

© University of Venda

Table A28: % removal of As, B, Cr, Mo and Se, pH, EC and TDS as a function of adsorbent dosage onto Fe^{3+} bentonite clay (30 minutes of contact time, 10 mg/L adsorbate concentration, 250 rpm, and 26°C).

	% Removal							
Dosage (g)	As (mg/L)	B (mg/L)	Cr (mg/L)	Mo (mg/L)	Se (mg/L)	Solution pH	EC (µS/cm)	TDS (mg/L)
0	0	0	0	0	0	2.26	1019	652
0.5	15	70	54	49	32	2.33	905	585
1	61	91	73	79	66	2.56	835	535
2	85	97	99	97	83	2.57	660	422
3	91	99	99.9	99.9	97	2.62	551	356
4	99.9	99.1	99.9	99.9	98	2.86	414	274
5	99.8	99.9	99.7	99.9	99	2.98	398	251

N = 3

Table A29: Initial pH, EC and TDS on adsorption of As, B, Cr, Mo and Se onto Fe^{3+} bentonite clay as a function of adsorbate concentration (30 minutes contact time, 4 grams adsorbate dosage, 250 rpm, 26°C and 4g/100 mL S/L ratios).

Initialconcentration (mg/L)	pH	EC (µS/cm)	TDS (mg/L)
0.1	2.84	21.9	14.04
0.5	3.05	57.6	36.8
1	3.25	105.7	67.7
3	2.70	377	241
6	2.51	575	368
10	2.26	1019	652
15	2.14	1526	1191

N = 3

© University of Venda

Table A30: % removal of As, B, Cr, Mo and Se, pH, EC and TDS as a function of adsorbate concentration onto Fe^{3+} bentonite clay (30 minutes contact time, 4 grams adsorbate dosage, 250 rpm, 26°C and 4g/100 mL S/L ratios).

	% Removal							
Concentration (mg/L)	As (mg/L)	B (mg/L)	Cr (mg/L)	Mo (mg/L)	Se (mg/L)	Solution pH	EC (µS/cm)	TDS (mg/L)
0.1	99.999	99.998	99.995	99.97	99.999	3.51	81.4	51.1
0.5	99.991	99.999	99.991	99.99	98.6	3.43	100.1	63.4
1	99.91	99.99	99.98	99.91	99.99	3.25	130.7	83.4
3	99.9	99.9	99.94	99.81	99.91	2.70	359	231
6	99.1	99.1	99.91	99.66	99.73	2.43	583	371
10	98.6	98.1	99.8	99.37	99.37	2.19	631	398
15	98.1	97.7	99.1	99.1	99.03	2.08	651	403

N = 3

Table A31: % removal of As, B, Cr, Mo and Se, pH, EC and TDS as a function of pH onto Fe^{3+} bentonite clay (30 minutes of contact time, 4 grams of adsorbent dosage, 10 mg/L of adsorbate concentration, 250 rpm, 26°C and 4g/100 mL S/L ratios).

	% Removal							
Initial pH	As (mg/L)	B (mg/L)	Cr (mg/L)	Mo (mg/L)	Se (mg/L)	Final pH	EC (µS/cm)	TDS (mg/L)
2	82	92	76	77.675	98.75	2.43	1309	8380
4	77	99.1	63	87.7	99.925	3.58	1795	1150
6	84	99.5	81	99.9957	99.975	3.8	1602	1026
8	87	99.96	90	99.9902	99.9975	3.87	1522	974
10	97	99.6	96	99.9895	99.975	4.38	1491	954
12	99.1	87	57	24.375	98.775	7.48	1525	976

N = 3

© University of Venda

Table A32: Langmuir and Freundlich adsorption isotherms for Fe^{3+} modified bentonite clay (30 minutes contact time, 4 grams adsorbate dosage, 250 rpm, and 1/100 S/L ratios) for As.

Initial Conc	**Final Conc**	**Langmuir Isotherm (As)**		**Freundlich Isotherm (As)**	
Co (mg/L)	Ce (mg/L)	Qe	Ce/Qe	log Ce	Log Qe
0.1	0.0001	0.002	0.04	-4.0	-2.6
0.5	0.0009	0.012	0.07	-3.0	-1.9
1	0.009	0.025	0.36	-2.0	-1.6
3	0.01	0.074	0.13	-2.0	-1.1
6	0.09	0.149	0.61	-1.0	-0.8
10	0.14	0.247	0.57	-0.9	-0.6
15	0.19	0.370	0.51	-0.7	-0.4

Table A33: Langmuir and Freundlich adsorption isotherms for Fe^{3+} modified bentonite clay (30 minutes contact time, 4 grams adsorbate dosage, 250 rpm, and 1/100 S/L ratios) for B.

Initial Conc	**Final Conc**	**Langmuir Isotherm (B)**		**Freundlich Isotherm (B)**	
Co (mg/L)	Ce (mg/L)	Qe	Ce/Qe	log Ce	Log Qe
0.1	0.0002	0.002	0.08	-3.7	-2.6
0.5	0.0001	0.012	0.01	-4.0	-1.9
1	0.001	0.025	0.04	-3.0	-1.6
3	0.01	0.075	0.13	-2.0	-1.1
6	0.09	0.149	0.61	-1.0	-0.8
10	0.19	0.247	0.77	-0.7	-0.6
15	0.23	0.370	0.62	-0.6	-0.4

© University of Venda

Table A34: Langmuir and Freundlich adsorption isotherms for Fe^{3+} modified bentonite clay (30 minutes contact time, 4 grams adsorbate dosage, 250 rpm and 1/100 S/L ratios) for Cr.

Initial Conc	**Final Conc**	**Langmuir Isotherm (Cr)**		**Freundlich Isotherm (Cr)**	
Co (mg/L)	Ce (mg/L)	Qe	Ce/Qe	log Ce	Log Qe
0.1	0.0005	0.002	0.20	-3.3	-2.6
0.5	0.0009	0.012	0.07	-3.0	-1.9
1	0.002	0.025	0.08	-2.7	-1.6
3	0.006	0.075	0.08	-2.2	-1.1
6	0.009	0.150	0.06	-2.0	-0.8
10	0.02	0.249	0.08	-1.7	-0.6
15	0.09	0.373	0.24	-1.0	-0.4

Table A35: Langmuir and Freundlich adsorption isotherms for Fe^{3+} modified bentonite clay (30 minutes contact time, 4 grams adsorbate dosage, 250 rpm and 1/100 S/L ratios) for Mo

Initial Conc	**Final Conc**	**Langmuir Isotherm (Mo)**		**Freundlich Isotherm (Mo)**	
Co (mg/L)	Ce (mg/L)	Qe	Ce/Qe	log Ce	Log Qe
0.1	0.003	0.002	1.21	-2.5	-2.6
0.5	0.001	0.012	0.08	-3.0	-1.9
1	0.009	0.025	0.36	-2.0	-1.6
3	0.019	0.074	0.26	-1.7	-1.1
6	0.034	0.149	0.23	-1.5	-0.8
10	0.063	0.248	0.25	-1.2	-0.6
15	0.09	0.373	0.24	-1.0	-0.4

© University of Venda

Table 36A: Langmuir and Freundlich adsorption isotherms for Fe^{3+} modified bentonite clay (30 minutes contact time, 4 grams adsorbate dosage, 250 rpm, and 1/100 S/L ratios) for Se.

Initial Conc	**Final Conc**	**Langmuir Isotherm (Se)**		**Freundlich Isotherm (Se)**	
Co (mg/L)	Ce (mg/L)	Qe	Ce/Qe	log Ce	Log Qe
0.1	0.0001	0.002	0.04	-4.0	-2.6
0.5	0.0001	0.012	0.01	-4.0	-1.9
1	0.001	0.025	0.04	-3.0	-1.6
3	0.009	0.075	0.12	-2.0	-1.1
6	0.027	0.149	0.18	-1.6	-0.8
10	0.063	0.249	0.25	-1.2	-0.6
15	0.097	0.373	0.26	-1.0	-0.4

© University of Venda